

Calcium- and BTB domain protein-modulated PINOID protein kinase directs polar auxin transport

Robert-Boisivon, H.S.

Citation

Robert-Boisivon, H. S. (2008, May 21). *Calcium- and BTB domain protein-modulated PINOID protein kinase directs polar auxin transport*. Retrieved from https://hdl.handle.net/1887/12863

Version:	Not Applicable (or Unknown)
License:	Leiden University Non-exclusive license
Downloaded from:	https://hdl.handle.net/1887/12863

Note: To cite this publication please use the final published version (if applicable).

Calcium- and BTB domain protein-modulated PINOID kinase directs polar auxin transport

Hélène Robert-Boisivon

Cover	Inflorescence of *pinoid-14 pinoid binding protein1-1* (front cover) GFP:FABD localization in Arabidopsis root hairs at the hypocotyl-root junction (back cover) GFP:FABD line was kindly provided by Tijs Ketelaar, Plant Cell Biology Lab., Wageningen University. Designed by Martin Brittijn
Invitation	Pin-like structure of *pinoid-14*
Printed by:	Ponsen & Looijen bv, The Netherlands
ISBN:	978-90-6464-250-0

Calcium- and BTB domain protein-modulated PINOID kinase directs polar auxin transport

Proefschrift

Ter verkrijging van
de graad van Doctor aan de Universiteit Leiden,
op gezag van Rector Magnificus Prof. Mr. P.F. van der Heijden,
volgens besluit van het College voor Promoties
te verdedigen op woensdag 21 mei 2008
klokke 13:45 uur

door

Hélène Stéphanie Robert-Boisivon

geboren te Mont Saint Aignan (France) in 1977

Promotor:	Prof. Dr. P.J.J. Hooykaas
Co-promotor:	Dr. R. Offringa
Referent:	Dr. P. Genschik (IBMP, Strasbourg, France)
Overige leden:	Prof. Dr. J. Memelink
	Prof. Dr. P.M. Brakefield
	Prof. Dr. B. van Duijn

“Calcium- and BTB domain protein-modulated PINOID kinase directs polar auxin transport”

by Hélène Robert-Boisivon

A ma p’tite KRob,
du plaisir que j’ai à la retrouver tous les soirs ;
A mon Grand Homme à la Maison,
pour son soutien durant ces années de labeur.

Contents

		Page
Abbreviations		9
Chapter 1	Calcium and BTB proteins: generic signaling components with specific roles in auxin transport	13
	Thesis outline	26
Chapter 2	TOUCHing PINOID: regulation of kinase activity by calcium-dependent sequestration	35
Chapter 3	Cell-type and tissue-specific regulation of PID signaling by small calcium-binding proteins	63
Chapter 4	BT scaffold proteins: a crucial function in plant development	87
Chapter 5	A BTB domain protein interacts with the protein kinase PINOID to fine tune its activity	115
Summary		143
Samenvatting		153
Curriculum vitae		161
Color supplements		163

List of abbreviations

ATP	Adenosine tri-phosphate
ATTERT	*Arabidopsis thaliana* telomerase reverse transcriptase
BB	Binding buffer
BELL	BEL1-like homeobox protein
BET/GTE	Bromodomain and extraterminal domain protein/Global transcriptional factor group E
BP	BREVIPEDICELLUS
BSA	Bovine serum albumin
BTB	Broad-Complex, Tramtrack, Bric-a-brac domain
BT	BTB and TAZ domain protein
Ca^{2+}	Calcium
CaD	Catalytic domain
Cam	Chloramphenicol
CaM/CaML	Calmodulin/calmodulin-like
CaMBD	Calmodulin binding domain
Cb	Carbenicillin
CBP	p1300/CREB binding protein
cDNA	Complementary DNA
CDPK	Calcium-dependent protein kinase
CFP	Cyan Fluorescent protein
CHZ	Chalazal pole
Col	Columbia
cort	Cortex cells
CSy	Collapsed synergid cell
CT	C-terminal
CUL3	Cullin 3
dag	Days after germination
DIC	Differential interference contrast
DMSO	Dimethyl sulfoxide
DNA	Deoxyribonucleic acid
Ds element	Dissociation element
EB	Extraction buffer
EC	Egg cell
EDTA	Ethylene diamine tetra-acetic acid
ENP	Enhancer of PINOID
EOL	ETO1-like
ep	Epidermis cells
EtBr	Ethidium bromide
ETO1	Ethylene overproducer1
FG	Female gametophyte development stage
FMN	Flavin mononucleotide
FRET	Förster (fluorescence) resonance energy transfer
gDNA	genomic DNA
gfa	GAMETOPHYTIC FACTOR
GFP	Green fluorescent protein

GST	Glutathione S-transferase
GT	Gene trap
GUS	(beta-) glucuronidase
h	hour
HEPES	4-(2-Hydroxyethyl)piperazine-1-ethanesulfonic acid
His	Histidine
Hm	Hygromycin
hpPBP1H	hairpin RNA spanning the complete PBP1H coding region
HRP	Horse radish peroxidase
IAA	3-Indoleacetic acid, natural auxin
IPTG	Isopropyl β-D-1-thiogalactopyranoside
JLO	JAGGED LATERAL ORGANS
KCBP	Kinesin-like calmodulin-binding protein
KIC	KCBP-interacting calcium-binding protein
KIPK	KCBP-interacting protein kinase
Km	Kanamycin
KNOX	KNOTTED-1 like homeobox proteins
KRP	KIC-related protein
La	Lanthanum
LB	Lysis buffer
LC	Luria–Bertani medium containing 10 mM MgSO4 and 5 mM CaCl2
L*er*	Landsberg *erecta*
LOB domain	Lateral organ boundaries domain
LOV domain	light, oxygen, or voltage domain
MAB4	MACCHI-BOU4
MADS box	MCM1, AGAMOUS, DEFICIENS and SRF box
MATH domain	Meprin and TRAF-C homology domain
MBP	Myelin basic protein
MC	Micropyle pole
min	minute
ml	milliliter
mM	millimolar
MT	microtubules
MYB domain	Myeloblastosis domain
NAA	1-naphthaleneacetic acid, synthetic auxin
NASC	Nottingham Arabidopsis Stock Centre
NES	Nuclear export signal
NLS	Nuclear localization signal
nm	nanometer
NPA	1-naphthylphthalamic acid
NPH3	NON-PHOTOTROPIC HYPOCOTYL3
NPY1	NAKED PINS IN YUC MUTANTS1
NT	N-terminal
(Ni-)NTA	Nickel nitrilotriacetic resin
PAT	Polar auxin transport
PBP1/PBP1H	PINOID BINDING PROTEIN1/PINOID BINDING PROTEIN1 HOMOLOGUE

PBP2	PINOID BINDING PROTEIN2
PBS	Phosphate buffer saline
PCR	Polymerase chain reaction
PDK1	3-phosphoinositide-dependent protein kinase1
PDVF	Polyvinylidene Difluoride
PHOT	Phototropin
PID	PINOID
PIF	PDK-interacting fragment
PIN	PIN-FORMED
PKA	Protein kinase A
PKC	Protein kinase C
PKG	Protein kinase G
PMSF	Phenylmethanesulfonyl Fluoride
PN	Polar nuclei
PNF	POUND-FOOLISH
PNY	PENNYWISE
PP2A	Protein phosphatase 2A
pro	promoter
Rif	Rifampicin
(m)RNA	(Messenger) riboxynucleic acid
RNAi	RNA interference
ROC	ROTAMASE CYLOPHILIN protein
ROI	Region of interest
RPS5A	RIBOSOMAL. PROTEIN S5A
RPT2	ROOT PHOTOTROPISM2
RT-PCR	Reverse transcriptase-PCR
SAM	Shoot apical meristem
SDS	Sodium Dodecyl Sulfate
SDS-PAGE	SDS-poly acrylamide gel electrophoresis
Spc	Spectinomycin
STM	SHOOTMERISTEMLESS
Sy	Synergids
TAC1	TELOMERASE ACTIVATOR1
TAZ/POZ	Transcriptional adaptor zinc finger/Pox virus zinc finger
Tc	Tetracain
TCH3	TOUCH3
T-DNA	Transfer-DNA
TIR	TRANSPORT INHIBITOR RESPONSE1
UPN	Unfused polar nuclei
YFP	Yellow fluorescent protein
ZZ	Zinc
αTUB	alfa Tubulin
µg	microgram
µl	microliter
µm	micrometer
µM	micromolar

Chapter 1

Calcium and BTB proteins: generic signaling components with specific roles in auxin transport

Hélène Robert, Remko Offringa

Transport driven auxin gradients and maxima orient plant development

As sessile organisms, plants have developed various mechanisms for perceiving and responding to changes in their environment such as light, temperature, gravity and drought. Auxin is a central regulator in many of these adaptive responses. Studies of Darwin on the tropic bending of canary grass and oat coleoptiles towards a unidirectional light source provided the first indications of a transported growth substance that mediates this adaptive response (Darwin, 1880). Later, the plant hormone indole-3-acetic acid (IAA) was identified as the key regulator of tropic responses and was named auxin after the greek word for "to grow" (Went, 1937). The asymmetric lateral distribution of auxin during tropic responses is mediated by its polar cell-to-cell transport. This polar auxin transport (PAT) is crucial for many developmental processes, creating auxin gradients and maxima in specific tissues in the plant, e.g. embryo, root tip, leaves and flowers primordia, that regulate cell division, elongation and differentiation, and in this way are instrumental for plant architecture (Sabatini et al., 1999, Reinhardt et al., 2003, Benková et al., 2003, Weijers et al., 2005).

The chemiosmotic model proposed for PAT in the 1970's predicted that polar auxin flow is driven by specific carriers that due to their localization at one side of the cell mediate polar auxin efflux. Molecular genetic research in Arabidopsis has identified the PIN transmembrane proteins as auxin efflux carriers (Gälweiler et al., 1998, Luschnig et al., 1998, Petrášek et al., 2006), that determine the direction of PAT through their asymmetric subcellular localization (Wisniewska et al., 2006). PIN localization is highly dynamic, regulated by vesicles trafficking, protein degradation and phosphorylation, and is responsive to both internal and external signals, among which auxin itself (Geldner et al., 2001, Friml et al., 2004, Abas et al., 2006, Sauer et al., 2006).

The first, and yet only identified determinant in the polar distribution of PIN proteins is the PINOID (PID) serine/threonine protein kinase. Above threshold levels of PID activity induce movement of PIN proteins from the basal (root facing) to the apical (shoot facing) side of cells, thereby changing the direction of auxin transport (Friml et al., 2004). Recently it has been demonstrated that PID directly phosphorylates PIN proteins in their hydrophilic loop, and that PP2A phosphatases counteract the activity of this kinase (Michniewicz et al., 2007).

PID activity is determined on the one hand by expression of the *PID* gene, which is auxin responsive (Benjamins et al., 2001) and under strict spatio-temporal regulation (Christensen et al., 2000, Benjamins et al., 2001, Michniewicz et al., 2007). On the other hand, several PID binding proteins have been identified that appear to regulate its enzymatic activity. Two of these are the calcium-binding proteins TOUCH3 (TCH3) and PINOID BINDING PROTEIN1 (PBP1) that interact with PID in a calcium-dependent manner and respectively repress or enhance its *in vitro* activity (Benjamins et al., 2003).

Furthermore, PID was found to interact with the Broad-Complex, Tramtrack, Bric-a-Brac (BTB) and Transcriptional Adaptor Zinc finger (TAZ) domain protein1 (BT1) (Benjamins, 2004), an interaction that may recruit PID into a multi-protein regulatory complex for which BT1 functions as scaffold (Kemel Zago, 2006). In other words, the AGCVIII kinase PID, a key regulator of auxin transport, is modulated through its interaction with calcium-binding- and BTB domain proteins. In this chapter we provide a survey on what is known on calcium signaling and BTB proteins in relation to plant development. Since calcium signaling and calcium-binding proteins have been widely reviewed, we will focus on the role of calcium in signaling pathways involving AGC kinases. We will further discuss the role of calcium and BTB proteins in the regulation of auxin transport in tropic responses such gravi-, photo- and thigmotropism.

Calcium: from plant nutrient to signaling molecule

Calcium is an essential nutrient for plants. It functions as structural component in the cell wall and the plasma membrane, and as a counter-cation in the vacuole. In addition, the cytosolic calcium concentration is an important second messenger in signal transduction pathways. In fact, cytosolic calcium excess is toxic for plants. In nature, plants succeed to adapt their requirement to the available calcium in the surrounding environment. Calcium is taken up by the roots and transported via the xylem to all parts of the plants, especially the leaves, where it is stored in the apoplast or in intracellular organelles such as the nucleus, vacuole, endoplasmic reticulum and plastids (White and Broadley, 2003). A set of calcium transporters (such as the Ca^{2+} ATPases) keeps the calcium concentration in the cytosol low by actively transporting calcium to the stores. This allows the cell to respond quickly and specifically to external stimuli by calcium channel-mediated release of calcium from these stores into the cytosol. In order for these transient cytosolic calcium-peaks to activate the appropriate pathway, cells have developed specific tools that will be discussed below.

Signal identity maintained by signature of transient cytosolic calcium peaks

Since calcium is involved as second messenger in multiple signaling pathways, the downstream components have to be able to distinguish what caused the transient cytosolic calcium peaks. Each signal appears to result in transient peaks of cytosolic calcium with a signal-specific signature that is characterized by its frequency, amplitude, location and duration (Malhó et al., 1998, McAinsh and Hetherington, 1998, Sanders et al., 1999, Rudd and Franklin-Tong, 2001, Ng and McAinsh, 2003). These signatures take the form of calcium spikes, waves and plateaus (McAinsh and Hetherington, 1998, Sanders et al., 1999). The dynamics of calcium signals is the consequence of calcium buffering (by proteins) in the cytoplasm and of the activity of calcium channels and other transporters

present on the membranes of different calcium stores. Each channel type is unique with respect to activation and deactivation or inactivation, localization, gating properties and sensitivity to other cellular parameters, such as membrane potential or pH (Sanders et al., 1999). Opening of calcium channels itself may lead to membrane depolarization and the subsequent activation of other channels. In the end, appropriate calcium "sensor" or "receptor" proteins are needed to interpret the calcium signature and activate the proper transduction pathways (Figure 1) (Sanders et al., 1999, Luan et al., 2002, White and Broadley, 2003, Bouché et al., 2005).

Calcium Receptors: different types for a variety of signaling pathways

Calcium receptors are proteins that monitor the changes in calcium concentration by binding calcium through specific domains called EF hands (Strynadka and James, 1989). Binding of calcium to the EF hands induces conformational changes of the calcium receptor proteins that either activate them or enhance their interaction with other proteins that are in turn activated or repressed (Travé et al., 1995, Sanders et al., 1999, Luan et al., 2002). Several types of calcium receptors are distinguished based on their structural domains (Reddy and Reddy, 2004). The ones called "sensors", the calmodulins (CaM) and calmodulin-like (CaML), are proteins with typically four EF-hands but no effector domain (McCormack and Braam, 2003). They relay a signal through their calcium-dependent interaction with an effector protein, which consecutively leads to its activation or

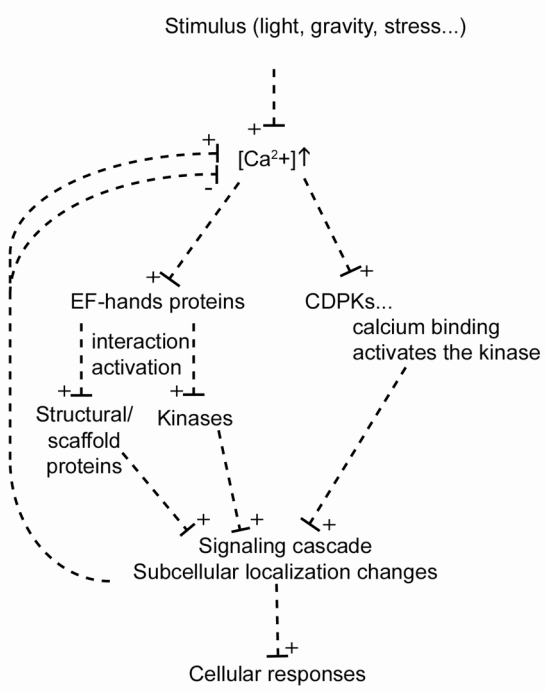


Figure 1. Calcium as second messenger in signal transduction.

Some stimuli (biotic or abiotic, hormone) can induce an increase of the cytoplasmic calcium concentration, which is sensed by at least two types of calcium receptors: the calmodulins and calmodulin-like proteins, or the calcium-dependent protein kinases (CDPKs). In the case of the CDPKs, the calcium signal is directly transmitted to the kinase domain, the activity of which is then enhanced. For the calmodulin(-like) proteins, calcium binding leads to enhanced affinity for other proteins, such as kinases (e.g. the AGCVIII kinases), scaffold proteins (e.g. BT1), or structural proteins (e.g. the kinesin-like calmodulin binding protein KCBP). Activation of the CDPKs, kinases or other calmodulin-binding proteins relays the signal transduction, which gives rise to the appropriate cellular responses, such as bending towards the light source, or activation of defense genes. Additionally, the calcium signal can be enhanced and entertained (spiking, waves) or stopped by a negative feed-back on the calcium channels.

repression (Snedden and Fromm, 2001, Bouché et al., 2005). Downstream targets of the CaMs have non-conserved CaM-Binding domains (Reddy and Reddy, 2004) that are found in a large range of proteins, from enzymes, such as protein kinases, to scaffold proteins (Reddy and Reddy, 2004). Another calcium receptor family is composed of the calcium-dependent protein kinases (CDPK) (Harper et al., 2004). These proteins, called "responders", combine a CaM-like domain with a kinase domain, and binding of calcium directly activates the protein kinase (Cheng et al., 2002). Another important class of calcium sensors is the calcium-dependent ion channels. CaMs, CDPKs and calcium-dependent ion channels have been extensively reviewed before (Luan et al., 2002, McCormack and Braam, 2003, Harper et al., 2004, Reddy and Reddy, 2004). Next to the EF-hand containing CDPKs, the animal protein kinase C (PKC) is also activated by binding calcium, in this case through a C2 domain. Plant homologues of PKCs have not been identified, but instead plants have the related but plant-specific AGCVIII protein kinases (Bögre et al., 2003, Galván-Ampudia and Offringa, 2007). The AGCVIII kinases do not directly bind calcium, but several of these kinases have been linked to calcium signaling through binding with CaM, CaML or CaM-Binding proteins (Baum et al., 1999, Benjamins et al., 2003, Harada et al., 2003, Reddy et al., 2004), and some of them participate in signal transduction pathways that modulate PAT (Friml et al., 2004, Celaya and Liscum, 2005, Santner and Watson, 2006). Below we describe the current knowledge concerning calcium regulation of AGCVIII kinases, and the role it plays in plant development.

Calcium and plant development: the AGCVIII kinases

The AGC family of serine/threonine kinases is named after the cAMP-dependent protein kinase A (PKA), cGMP-dependent protein kinase G (PKG) and calcium-dependent protein kinase C (PKC), animal kinases that are involved in receptor-mediated growth factor signal transduction (Hanks and Hunter, 1995). In plants, the typical PKA, PKG and PKC are not present, but instead a plant specific subfamily of the AGC kinases, AGCVIII, has been identified (Bögre et al., 2003, Galván-Ampudia and Offringa, 2007). The main common feature between animal and plant AGC kinases is their activation by the 3-phosphoinositide-dependent protein kinase1 (PDK1). PDK1 also belongs to the AGC kinase family, and is well-known as a key regulator of other animal AGC kinases (Toker and Newton, 2000, Newton, 2003). PDK1 recruits the kinases at the plasma membrane by binding to a hydrophobic C-terminal domain, called PDK1 Interacting Fragment (PIF), which promotes PDK1-dependent phosphorylation of the AGC kinases in the activation loop. Phosphorylation leads to conformational changes, and PDK1 is released and an auto-phosphorylation in the PIF domain fully matures the kinases, which are then located in the cytosol, ready for activation upon stimulation (Toker and Newton, 2000, Newton, 2003). The majority of the plant-specific AGCVIII kinases are also *in vitro* substrates of PDK1 (Zegzouti et al., 2006), but the *in planta* significance of the PDK1-dependent activation is

still unclear. For the animal PKC, direct calcium binding through the C2 domain induces conformational changes that activates the kinase and targets the protein to the plasma membrane (Shirai and Saito, 2002, Newton, 2003, Halet et al., 2004). The plant-specific AGCVIII kinases have neither a C2 domains, nor EF-hands. Nevertheless some of them were found to be regulated by calcium (Baum et al., 1999, Benjamins et al., 2003, Harada et al., 2003). For three of the AGCVIII kinases, we will further discuss how EF-hand proteins may modulate their activity to translate the calcium signal into a developmental response.

The PINOID kinase links calcium and polar auxin transport

The role of calcium as second messenger in modulating auxin responses and PAT is well established. Evidence that calcium is one of the early signals in auxin response came from experiments on wheat protoplasts (Shishova and Lindberg, 2004), maize coleoptile cells (Felle, 1988, Gehring et al., 1990a), parsley cells (Gehring et al., 1990a) and maize and pea roots (Gehring et al., 1990a). A rapid increase in the cytosolic calcium concentration was detected within minutes after auxin application using calcium fluorescent dyes or ion-sensitive electrodes. It was also found that auxin transport is suppressed by application of the calcium chelator EDTA, and restored after application of a calcium solution (Dela Fuente and Leopold, 1973). The finding that the plant AGC kinase PID, involved in the regulation of the PAT, interacts with two calcium-binding proteins, TCH3 and PBP1, in a calcium-dependent manner provided the first molecular link between calcium signaling and PAT (Benjamins et al., 2003). TCH3 is a CaML protein with six EF-hand domains encoded by a touch-responsive gene (Braam and Davis, 1990, Sistrunk et al., 1994). PBP1 is a small protein of the single EF-hand family (Benjamins et al., 2003, Reddy et al., 2004). Neither of the calcium binding proteins is a phospho-target of PID, but instead they regulate PID kinase activity (Benjamins et al., 2003). TCH3 is a negative regulator of PID activity, whereas PBP1 positively regulates the kinase in *in vitro* phosphorylation assays (Benjamins et al., 2003). PID groups to the AGC3 clade of the Arabidopsis AGCVIII kinases, together with three other kinases, WAG1, WAG2 and AGC3-4 (Galván-Ampudia and Offringa, 2007). Functional analysis of WAG1 and WAG2 has indicated that these kinases play a role in root growth. Roots of *wag1 wag2* loss-of-function seedlings show enhanced sensitivity to the PAT inhibitor NPA, and, like PID, the WAG kinases are membrane-associated, suggesting that they may also be involved in the regulation of PIN polar targeting (Galván-Ampudia and Offringa, 2007). Interestingly, similar to *PID* overexpression, overexpression of *WAG2* in Arabidopsis results in agravitropic seedling growth and primary root meristem collapse (C. Galván-Ampudia, unpublished results). It will therefore be interesting to test whether the calcium-dependent regulation by TCH3 and PBP1, as observed for PID, is conserved for the other AGC3 kinases.

Calcium regulation of the trichome development through the KIC-KCBP complex

There is a striking analogy between the components involved in PID signaling and that of another AGCVIII kinase, the kinesin-like calmodulin-binding protein (KCBP) interacting protein kinase (KIPK). KIPK does not classify to the PID clade, but to the largest AGCVIII clade AGC1 (Galván-Ampudia and Offringa, 2007), and interacts with, but does not phosphorylate KBCP (Day et al., 2000). KCBP is a microtubule (MT) motor protein involved in trichome morphology by regulating branching and polar growth (Reddy and Day, 2000, Reddy et al., 2004). In the presence of calcium, KCBP interacts with AtCaM2, and with a small single EF-hand protein, KCBP-interacting calcium binding protein (KIC) (Reddy et al., 2004). Binding of KIC dissociates KCBP from the MT and inhibits its motor activity (Kao et al., 2000, Reddy et al., 2004). *In vivo KIC* overexpression phenocopies *kcbp* loss-of-function mutants and affects trichome morphology, supporting the *in vitro* observation of the negative regulatory function of KIC on KCBP activity (Reddy et al., 2004). The role of KIPK in this pathway is not clear. KIPK may phosphorylate the other KCBP-associated proteins KIC or CaM2. Another option is that KCBP is involved in the subcellular targeting of KIPK. The relationship between KIC, CaM2 and KIPK has not been elucidated yet. Interestingly, KIC belongs to the same protein family as PBP1 (Reddy et al., 2004), and CaM2 is a close homologue of TCH3 (McCormack and Braam, 2003). Taking into account the role of PBP1 and TCH3 on PID kinase activity, KIC and CaM2 may also regulate KIPK kinase activity, suggesting a conserved function of the EF-hand proteins and a conserved regulation of the AGCVIII kinases by calcium.

Light-induced calcium spikes depend on PHOTOTROPIN activity

Light is an important environmental factor required for plant growth and development. To guarantee optimal positioning of the main photosynthetic organs of a plant, the leaves, toward the light source, plants have developed several photoreceptor-dependent mechanisms to orient plant growth, one of which is phototropic growth. Phototropism is a blue light-induced differential growth response resulting in bending of a plant organ in the direction or away of a unidirectional light stimulus (Liscum, 2002). The light receptors involved in phototropism are the phototropins, which are named PHOTOTROPIN1 (PHOT1) and PHOT2 in Arabidopsis (Briggs and Christie, 2002). The PHOT proteins consist of a kinase domain, based on which they classify to the AGCVIII kinase family, and a photoreceptor domain containing two LOV domains that bind the chromophore flavin mononucleotide (FMN) (Liscum and Briggs, 1995, Huala et al., 1997). Based on the current understanding PHOT1 induces phototropic growth in response to unidirectional low intensity light (Briggs and Christie, 2002). In dark conditions, PHOT1 is a membrane-associated protein, and the LOV domains are believed to repress the PHOT kinase activity. Light stimulation alters the redox state of the FMN, which is sensed by the LOV domains and results in a conformational change that releases the LOV-dependent repression on the

kinase domain (Christie et al., 1998). Upon autophosphorylation, PHOT1 moves to the cytoplasm where it triggers an unknown signaling cascade that leads to differential growth between the lit and shaded side of the plant (Gallagher et al., 1988, Reymond et al., 1992a, Reymond et al., 1992b, Sakamoto and Briggs, 2002). Unfortunately, up to now, besides the autophosphorylation sites, no other PHOT1 phosphorylation targets are known. An early event in the transduction cascade is a PHOT1-dependent calcium release from the apoplast through plasma membrane channels (Baum et al., 1999, Harada et al., 2003). This light-induced peak in cytosolic calcium has been observed in cells at the shaded side of maize coleoptiles where cells show increased elongation, resulting in the coleoptile bending in response to unidirectional light (Gehring et al., 1990b). This is seemingly in contrast with the action of PHOTs, which, as light receptors, are expected to act at the lit side. This suggests that the light-dependent activation of PHOT leads to a mobile signal that induces calcium peaks in cells at the shaded side. Furthermore, in monocotyledons calcium peaks are not immediate, and only start after 5 minutes and reach their maximal level around 15 minutes, whereas in dicotyledonous plants, increase of calcium is observed within seconds after the light stimulus (Harada and Shimazaki, 2007). The meaning of the involvement of calcium in the phototropic response remains to be elucidated. An interesting possibility is that PHOT1, as initiator of a phototropic signaling cascade, modulates the activity of other AGCVIII kinases through their calcium-induced interaction with TCH3 and PBP1 in cells at the shaded side.

Scaffold proteins in plant development

Scaffold proteins are important for bringing proteins together during signal transduction, and are characterized by the presence of multiple protein-protein interaction domains. The 14-3-3 proteins are well known for their role of multi-functional scaffold proteins. Dimerized 14-3-3 proteins interact with phosphorylated proteins and allow transduction of the signals (Sehnke et al., 2002, Ferl, 2004, Bridges and Moorhead, 2005). BTB domain proteins are also typical scaffold proteins. BTB domain proteins have been first described in *Drosophila melanogaster* as scaffolds in transcription factor complexes, are found in many eukaryotes including mammals and plants and are involved in various cellular processes (Bardwell and Treisman, 1994, Albagli et al., 1995, Stogios et al., 2005, Gingerich et al., 2005, Gingerich et al., 2007). In Arabidopsis, eighty BTB proteins have been classified in ten subfamilies depending on other domains present (Gingerich et al., 2005). Up to now, only few of these proteins have been functionally characterized.

Studies in both plants and in animals indicated that several families of BTB proteins serve as a substrate adapter protein in CULLIN3 (CUL3)-containing E3 ligase complexes (Krek, 2003, Xu et al., 2003, Pintard et al., 2004, Moon et al., 2004, Wang et al.,

2004, Gingerich et al., 2005, Dieterle et al., 2005, Weber et al., 2005, Figueroa et al., 2005). Their BTB domain interacts with CUL3 whereas a second protein-protein interaction motif, such as MATH or NPH3, is used to specifically recruit target proteins for ubiquitination and subsequent degradation by the 26S proteasome. Both in animals and in plants, the BTB-MATH protein family has been well characterized for the identification of the target proteins (Xu et al., 2003, Pintard et al., 2004, Dieterle et al., 2005, Figueroa et al., 2005, Gingerich et al., 2005, Weber et al., 2005).

The BTB domain proteins in PHOT signaling

BTB proteins have been reported to be involved in the PID and the PHOT pathways as scaffold and regulator proteins. Two BTB domain proteins of the same family, NON PHOTOTROPIC HYPOCOTYL3 (NPH3) and ROOT PHOTOTROPISM2 (RPT2), interact with PHOT1 (Motchoulski and Liscum, 1999, Sakai et al., 2000). The LOV domains of PHOT1 bind to the coiled-coil domain of NPH3 and with the BTB domain of RPT2, whereas the two BTB proteins homo- and heterodimerize with their respective BTB domain (Motchoulski and Liscum, 1999, Inada et al., 2004). Genetic analyses suggest that both BTB proteins are required for the phototropic response, with *nph3* resembling *phot1* and *rpt2* phenocopying *phot2*, indicating that they are downstream components of the PHOT1 and the PHOT2 signaling pathways, respectively. They are both associated with the plasma membrane where they may be part of a PHOT complex in darkness (Motchoulski and Liscum, 1999, Inada et al., 2004, Celaya and Liscum, 2005). Recent data indicate that NPH3 is phosphorylated in the dark, and that its dephosphorylation in the light is dependent on PHOT1 (Pedmale and Liscum, 2007). The two BTB proteins are proposed to act as modular scaffold proteins bringing together in a dynamic signaling complex comprising PHOT1, or PHOT2, and the early actors of the phototropic response, such as phosphatases and kinases (Liscum, 2002). The fact that the BTB domain of NPH3 may interact with CUL3 suggests that NPH3-dependent recruitment of proteins for degradation by the 26S proteasome is a crucial part of the phototropic response (Pedmale and Liscum, 2007).

BTB proteins in PID signaling

Two BTB proteins have been reported to act in or in parallel to the PID signaling pathway. Firstly, the PINOID BINDING PROTEIN2 (PBP2), initially identified as CaM binding protein BT1, for BTB and TAZ domain1 (Du and Poovaiah, 2004), was identified as interactor of PID (Benjamins, 2004). PBP2/BT1 is part of the land plant specific *Arabidopsis thaliana* BT protein family which includes four other members (Du and Poovaiah, 2004). Interaction studies and functional analyses of the BT protein family suggest that these proteins may be scaffold proteins that provide cross-talk between various signaling pathways (Du and Poovaiah, 2004, Kemel Zago, 2006, Ren et al., 2007).

Interestingly, BT2 is involved in the auxin-induced enhancement of telomerase activity, and *BT2* overexpression lines show reduced auxin sensitivity (Ren et al., 2007).

A second BTB protein of the NPH3-like family, MACCHI-BOU4/ENHANCER OF PINOID/NAKED PINS IN YUC MUTANTS1 (MAB4/ENP/NPY1), has recently been implied in or parallel to the PID signaling pathway. *mab4/npy1* loss-of-function mutants show auxin transport-related phenotypes, such as aberrant cotyledon numbers and deviations in floral organ patterning (Treml et al., 2005, Cheng et al., 2007, Furutani et al., 2007). Genetic analysis of *mab4* indicates that MAB4 is involved in organogenesis synergistically with PID by controlling PIN1 localization in embryo and inflorescence meristems (Furutani et al., 2007).

Calcium and BTB proteins regulate development through the AGC kinases

From the previous part we conclude that the PHOTs and the AGC3 kinases are key regulators of auxin-dependent growth and patterning, and that the signal transduction by both types of AGCVIII kinases involves BTB proteins and calcium. Below we discuss the possible role of these two components based on different examples of auxin-controlled plant development.

Organogenesis

Auxin transport is an important regulator for the positioning and the emergence of a newly formed organ. It generates auxin maxima that precede the occurence of the primordial of future lateral organs, such as lateral roots, leaves and flowers (Benková et al., 2003, Reinhardt et al., 2003, Heisler et al., 2005). Mutants impaired in auxin transport and signaling, such as *pin1*, *pid* and *monopteros* are defective in the formation and positioning of lateral organs at the inflorescence meristem (Okada et al., 1991, Bennett et al., 1996, Hardtke and Berleth, 1998). PID regulates auxin transport by directing the subcellular localization of the PIN auxin-efflux transporters proteins (Friml et al., 2004). And the PID kinase activity during lateral organ formation is crucial for the formation of proper inflorescence in Arabidopsis (Reinhardt et al., 2003). The scaffold protein MAB4/NPY1 undoubtedly acts synergistically with PID-dependent signal transduction. But its role in PID signaling is unclear. Also for BT1 and cytosolic calcium, a role in organogenesis is still elusive (Kemel Zago, 2006, Cheng et al., 2007, Furutani et al., 2007). Interestingly, organ formation is responsive to touch (Jaffe, 1973, Braam, 2005), and we could speculate on the involvement of TCH3 in regulating polar auxin transport by repressing PID-dependent phospho-signal to the PIN proteins (Benjamins et al., 2003). In addition, BT1 has a CaM-binding domain, but it is not known whether TCH3 or PBP1 can interact with it (Du and Poovaiah, 2004). The exact function of this CaM-binding to BT proteins is not known, but

a study on the regulation of telomerase by BT2 suggests that BT proteins become activated by increase cytosolic calcium (Ren et al., 2007).

Phototropism

Phototropic response induces a differential cellular expansion between the lit side and the shaded side, causing a phototropic stem bending towards the unidirectional light source. The unequal growth response appeared to be triggered by an auxin gradient across the stem. This differential auxin distribution between the lit and shaded sides was initially vizualized using the auxin responsive reporters in etiolated seedlings (Li et al., 1991, Friml et al., 2002), and was recently demonstrated by auxin measurements in etiolated Brassica seedlings (Esmon et al., 2006). This auxin gradient requires lateral movement of active auxin, as observed in maize, Arabidopsis and Brassica seedlings (Briggs et al., 1957, Briggs, 1963, Baskin et al., 1986, Friml et al., 2002, Esmon et al., 2006). As discussed above, the direction of auxin transport is determined by the asymmetric placement of the PIN auxin efflux carriers at the plasma membrane (Wisniewska et al., 2006). *pin3* loss-of-function mutants are partially defective in phototropic responses and PIN3 proteins show lateral localization in the hypocotyl (Friml et al., 2002), making PIN3 an excellent candidate for driving a lateral auxin distribution to the shaded hypocotyl side. The current hypothesis is that the blue light-induced PHOT1 signal transduction leads to a change in PIN3 localization, which induces lateral auxin transport to the dark side of the hypocotyl. This implicates that a PHOT1-activated signaling is directly involved in the regulation of the PIN localization. Since PID and possibly the other AGC3 kinases are determinants of PIN polar targeting, it may be interesting to test their involvement in the phototropic growth response. One interesting possibility is that the PHOT1-induced calcium peak that regulate the activity of the kinases via their interaction with TCH3 and PBP1 (Galván-Ampudia and Offringa, 2007). On the other hand, the BTB protein NPH3 is crucial for the lateral redistribution of auxin, since in mutants of the *NPH3* rice homologue *COLEOPTILE PHOTOTROPISM1*, auxin is not found in the shaded side after blue-light stimulation and coleoptile bending is not observed (Haga et al., 2005). It is interesting to note that NPH3 is a phospho-protein, and that blue light induces PHOT1-dependent dephosphorylation (Pedmale and Liscum, 2007). Again, the AGC3 kinases may play a role in keeping NPH3 in the phosphorylated state that interacts with PHOT1, while repression of kinase activity followed by dephosphorylation of NPH3 may lead to its release to the cytosol, where it will be able to initiate changes in auxin transport.

Root growth: gravi- and thigmotropism

Another tropic response is the root response to gravity reorientation, called gravitropism. Gravity is sensed by specialized cellular organs named statoliths, derived from plastids and filled with starch granules. Evidence of their involvement in the gravitropism comes from

starchless mutants. The columella cells, located at the root tip, are the sensors of the gravity vector in the root and responsible for the reorientation of the root growth upon alterations in this gravity vector (Blancaflor et al., 1998). In the shoot the statoliths are located in the endodermis, and some shoot agravitropic mutants identified indeed lack the endodermis. Dynamic auxin movement was observed using auxin responsive *DR5* promoter-reporter constructs in gravi-stimulated roots (Friml et al., 2002, Ottenschlager et al., 2003, Paciorek et al., 2005, Swarup et al., 2005). Moreover, several loss-of-function mutants with altered in auxin transport in roots display agravitropic phenotypes, confirming a role for auxin transport in the root growth response to gravity changes (Bennett et al., 1996, Benjamins et al., 2001, Friml et al., 2002). The PIN3 auxin efflux transporter randomly localizes at the plasma membrane in the root columella initials, but rapidly relocates to the new bottom side of the cells upon changes in the gravity vector, thereby creating a lateral auxin gradient between the lower and the upper side of the root (Friml et al., 2002). Consequently, the auxin-induced differential cell elongation between the two sides results in the root reorientation toward the gravity vector (Ottenschlager et al., 2003). Calcium was found to be involved in and to enhance the auxin transport in gravi-stimulated roots (Lee and Evans, 1985, Plieth and Trewavas, 2002). Several studies suggest a correlated polar mouvement of calcium and of auxin in gravi-stimulated roots (Lee and Evans, 1985 and references within). Moreover gravitropic stimulation of Arabidopsis seedlings induces a specific calcium signature in cells of the root (Plieth and Trewavas, 2002). However up to now, no BTB proteins or kinases have been identified that are clearly involved in PIN3 re-localization, which is the primary cue for gravitropic root growth. In fact, the polarity of PIN3 does not seem to be sensitive to *PID* overexpression (Friml et al., 2004). And the complete agravitropy of *PID* overexpression seedlings can be attributed to the apicalization of the other three PIN proteins expressed in the root tip.

During growth, roots are constitutively submitted to environmental cues such as gravity and contact with the soil. As a consequence, root growth follows a wavy pattern, as a result of concomitant circumnutation (natural rotating movement of the root during growth) and gravitropic and thigmotropic (touch) stimulation. As it is unlikely that PID is involved in triggering gravitropic responses, the other two kinases of the AGC3 clade, WAG1 and WAG2, which have been implied in the regulation of root waving (Santner and Watson, 2006), are probably involved in re-directing PIN3 localization during gravitropic and thigmotropic root growth. It will be interesting to test whether the interaction of TCH3 and PBP1 with the WAG kinases is conserved, since they could provide the missing link between gravitropism-induced increases in cytosolic calcium and re-orientation of auxin transport.

Thesis outline

The function of the PID protein kinase in auxin transport has been largely clarified by the demonstration of its activity on the polar targeting of PIN auxin efflux carriers (Friml et al., 2004), and by the identification of the large central hydrophilic loop of PIN proteins as its likely phosphorylation substrates (Michniewicz et al., 2007). However, importamt questions that remain are how PID activity and subcellular localization are regulated and what could be the *in planta* significance of the PID-dependent PIN phosphorylation. Some of the answers come from the isolation of calcium-binding proteins and BTB domain proteins as PID-binding partners (Benjamins et al., 2003, Benjamins, 2004). PID BINDING PROTEIN1 (PBP1) and TOUCH3 (TCH3) are calcium-dependent regulators of PID kinase activity *in vitro*, and the fact that the *PID* overexpression phenotype is enhanced by calcium channel and calmodulin inhibitors suggests that these PBPs link calcium signaling and auxin transport regulation by the PID kinase (Benjamins et al., 2003).

Chapter 2 and **Chapter 3** describe the further study on the role of TCH3 and PBP1 in Arabidopsis. Alterations in the expression of these genes in the *pid-14* loss-of-function mutant confirmed the function of a negative regulator, for TCH3, and positive regulators, for PBP1 and its close homologue PBP1H, of the PID kinase activity (Chapters 2 and 3). Further analysis in Chapter 3 indicated that PBP1 and PBP1H function redundantly.

Besides regulating the enzymatic PID activity, calcium was also implied in determining the subcellular localization of PID (Chapter 2). In epidermal cells of the root tip PID is mainly plasma membrane-associated (Michniewicz et al., 2007). Upon exogenous auxin application, however, PID was found to be rapidly and transiently released into the cytoplasm (Chapter 2). Inhibitor studies indicated the involvement of calcium channels and CaMs in PID sequestration, and suggested that this was mediated by binding to CaM or CaMLs, such as TCH3, due to auxin-increased cytoplasmic calcium concentrations (Dela Fuente and Leopold, 1973, Felle, 1988, Gehring et al., 1990a, Shishova and Lindberg, 2004) (Chapter 2). On the other hand, *PBP1* overexpression partially stabilized PID at the plasma membrane of root epidermis cells (Chapter 3). In conclusion, auxin seems to regulate both the subcellular localization and the enzymatic activity of the PID kinase through the action of calcium and calcium binding proteins.

The BTB domain protein PBP2/BT1 has been previously identified as a third PID-binding partner (Benjamins, 2004). Here we further analyzed the function of this protein. **Chapter 4** first describes a detailed functional analysis of the Arabidopsis family of land plant-specific BT proteins, which comprises five members (Du and Poovaiah, 2004). Interestingly, BT1 is an unstable protein and a target for degradation by the 26S proteasome. However, reports concerning its interaction with CUL3 are contradictory (Gingerich et al., 2005, Dieterle et al., 2005, Weber et al., 2005, Figueroa et al., 2005).

Genetic and expression analyses showed that the five BT proteins are functionally redundant and essential for female gametophyte development.

In **Chapter 5** we analyze in more detail the function of BT1 and its family members in the PID pathway. The results indicate that the BT proteins bind to PID through their BTB domain, and have a negative regulatory function on PID kinase activity *in vitro*. The instability of the protein may be necessary to fine tune this effect of BT1 on PID activity *in vivo*. For at least four of the five BT proteins we were able to show that they interact with PID, suggesting that all BT act in PID signaling. Interestingly, the absence of BT function rescued the *PID* overexpression seedlings phenotypes, suggesting that BT proteins are crucial regulatory components for PID function. Co-expression studies in Arabidopsis protoplasts indicate a yet unrevealed function for PID in the nucleus, and suggest that the BT proteins function by regulating the subcellular localization of the kinase.

References

Abas,L., Benjamins,R., Malenica,N., Paciorek,T., Wisniewska,J., Moulinier-Anzola,J.C., Sieberer,T., Friml,J., and Luschnig,C. (2006). Intracellular trafficking and proteolysis of the Arabidopsis auxin-efflux facilitator PIN2 are involved in root gravitropism. Nat.Cell Biol. **8**:249-256.

Albagli,O., Dhordain,P., Deweindt,C., Lecocq,G., and Leprince,D. (1995). The BTB/POZ domain: a new protein-protein interaction motif common to DNA- and actin-binding proteins. Cell Growth Differ **6**:1193-1198.

Bardwell,V.J. and Treisman,R. (1994). The Poz Domain - A Conserved Protein-Protein Interaction Motif. Genes & Development **8**:1664-1677.

Baskin,T.I., Briggs,W.R., and Iino,M. (1986). Can Lateral Redistribution of Auxin Account for Phototropism of Maize Coleoptiles? Plant Physiol **81**:306-309.

Baum,G., Long,J.C., Jenkins,G.I., and Trewavas,A.J. (1999). Stimulation of the blue light phototropic receptor NPH1 causes a transient increase in cytosolic Ca2+. PNAS **96**:13554-13559.

Benjamins, R. (2004). Functional analysis of the PINOID protein kinase in *Arabidopsis thaliana*. Institute of Biology, Leiden University, The Netherlands.

Benjamins,R., Ampudia,C.S., Hooykaas,P.J., and Offringa,R. (2003). PINOID-mediated signaling involves calcium-binding proteins. Plant Physiol **132**:1623-1630.

Benjamins,R., Quint,A., Weijers,D., Hooykaas,P., and Offringa,R. (2001). The PINOID protein kinase regulates organ development in Arabidopsis by enhancing polar auxin transport. Development **128**:4057-4067.

Benková,E., Michniewicz,M., Sauer,M., Teichmann,T., Seifertova,D., Jurgens,G., and Friml,J. (2003). Local, efflux-dependent auxin gradients as a common module for plant organ formation. Cell **115**:591-602.

Bennett,M.J., Marchant,A., Green,H.G., May,S.T., Ward,S.P., Millner,P.A., Walker,A.R., Schulz,B., and Feldmann,K.A. (1996). Arabidopsis AUX1 gene: a permease-like regulator of root gravitropism. Science **273**:948-950.

Blancaflor,E.B., Fasano,J.M., and Gilroy,S. (1998). Mapping the functional roles of cap cells in the response of Arabidopsis primary roots to gravity. Plant Physiol **116**:213-222.

Bögre,L., Okrész,L., Henriques,R., and Anthony,R.G. (2003). Growth signalling pathways in Arabidopsis and the AGC protein kinases. Trends Plant Sci. **8**:424-431.

Bouché,N., Yellin,A., Snedden,W.A., and Fromm,H. (2005). PLANT-SPECIFIC CALMODULIN-BINDING PROTEINS. Annual Review of Plant Biology **56**:435-466.

Braam,J. and Davis,R.W. (1990). Rain-, wind-, and touch-induced expression of calmodulin and calmodulin-related genes in Arabidopsis. Cell **60**:357-364.

Braam,J. (2005). In touch: plant responses to mechanical stimuli. New Phytol. **165**:373-389.

Bridges,D. and Moorhead,G.B.G. (2005). 14-3-3 Proteins: A Number of Functions for a Numbered Protein. Sci.STKE **2005**:re10.

Briggs,W.R. (1963). Mediation of Phototropic Responses of Corn Coleoptiles by Lateral Transport of Auxin. Plant Physiol **38**:237-247.

Briggs,W.R. and Christie,J.M. (2002). Phototropins 1 and 2: versatile plant blue-light receptors. Trends Plant Sci. **7**:204-210.

Briggs,W.R., Tocher,R.D., and Wilson,J.F. (1957). Phototropic auxin redistribution in corn coleoptiles. Science **126**:210-212.

Celaya,R.B. and Liscum,E. (2005). Phototropins and associated signaling: providing the power of movement in higher plants. Photochem.Photobiol. **81**:73-80.

Cheng,S.H., Willmann,M.R., Chen,H.C., and Sheen,J. (2002). Calcium signaling through protein kinases. The Arabidopsis calcium-dependent protein kinase gene family. Plant Physiol **129**:469-485.

Cheng,Y., Qin,G., Dai,X., and Zhao,Y. (2007). NPY1, a BTB-NPH3-like protein, plays a critical role in auxin-regulated organogenesis in Arabidopsis. Proc.Natl.Acad.Sci.U.S.A.

Christensen,S.K., Dagenais,N., Chory,J., and Weigel,D. (2000). Regulation of auxin response by the protein kinase PINOID. Cell **100**:469-478.

Christie,J.M., Reymond,P., Powell,G.K., Bernasconi,P., Raibekas,A.A., Liscum,E., and Briggs,W.R. (1998). Arabidopsis NPH1: a flavoprotein with the properties of a photoreceptor for phototropism. Science **282**:1698-1701.

Darwin,C. (1880). *The Power of Movement in Plants*. London: John Murray.

Day,I.S., Miller,C., Golovkin,M., and Reddy,A.S. (2000). Interaction of a kinesin-like calmodulin-binding protein with a protein kinase. J.Biol.Chem. **275**:13737-13745.

Dela Fuente,R.K. and Leopold,A.C. (1973). A Role for Calcium in Auxin Transport. Plant Physiol **51**:845-847.

Dieterle,M., Thomann,A., Renou,J.P., Parmentier,Y., Cognat,V., Lemonnier,G., Muller,R., Shen,W.H., Kretsch,T., and Genschik,P. (2005). Molecular and functional characterization of Arabidopsis Cullin 3A. Plant J. **41**:386-399.

Du,L.Q. and Poovaiah,B.W. (2004). A novel family of Ca2+/calmodulin-binding proteins involved in transcriptional regulation: interaction with fsh/Ring3 class transcription activators. Plant Molecular Biology **54**:549-569.

Esmon,C.A., Tinsley,A.G., Ljung,K., Sandberg,G., Hearne,L.B., and Liscum,E. (2006). A gradient of auxin and auxin-dependent transcription precedes tropic growth responses. PNAS **103**:236-241.

Felle,H. (1988). Auxin causes oscillations of cytosolic free calcium and pH in Zea mays coleoptiles. Planta **V174**:495-499.

Ferl,R.J. (2004). 14-3-3 proteins: regulation of signal-induced events. Physiologia Plantarum **120**:173-178.

Figueroa,P., Gusmaroli,G., Serino,G., Habashi,J., Ma,L.G., Shen,Y.P., Feng,S.H., Bostick,M., Callis,J., Hellmann,H., and Deng,X.W. (2005). Arabidopsis has two redundant Cullin3 proteins that are essential for embryo development and that interact with RBX1 and BTB proteins to form multisubunit E3 ubiquitin ligase complexes in vivo. Plant J. **17**:1180-1195.

Friml,J., Wisniewska,J., Benkova,E., Mendgen,K., and Palme,K. (2002). Lateral relocation of auxin efflux regulator PIN3 mediates tropism in Arabidopsis. Nature **415**:806-809.

Friml,J., Yang,X., Michniewicz,M., Weijers,D., Quint,A., Tietz,O., Benjamins,R., Ouwerkerk,P.B.F., Ljung,K., Sandberg,G., Hooykaas,P.J.J., Palme,K., and Offringa,R. (2004). A PINOID-dependent binary switch in apical-basal PIN polar targeting directs auxin efflux. Science **306**:862-865.

Furutani,M., Kajiwara,T., Kato,T., Treml,B.S., Stockum,C., Torres-Ruiz,R.A., and Tasaka,M. (2007). The gene MACCHI-BOU 4/ENHANCER OF PINOID encodes a NPH3-like protein and reveals similarities between organogenesis and phototropism at the molecular level. Development.

Gallagher,S., Short,T.W., Ray,P.M., Pratt,L.H., and Briggs,W.R. (1988). Light-mediated changes in two proteins found associated with plasma membrane fractions from pea stem sections. Proc.Natl.Acad.Sci.U.S.A **85**:8003-8007.

Galván-Ampudia,C.S. and Offringa,R. (2007). Plant evolution: AGC kinases tell the auxin tale. Trends Plant Sci. **12**.

Gälweiler,L., Guan,C., Müller,A., Wisman,E., Mendgen,K., Yephremov,A., and Palme,K. (1998). Regulation of polar auxin transport by AtPIN1 in Arabidopsis vascular tissue. Science **282**:2226-2230.

Gehring,C.A., Irving,H.R., and Parish,R.W. (1990a). Effects of auxin and abscisic acid on cytosolic calcium and pH in plant cells. Proc.Natl.Acad.Sci.U.S.A **87**:9645-9649.

Gehring,C.A., Williams,D.A., Cody,S.H., and Parish,R.W. (1990b). Phototropism and geotropism in maize coleoptiles are spatially correlated with increases in cytosolic free calcium. Nature **345**:528-530.

Geldner,N., Friml,J., Stierhof,Y.D., Jurgens,G., and Palme,K. (2001). Auxin transport inhibitors block PIN1 cycling and vesicle trafficking. Nature **413**:425-428.

Gingerich,D.J., Gagne,J.M., Salter,D.W., Hellmann,H., Estelle,M., Ma,L.G., and Vierstra,R.D. (2005). Cullins 3a and 3b assemble with members of the broad complex/tramtrack/bric-a-brac (BTB) protein family to form essential ubiquitin-protein ligases (E3s) in Arabidopsis. J.Biol.Chem. **280**:18810-18821.

Gingerich,D.J., Hanada,K., Shiu,S.H., and Vierstra,R.D. (2007). Large-Scale, Lineage-Specific Expansion of a Bric-a-Brac/Tramtrack/Broad Complex Ubiquitin-Ligase Gene Family in Rice. Plant Cell:tpc.

Haga,K., Takano,M., Neumann,R., and Iino,M. (2005). The Rice COLEOPTILE PHOTOTROPISM1 gene encoding an ortholog of Arabidopsis NPH3 is required for phototropism of coleoptiles and lateral translocation of auxin. Plant Cell **17**:103-115.

Halet,G., Tunwell,R., Parkinson,S.J., and Carroll,J. (2004). Conventional PKCs regulate the temporal pattern of Ca2+ oscillations at fertilization in mouse eggs. J.Cell Biol. **164**:1033-1044.

Hanks,S.K. and Hunter,T. (1995). Protein kinases 6. The eukaryotic protein kinase superfamily: kinase (catalytic) domain structure and classification. FASEB J. **9**:576-596.

Harada,A., Sakai,T., and Okada,K. (2003). Phot1 and phot2 mediate blue light-induced transient increases in cytosolic Ca2+ differently in Arabidopsis leaves. Proc.Natl.Acad.Sci.U.S.A **100**:8583-8588.

Harada,A. and Shimazaki,K. (2007). Phototropins and blue light-dependent calcium signaling in higher plants. Photochem.Photobiol. **83**:102-111.

Hardtke,C.S. and Berleth,T. (1998). The Arabidopsis gene MONOPTEROS encodes a transcription factor mediating embryo axis formation and vascular development. EMBO J. **17**:1405-1411.

Harper,J.F., Breton,G., and Harmon,A. (2004). Decoding Ca(2+) signals through plant protein kinases. Annu.Rev.Plant Biol. **55**:263-288.

Heisler,M.G., Ohno,C., Das,P., Sieber,P., Reddy,G.V., Long,J.A., and Meyerowitz,E.M. (2005). Patterns of auxin transport and gene expression during primordium development revealed by live imaging of the Arabidopsis inflorescence meristem. Curr.Biol. **15**:1899-1911.

Huala,E., Oeller,P.W., Liscum,E., Han,I.S., Larsen,E., and Briggs,W.R. (1997). Arabidopsis NPH1: a protein kinase with a putative redox-sensing domain. Science **278**:2120-2123.

Inada,S., Ohgishi,M., Mayama,T., Okada,K., and Sakai,T. (2004). RPT2 is a signal transducer involved in phototropic response and stomatal opening by association with phototropin 1 in Arabidopsis thaliana. Plant Cell **16**:887-896.

Jaffe,M.J. (1973). Thigmomorphogenesis: The response of plant growth and development to mechanical stimulation. Planta **114**:143-157.

Kao,Y.L., Deavours,B.E., Phelps,K.K., Walker,R.A., and Reddy,A.S. (2000). Bundling of microtubules by motor and tail domains of a kinesin-like calmodulin-binding protein from Arabidopsis: regulation by Ca(2+)/Calmodulin. Biochem.Biophys.Res.Commun. **267**:201-207.

Kemel Zago, M. (2006). Components and targets of the PINOID signaling complex in *Arabidopsis thaliana*. Institute of Biology, Leiden University, The Netherlands.

Krek,W. (2003). BTB proteins as henchmen of Cul3-based ubiquitin ligases. Nat.Cell Biol. **5**:950-951.

Lee,J.S. and Evans,M.L. (1985). Polar transport of auxin across gravistimulated roots of maize and its enhancement by calcium. Plant Physiol **77**:824-827.

Li,Y., Hagen,G., and Guilfoyle,T.J. (1991). An Auxin-Responsive Promoter Is Differentially Induced by Auxin Gradients during Tropisms. Plant Cell **3**:1167-1175.

Liscum,E. (2002) Phtotropism: Mechanism and Outcomes. In The Arabidopsis Book, C.R.Somerville and E.M.Meyerowitz, eds (Rockville, Maryland: American Society of Plant Biologists).

Liscum,E. and Briggs,W.R. (1995). Mutations in the NPH1 locus of Arabidopsis disrupt the perception of phototropic stimuli. Plant Cell **7**:473-485.

Luan,S., Kudla,J., Rodriguez-Concepcion,M., Yalovsky,S., and Gruissem,W. (2002). Calmodulins and calcineurin B-like proteins: calcium sensors for specific signal response coupling in plants. Plant Cell **14 Suppl**:S389-S400.

Luschnig,C., Gaxiola,R.A., Grisafi,P., and Fink,G.R. (1998). EIR1, a root-specific protein involved in auxin transport, is required for gravitropism in Arabidopsis thaliana. Genes Dev. **12**:2175-2187.

Malhó,R., Moutinho,A., van der Luit,A., and Trewavas,A.J. (1998). Spatial characteristics to calcium signalling; the calcium wave as a basic unit in plant cell calcium signalling. Philosophical Transactions of the Royal Society B: Biological Sciences **353**:1463-1473.

McAinsh,M.R. and Hetherington,A.M. (1998). Encoding specificity in Ca2+ signalling systems. Trends in Plant Science **3**:32-36.

McCormack,E. and Braam,J. (2003). Calmodulins and related potential calcium sensors of Arabidopsis. New Phytologist **159**:585-598.

Michniewicz,M., Zago,M.K., Abas,L., Weijers,D., Schweighofer,A., Meskiene,I., Heisler,M.G., Ohno,C., Huang,F., Weigel,D., Meyerowitz,E.M., Luschnig,C., Offringa,R., and Friml,J. (2007). Phosphatase 2A and PID kinase activities antagonistically mediate PIN phosphorylation and apical/basal targeting in *Arabidopsis*. Cell **130**:1044-1056.

Moon,J., Parry,G., and Estelle,M. (2004). The Ubiquitin-Proteasome Pathway and Plant Development. Plant Cell **16**:3181-3195.

Motchoulski,A. and Liscum,E. (1999). Arabidopsis NPH3: A NPH1 photoreceptor-interacting protein essential for phototropism. Science **286**:961-964.

Newton,A.C. (2003). Regulation of the ABC kinases by phosphorylation: protein kinase C as a paradigm. Biochem.J. **370**:361-371.

Ng,C.K. and McAinsh,M.R. (2003). Encoding specificity in plant calcium signalling: hot-spotting the ups and downs and waves. Ann.Bot.(Lond) **92**:477-485.

Okada,K., Ueda,J., Komaki,M.K., Bell,C.J., and Shimura,Y. (1991). Requirement of the Auxin Polar Transport System in Early Stages of Arabidopsis Floral Bud Formation. Plant Cell **3**:677-684.

Ottenschlager,I., Wolff,P., Wolverton,C., Bhalerao,R.P., Sandberg,G., Ishikawa,H., Evans,M., and Palme,K. (2003). Gravity-regulated differential auxin transport from columella to lateral root cap cells. Proc.Natl.Acad.Sci.U.S.A **100**:2987-2991.

Paciorek,T., Zazimalova,E., Ruthardt,N., Petrasek,J., Stierhof,Y.D., Kleine-Vehn,J., Morris,D.A., Emans,N., Jurgens,G., Geldner,N., and Friml,J. (2005). Auxin inhibits endocytosis and promotes its own efflux from cells. Nature **435**:1251-1256.

Pedmale,U.V. and Liscum,E. (2007). Regulation of phototropic signaling in Arabidopsis via phosphorylation state changes in the phototropin 1-interacting protein NPH3. J.Biol.Chem. **282**:19992-20001.

Petrášek,J., Mravec,J., Bouchard,R., Blakeslee,J.J., Abas,M., Seifertová,D., Wisniewska,J., Tadele,Z., Kubes,M., Covanová,M., Dhonukshe,P., Skupa,P., Benková,E., Perry,L., Krecek,P., Lee,O.R., Fink,G.R., Geisler,M., Murphy,A.S., Luschnig,C., Zazimalova,E., and Friml,J. (2006). PIN Proteins Perform a Rate-Limiting Function in Cellular Auxin Efflux. Science **312**:914-918.

Pintard,L., Willems,A., and Peter,M. (2004). Cullin-based ubiquitin ligases: Cul3-BTB complexes join the family. EMBO J. **23**:1681-1687.

Plieth,C. and Trewavas,A.J. (2002). Reorientation of seedlings in the earth's gravitational field induces cytosolic calcium transients. Plant Physiol **129**:786-796.

Reddy,A.S. and Day,I.S. (2000). The role of the cytoskeleton and a molecular motor in trichome morphogenesis. Trends Plant Sci. **5**:503-505.

Reddy,V.S., Day,I.S., Thomas,T., and Reddy,A.S. (2004). KIC, a novel Ca2+ binding protein with one EF-hand motif, interacts with a microtubule motor protein and regulates trichome morphogenesis. Plant Cell **16**:185-200.

Reddy,V.S. and Reddy,A.S. (2004). Proteomics of calcium-signaling components in plants. Phytochemistry **65**:1745-1776.

Reinhardt,D., Pesce,E.R., Stieger,P., Mandel,T., Baltensperger,K., Bennett,M., Traas,J., Friml,J., and Kuhlemeier,C. (2003). Regulation of phyllotaxis by polar auxin transport. Nature **426**:255-260.

Ren,S., Mandadi,K.K., Boedeker,A.L., Rathore,K.S., and McKnight,T.D. (2007). Regulation of Telomerase in Arabidopsis by BT2, an Apparent Target of TELOMERASE ACTIVATOR1. Plant Cell **19**:23-31.

Reymond,P., Short,T.W., and Briggs,W.R. (1992a). Blue Light Activates a Specific Protein Kinase in Higher Plants. Plant Physiol **100**:655-661.

Reymond,P., Short,T.W., Briggs,W.R., and Poff,K.L. (1992b). Light-induced phosphorylation of a membrane protein plays an early role in signal transduction for phototropism in Arabidopsis thaliana. Proc.Natl.Acad.Sci.U.S.A **89**:4718-4721.

Rudd,J.J. and Franklin-Tong,V.E. (2001). Unravelling response-specificity in Ca2+ signalling pathways in plant cells. New Phytologist **151**:7-33.

Sabatini,S., Beis,D., Wolkenfelt,H., Murfett,J., Guilfoyle,T., Malamy,J., Benfey,P., Leyser,O., Bechtold,N., Weisbeek,P., and Scheres,B. (1999). An auxin-dependent distal organizer of pattern and polarity in the Arabidopsis root. Cell **99**:463-472.

Sakai,T., Wada,T., Ishiguro,S., and Okada,K. (2000). RPT2. A signal transducer of the phototropic response in Arabidopsis. Plant Cell **12**:225-236.

Sakamoto,K. and Briggs,W.R. (2002). Cellular and subcellular localization of phototropin 1. Plant Cell **14**:1723-1735.

Sanders,D., Brownlee,C., and Harper,J.F. (1999). Communicating with calcium. Plant Cell **11**:691-706.

Santner,A.A. and Watson,J.C. (2006). The WAG1 and WAG2 protein kinases negatively regulate root waving in Arabidopsis. Plant J **45**:752-764.

Sauer,M., Balla,J., Luschnig,C., Wisniewska,J., Reinohl,V., Friml,J., and Benkova,E. (2006). Canalization of auxin flow by Aux/IAA-ARF-dependent feedback regulation of PIN polarity. Genes Dev. **20**:2902-2911.

Sehnke,P.C., DeLille,J.M., and Ferl,R.J. (2002). Consummating signal transduction: the role of 14-3-3 proteins in the completion of signal-induced transitions in protein activity. Plant Cell **14 Suppl**:S339-S354.

Shirai,Y. and Saito,N. (2002). Activation mechanisms of protein kinase C: maturation, catalytic activation, and targeting. J.Biochem.(Tokyo) **132**:663-668.

Shishova,M. and Lindberg,S. (2004). Auxin induces an increase of Ca2+ concentration in the cytosol of wheat leaf protoplasts. J Plant Physiol **161**:937-945.

Sistrunk,M.L., Antosiewicz,D.M., Purugganan,M.M., and Braam,J. (1994). Arabidopsis TCH3 encodes a novel Ca2+ binding protein and shows environmentally induced and tissue-specific regulation. Plant Cell **6**:1553-1565.

Snedden,W.A. and Fromm,H. (2001). Calmodulin as a versatile calcium signal transducer in plants. New Phytologist **151**:35-66.

Stogios,P., Downs,G., Jauhal,J., Nandra,S., and Prive,G. (2005). Sequence and structural analysis of BTB domain proteins. Genome Biology **6**:R82.

Strynadka,N.C.J. and James,M.N.G. (1989). Crystal Structures of the Helix-Loop-Helix Calcium-Binding Proteins. Annual Review of Biochemistry **58**:951-999.

Swarup,R., Kramer,E.M., Perry,P., Knox,K., Leyser,H.M., Haseloff,J., Beemster,G.T., Bhalerao,R., and Bennett,M.J. (2005). Root gravitropism requires lateral root cap and epidermal cells for transport and response to a mobile auxin signal. Nat.Cell Biol. **7**:1057-1065.

Toker,A. and Newton,A.C. (2000). Cellular signaling: pivoting around PDK-1. Cell **103**:185-188.

Travé,G., Lacombe,P.J., Pfuhl,M., Saraste,M., and Pastore,A. (1995). Molecular mechanism of the calcium-induced conformational change in the spectrin EF-hands. EMBO J. **14**:4922-4931.

Treml,B.S., Winderl,S., Radykewicz,R., Herz,M., Schweizer,G., Hutzler,P., Glawischnig,E., and Ruiz,R.A.T. (2005). The gene ENHANCER OF PINOID controls cotyledon development in the Arabidopsis embryo. Development **132**:4063-4074.

Wang,K.L.C., Yoshida,H., Lurin,C., and Ecker,J.R. (2004). Regulation of ethylene gas biosynthesis by the Arabidopsis ETO1 protein. Nature **428**:945-950.

Weber,H., Bernhardt,A., Dieterle,M., Han,P., Hano,P., Mutlu,A., Estelle,M., Genschik,P., and Hellmann,H. (2005). Arabidopsis AtCUL3a and AtCUL3b form complexes with members of the BTB/POZ-MATH protein family. Plant Physiol. **137**:83-93.

Weijers,D., Sauer,M., Meurette,O., Friml,J., Ljung,K., Sandberg,G., Hooykaas,P., and Offringa,R. (2005). Maintenance of embryonic auxin distribution for apical-basal patterning by PIN-FORMED-dependent auxin transport in Arabidopsis. Plant Cell **17**:2517-2526.

Went,F.W. (1937) *Phytohormones*.

White,P.J. and Broadley,M.R. (2003). Calcium in plants. Ann.Bot.(Lond) **92**:487-511.

Wisniewska,J., Xu,J., Seifertova,D., Brewer,P.B., Ruzicka,K., Blilou,I., Rouquie,D., Scheres,B., and Friml,J. (2006). Polar PIN localization directs auxin flow in plants. Science **312**:883.

Xu,L., Wei,Y., Reboul,J., Vaglio,P., Shin,T.H., Vidal,M., Elledge,S.J., and Harper,J.W. (2003). BTB proteins are substrate-specific adaptors in an SCF-like modular ubiquitin ligase containing CUL-3. Nature **425**:316-321.

Zegzouti,H., Li,W., Lorenz,T.C., Xie,M., Payne,C.T., Smith,K., Glenny,S., Payne,G.S., and Christensen,S.K. (2006). Structural and functional insights into the regulation of Arabidopsis AGC VIIIa kinases. J.Biol.Chem. **281**:35520-35530.

Chapter 2

TOUCHing PINOID: regulation of kinase activity by calcium-dependent sequestration

Hélène Robert[1], Carlos Samuel Galvan-Ampudia[1], Karen Sap, Remko Offringa

[1] These authors contributed equally to this manuscript

Abstract

Calcium is a broadly used second messenger in signaling pathways. For the specificity of its response, not only the spatio-temporal pattern, but also calcium "receptors" are essential. The signaling and polar transport of the plant hormone auxin are well-studied examples of processes modulated by calcium. PIN efflux carrier-driven auxin transport generates gradients and maxima that are essential for plant development. The Arabidopsis PINOID (PID) protein serine/threonine kinase has been identified as determinant in the polar subcellular targeting of PIN proteins, and thereby of the direction of transport. The finding that PID shows a calcium-dependent interaction with the calmodulin-related protein TOUCH3 (TCH3) provided the first molecular link between calcium and auxin transport. Here we show that TCH3 inhibits PID kinase activity by interacting with its catalytic domain, and we provide genetic evidence for the *in vivo* significance of this interaction. Furthermore, we show auxin-dependent sequestration of PID from the plasma membrane to the cytosol in protoplasts upon co-expression of TCH3. In root epidermal cells, where PID and TCH3 are co-expressed, auxin induces rapid and transient dissociation of PID from the plasma membrane away from its phospho-targets, the PIN proteins. This response requires the action of calmodulins and calcium channels. These results suggest that TCH3 is part of a feedback loop that modulates PIN polar targeting by rapid inhibition of PID activity in response to stimuli, such as auxin, that induce cytosolic calcium peaks.

Introduction

Calcium plays an important role as intracellular second messenger in a variety of signaling pathways. In plants, rapid changes in the cytosolic calcium concentration are required for the transduction of both abiotic signals and biotic stimuli (Bouché et al., 2005). In order to give an appropriate response, cells need to distinguish the calcium signals produced by these different stimuli. Spatial and temporal patterns of calcium responses, and also the presence of calcium "receptors" or sensors in the cell, are needed to give specificity to the signal (Luan et al., 2002, Sanders et al., 2002). These receptor proteins are able to monitor the changes in the calcium concentration by binding calcium through specific domains called EF hands (Strynadka and James, 1989). The conformational changes induced by binding of calcium to these proteins either induces their activation, or enhances their interaction with other proteins that are in turn activated or repressed (Travé et al., 1995, Luan et al., 2002, Sanders et al., 2002). Two main types of sensors are known: the calmodulins (CaMs) and the calcium-dependent protein kinases (CDPKs). CaMs are small proteins with typically four EF-hands without an effector domain. The transmission of the signal occurs through the interaction with a target enzyme to influence its activity (Snedden

and Fromm, 2001, Bouché et al., 2005). The CDPKs combine a calmodulin-like domain with a kinase domain. Binding of calcium directly activates the protein kinase (Cheng et al., 2002).

The phytohormone auxin regulates plant development by controlling basic cellular processes such as cell division, -differentiation and -elongation (Reinhardt et al., 2000, Nakajima and Benfey, 2002, Weijers and Jurgens, 2005). Several studies suggest that the auxin signaling pathway involves rapid changes in the cytosolic calcium concentration. For example, in wheat protoplasts (Shishova and Lindberg, 2004), maize coleoptile cells (Felle, 1988, Gehring et al., 1990a) and parsley cells (Gehring et al., 1990a), an increase of the cytosolic calcium concentration was detected within minutes after auxin application using calcium fluorescent dyes or ion-sensitive microelectrodes. The observation of an auxin-induced calcium pulse was not limited to protoplasts, but was also observed in intact plant tissues such as maize and pea roots (Gehring et al., 1990a).

Ever since the first observations of Darwin on the growth response of Canary grass coleoptiles to unidirectional light (Darwin, 1880), it is well-established now that auxin is transported from cell to cell in a polar fashion from its sites of synthesis to its sites of action (Muday and DeLong, 2001). This polar auxin transport (PAT) generates auxin gradients and maxima that mediate photo- and gravitropic growth responses, and are instructive for embryogenesis, meristem maintenance and organ positioning (Sabatini et al., 1999, Friml et al., 2002, Friml et al., 2003, Reinhardt et al., 2003). The mechanism of auxin transport has been widely studied, and PIN transmembrane proteins have been identified as auxin efflux carriers that direct this polar intercellular transport through their asymmetric subcellular localization (Morris et al., 2004, Petrášek et al., 2006, Wisniewska et al., 2006). The plant-specific AGC protein serine/threonine kinase PINOID (PID) was identified as a regulator of auxin transport and is the only determinant identified up to now in the polar targeting of PIN proteins. PID directs their localization at the apical (shoot facing) cell membrane, by phosphorylation of the PIN central hydrophilic loop (Benjamins et al., 2001, Friml et al., 2004, Michniewicz et al., 2007).

Calcium has also been implied as an important signal in the regulation of PAT in sunflower hypocotyls (Dela Fuente and Leopold, 1973), in gravistimulated roots (Lee and Evans, 1985) and in the phototropism signaling pathway. The light signal inducing phototropic growth is perceived by the PHOT1 blue receptor kinase. This induces a rapid increase in the cytoplasmic calcium concentration (Baum et al., 1999, Harada et al., 2003) and triggers a PIN-dependent auxin gradient. Auxin accumulation in the shaded side results in auxin-dependent transcriptions, leading to a shoot bending toward the light source (Friml et al., 2002, Esmon et al., 2006). The function of the rapid calcium response in phototropic growth and the downstream components of the signaling pathway are still uncharacterized.

Our previous finding that PID interacts in a calcium-dependent manner with the calcium-binding proteins PINOID BINDING PROTEIN1 (PBP1) and TOUCH3 (TCH3)

provided the first molecular evidence for calcium as a signal transducer in the regulation of auxin transport (Benjamins et al., 2003). TCH3 is a CaM-like protein containing 6 EF-hands, and its corresponding gene was initially identified as a touch-responsive gene (Braam and Davis, 1990, Sistrunk et al., 1994). Here we present a detailed study of the *in vivo* interaction between PID and TCH3. Using loss- and gain-of-function mutant lines, we confirm *in vitro* observations that TCH3 is a negative regulator of the PINOID kinase activity. This regulation occurs directly by inhibition of the kinase activity, as shown in phosphorylation assays, and by sequestration of PID from the plasma membrane where its phospho-targets are located (Michniewicz et al., 2007). Interestingly, auxin treatment also results in rapid transient re-localization of the membrane-associated kinase to the cytosol. We speculate that this occurs through its interaction with TCH3, which is enhanced by the auxin-induced increase in cytosolic calcium.

Results

TCH3 reduces the kinase activity by binding to the catalytic domain of PID

Previously we identified the calmodulin-like protein TCH3 as PID binding protein in a yeast two-hybrid screen. With *in vitro* pull-down assays we could show that the kinase-CaM interaction is calcium-dependent (Benjamins et al., 2003). In order to roughly map the TCH3 interaction site in PID, we incubated GST-tagged isolates of full-length PID, the N-terminal domain (aa 2-103), the catalytic domain (aa 75-398) or C-terminal domain (aa 339-438) with crude *E. coli* extracts containing Histidine (His)-tagged TCH3 (Figure 1A). Protein complexes were pulled down with glutathione beads and separated on gel. Western blot analysis using anti-His antibodies showed that TCH3 interacts with full-length PID or with its catalytic domain (Figure 1B, lanes 2 and 4) but not with the N- or C-terminal domains (Figure 1B, lanes 3 and 5) nor with GST alone (Figure 1B, lane 1). Binding to the catalytic domain suggested that TCH3 might affect PID kinase activity. Indeed, our previous studies showed that TCH3 reduces the *in vitro* phosphorylation activity of PID using traditional kinase assay with Myelin Basic Protein (MBP) as substrate (Benjamins et al., 2003). To confirm these results with a wider array of substrates, we incubated a commercial phospho-peptide chip with radiolabelled ATP and PID alone or in the presence of PBP1, a PID positive regulator (Benjamins et al., 2003), or of both PBP1 and TCH3. For a quantitative comparison of the differences in PID activity, we focused on the phosphorylation intensity of four peptides, one of which represented a phospho-target in MBP. PID efficiently phosphorylated all four peptides (Figures 2A and 2D) and in presence of PBP1, the phosphorylation intensity was significantly increased (Figures 2B and 2D) which corroborated the role of PBP1 as positive regulator of PID (Benjamins et al., 2003). When TCH3 was added to the last mix, the phosphorylation intensity was significantly

reduced to even below the basal level of PID alone (Figures 2C and 2D). These data corroborate our previous data that TCH3 is a negative regulator of PID kinase activity *in vitro* and indicate that TCH3 binding to PID is able to overrule this positive effect of PBP1.

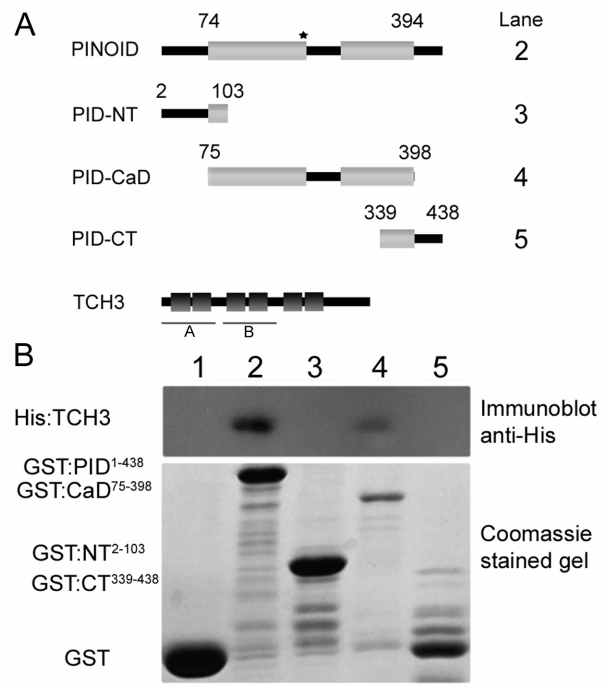


Figure 1. TCH3 interacts with the catalytic domain of PID.
(A) A schematic representation of the proteins used in the *in vitro* pull-down assay. Full-length PID (498 aa) and its deletion mutants: the N-terminal portion (PID-NT, aa 2-103), the catalytic domain (PID-CaD, aa 75-398) and the C-terminal portion (PID-CT, aa 339-438), are shown. The light grey boxes represent the PID catalytic domain (aa 74-394), comprising 11 conserved sub-domains and the amino acid insertion between sub-domain VII and VIII (aa 226-281). The star indicates the DFG to DFD mutation characteristic for the plant-specific AGCVIII protein kinases. The numbers indicated on the right correspond to the lane numbers of the Western blot in (B). TCH3 (324 aa) is depicted with the six EF-hand domains (aa 12-38, 50-74, 101-127, 139-163, 191-217, 228-253) as dark grey boxes. The lines A and B represent the perfect tandem repeat comprising EF-hands pairs 1-2 and 3-4.
(B) Western blot analysis (top) with anti-His antibodies detects His-tagged TCH3 after pull-down with GST-tagged PID (lane 2) or GST-tagged PID catalytic domain (GST:CaD, lane 4), but not after pull-down with GST-tagged PID N-terminal (GST:NT, lane 3) or C-terminal (GST:CT, lane 5) domains or with GST alone (lane 1). Coomassie stained gel (bottom) showing the input of proteins used in the pull-down assay.

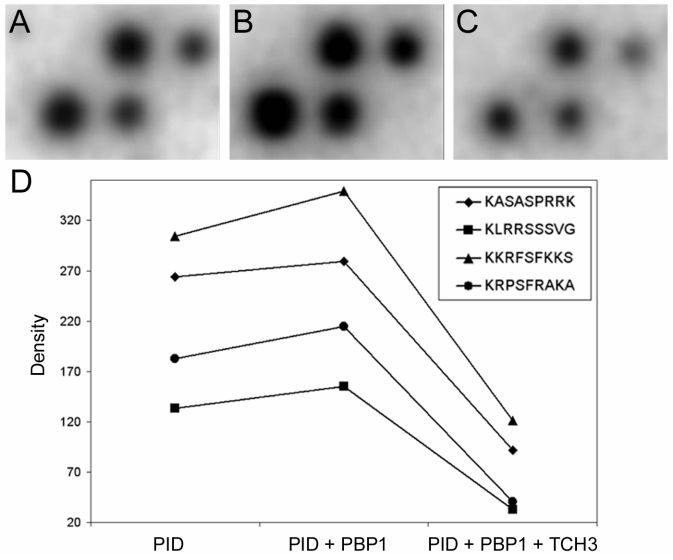


Figure 2. TCH3 reduces PID kinase activity *in vitro.*
(A-C) Kinase assay using a chip where PID alone (A), PID and the positive regulator PBP1 (B), or PID, PBP1 and TCH3 (C) were incubated with radiolabelled ATP.
(D) Quantification of the phosphorylation density of the four peptides shown in (A-C) confirms that TCH3 represses PID kinase activity *in vitro*.

TCH3 *overexpression lines and* **tch3** *loss-of-function mutants do not show phenotypes*

To further analyze the possible function of TCH3 as a regulator of the PID pathway *in planta*, we obtained the mutant alleles *tch3-2* and *tch3-1* from the SALK collection with a T-DNA inserted at respectively positions -134 and -120 relative to the ATG of *TCH3*. Northern blot analysis indicated that *tch3-2* was a null allele, whereas in *tch3-1* the expression was enhanced (Figure 3A). Another SALK line with a T-DNA insertion at position -71, named *tch3-3*, was found to be a complete knock-out both on Northern and Western blots (J. Braam, pers. com.). Both *tch3-2* and *tch3-3* (J. Braam, pers. com.) alleles did not show any obvious phenotypes, suggesting that TCH3 is functionally redundant with the most related calmodulin-like proteins CaML9 and CML10 (McCormack and Braam, 2003).

In order to generate gain-of-function alleles, *TCH3* full-length cDNA was overexpressed in Arabidopsis Columbia under the strong *35S* promoter. Despite high expression levels in four independent single locus insertion lines (Figure 3B), no obvious phenotypes were observed in the *35S::TCH3* plants. Our analysis focused on auxin-related phenotypes (gravitropic growth, sensitivity to IAA and NPA and lateral root development) and we may have therefore missed phenotypes related to the touch response pathway.

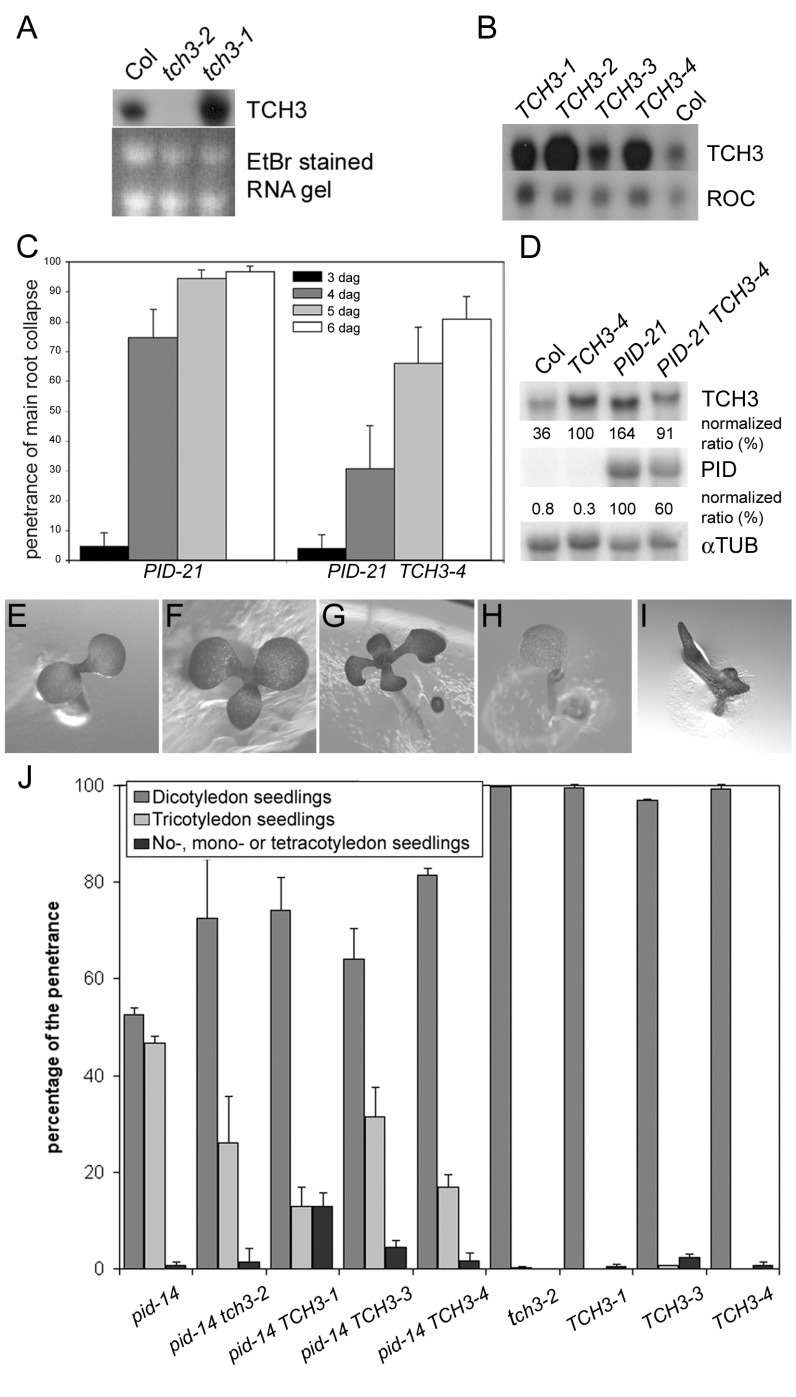

A
Col
tch3-2
tch3-1
TCH3
EtBr stained
RNA gel
B
TCH3-1
TCH3-2
TCH3-3
TCH3-4
Col
TCH3
ROC
C
penetrance of main root collapse
3 dag
4 dag
5 dag
6 dag
PID-21
PID-21 TCH3-4
D
Col
TCH3-4
PID-21
PID-21 TCH3-4
TCH3
36 100 164 91
normalized ratio (%)
PID
0.8 0.3 100 60
normalized ratio (%)
αTUB
E
F
G
H
I
J
percentage of the penetrance
Dicotyledon seedlings
Tricotyledon seedlings
No-, mono- or tetracotyledon seedlings
pid-14
pid-14 tch3-2
pid-14 TCH3-1
pid-14 TCH3-3
pid-14 TCH3-4
tch3-2
TCH3-1
TCH3-3
TCH3-4

Figure 3: TCH3 is a negative regulator of PID *in vivo*.
(A) Northern blot showing *TCH3* expression in *tch3-2* (SALK_090554) and *tch3-1* (SALK_056345), having T-DNA insertions at respectively position -140 and -120 relative to the ATG of the *TCH3* gene: *tch3-2* shows no detectable mRNA expression, whereas the expression in *tch3-1* is enhanced. An Ethidium bromide stained RNA gel is shown to compare loading.
(B) Northern blot showing the level of *TCH3* overexpression in four independent transgenic lines carrying the *35Spro:TCH3* construct. The blot was first hybridized with the *TCH3* cDNA (top), and subsequently stripped and hybridized with the *ROC* cDNA to show the loading (bottom).
(C) The percentage of the main root meristem collapse in the *35Spro:PID-21* and in *35Spro:PID-21 35Spro:TCH3-4* lines. When *TCH3* is overexpressed the root meristem collapse is significantly delayed (Student's t-test, $p < 0.05$).
(D) Northern blot analysis showing the expression level of *TCH3* (top), *PID* (middle) and *αTubulin* (bottom) in seedlings of the lines used in (C). The same blot was successively hybridized with the *PID*, *TCH3* and *αTubulin* cDNA. Intensities were quantified using ImageQuant and normalized to the corresponding *αTubulin* sample to compensate for loading differences. The sample with *TCH3* or *PID* overexpression alone was put at 100%.
(E-I) Observed seedling phenotypes, ranging from di- (E) and tri-cotyledon seedlings (F) as seen in the *pid-14* allele, to tetra- (G), mono- (H) and no-cotyledon seedlings (I) as seen in the *pid-14 tch3-2*, and *pid-14 35Spro:TCH3* lines.
(J) The percentage of the penetrance of the aberrant number of cotyledons was analyzed in seedling population of *pid-14/+*, *pid-14/+ tch3-2*, *pid-14/+ 35Spro:TCH3-1*, *pid-14/+ 35Spro:TCH3-3*, *pid-14/+ 35Spro:TCH3-4*.

TCH3 *overexpression reduces* PID *gain-of-function root meristem collapse*

The above data suggest that TCH3 provides feedback regulation on the PID kinase activity, in response to auxin or other signals that induce rapid changes in the cytosolic calcium concentration. As both loss-of-function and gain-of-function lines did not provide further information, we crossed the *TCH3* overexpression line *35Spro:TCH3-4* with the overexpression line *35Spro:PID-21*. High *PID* expression in the root causes the collapse of the main root meristem, which is triggered by the lack of an auxin maximum due to the basal-to-apical PIN polarity switch (Benjamins et al., 2001, Friml et al., 2004). This phenotype is observed in only 5 % of the seedlings at 3 days after germination (dag), but has occurred in up to 97 % of the seedlings at 6 dag (Figure 3C). Overexpression of *TCH3* significantly reduced the root meristem collapse (Figure 3C) from 75 % to 31 % at 4 dag (Student's t-test, $p < 0.05$) and from 97 % to 81 % at 6 dag (Student's t-test, $p = 0.06$). The levels of *PID* and *TCH3* expression were slightly lower in 5 days old *35Spro:PID-21 35Spro:TCH3-4* seedlings than in *35Spro:PID-21* and *35Spro:TCH3-4* seedlings (Figure 3D), but not enough to explain the difference in timing of the root meristem collapse phenotype between *35Spro:PID-21* and *35Spro:PID-21 35Spro:TCH3-4*. These observations corroborate the proposed role of TCH3 as negative regulator of PID kinase activity (above and (Benjamins et al., 2003).

pid *loss-of-function mutant is sensitized to changes in* TCH3 *expression*

Loss-of-function *pid* alleles have a characteristic defect in embryo development mostly leading to seedlings with three cotyledons. The penetrance of this phenotype varies between

10 and 50 % depending on the strength of the mutant allele (Bennett et al., 1995, Christensen et al., 2000, Benjamins et al., 2001). In the *pid-14* allele, 46 % of the homozygous seedlings have three cotyledons (Figures 3F and 3J) and less than 1 % develops a single cotyledon (Figures 3H and 3J). To investigate the influence of TCH3 on the *pid* embryo phenotype, the *tch3-2* allele and the *35Spro:TCH3-1*, *-3* and *-4* overexpression lines were crossed with *pid-14*, and progeny homozygous for the *tch3-2* loss-of-function or the *35Spro:TCH3* gain-of-function locus and segregating for the *pid-14* allele were scored for cotyledon defects. The percentages were calculated relative to the expected number of *pid-14* homozygous individuals. The *tch3-2* loss-of-function allele did not show aberrant cotyledon phenotypes and in the three *TCH3* overexpressing lines only a low percentage of monocotyledon seedlings was observed (up to 2 % for *35Spro:TCH3-3*, Figure 3J). In all the double mutant lines, the overall penetrance of aberrant cotyledon phenotypes was reduced (17 to 31 % for the double mutants versus 46 % for *pid-14*, Figure 3J), whereas a significantly higher number of seedlings showed stronger cotyledon defects, such as four cotyledons (< 1 % for *pid-14 35Spro:TCH3-4*, Figure 3G), one cotyledon (ranging from 2 % for *pid-14 tch3-2* and *pid-14 35Spro:TCH3-4*, up to 10 % for *pid-14 35Spro:TCH3-1*, Figure 3H) or even no cotyledons (3 % for *pid-14 35Spro:TCH3-1*, Figure 3I). Although there is a clear effect of both *TCH3* overexpression and loss-of-function on the severity of the *pid* loss-of-function seedling phenotypes, the data do not indicate a clear negative regulatory function for TCH3, as observed in the *in vitro* phosphorylation assays or for the PID overexpression-induced root meristem collapse phenotype. No correlation between the level of *TCH3* overexpression and the increase in number of mono-, no- and tetracotyledon seedlings is found. Possibly, during embryo development, a critical balance between the cellular PID activity and TCH3 levels is required for proper cotyledon positioning, and both *TCH3* overexpression and loss-of-function can disturb this balance, as indicated by the significant number of seedlings with defects in cotyledon positioning. The fact that the *pid* loss-of-function mutant background is sensitized to changes in *TCH3* expression, corroborates the functional relationship between PID and TCH3.

TCH3 mediates auxin-dependent sequestration of PID from the plasma membrane

The subcellular localization of TCH3 was tested by transfecting Arabidopsis protoplasts with a *35Spro:TCH3:YFP* construct. The TCH3:YFP fusion protein was found to be cytoplasmic (Figure 4A), overlapping with soluble CFP (Figures 4B and 4C). In contrast to soluble CFP (Figure 4B), however, TCH3:YFP was excluded from the nucleus (Figures 4B and 4C). This localization differed significantly from that of PID, which is membrane-associated both in protoplasts (Figure 4E), or *in planta* (Figure 6E) (Lee and Cho, 2006, Michniewicz et al., 2007).

When *35Spro:PID:CFP* and *35Spro:TCH3:YFP* were co-transfected in auxin-starved Arabidopsis protoplasts, PID:CFP and TCH3:YFP did not co-localize and remained

at their respective subcellular location, the plasma membrane and the cytoplasm (Figures 4F-H). Interestingly, when cells were cultured in normal auxin-containing medium, PID subcellular localization became cytoplasmic in presence of TCH3 (Figures 4I-K), suggesting that the auxin-dependent interaction with TCH3 sequesters PID from the plasma membrane. The fact that auxin treatment of auxin-starved protoplasts does not lead to PID sequestration when TCH3 is co-transfected (results not shown), suggests that protoplasts are desensitized to auxin, and that the sequestration observed in auxin grown protoplasts is probably the result of PID and TCH3 overexpression and constitutively elevated calcium levels.

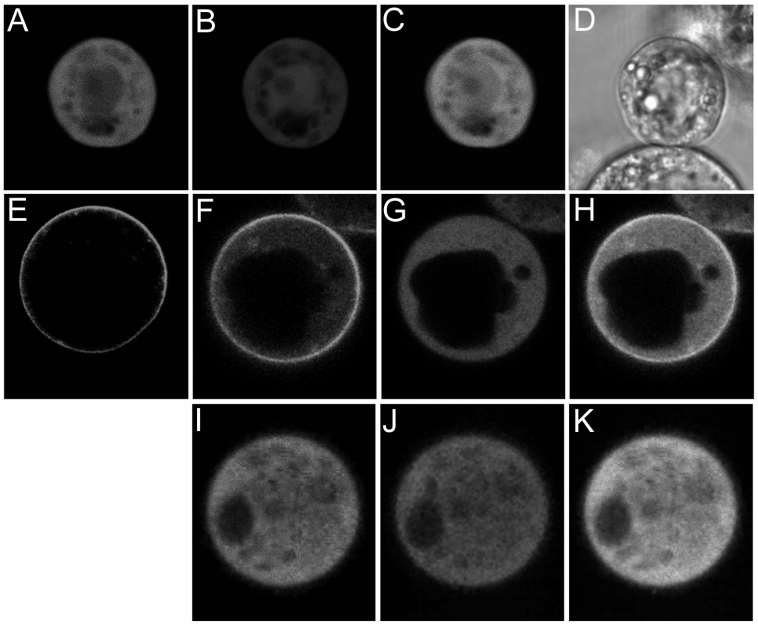
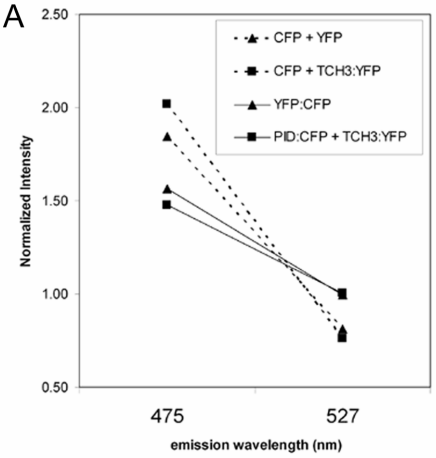


Figure 4. TCH3 and PID co-localization is auxin-dependent.
(A-D) *35Spro:TCH3:YFP* was co-transfected with *35Spro:CFP* in Arabidopsis protoplasts. Comparison of the YPF image (A) with the CFP image (B) or the merged image (C) indicates that TCH3 is cytoplasmic and excluded from the nucleus. (D) A transmitted light image of the protoplast in (A-C).
(E) Arabidopsis cell suspension protoplast transfected with *35Spro:PID:CFP* shows a plasma membrane localization.
(F-K) Auxin-starved (F-H) or auxin-cultured (I-K) Arabidopsis protoplasts co-transfected with *35pro:PID:CFP* and *35Spro:TCH3:YFP*. Shown are the CFP channel (F, I), the YFP channel (G, J) or the merged image (H, K). PID is membrane localized in auxin-starved protoplasts but co-localizes with TCH3 in the cytoplasm when cells are cultured in presence of auxin.

A



B

		Student T test p<0.05	
	Slope	475 nm	527 nm
CFP + YFP	-0.020		
CFP + TCH3:YFP	-0.024	0.394	0.515
YFP:CFP	-0.011	0.046	0.016
PID:CFP + TCH3:YFP	-0.009	0.040	0.036

Figure 5. TCH3 interacts with PID *in vivo*.
(A) Graph showing the fluorescence intensities at 475 nm (CFP emission peak) and 527 nm (YFP emission peak) during lambda scanning using an excitation wavelength of 457 nm (donor, CFP) in Arabidopsis protoplasts expressing a translational fusion between YFP and CFP (triangle, plain line, positive control), or co-expressing PID:CFP and TCH3:YFP (square, plain line), CFP and TCH3:YFP (square, dotted line, negative control) or CFP and YFP (triangle, dotted line, negative control). The observed quenched intensities at the CFP emission peak and enhanced intensities at the YFP emission peak of the PID:CFP-TCH3:YFP sample are indicative for FRET, and corroborate the *in vivo* interaction between TCH3 and PID.
(B) Table indicating the slope of the curves shown in (A) and the *P*-values of Student's t-tests, in which the 475 nm (CFP) and the 527 nm (YFP) emission intensities of CFP and TCH3:YFP, and YFP:CFP were compared with those of YFP and CFP expressing protoplasts; and of PID:CFP and TCH3:YFP compared with those of TCH3:YFP and 35Spro:CFP.

To confirm the *in vivo* interaction between the two proteins, we checked for the presence of Förster (Fluorescence) Resonance Energy Transfer (FRET) between the CFP and YFP moieties of the co-expressed fusion proteins using confocal lambda scanning (Siegel et al., 2000). No bleed-through occurred in protoplasts co-expressing with CFP and YFP, meaning that YFP was not excited by CFP excitation wavelength (457 nm) and vice versa (data not shown). However, excitation with 457 nm leads to a significant CFP-derived signal at the YFP emission wavelength (527 nm). FRET in the test sample is therefore signified by a quenched signal at the CFP emission wavelength (475 nm) and higher signal at the YFP emission wavelength (527 nm), as compared to control transfections with non-interacting versions of CFP and YFP (*35Spro:CFP* co-transfected either with *35Spro:TCH3:YFP* or with *35Spro:YFP*). Indeed, a significant FRET signal could be detected in protoplast that co-expressed TCH3:YFP and PID:CFP. The lambda scanning profile matched that of protoplasts expressing the YFP:CFP fusion protein for which FRET is expected (Figures 5A and 5B). These data corroborate our earlier hypothesis that TCH3 sequesters PID from the plasma membrane to the cytoplasm by interaction with the protein kinase.

Auxin-induced calcium-dependent sequestration of PID in root epidermal cells

Previous studies (Sistrunk et al., 1994, Antosiewicz et al., 1995, Benjamins et al., 2001) already indicated that expression patterns of *PID* and *TCH3* overlap to allow a functional *in vivo* interaction between the two proteins. As shown by a *TCH3pro:TCH3:GUS* translation fusion, *TCH3* is expressed in epidermis cells of the elongation zone of the root tip (Figure 6A), in the vasculature of the root at the root-hypocotyl junction (Figure 6B), in the vasculature and in the stomata of leaves and cotyledons (Figure 6C), and at the shoot apical meristem (Figure 6C). As the expression of *TCH3* is auxin responsive, it preferentially accumulates in cells that are part of auxin response maxima, e.g., in the shoot apical meristem and root columella, in vascular tissues in roots, leaves and sepals and in the anthers and stigmas of flowers (Sistrunk et al., 1994, Antosiewicz et al., 1995). Upon IAA treatment, *TCH3* expression is strongly induced in the root, where it is extended to the vasculature and the epidermis of the complete root (Figure 6D). *PID* is also auxin responsive and is co-expressed with *TCH3* in the epidermis cells in the elongation zone of the root tip, in the shoot apical meristem and in flowers (Benjamins et al., 2001), suggesting a functional interaction between the two proteins in these tissues.

To investigate the biological relevance of the auxin-dependent, TCH3-mediated sequestration of PID observed in protoplasts, we used the *PIDpro:PID:VENUS* line (Michniewicz et al., 2007) to study the dynamics of the subcellular localization of PID in wild type Arabidopsis and *35Spro:TCH3* overexpression epidermis root cells. In both backgrounds, PID localized at the membrane (Figures 6E and 6M) (Lee and Cho, 2006, Michniewicz et al., 2007), suggesting that overexpression of *TCH3* alone is not sufficient to trigger the change in PID subcellular localization *in planta*. Upon auxin treatment, however, PID was rapidly released in the cytoplasm within 5 minutes of treatment (Figure 6F), and plasma membrane localization was restored 10 minutes after auxin addition (Figures 6G-J). Pre-treatment of seedlings with tetracain (Tc), a calmodulin inhibitor, or lanthanum (La), a calcium channel blocker, did not influence the PID localization by itself (Figures 6K and 6S), but did inhibit IAA-induced dissociation of PID from the plasma membrane (Figures 6L and 6T). PID localization was not influenced by TCH3 overexpression. These data suggest that this dissociation is dependent on an increase in the cytoplasmic calcium concentration involving plasma membrane calcium channels, and that this calcium signal is translated by one or more CaMs. In view of our results in protoplasts, it is likely that the CaM-like protein TCH3 is involved in this process.

Together the results described here suggest that TCH3 acts as a calcium receptor in the PID signaling pathway that translates rapid peaks in cytosolic calcium into subtle changes in PIN polarity, by influencing the activity and by sequestering the kinase from the plasma membrane to the cytoplasm.

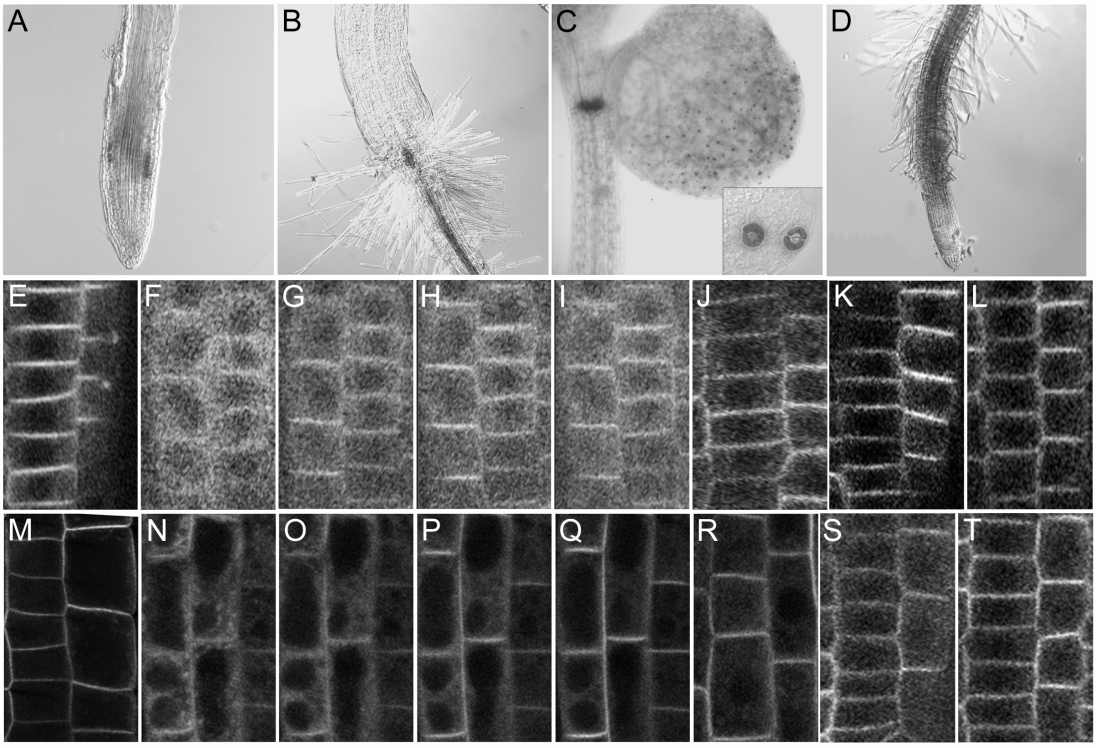


Figure 6. TCH3 and auxin cause PID to dissociate from the plasma membrane.
(A-D) Histochemical staining of *TCH3pro:TCH3:GUS* seedlings (Sistrunk et al., 1994) showing that *TCH3* is expressed in epidermis cells of the elongation zone of the root tip (A), in vascular tissues at the root-hypocotyl junction (B), in the shoot apical meristem and in vascular tissues and stomata (inset) of the cotyledon (C). *TCH3* expression in roots is enhanced when grown on 0.1μM IAA (D).
(E) PID is membrane localized in *PIDpro:PID:VENUS* epidermal cells of seedling root tips.
(F-J) PID transiently dissociates from the plasma membrane 5 min after IAA treatment (F), but rapidly returns to the plasma membrane (10 min (G), 20min (H), 30 min (I) and 1 h (J) treatment).
(K-L, S-T) Pre-treatment with tetracain (30 min incubation, K-L), a CaM inhibitor, or Lanthanum (30 min incubation, S-T), a calcium channel inhibitor, does not influence PID localization (K, S) but blocks the auxin-induced dissociation of PID from the plasma membrane (5 min treatment with IAA and inhibitors, L, T).
(M-R) PID shows normal plasma membrane localization (M) and IAA-induced transient dissociation from the plasma membrane (5min (N), 10min (O), 20 min (P), 30 min (Q), 1h (R)) in seedling root tips of the *PIDpro:PID:YFP 35Spro:TCH3-2* line.

Discussion

Calcium is a common second messenger in signaling pathways, and has been found as one of the early signals in auxin responses. Experiments on plant cells showed that the cytosolic calcium concentration is increased within few minutes after auxin application (Felle, 1988,

Gehring et al., 1990a, Shishova and Lindberg, 2004). Furthermore polar auxin transport (PAT) is suppressed by application of the calcium chelator EDTA, and restored after application of a calcium solution (Dela Fuente and Leopold, 1973) indicating that calcium is also an important second messenger in the regulation of auxin transport.

PIN proteins are components of the cellular auxin efflux machinery. Their subcellular localization determines the direction of the auxin transport (Wisniewska et al., 2006, Petrášek et al., 2006). The protein serine/threonine kinase PINOID regulates PAT by establishing the proper apico-basal polarity of the PIN auxin efflux carriers (Friml et al., 2004). The finding that two calcium binding proteins PBP1 and TCH3 interact with PID to regulate its kinase activity *in vitro*, provided a first molecular link between calcium and the regulation of PAT (Benjamins et al., 2003). Here we investigated the *in vivo* role of TCH3 in the PID signaling pathway. First, we identified that TCH3 binds the catalytic domain of the PID kinase, and used *in vitro* kinase assays and genetic analysis to confirm the previous observations that TCH3 is a regulator of PID kinase activity (Benjamins et al., 2003). Next, we showed the co-localization and the interaction between TCH3 and PID in Arabidopsis protoplasts. Finally, we could demonstrate that TCH3 is involved in PID subcellular localization dynamics, clarifying the molecular link between calcium signaling and auxin transport.

TOUCHing PID: a regulatory loop that translates cellular calcium levels to PIN polarity

Previously, we used *in vitro* pull down assays to show that TCH3 interacts with PID in a calcium-dependent manner (Benjamins et al., 2003). Here, a similar assay was used in combination with PID deletion constructs to show that TCH3 interacts with the PID catalytic domain. Moreover, co-expression of TCH3 and PID in Arabidopsis protoplasts and subsequent FRET measurements demonstrated the *in vivo* interaction between the two proteins, and showed that TCH3 sequesters the normally plasma membrane-associated PID kinase to the cytoplasm. This suggests that interaction with TCH3 with the catalytic domain of PID provokes the release of the kinase from the plasma membrane. The cytoplasmic PID sequestration is auxin-dependent, as auxin-starved protoplasts do not show internalization of PID. Most likely, auxin treatment of protoplasts results in elevated levels of cytosolic calcium, which in turn enhances the affinity of the TCH3 CaM-like protein for PID.

Recent data by Zegzouti and co-workers indicated that PID binds to phosphorylated inositides and phosphatidic acid, and that the amino acid insertion in the PID catalytic domain (insertion domain) is the key determinant in membrane association of the kinase (Zegzouti et al., 2006). We therefore hypothesize that PID co-localizes at the plasma membrane with its phosphorylation targets, the PIN auxin efflux carriers (Michniewicz et al., 2007), through direct binding of membrane components to the insertion domain. An increase in cytosolic calcium, e.g. induced by auxin, facilitates

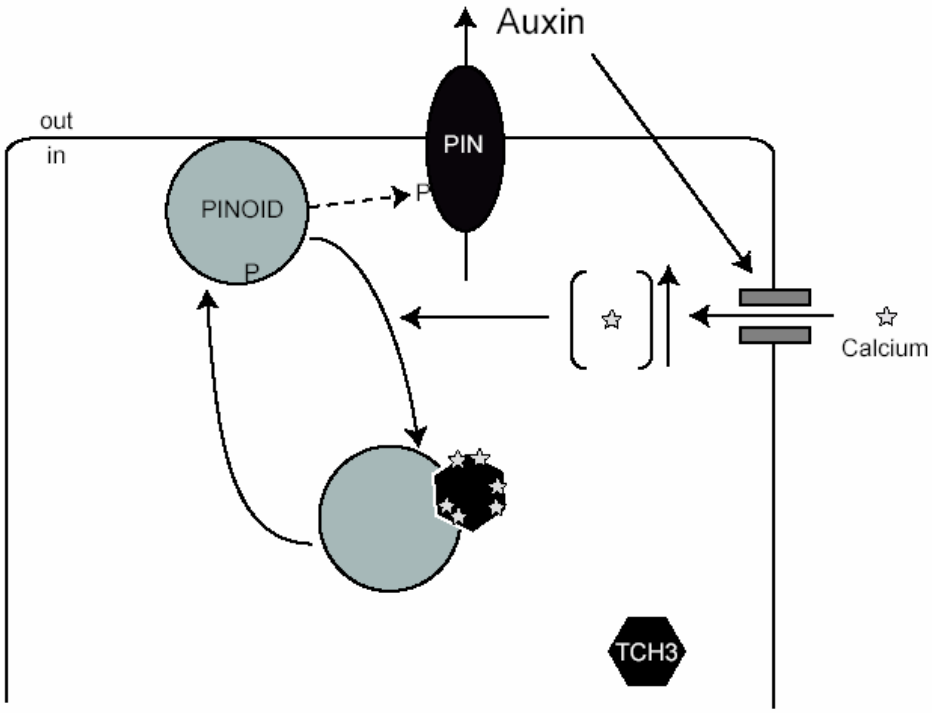


Figure 7. PID activity and subcellular localization is mediated by calcium and the calcium-binding proteins TCH3.
PID is a plasma membrane-associated protein kinase in proximity of its phospho-targets, the PIN auxin efflux carriers. Low calcium levels stabilize membrane association PID activity. Increases in calcium concentrations, via calcium channels in the plasma membrane, for example in response to elevated auxin levels, stimulate the interaction with the calmodulin-like TCH3, and this inhibits PID activity and triggers the dissociation of PID from the plasma membrane. P: phosphate group from a phosphorylation event, stripped line: phosphorylation reaction, plain line: signaling events, stars: calcium.

binding of TCH3 to the catalytic domain of PID, thereby preventing the kinase-lipid interaction and resulting in sequestration of the kinase away from its phospho-targets to the cytoplasm (Figure 7). Based on this model, it would be interesting to test whether TCH3 and phosphoinositides are competing for the interaction with the PID catalytic domain.

PKC, one of the animal orthologs of the plant specific AGCVIII kinases to which PID belongs (Galván-Ampudia and Offringa, 2007) directly binds calcium through a C2 domain. Calcium binding to this domain promotes a change in PKC subcellular localization from the cytosol to the plasma membrane and enhances the affinity of the C2 domain for phosphorylated inositides (Corbálan-Garcia et al., 2007). This plasma membrane translocation activates the PKC kinase. PID is also thought to be active at the plasma membrane. However in this case the (auxin-induced) increase in cytosolic calcium levels

results in the opposite effect and removes the kinase from the plasma membrane. PID does not have the typical calcium binding domains, and instead the kinase has evolved to interact in a calcium-dependent manner with calcium receptors, such as TCH3. Changes in subcellular localization are commonly used cellular mechanism to regulate protein activity by sequestering proteins away from their targets. To our knowledge, the calcium- and CaM-dependent release of the PID kinase is a new form of regulating the activity of a kinase that steers the polar subcellular targeting of transporter proteins.

TCH3: part of feedback loop of auxin on the direction of its own transport?

The proposed model in Figure 7 implies that a calcium release negatively and transiently regulates PID activity through its TCH3-induced dissociation from the plasma membrane, away from its phospho-targets, the PIN proteins. This TCH3-dependent inactivation of PID may be part of a regulatory loop that allows fast and possibly subtle alterations in PIN polarity in response to signals that lead to rapid changes in cytosolic calcium levels, such as auxin (Felle, 1988, Gehring et al., 1990a, Shishova and Lindberg, 2004), unidirectional blue light or gravity (Lee and Evans, 1985, Gehring et al., 1990b, Baum et al., 1999, Harada et al., 2003). Auxin is known to regulate its own transport, firstly by inhibiting PIN endocytosis (Paciorek et al., 2005), and secondly by regulating the subcellular PIN localization in Arabidopsis roots (Sauer et al., 2006), probably in order to canalize and increase the auxin flow in response to increased cellular auxin concentrations. Sauer and co-workers concluded that PID is not required for auxin-dependent PIN lateralization in root cells, because they still observed PIN lateralization in auxin-treated *35Spro:PID* seedlings (Sauer et al., 2006).

Auxin-induced PIN lateralization involves TIR1-dependent induction of auxin responsive gene expression, and does not occur as rapid as the auxin-induced dissociation of PID from the membrane that we report here. Our results suggest that elevated cellular auxin levels may transiently alter PID kinase activity by subcellular localization changes and inhibition of its kinase activity via TCH3 interaction. This may set the stage for the auxin-dependent PIN lateralization, or may only lead to a subtle modulation of PIN polar targeting. The fact that none of *TCH3* loss- and gain-of-function mutants display obvious phenotypes, and that we have not been able to detect changes in PIN polar targeting in roots of *35Spro:TCH3* and *tch3* mutant lines (M. Sauer, unpublished results) nor in *pid* knock-out roots (Friml et al., 2004), may be explained by calcium dependency of the PID-TCH3 interaction (*35Spro:TCH3*) and by functional redundancy with other CaMs (*tch3*) or with the PID-related kinases (*pid*).

Material and methods

Molecular cloning and constructs

Molecular cloning was performed following standard procedures (Sambrook et al., 1989). Bacteria were grown on LC medium containing 100 µg/ml carbenicillin (Cb, all high copy plasmids), 50 µg/ml kanamycin (Km, pGreen) or 250 µg/ml spectinomycin (Spc, pART27) for *E. coli* strains DH5α or Rosetta (Novagen) or 20 µg/ml rifampicin (Rif) and 50 µg/ml Km, or 250 µg/ml Spc for Agrobacterium strain LBA1115. The constructs pSDM6008 (pET16H:TCH3), pSDM6004 (pGEX:PID) and pSDM6005 (pBluescript SK-PID) were described previously (Benjamins et al., 2003). Primers used in this study are listed in Table 1. To obtain a plasmid encoding the GST tagged first 100 amino acids of PID, the *Sal*I-*Sac*I (blunted) fragment from pSDM6005 was cloned into the *Xho*I and *Hin*dIII (blunted) sites of pGEX-KG (Guan and Dixon, 1991). Fragments encoding the PID catalytic domain (aa 75-398) and the C-terminal part of PID (aa 339-438) were obtained by PCR amplification using the primer pairs PID PK CaD F - PID PK CaD R and PID PK CT F - PID PK CT R, respectively and cloned into pGEX-KG using *Xho*I-*Hin*dIII (blunted) and *Eco*RI-*Hin*dIII (blunted), respectively. To overexpress *TCH3* in *Arabidopsis thaliana*, its complete coding region was cloned from pSDM6008 as a *Bam*HI fragment into pART7 and the expression cassette was inserted as a *Not*I fragment into the pART27 binary vector. To construct *35Spro:TCH3:YFP*, *35Spro:PID:YFP* and *35Spro:PID:CFP,* the coding regions were amplified by PCR from pSDM6008 and pSDM6004 with respectively primers TCH3 attB F1 and TCH3 attB R1, and PID attB F1 and PID attB R1 and the resulting PCR fragments were recombined into pDONOR207 (BP reaction) and subsequently into pART7-derived destination vectors (LR reaction), containing either the *CFP* (PID) or the *YFP* (TCH3 and PID) coding region in frame with the Gateway cassette (Invitrogen). The *35Spro:PID:YFP* expression cassette was inserted as a *Not*I fragment into the pGreenII0179 binary vector.

In vitro *pull-down*

E. coli strain Rosetta (Novagen) was transformed with pSDM6008, pSDM6004, pGEX-PIDaa2-103, pGEX-PIDaa75-398 and pGEX-PIDaa339-438. Single colonies were picked and grown overnight (o/n) at 37^{o}C in 5 ml liquid LC medium containing Cb, 15 µg/ml Km and 34 µg/ml Chloramphenicol (Cam). The o/n culture was diluted 1/20 in 100 ml of fresh LC medium containing Cb and Cam and grown at 37^{o}C until an OD_{600} of 0.8. The cultures were induced with 1 mM IPTG for 4 h and bacteria were harvested by centrifugation and frozen. For GST-tagged PID, frozen bacterial pellets were resuspended in 5 ml Extraction Buffer (EB: 20 mM Tris pH 7.5, 500 mM NaCl, 5 mM EDTA, 1 mM EGTA, 1 mM DTT, 0.2 % Triton X-100, 0.05 % Tween-20) supplemented with 0.1 mM Phenylmethanesulfonylfluoride (PMSF), 0.5 µg/ml Leupeptin and 5 µg/ml Trypsin Inhibitor and incubated on ice for 5 min. After sonication for 2 min, the mixtures were

centrifuged at 10000 g for 15 min at 4°C. Supernatants were added to 500 µl of pre-equilibrated 50 % Glutathione sepharose 4B beads (Amersham-Pharmacia) and incubated for 1 h at 4°C. Beads were washed once with 10 ml EB, and twice with 10 ml Washing Buffer 1 (10 mM Tris pH 7.5, 150 mM NaCl, 5 mM EDTA, 1 mM EGTA, 1 mM DTT). Proteins were eluted by incubating beads at room temperature with 2 ml Elution Buffer 1 (50 mM Tris pH 8.0, 10 mM reduced glutathione). Eluates were passed through MicroSpin chromatography columns (BioRad) and concentrated using Vivaspin 6 device 10000 MWCO (Sartorius). For His-tagged TCH3, bacteria pellets were resuspended in Binding Buffer (BB: 20 mM Tris pH 7.5, 500 mM NaCl, 5 mM $MgCl_2$, 2 mM $CaCl_2$, 1 mM DTT, 0.2 % Triton X-100, 0.05 % Tween-20) supplemented with 0.1 mM PMSF, 0.5 µg/ml Leupeptin and 5 µg/ml Trypsin Inhibitor, incubated for 5 min on ice prior to lysis of cells by 2 min sonication. For *in vitro* pull down assays, 2 µg of purified GST-tagged protein was immobilized on Glutathione High Capacity Coated Plates (Sigma). After three washes with BB, 200 µl of total protein extract containing His-tagged TCH3 was added to each well and incubated for 1 h at 4°C, washed once with BB and twice with Washing Buffer 2 (10 mM Tris pH 7.5, 150 mM NaCl, 5 mM $MgCl_2$, 2 mM $CaCl_2$, 1 mM DTT). Protein complexes were eluted with 25 µl of 2x Laemmli sample buffer and boiled. Eluate samples were analyzed by SDS-PAGE (12 % gel). Proteins were blotted on a PDVF membrane (Millipore, USA) and detected using penta-his antibodies (Qiagen) according to the manufacturer's instructions.

Table 1. Primer list

PID PK CaD F	5'TTC-*Xho*I-TTTCGCCTCAT3'
PID PK CaD R	5'GCGCTCAGTTTAGACCTTTGA3'
PID PK CT F	5'TAATGACG-*Eco*RI-TCCGTAACAT3'
PID PK CT R	5'AAGCTCGTTCAAAAGTAATCGAAC3'
TCH3 attB F1	5'GGGGACAAGTTTGTACAAAAAAGCAGGCTTAATGGCGGATAAGCTCACT3'
TCH3 attB R1	5'GGGGACCACTTTGTACAAGAAAGCTGGGTAAGATAACAGCGCTTCGAACA3'
PID attB F1	5'GGGGACAAGTTTGTACAAAAAAGCAGGCTTCAGCATGTTACGAGAATCAGACGGT3'
PID attB R1	5'GGGGACCACTTTGTACAAGAAAGCTGGGTCAAAGTAATCGAACGCCGCTGG3'
PID exon1 F1	5'TCTCTTCCGCCAGGTAAAAA3'
PID exon2 R1	5'CGCAAGACTCGTTGGAAAAG3'
TCH3pr F1	5'AAATGTCCACTCACCCATCC3'
TCH3pr R1	5'GGGAATTCTGAAGATCAGCTTTTGTCG3'
LBaI	5'TGGTTCACGTAGTGGGCCATCG3'
AtROC5 F	5'CGGGAAGGATCGTGATGGA3'
AtROC5 R	5'CCAACCTTCTCGATGGCCT3'
αTUB F	5'CGGAATTCATGAGAGAGATCCTTCATATC3'
αTUB R	5'CCCTCGAGTTAAGTCTCGTACTCCTCTTC3'

The attB recombination sites are underlined.

Phosphorylation assays

His-tagged proteins were purified by immobilized-metal affinity chromatography. Bacterial pellets were resuspended in 2 ml of Lysis Buffer (LB: 25 mM Tris pH 8.0, 500 mM NaCl, 20 mM imidazole, 0.05 % Tween-20, 10 % glycerol) and incubated 5 min on ice. After sonication for 2 min, 100 µl of 20 % Triton X-100 was added and the mixture was incubated 5 min on ice, followed by centrifugation at 10000 g for 15 min at 4°C. The soluble fraction was added with 400 µl of pre-equilibrated 50 % NTA-agarose matrix (Qiagen) and mixed gently for 1.5 h at 4°C. Beads were washed three times with 2 ml of LB, 2 ml of Washing Buffer 3 (25 mM Tris pH 7.5, 500 mM NaCl, 40 mM imidazole, 0.01 % Tween-20, 10 % glycerol), and 2 ml of Wash Buffer 4 (25 mM Tris pH 7.0, 500 mM NaCl, 80 mM imidazole and 10 % glycerol). Elution was performed by incubating the beads on 600 µl Elution Buffer 2 (25 mM Tris pH 7.0, 300 mM NaCl, 300 mM imidazole, 10 % glycerol) for 30 min at 4°C. Samples were analyzed by SDS-PAGE and quantified.

The Pepchip Kinase Slide A (Pepscan) was used for *in vitro* phosphorylation assays for PID in the presence of TCH3. Thirty ng of His:PID, His:TCH3 and His:PBP1 (Chapter 3, this thesis) were mixed with Kinase Mastermix (50 mM HEPES pH 7.4, 20 mM $MgCl_2$, 20 % v/v glycerol, 0.01 mg/ml BSA, 0.01 % v/v Brij-35, 2 mM $CaCl_2$), 10 µM ATP and 300 µCi/ml γ-^{33}P-ATP (specific activity ~ 3000 Ci/mmol, Amersham). Fifty µl of the reaction mix was incubated with the Pepchip Kinase Slide A for 4 h at 30°C in a humid chamber. Slides were washed twice with 2 M NaCl, twice with water and dried for 30 min. Slides were exposed to X-ray film FUJI Super RX for 12 and 24 h.

Arabidopsis lines, plant growth, transformation and protoplast transfections

The *35Spro:PID-21*, *TCH3pro:TCH3:GUS* and *PIDpro:PID:VENUS* lines were described previously (Sistrunk et al., 1994, Benjamins et al., 2001, Michniewicz et al., 2007). Loss-of-function alleles *pid-14* (SALK_049736), *tch3-1* (SALK_056345) and *tch3-2* (SALK_090554) were obtained from NASC (Alonso et al., 2003).

Arabidopsis seeds were surfaced-sterilized by incubation for 15 min in 50 % commercial bleach solution and rinsed four times with sterile water. Seeds were vernalized for 2 to 4 days and germinated at 21°C, 16 h photoperiod and 3000 lux on solid MA medium (Masson and Paszkowski, 1992) supplemented with antibiotics when required. Two- to three-week old plants were transferred to soil and grown in growth room at 21°C, 16 h photoperiod, 70 % relative humidity and 10000 lux.

To screen for the presence of the different T-DNA insertions, the T-DNA-specific LBaI primer was combined in a PCR reaction with the gene-specific PCR primers PID exon1 F1 or PID exon2 R1 for *pid-14* and TCH3pr F1 or TCH3pr R1 for *tch3-1* and *tch3-2*. Sequencing of the junction fragment and Northern blot analysis were used to confirm the insertion position and full knock-out of the loss-of-function alleles.

Arabidopsis thaliana ecotype Columbia wild type (for *35Spro:TCH3*) or the *35Spro:TCH3-2* line (for *35Spro:PID:YFP*) were transformed by a floral dip method as described (Clough and Bent, 1998) using Agrobacterium LBA1115 strain. The T1 transformants were selected on medium supplemented with 50 µg/ml Km for *35Spro:TCH3* or 20 µg/ml hygromycin (Hm) for *35Spro:PID* and with 100 µg/ml timentin to inhibit the Agrobacterium growth. For further analysis, single locus insertion lines were selected by germination on 25 µg/ml Km or 10 µg/ml Hm.

Protoplasts were obtained from *Arabidopsis thaliana* Columbia cell suspension cultures that were propagated as described (Schirawski et al., 2000). Protoplast isolation and PEG-mediated transfections with 10 µg plasmid DNA were performed as initially indicated (Axelos et al., 1992) and adapted by Schirawski and coworkers (Schirawski et al., 2000). To obtain auxin-starved protoplasts, auxin (NAA) was removed from the media during protoplast isolation. Following transfection, the protoplasts were incubated for at least 16 h prior to observation.

Histochemical staining and microscopy

For the Histochemical detection of *GUS* expression, seedlings were fixed in 90 % acetone for 1 h at -20°C, subsequently washed three times in 10 mM EDTA, 100 mM sodium phosphate (pH 7.0), 2 mM $K_3Fe(CN)_6$ and stained for 2 h in 10 mM EDTA, 100 mM sodium phosphate (pH 7.0), 1 mM $K_3Fe(CN)_6$, 1 mM $K_4Fe(CN)_6$ containing 1 mg/ml 5-bromo-4-chloro-3-indolyl-β-D-glucuronic acid, cyclohexylammonium salt (Duchefa). Seedlings were post-fixed in ethanol-acetate (3:1), cleared in 70 % ethanol and stored in 100 mM sodium phosphate (pH 7.0). *GUS* expression patterns in cleared Arabidopsis seedlings were analyzed using a Zeiss Axioplan II microscope with DIC optics. Images were recorded by a ZEISS camera. Arabidopsis lines expressing YFP-fusion proteins were analyzed with a ZEISS Axioplan microscope equipped with a confocal laser scanning unit (MRC1024ES, BioRad, Hercules, CA), using a 40x oil objective. The YFP fluorescence was monitored with a 522-532 nm band pass emission filter (488 nm excitation). All images were recorded using a 3CCD Sony DKC5000 digital camera. For the protoplast experiments, a Leica DM IRBE confocal laser scanning microscope was used with a 63x water objective, digital zoom and 51 % laser intensity. The fluorescence was visualized with an Argon laser for excitation at 514 nm (YFP) and 457 nm (CFP), with 522-532 nm (for the YFP) and 471-481 nm (for the CFP) emission filters. A transmitted light picture was taken for a reference. The images were processed by ImageJ (http://rsb.info.nih.gov/ij/) and assembled in Adobe Photoshop 7.0.

Förster (Fluorescence) Resonance Energy Transfer (FRET)

Protoplasts were prepared and their fluorescence monitored using a Leica confocal microscope as described above. Lambda scanning was done by excitation at 457 nm (donor,

CFP) and by measuring emission at 5 nm intervals from 460 to 585 nm using a RSP465 filter. Of every interval an image was obtained and the intensity of three fixed areas (regions of interest, ROIs) was quantified using the Leica confocal laser scanning software. The intensity of these three ROIs was averaged and normalized. Per sample lambda scanning was performed on three protoplasts and the obtained normalised intensity of all three protoplasts was averaged and used to calculate the standard deviation. The Student's t-test was used to test for significant differences in wavelength specific intensities between the test sample and the negative control. Significantly quenched donor emission wavelength intensity, combined with significantly increased acceptor emission wavelength intensity was considered indicative for protein-protein interaction-dependent FRET. Similar results were obtained for three independent transfections.

RNA extraction and Northern Blots

Total RNA was purified using the RNeasy Plant Mini kit (Qiagen). Subsequent RNA blot analysis was performed as described (Memelink et al., 1994) using 10 µg of total RNA per sample. The following modifications were made: pre-hybridizations and hybridizations were conducted at 65^{o}C using 10 % Dextran sulfate, 1 % SDS, 1 M NaCl, 50 µg/ml of single strand Herring sperm DNA as hybridization mix. The hybridized blots were washed for 20 min at 65^{o}C in 2x SSPE 0.5 % SDS, and for 20 min at 42^{o}C in respectively 0.2x SSPE 0.5 % SDS, 0.1x SSPE 0.5 % SDS and 0.1x SSPE. Blots were exposed to X-ray film FUJI Super RX. The probe for *TCH3* was isolated from pSDM6008 as a *Bam*HI fragment. The probes for *AtROC5*, for *αTubulin* and *PID* were PCR amplified from Col genomic DNA and column purified (Qiagen). Probes were radioactively labeled using a Prime-a-gene kit (Promega).

Biological assays

For the root collapse assay, about 200 seedlings per line were grown in triplicate on vertical plates on MA medium, while the development of the seedling root was monitored and scored each day during 8 days for the collapse of the primary root meristem. For the phenotypic analysis of *pid-14/+ 35Spro:TCH3-1, pid-14/+ 35Spro:TCH3-3*, *pid-14/+ 35Spro:TCH3-4* and *pid-14/+ tch3-2* lines, about 300 seeds were plated in triplicate on MA medium and germinated for one week. The number of dicotyledon seedlings and of seedlings with specific cotyledon defects was counted and the penetrance of the specific phenotypes was calculated based on a 1:3 segregation ratio for *pid/pid* seedlings. For GUS analysis, seeds of *TCH3pro:TCH3:GUS* were grown for 4 days on MA medium, supplemented with 5 µM IAA when indicated. For the subcellular localization of PID in Arabidopsis roots, vertically grown 3 day-old *PIDpro:PID:VENUS* seedlings were treated with 5 µM IAA (in MA medium) with 30 min pre-treatment with a calmodulin inhibitor (0.5 mM Tetracain, Sigma) or calcium channel blocker (1.25 mM Lanthanum, Sigma)

when indicated. Analysis of the subcellular localization was done using the BioRad confocal microscope as described above.

Accession Numbers

The *Arabidopsis* Genome Initiative locus identifiers for the genes mentioned in this chapter are as follows: *PBP1* (At5g54490), *PID* (At2g34650), *TCH3* (At2g41100), *ROC* (At4g38740), *αTubulin* (At5g44340).

Acknowledgments

The authors would like to thank M. Heisler and J. Braam for kindly providing us with the *PIDpro:PID:VENUS* line and the *TCH3pro:TCH3:GUS* line, respectively, J. Braam for sharing her unpublished data on the *tch3-3* allele, Michael Sauer for PIN localization on *TCH3* gain- and loss-of-function mutants, Arnoud van Marion for technical assistance, and Gerda Lamers and Ward de Winter for their help with the microscopy and the tissue culture, respectively. This work was funded through grants from the Research Council for Earth and Life Sciences (C.G-A.: ALW 813.06.004) with financial aid from the Dutch Organization of Scientific Research (NWO).

References

Alonso,J.M., Stepanova,A.N., Leisse,T.J., Kim,C.J., Chen,H., Shinn,P., Stevenson,D.K., Zimmerman,J., Barajas,P., Cheuk,R., Gadrinab,C., Heller,C., Jeske,A., Koesema,E., Meyers,C.C., Parker,H., Prednis,L., Ansari,Y., Choy,N., Deen,H., Geralt,M., Hazari,N., Hom,E., Karnes,M., Mulholland,C., Ndubaku,R., Schmidt,I., Guzman,P., Aguilar-Henonin,L., Schmid,M., Weigel,D., Carter,D.E., Marchand,T., Risseeuw,E., Brogden,D., Zeko,A., Crosby,W.L., Berry,C.C., and Ecker,J.R. (2003). Genome-Wide Insertional Mutagenesis of Arabidopsis thaliana. Science **301**:653-657.

Antosiewicz,D.M., Polisensky,D.H., and Braam,J. (1995). Cellular localization of the Ca2+ binding TCH3 protein of Arabidopsis. Plant J. **8**:623-636.

Axelos,M., Curie,C., Mazzolini,L., Bardet,C., and Lescure,B. (1992). A Protocol for Transient Gene-Expression in Arabidopsis-Thaliana Protoplasts Isolated from Cell-Suspension Cultures. Plant Physiology and Biochemistry **30**:123-128.

Baum,G., Long,J.C., Jenkins,G.I., and Trewavas,A.J. (1999). Stimulation of the blue light phototropic receptor NPH1 causes a transient increase in cytosolic Ca2+. PNAS **96**:13554-13559.

Benjamins,R., Ampudia,C.S., Hooykaas,P.J., and Offringa,R. (2003). PINOID-mediated signaling involves calcium-binding proteins. Plant Physiol **132**:1623-1630.

Benjamins,R., Quint,A., Weijers,D., Hooykaas,P., and Offringa,R. (2001). The PINOID protein kinase regulates organ development in Arabidopsis by enhancing polar auxin transport. Development **128**:4057-4067.

Bennett,S.R.M., Alvarez,J., Bossinger,G., and Smyth,D.R. (1995). Morphogenesis in Pinoid Mutants of Arabidopsis-Thaliana. Plant Journal **8**:505-520.

Bouché,N., Yellin,A., Snedden,W.A., and Fromm,H. (2005). PLANT-SPECIFIC CALMODULIN-BINDING PROTEINS. Annual Review of Plant Biology **56**:435-466.

Braam,J. and Davis,R.W. (1990). Rain-, wind-, and touch-induced expression of calmodulin and calmodulin-related genes in Arabidopsis. Cell **60**:357-364.

Cheng,S.H., Willmann,M.R., Chen,H.C., and Sheen,J. (2002). Calcium signaling through protein kinases. The Arabidopsis calcium-dependent protein kinase gene family. Plant Physiol **129**:469-485.

Christensen,S.K., Dagenais,N., Chory,J., and Weigel,D. (2000). Regulation of auxin response by the protein kinase PINOID. Cell **100**:469-478.

Clough,S.J. and Bent,A.F. (1998). Floral dip: a simplified method for Agrobacterium-mediated transformation of Arabidopsis thaliana. The Plant Journal **16**:735-743.

Corbálan-Garcia,S., Guerrero-Valero,M., Marin-Vicente,C., and Gomez-Fernández,J.C. (2007). The C2 domains of classical/conventional PKCs are specific PtdIns(4,5)P(2)-sensing domains. Biochem.Soc.Trans. **35**:1046-1048.

Darwin,C. (1880). *The Power of Movement in Plants*. London: John Murray.

Dela Fuente,R.K. and Leopold,A.C. (1973). A Role for Calcium in Auxin Transport. Plant Physiol **51**:845-847.

Esmon,C.A., Tinsley,A.G., Ljung,K., Sandberg,G., Hearne,L.B., and Liscum,E. (2006). A gradient of auxin and auxin-dependent transcription precedes tropic growth responses. PNAS **103**:236-241.

Felle,H. (1988). Auxin causes oscillations of cytosolic free calcium and pH in Zea mays coleoptiles. Planta **V174**:495-499.

Friml,J., Yang,X., Michniewicz,M., Weijers,D., Quint,A., Tietz,O., Benjamins,R., Ouwerkerk,P.B.F., Ljung,K., Sandberg,G., Hooykaas,P.J.J., Palme,K., and Offringa,R. (2004). A PINOID-dependent binary switch in apical-basal PIN polar targeting directs auxin efflux. Science **306**:862-865.

Friml,J., Vieten,A., Sauer,M., Weijers,D., Schwarz,H., Hamann,T., Offringa,R., and Jurgens,G. (2003). Efflux-dependent auxin gradients establish the apical-basal axis of Arabidopsis. Nature **426**:147-153.

Friml,J., Wisniewska,J., Benková,E., Mendgen,K., and Palme,K. (2002). Lateral relocation of auxin efflux regulator PIN3 mediates tropism in Arabidopsis. Nature **415**:806-809.

Galván-Ampudia,C.S. and Offringa,R. (2007). Plant evolution: AGC kinases tell the auxin tale. Trends Plant Sci. **12**: 541-547.

Gehring,C.A., Irving,H.R., and Parish,R.W. (1990a). Effects of auxin and abscisic acid on cytosolic calcium and pH in plant cells. Proc.Natl.Acad.Sci.U.S.A **87**:9645-9649.

Gehring,C.A., Williams,D.A., Cody,S.H., and Parish,R.W. (1990b). Phototropism and geotropism in maize coleoptiles are spatially correlated with increases in cytosolic free calcium. Nature **345**:528-530.

Guan,K.L. and Dixon,J.E. (1991). Eukaryotic Proteins Expressed in Escherichia-Coli - An Improved Thrombin Cleavage and Purification Procedure of Fusion Proteins with Glutathione-S-Transferase. Analytical Biochemistry **192**:262-267.

Harada,A., Sakai,T., and Okada,K. (2003). Phot1 and phot2 mediate blue light-induced transient increases in cytosolic Ca2+ differently in Arabidopsis leaves. Proc.Natl.Acad.Sci.U.S.A **100**:8583-8588.

Lee,J.S. and Evans,M.L. (1985). Polar transport of auxin across gravistimulated roots of maize and its enhancement by calcium. Plant Physiol **77**:824-827.

Lee,S.H. and Cho,H.T. (2006). PINOID Positively Regulates Auxin Efflux in Arabidopsis Root Hair Cells and Tobacco Cells. Plant Cell **18**:1604-1616.

Luan,S., Kudla,J., Rodriguez-Concepcion,M., Yalovsky,S., and Gruissem,W. (2002). Calmodulins and calcineurin B-like proteins: calcium sensors for specific signal response coupling in plants. Plant Cell **14 Suppl**:S389-S400.

Masson,J. and Paszkowski,J. (1992). The Culture Response of Arabidopsis-Thaliana Protoplasts Is Determined by the Growth-Conditions of Donor Plants. Plant Journal **2**:829-833.

McCormack,E. and Braam,J. (2003). Calmodulins and related potential calcium sensors of Arabidopsis. New Phytologist **159**:585-598.

Memelink,J., Swords,K.M.M., Staehelin,L.A., and Hoge,J.H.C. (1994) Southern, Northern and Western blot analysis. In Plant Molecular Biology Manuel, (Dordrecht, NL: Kluwer Academic Publishers).

Michniewicz,M., Zago,M.K., Abas,L., Weijers,D., Schweighofer,A., Meskiene,I., Heisler,M.G., Ohno,C., Huang,F., Weigel,D., Meyerowitz,E.M., Luschnig,C., Offringa,R., and Friml,J. (2007). Phosphatase 2A and PID kinase activities antagonistically mediate PIN phosphorylation and apical/basal targeting in *Arabidopsis*. Cell **130**:1044-1056.

Morris,D.A., Friml,J., and Zazimalova,E. (2004) The functioning of hormones in plant growth and development, the transport of auxins. In Plant hormones: Biosynthesis, signal transduction, action!, kluwer Academic Publishers, Dordrecht, NL), pp. 437-470.

Muday,G.K. and DeLong,A. (2001). Polar auxin transport: controlling where and how much. Trends Plant Sci. **6**:535-542.

Nakajima,K. and Benfey,P.N. (2002). Signaling in and out: Control of cell division and differentiation in the shoot and root. Plant Cell **14**:S265-S276.

Paciorek,T., Zazimalová,E., Ruthardt,N., Petrášek,J., Stierhof,Y.D., Kleine-Vehn,J., Morris,D.A., Emans,N., Jürgens,G., Geldner,N., and Friml,J. (2005). Auxin inhibits endocytosis and promotes its own efflux from cells. Nature **435**:1251-1256.

Petrášek,J., Mravec,J., Bouchard,R., Blakeslee,J.J., Abas,M., Seifertová,D., Wisniewska,J., Tadele,Z., Kubes,M., Covanová,M., Dhonukshe,P., Skupa,P., Benková,E., Perry,L., Krecek,P., Lee,O.R., Fink,G.R., Geisler,M., Murphy,A.S., Luschnig,C., Zazimalová,E., and Friml,J. (2006). PIN Proteins Perform a Rate-Limiting Function in Cellular Auxin Efflux. Science **312**:914-918.

Reinhardt,D., Mandel,T., and Kuhlemeier,C. (2000). Auxin regulates the initiation and radial position of plant lateral organs. Plant Cell **12**:507-518.

Reinhardt,D., Pesce,E.R., Stieger,P., Mandel,T., Baltensperger,K., Bennett,M., Traas,J., Friml,J., and Kuhlemeier,C. (2003). Regulation of phyllotaxis by polar auxin transport. Nature **426**:255-260.

Sabatini,S., Beis,D., Wolkenfelt,H., Murfett,J., Guilfoyle,T., Malamy,J., Benfey,P., Leyser,O., Bechtold,N., Weisbeek,P., and Scheres,B. (1999). An auxin-dependent distal organizer of pattern and polarity in the Arabidopsis root. Cell **99**:463-472.

Sambrook,J., Fritsch F., and Maniatis,T. (1989) Molecular cloning - A laboratory Manual. C.Nolan, ed Cold Spring Harbor Laboratory press, NY, USA).

Sanders,D., Pelloux,J., Brownlee,C., and Harper,J.F. (2002). Calcium at the crossroads of signaling. Plant Cell **14 Suppl**:S401-S417.

Sauer,M., Balla,J., Luschnig,C., Wisniewska,J., Reinöhl,V., Friml,J., and Benková,E. (2006). Canalization of auxin flow by Aux/IAA-ARF-dependent feedback regulation of PIN polarity. Genes Dev. **20**:2902-2911.

Schirawski,J., Planchais,S., and Haenni,A.L. (2000). An improved protocol for the preparation of protoplasts from an established Arabidopsis thaliana cell suspension culture and infection with RNA of turnip yellow mosaic tymovirus: a simple and reliable method. Journal of Virological Methods **86**:85-94.

Shishova,M. and Lindberg,S. (2004). Auxin induces an increase of Ca2+ concentration in the cytosol of wheat leaf protoplasts. J Plant Physiol **161**:937-945.

Siegel,R.M., Chan,F.K., Zacharias,D.A., Swofford,R., Holmes,K.L., Tsien,R.Y., and Lenardo,M.J. (2000). Measurement of molecular interactions in living cells by fluorescence resonance energy transfer between variants of the green fluorescent protein. Sci STKE. **2000**:L1.

Sistrunk,M.L., Antosiewicz,D.M., Purugganan,M.M., and Braam,J. (1994). Arabidopsis TCH3 encodes a novel Ca2+ binding protein and shows environmentally induced and tissue-specific regulation. Plant Cell **6**:1553-1565.

Snedden,W.A. and Fromm,H. (2001). Calmodulin as a versatile calcium signal transducer in plants. New Phytologist **151**:35-66.

Strynadka,N.C.J. and James,M.N.G. (1989). Crystal Structures of the Helix-Loop-Helix Calcium-Binding Proteins. Annual Review of Biochemistry **58**:951-999.

Travé,G., Lacombe,P.J., Pfuhl,M., Saraste,M., and Pastore,A. (1995). Molecular mechanism of the calcium-induced conformational change in the spectrin EF-hands. EMBO J. **14**:4922-4931.

Weijers,D. and Jurgens,G. (2005). Auxin and embryo axis formation: the ends in sight? Current Opinion in Plant Biology **8**:32-37.

Wisniewska,J., Xu,J., Seifertová,D., Brewer,P.B., Ruzicka,K., Blilou,I., Rouquié,D., Benková,E., Scheres,B., and Friml,J. (2006). Polar PIN Localization Directs Auxin Flow in Plants. Science **312**:883.

Zegzouti,H., Li,W., Lorenz,T.C., Xie,M., Payne,C.T., Smith,K., Glenny,S., Payne,G.S., and Christensen,S.K. (2006). Structural and functional insights into the regulation of Arabidopsis AGC VIIIa kinases. J Biol.Chem. **281**:35520-35530.

Chapter 3

Cell-type and tissue-specific regulation of PID signaling by small calcium-binding proteins

Hélène Robert, Yang Xiong[1], Remko Offringa

[1] Current address: College of Life Sciences, Peking University, Beijing 100871, China

Abstract

The plant hormone auxin regulates plant development and tropic growth responses through its unidirectional transport, creating auxin gradients and maxima that are instrumental for basic cellular processes such as elongation, differentiation and division. The direction of this intercellular auxin transport is determined by the asymmetric localization of PIN auxin transporters whose subcellular targeting is dependent on their phosphorylation by the protein serine/threonine kinase PINOID (PID). Here we investigated the role of two small calcium-binding proteins, PINOID BINDING PROTEIN1 (PBP1) and its close homolog, whose interaction with PID is enhanced by calcium. Genetic experiments with different loss- and gain-of-function lines indicate that PBP1 and PBP1H act redundantly to enhance PID activity during embryo development, and that they suppress root growth, possibly through their stimulatory effect on PID. *PBP1* overexpression partially inhibits the auxin-induced calcium-dependent sequestration of PID from the plasma membrane, indicating that apart from enhancing the activity of the PID kinase, PBP1 also stabilizes the association of PID with the plasma membrane, close to the PIN phosphorylation targets. Interestingly, *pbp1-1* loss-of-function partially rescues the inflorescence phenotypes of the *pid-14* mutant allele, which seemingly contradicts the role of PBP1 as positive regulator of PID activity. We conclude that PBP1 and PBP1H fine-tune PID signaling in response to changes in cytosolic calcium, in a cell-type and tissue-specific manner.

Introduction

Auxin plays important roles as informative molecule in many cellular processes and in plant development (reviewed in Tanaka et al., 2006). Intercellular polar auxin transport (PAT) generates auxin gradients and maxima, essential for tropic growth responses, embryogenesis, organ positioning and meristem maintenance (Sabatini et al., 1999, Friml et al., 2002, Friml et al., 2003, Reinhardt et al., 2003, Benková et al., 2003). Auxin transport is tightly regulated by the presence of the polar localized PIN efflux carriers (Tanaka et al., 2006). These transmembrane facilitator proteins are the rate limiting factors in auxin efflux (Petrášek et al., 2006) and determine the direction of PAT through their asymmetric subcellular localization (Wisniewska et al., 2006). The plant specific protein serine/threonine kinase PINOID (PID) regulates PAT by controlling PIN localization, and thereby determining the direction of PAT (Benjamins et al., 2001, Friml et al., 2004). Recent data indicate that PID is a plasma membrane-associated kinase that acts antagonistic to trimeric PP2A phosphatases, through direct phosphorylation of PINs (Lee and Cho, 2006, Michniewicz et al., 2007).

Calcium is a common second messenger in signaling pathways. Early studies on sunflowers stem sections showed that PAT was abolished by the presence of calcium chelators and restored by application of calcium solutions, which suggested an important role for calcium in the regulation of PAT (Dela Fuente and Leopold, 1973). The first molecular evidence for a link between calcium and PAT was provided by the identification of the calcium-binding proteins PINOID BINDING PROTEIN1 (PBP1) and TOUCH3 (TCH3) as interacting proteins of PID (Benjamins et al., 2003). The calcium-dependent binding of PBP1 and TCH3 to PID was found to respectively up-regulate and repress the PID kinase autophosphorylation activity in *in vitro* phosphorylation assays (Benjamins et al., 2003). Further analysis of the *in vivo* difference of the interaction between the calmodulin-related protein TCH3 and PID indicated that binding of TCH3 to the catalytic domain not only suppresses the activity of the kinase, but also sequesters the plasma membrane-associated kinase to the cytoplasm, away from the PIN phosphorylation targets (Chapter 2, this thesis). In contrast to TCH3, which has six calcium-binding pockets, or EF-hands, PBP1 has a single EF-hand. PBP1 is also known as KRP2 (for KIC-related protein2), as it is part of a small protein family that includes KIC (KCBP-interacting Calcium binding protein) and the close PBP1 homologue PBP1H/KRP1 (Reddy et al., 2004). KIC is involved in the regulation of trichome development by a calcium-dependent interaction with the kinesin-like calmodulin-binding protein KCBP (Reddy et al., 2004). KCBP is a microtubule (MT) motor protein that determines trichome morphology by regulating branching and polar growth (Reddy and Day, 2000). Calcium-dependent KIC-KCBP interaction inhibits binding of KCBP with the MT, thereby affecting trichome development (Reddy et al., 2004). Interestingly, this pathway also implicates KIPK, a KCBP-interacting protein kinase that belongs to the same AGCVIII kinase family as PID (Day et al., 2000, Lee and Cho, 2006, Galván-Ampudia and Offringa, 2007). Up to now, a direct interaction between KIC and KIPK, as shown for PBP1 and PID, has not been reported.

Here we present a more detailed functional and genetic analysis to further elucidate the regulatory role of PBP1 and its close homologue PBP1H in PID signaling. Experiments with combinations of loss- and gain-of-function mutant lines of *PBP1*, *PBP1H* and *PID* indicate that PBP1 and PBP1H act redundantly to enhance PID activity during embryo development, and that they partly suppress root growth, possibly through their stimulatory effect on PID. *PBP1* overexpression partially inhibits auxin-induced calcium-dependent sequestration of PID from the plasma membrane, suggesting that apart from enhancing the activity of the PID kinase, PBP1 also influences PID subcellular localization. These data confirm *in vitro* data, indicating a role for PBP1 and PBP1H as positive regulators of the PID kinase activity. Unexpectedly, however, *pbp1-1* loss-of-function was found to partially suppress *pid-14* inflorescence phenotypes, suggesting a repressing role for PBP1 on PID activity during inflorescence development. These seemingly contradictory

results imply that PBP1 and PBP1H have a cell-type and tissue-specific effect on the PID pathway.

Results

PBP1 *loss- and gain-of-function mutants are affected in root length*

Previously, PBP1/KRP2 was identified as an interactor of PINOID that enhances the *in vitro* autophosphorylation activity of this protein serine/threonine kinase (Benjamins et al., 2003). As a first approach to analyze the function of PBP1 as a regulator of the PID kinase activity *in planta*, we isolated the *pbp1-1* loss-of-function allele, and generated lines overexpressing the *PBP1* cDNA under control of the *35S* promoter.

The *pbp1-1* allele (line GT6553 in Landsberg *erecta* (L*er*) background) has a transposon inserted at 91bp after the ATG, before the region encoding the EF-hand domain (Figure 5A). RT-PCR analysis did not detect *PBP1* transcript in *pbp1-1* mutant seedlings, indicating that it is a complete loss-of-function allele (Figure 1A). Detailed phenotypic analysis revealed that the primary roots of *pbp1-1* were longer than wild type roots (120 % of the L*er* root length, Student's t-test, $p < 0.02$, Figure 1C). Apart from that, *pbp1-1* did not show any other phenotype, and since the expression of the closely homologous gene *PBP1H/KRP1* was not altered in *pbp1-1* (Figure 1A), this suggests that, except for a specific role for *PBP1* in root growth, *PBP1* and *PBP1H* act redundantly.

From the multiple overexpression lines that were generated, two single locus lines were selected for further studies: one with a strong (*35Spro:PBP1-29*) and one with a medium (*35Spro:PBP1-53*) *PBP1* overexpression level (Figure 1B). The only observed phenotype in these lines was a slight but significant reduction of the root length. The roots in the *35Spro:PBP1*-29 and *-53* were 86 % and 90 % of the wild type Col root length, respectively (Student's t-test, $p < 0.02$, Figure 1C). The root length reduction correlated with the level of overexpression of *PBP1* in these two lines. Seedlings of the two *PBP1* overexpressing lines still showed a significant reduction in root length when germinated on medium containing 0.1 µM of the auxin indole-3-acetic acid (IAA) or the auxin transport inhibitor naphthylphtalamic acid (NPA) (data not shown). Also other auxin-dependent responses such as root gravitropism or lateral root initiation were not affected (data not shown).

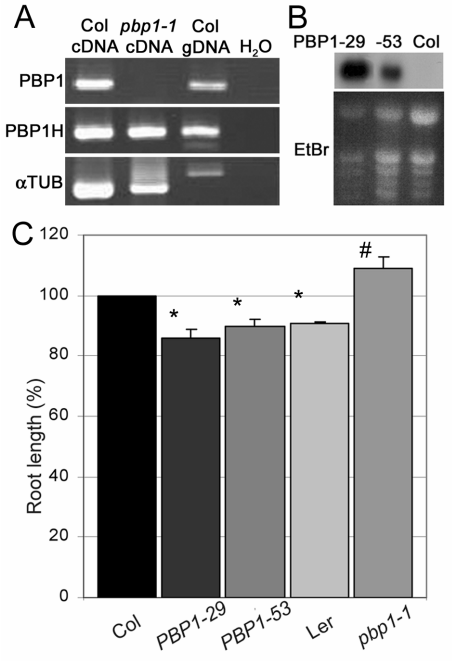


Figure 1. PBP1 represses root growth.
(A) RT-PCR on Col cDNA, *pbp1-1* cDNA and Col genomic DNA of one-week old seedlings indicates that *pbp1-1* is a null allele for *PBP1*, and that *PBP1H* expression is not affected.
(B) Northern blot analysis showing the level of *PBP1* overexpression in seedlings of the *PBP1* overexpression lines *35Spro:PBP1-29* and *-53*, as compared to Col wild type. The ethidium bromide stained RNA gel is shown as loading control.
(C) Percentage of root growth in eight day-old seedlings of *35Spro:PBP1-29* and *-53*, *pbp1-1* and L*er*, as compared to Col wild type. The mean of three experiments is shown, * significantly different from Col, # significantly different from L*er* (Student's t-test, $p < 0.02$).

PBP1 does not significantly influence the PID gain-of-function root collapse

To more specifically address the functionality of the PID-PBP1 interaction *in planta*, the *pbp1-1* allele and the two *PBP1* overexpression lines were crossed into the *35Spro:PID-21* overexpression line (Benjamins et al., 2001). The absence of auxin maxima in the root tip of *35Spro:PID-21*, due to a change of polarity of the PIN auxin efflux carriers localization, provokes differentiation of the main root meristem initials, thus leading to meristem collapse (Benjamins et al., 2001, Friml et al., 2004). This phenotype is not visible in all seedlings, but occurs gradually during seedling growth from three to six days after germination (dag). The percentage of seedlings showing the phenotype at a certain number of dag is a good measure for the PID activity- or overexpression levels. In line *35Spro:PID-21*, root collapse is observed in 6 % of the seedlings at three dag and in 96 % of the seedlings at five dag (Figure 2A) (Benjamins et al., 2001). In view of the positive effect of PBP1 on PID kinase activity *in vitro*, we expected *pbp1* loss-of-function to reduce and *PBP1* overexpression to enhance the root collapse phenotype.

The percentage of the root collapse in *35Spro:PID-21 pbp1-1* seedlings did not significantly differ from that in *35Spro:PID-21* seedlings (Figure 2A). For *PBP1* overexpression lines, a significant decrease of the *35Spro:PID*-induced root collapse was observed only at four dag (57 % and 45 % for *35Spro:PID-21 35Spro:PBP1-29* and *35Spro:PID-21 35Spro:PBP1-53*, respectively versus 82 % for *35Spro:PID-21*, Student's t-test, $p < 0.04$) (Figure 2A), but not at other time points. Since an increase rather than a

decrease of the root collapse penetrance was expected in the crossed lines due to the putative positive regulatory activity of PBP1, the level of expression of *PID* and *PBP1* was checked by Northern blot analysis. The *PID* overexpression levels were reduced to 48 % in *35Spro:PID-21 pbp1-1*, and this line did not show a significant change in root meristem collapse. We therefore are confident that the observed decrease in penetrance of the root collapse phenotype in the *35Spro:PID-21 35Spro:PBP1* seedlings is not due to a significant

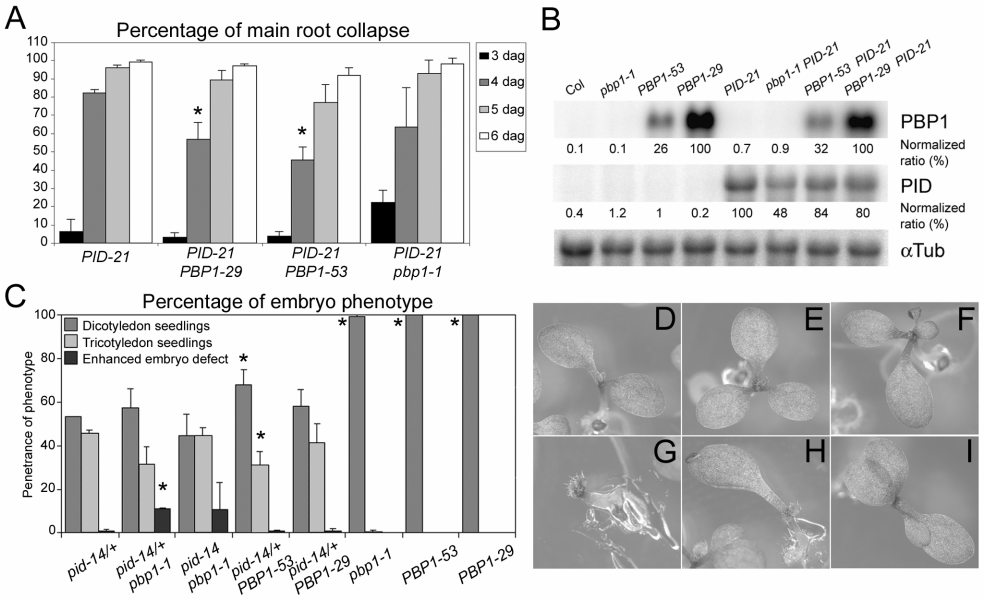


Figure 2. *pbp1-1* loss-of-function enhances *pid-14* embryo phenotypes.

(A) Graph showing the percentage of main root meristem collapse at 3, 4, 5 and 6 days after germination (dag) in *35Spro:PID-21* (n = 78, 117, 110), *35Spro:PID-21 35S: PBP1-29* (n = 201, 202, 235), *35Spro:PID-21 35Spro:PBP1-53* (n = 190, 244, 239) and *35Spro:PID-21 pbp1-1* (n = 58, 104, 102). Stars (*) indicated that the values are significantly different compared to *35Spro:PID-21* (Student's t-test, $p < 0.04$).

(B) Expression analysis of *PID* and *PBP1* by Northern blots showing that *PBP1* overexpression is strongest in line *35Spro:PBP1-29*, and that there are slight variations in the *PID* overexpression levels between the overexpression lines analyzed in (A).

(C) The percentage of cotyledon phenotypes in progeny of *pid-14/+* (n = 1469), *pid-14/+ pbp1-1* (n = 1040), *pid-14 pbp1-1* (n = 291), *pid-14/+ 35Spro:PBP1-29* (n = 1116), *pid-14/+ 35Spro:PBP1-53* (n = 1889), *pbp1-1* (n = 984), *35Spro:PBP1-29* (n = 595), *35Spro:PBP1-53* (n = 828). *pid-14/+* and *pid-14* indicate lines segregating or homozygous for the *pid-14* allele. Stars (*) indicated that the values are significantly different compared to *pid-14* (Student's t-test, $p < 0.05$).

(D-E) A segregating *pid-14/+* population typically consists of 53 % dicotyledonous seedlings (D) and 47 % tricotyledonous seedlings (E).

(F-I) Seedlings with an aberrant number of cotyledons were observed in *pid-14 pbp1-1*: four cotyledon (F, I), no cotyledon (G) and one cotyledon (H) seedlings.

decrease in *PID* overexpression levels (Figure 2B). Previously, we observed that collapse of the main root meristem is dependent on root growth, as it can only be prevented by exogenous auxin concentrations that completely inhibit root growth (Benjamins et al., 2001). The slight delay in root collapse at four dag by *PBP1* overexpression could thus be explained by the reduction in root growth in the *35Spro:PBP1* lines.

We have indications that PBP1 is a very unstable protein (F. Maraschin, unpublished data). Therefore the level of mRNA overexpression observed by Northern blot analysis may not reflect the actual protein level in the *35Spro:PBP1* seedlings, which would explain this unexpected result. Unfortunately, the above experiments do not permit to draw a clear conclusion concerning the *in planta* function of PBP1 in the PID signaling pathway.

pbp1-1 loss-of-function enhances _pid-14_ embryo phenotypes

A characteristic embryo-based phenotype of *pid* loss-of-function mutants is the aberrant number of cotyledons (mostly three), which is best scored in 5- to 7-day old seedlings and is only observed in part of the homozygous mutant seedlings (Bennett et al., 1995, Christensen et al., 2000, Benjamins et al., 2001). For the *pid-14* allele, an intermediately strong mutant allele caused by a T-DNA insertion in the intron of the *PID* gene, the penetrance of the tricotyledon phenotype is 47 % (n = 1469, Figures 2C and 2E). The influence of modified *PBP1* expression on *pid-14* was investigated by scoring the mutant phenotypes in *pid-14/+ 35Spro:PBP1-53*, *pid-14/+ 35Spro:PBP1-29* and *pid-14/+ pbp1-1* F3 populations.

PBP1 overexpression lead to a mild but significant reduction of the number of tricotyledon seedlings for line *35Spro:PBP1-53* (31 %, n = 1889, Student's t-test, $p < 0.05$, Figure 2C), whereas for line *35Spro:PBP1-29* the reduction was not significant (41 % of tricotyledons, n = 1116, Student's t-test, $p > 0.05$, Figure 2C). This result suggests that PBP1 reduces the severity of the *pid* embryo phenotype, although the decrease of the tricotyledon phenotype penetrance did not correlate with the level of the *PBP1* overexpression.

For the *pid-14/+ pbp1-1* F3 population, the global penetrance of cotyledon defects did not significantly differ from that in *pid-14/+* (43 %, n = 1040, Student's t-test, $p > 0.05$). However, *pbp1-1* loss-of-function did cause a reduction in the penetrance of the tricotyledon phenotype to 32 % (Figure 2C), and instead seedlings were observed with one cotyledon (5 %, Figure 2H), four cotyledons (2 %, Figures 2F and 2I) or even no cotyledon (4 %, Figure 2G). We considered this a significant shift, as tetra-, or nocotyledon seedlings were never observed for the *pid-14* allele, and monocotyledon seedlings only occasionally (0.5 %, n = 1469). Interestingly, *pid-14 pbp1-1* plants produced a few fertile flowers (see below), and this allowed us to reassess the penetrance of the cotyledon in a *pid-14 pbp1-1* double homozygous F4 population. This time, the penetrance of the tricotyledon phenotype

was not significantly changed (45 %, n = 291, Student's t-test, $p > 0.05$, Figure 2C), but on top of that 11 % of the seedlings showed the no-, mono- or tetracotyledon phenotypes as observed in *pid-14/+ pbp1-1*, indicating that *pbp1* loss-of-function does not only change the type of cotyledon defects, but also increases the penetrance of the cotyledon phenotypes. No-, mono- and tetracotyledon seedlings have been reported for some strong *pid* mutant alleles (Bennett et al., 1995), indicating that the absence of *PBP1* expression during embryo development enhances *pid-14* mutant phenotypes, which is in accordance with our conclusions from the *in vitro* kinase assays that PBP1 acts as a positive regulator of PID activity (Benjamins et al., 2003; Galván-Ampudia, unpublished data).

pbp1-1 loss-of-function partially rescues *pid-14* inflorescences

At bolting stage *pid* loss-of-function mutants are characterized by the formation of inflorescence stems with few aberrant flowers and ending in a pin-like structure, thereby mimicking Arabidopsis plants grown on auxin transport inhibitors (Figure 3A) (Okada et al., 1991). The *pid* inflorescence phenotypes are fully penetrant, but may vary in strength depending on the mutant allele. In 5-week old plants of the intermediate strong *pid-14* allele, almost no flowers are observed (Figures 3A and 3D-E). Only 44 % of the inflorescence stems carried flowers, which have the typical *pid* phenotype: fewer stamens and sepals, extra petals and a trumpet-shaped pistil (Figures 3A and 3D, Table 1) (Bennett et al., 1995). Interestingly, in *pid-14 pbp1-1* plants, up to 72 % of the stems carried flowers (Figures 3A-C, Table 1). All these flowers had *pid*-like phenotypes (Figures 3B, 3C, 3I and

Table 1. *pbp1-1* reduces the severity of the *pid-14* pin-like phenotype.

	Stems with flowers[1]	n
Col wild type	100 (0)	10
L*er* wild type	100 (0)	10
35Spro:PBP1-53	100 (0)	10
35Spro:PBP1-29	100 (0)	10
pbp1-1	100 (0)	11
pid-14	44* (19)	10
pid-14 35Spro:PBP1-53	60[!] (21)	7
pid-14 35Spro:PBP1-29	49[!] (28)	5
pid-14 pbp1-1	72[†#] (19)	15

[1] Percentage of stems per five week-old plant with flowers (s.d.)

* Significantly different from Col (Student's t-test, $p < 0.05$)

[†] Significantly different from *pid-14* (Student's t-test, $p < 0.02$)

[!] Significantly different from the respective *35Spro:PBP1* line (Student's t-test, $p < 0.05$)

[#] Significantly different from *pbp1-1* (Student's t-test, $p < 0.02$)

3J). Two kinds of inflorescence were observed in the same plant: wild type-like inflorescence with *pid*-like flowers (Figure 3B) and *pin*-like inflorescences with fewer *pid*-like flowers (Figure 3C). These results suggest that the absence of *PBP1* expression at bolting stage partially rescues the *pid* phenotype, allowing the formation of flowers and the production of few seeds. In contrast, *PBP1* did not have a significant effect on the *pid-14* bolting phenotype (Table 1).

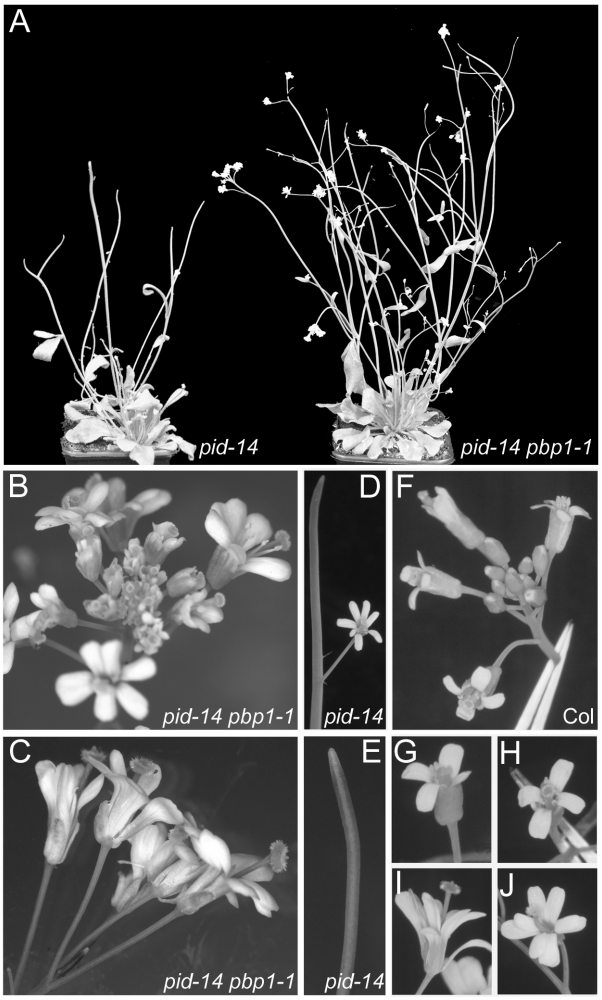


Figure 3. *pbp1-1* loss-of-function partially rescues *pid-14* inflorescences
(A) *pid-14 pbp1-1* plants (right) have a reduced apical dominance compared to *pid-14* (left).
(B, C) *pid-14 pbp1-1* has two types of inflorescences: wild-type with pid-like flowers (B) and pin-like with pid-like flowers (C).
(D, E) *pid-14* has inflorescences with (D) or without (E) flowers.
(F-H) Col wild-type inflorescence (F) has flowers (G, H) with four petals, six stamens and one carpel.
(I, J) *pid-14 pbp1-1* flowers are pid-like with extra number of petals and a trumpet-shaped pistil.

The above results suggest that the effect of PBP1 on PID differs per developmental stage. On the one hand, PBP1 seems to act synergistically with PID during embryo development, as indicated by the enhanced cotyledon defects in *pid-14 pbp1-1* seedlings. On the other hand, PBP1 seems to act antagonistically to PID during inflorescence development, as observed by the partially rescued inflorescences of *pid-14 pbp1-1* plants. The effect of

PBP1 overexpression is minor, and restricted to embryo development, where the observed reduction in the penetrance of cotyledon defects is in line with the proposed synergistic action between PBP1 and PID.

Auxin-induced sequestration of PID to the cytoplasm is PBP1-independent

To further analyze the effect of the PBP1-dependent regulation of PID in plants, we analyzed whether *PBP1* overexpression had any effect on PID expression and localization using the *PIDpro:PID:VENUS* marker line (Michniewicz et al., 2007). For this we focused our attention to epidermal cells in the distal elongation zone, as *PID* is expressed in this region (Michniewicz et al., 2007), and *PBP1* overexpression resulted in a significant reduction in root length.

PID is a plasma membrane-associated kinase (Figure 4A) (Lee and Cho, 2006, Michniewicz et al., 2007). Previously, we observed that PID localization is highly dynamic, and that auxin treatment induces its rapid and transient sequestration from the plasma membrane to the cytoplasm (Figure 4E and Chapter 2, this thesis). The auxin-dependent release of PID from the plasma membrane seems to rely on an increase of the cytoplasmic calcium concentration through plasma membrane calcium channels, and on calmodulin-like activity, as it can be inhibited by pre-incubation with the plasma membrane calcium channel inhibitor Tetracain (Figure 4G), or with the calmodulin inhibitor Lanthanum (Figure 4H). *PBP1* overexpression did not result in a clear alteration of PID localization (Figure 4B), but it did partially inhibit the transient sequestration of PID (Figure 4F). These results suggest that PBP1 itself is not involved in the auxin-induced sequestration of PID in root epidermal cells, but that instead its overexpression stabilizes the membrane association of PID.

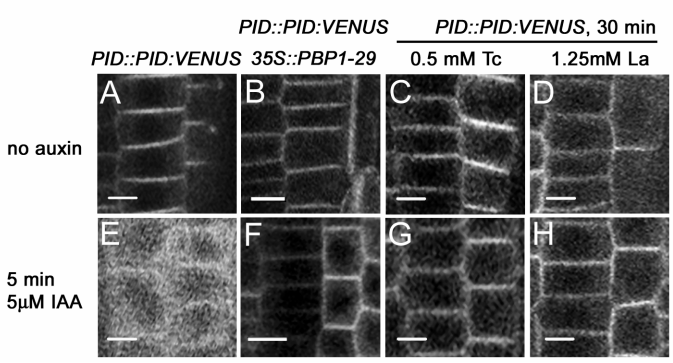


Figure 4. PBP1 stabilizes the plasma membrane association of PID.

(A-H) Confocal sections showing the subcellular localization of PID:VENUS in epidermal cells of the elongation zone of seedling root tips of the lines *PIDpro:PID:VENUS* (A, C-E, G, H) and *PIDpro:PID:VENUS 35Spro:PBP1-29* (B, F). PID is membrane localized in control medium (A, B), but is transiently sequestered to the cytoplasm after 5 min treatment with 5 μM IAA (E), but less when PBP1 is overexpressed (F). A 30 min pre-

treatment with 0.5 mM Tetracain (C, G) or 1.25 mM Lanthanum (D, H) did not affect PID localization, but blocked the auxin-induced transient sequestration to the cytosol (G, H). Scale bars represent 10 µm.

PBP1H acts redundantly with its close homolog PBP1 to positively regulate PID activity

PBP1 and PBP1H are highly conserved with 80 % amino acid sequence identity (Figure 5A), and pull down experiments indicated that PID also interacts with PBP1H (C. Galván-Ampudia, unpublished data). Since the loss-of-function allele *pbp1-1* did not give phenotypes, other than the increased root length, we suspected that the two proteins were functionally redundant, and tried to identify *pbp1h* loss-of-function alleles. Unfortunately, in the two available T-DNA insertion lines (SALK_013868 and SALK_048098) with T-DNAs at positions -673 and -582 relative to the *PBP1H* ATG, respectively, *PBP1H* expression was found to be at wild type levels (data not shown). Therefore, we attempted to knock-down both *PBP1* and *PBP1H* expression through RNA interference (RNAi), by overexpressing a hairpin RNA spanning the complete *PBP1H* coding region (*hpPBP1H*). Several lines were obtained containing a single locus insertion of the *hpPBP1H* construct, two of which (*hpPBP1H-13* and *hpPBP1H-16*) were studied in more detail. Expression analysis showed that *PBP1H* expression in both lines was significantly reduced (Figure 5B). The residual fragment amplified in both lines was also observed in the minus reverse transcriptase control, indicating that it was derived from contaminating DNA. In the *hpPBP1H-13* sample, a larger additional band was detected. Since Northern blot analysis indicated that line *hpPBP1H-13* shows the highest expression of the *hpPBP1H* RNA (results not shown), it is likely that this fragment represents the full length hairpin RNA amplified with the forward PCR primer. As anticipated based on the homology between the *PBP1* and *PBP1H* coding regions (78 % identity), *PBP1* expression was also suppressed in *hpPBP1H-13* and was even undetectable in *hpPBP1H-16* (Figure 5B).

Figure 5. (continued)

(C) The percentage of main root growth in L*er* wild type, *pbp1-1*, *hpPBP1H-13* and *hpPBP1H-16* seedlings, normalized to Col wild type seedlings. The mean of three experiments is shown. Stars (*) and hash signs (#) indicate significant differences compared to Col and L*er*, respectively (Student's t-test, $p < 0.06$).

(D) The percentage of main root meristem collapse in *35Spro:PID-21*, *35Spro:PID-21 hpPBP1H-13* and *35Spro:PID-21 hpPBP1H-16* seedlings at 3, 4, and 5 days after germination (dag).

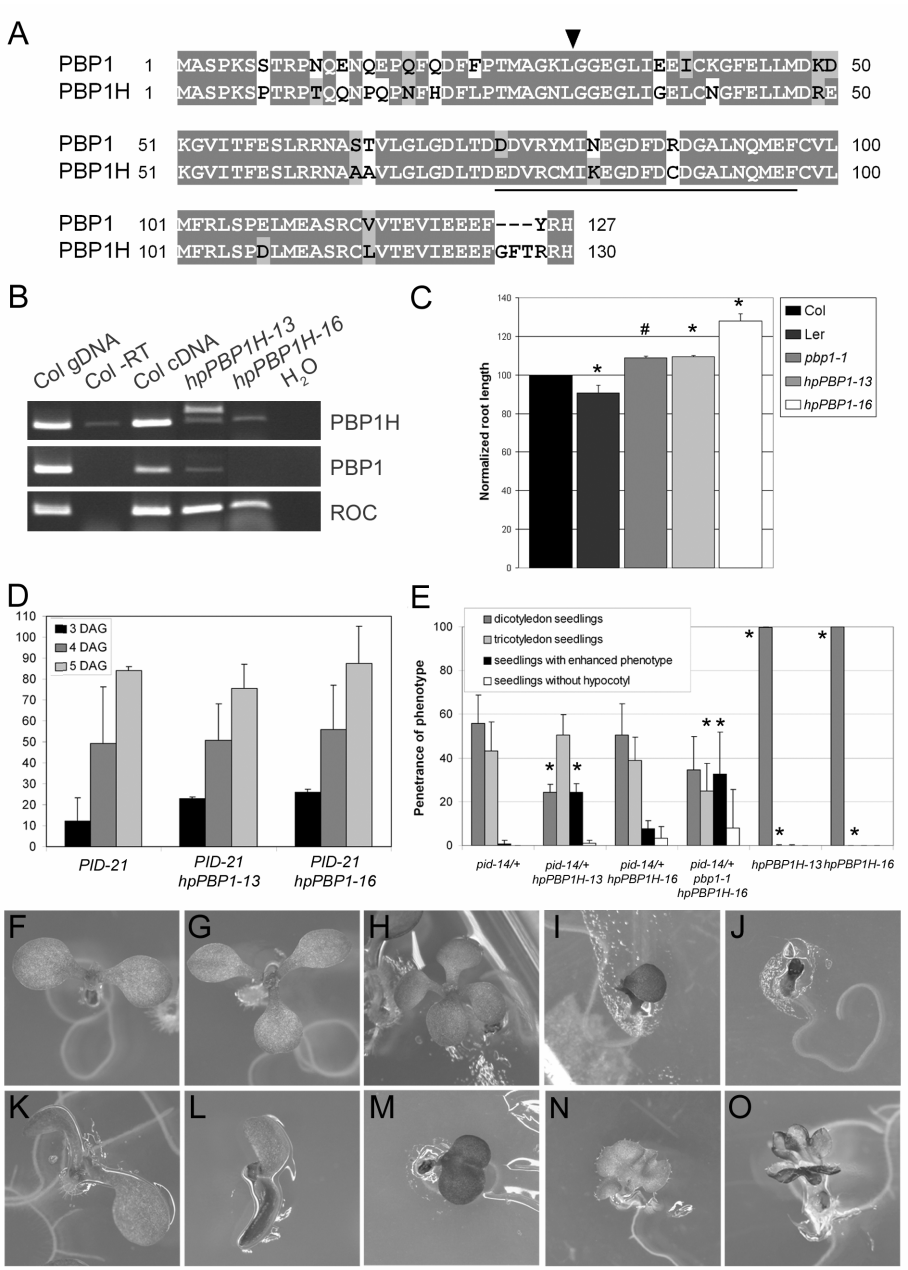
(E) The percentage of seedling phenotypes in *pid-14/+, pid-14/+ hpPBP1H-13, pid-14/+ hpPBP1H-16, pid-14/+ pbp1-1 hpPBP1H-16, hpPBP1H-13* and *hpPBP1H-16. pid-14/+* and *pid-14* indicate lines segregating or homozygous for the *pid-14* allele, respectively. Stars (*) indicate significant differences compared to *pid-14* (Student's t-test, $p < 0.06$).

(F-G) Seedling phenotypes observed in progeny of *pid-14/+*: a normal dicotyledonous seedling (F) and a tricotyledonous seedling (G) observed in 45% of the individuals homozygous for the *pid-14* loss-of-function mutation.

(H-J) Seedlings with four cotyledons (H), one cotyledon (I) and no cotyledon (J), as observed among progeny of the lines *pid-14/+ hpPBP1H-13, pid-14/+ hpPBP1H-16* and *pid-14/+ pbp1-1 hpPBP1H-16*.

(K-M) Seedlings without hypocotyl (K), without hypocotyl and root (L) and with fused cotyledons are found in *pid-14 hpPBP1H-13, pid-14 hpPBP1H-16* and *pid-14 pbp1-1 hpPBP1H-16* (M).

(N-O) Seedlings without cotyledons in *pid-14 pbp1-1 hpPBP1H-16* show defects in the phyllotaxis of the first



leaves, with either fused leaves (N) or fused petioles (O).

Figure 5. PBP1 and PBP1H act redundantly on root growth, embryo patterning and leaf phyllotaxis.
(A) Alignment of the PBP1 and PBP1H proteins. The arrowhead indicates the position of the transposon insertion in *pbp1-1*. The EF-hand domain is underlined.

(B) RT-PCR reactions showing that both *PBP1* (middle) and *PBP1H* (top) expression are reduced in *hpPBP1H-13* whereas *PBP1* expression is absent in *hpPBP1H-16*. Controls are Col genomic DNA (gDNA), Col RNA in which the reverse transcriptase was omitted during the RT reaction (Col -RT), Col cDNA and water.

Overall, *hpPBP1H-13* and *hpPBP1H-16* plants had a wild type phenotype, but similar to *pbp1-1*, the primary seedling roots were longer compared to the wild type control (109 % and 128 %, respectively, Student's t-test, $p < 0.06$, Figure 5C). Interestingly, the increase in root length correlated with the level of *PBP1* knock-down in these lines.

To further investigate the function of PBP1H in the PID pathway, the *hpPBP1H* lines were crossed with *35Spro:PID-21,* and the main root meristem collapse was analyzed in the progeny of double homozygous F2 plants. Similar to the *pbp1-1* loss-of-function allele, the *hpPBP1H*-induced knock-down of both *PBP1* and *PBP1H* did not significantly influence the root collapse kinetics of *PID* overexpression (Student's t-test, $p > 0.05$, Figure 5D).

In addition, we crossed *hpPBP1H* lines with the *pid-14* allele, and counted the number of seedlings with aberrant cotyledon phenotypes in progeny of *pid-14/+ hpPBP1H* F2 plants. A greater number of seedlings with cotyledon defects could be observed in *pid-14/+ hpPBP1H-13* (even up to 75 %) and *pid-14/+ hpPBP1H-16* compared to *pid-14/+* and *pid-14/+ pbp1-1* (Figures 5E and 5H-J). In both *pid-14/+ hpPBP1H-13* and *pid-14/+ hpPBP1H-16* the number of monocotyledon seedlings was increased (8 % and 6 %, respectively, Figure 5I), whereas a significant number of seedlings without cotyledon could be observed in *pid-14/+ hpPBP1H-13 (*15 %, Figure 5J). Furthermore, several seedlings without hypocotyl (Figure 5K) or without hypocotyl and root (Figure 5L) were observed in *pid-14/+ hpPBP1H-16* (> 3 %, Figure 5E), indicating that PID, PBP1, PBP1H are involved in broader aspects of embryo patterning than only cotyledon initiation and positioning.

To corroborate these data, we generated *pid-14/+ pbp1-1 hpPBP1H-16* triple lines, homozygous for *pbp1-1* and *hpPBP1H-16*, and heterozygous for *pid-14*, and scored for cotyledon defects in the progeny. The severity of the embryo/seedling phenotypes was enhanced compared to the two *pid-14 hpPBP1H* and the *pid-14 pbp1-1* lines, with 32 % of seedlings showing enhanced seedling phenotype (Figures 5E and 5H-O). The majority of these seedlings had one (14 %, Figure 5I) or no cotyledon (18 %, Figure 5J), and the number of seedlings without hypocotyl or without hypocotyl and root was increased to 8 % (Figure 5K and 5L). Furthermore, monocotyledon seedlings had defects in the formation of the first leaves, which were fused at the blade (Figure 5N) or at the petiole (Figure 5O). Normal plant growth and organ positioning were restored for the subsequent leaves. These data suggest that PBP1 and PBP1H act redundantly in the PID pathway and have a positive effect on the kinase function. Defects in embryo patterning and leaf phyllotaxis in *pid-14 pbp1-1 hpPBP1H-16* confirms the proposed role of PID in regulation of organ boundaries during embryogenesis (Furutani et al., 2004).

Discussion

The plant signaling molecule auxin controls plant development through transport-generated auxin gradients. Previous experiments have indicated that calcium is an important second messenger in auxin action. One of the earliest cellular responses to auxin is a rapid increase in cytosolic calcium (Felle, 1988, Gehring et al., 1990, Shishova and Lindberg, 2004) and calcium has been reported to play a crucial role in PAT (Dela Fuente and Leopold, 1973). The direction of PAT is determined by the asymmetrical subcellular localization of the PIN auxin efflux carriers (Wisniewska et al., 2006). The protein kinase PID has been shown to direct the polar targeting of PIN proteins by phosphorylation of residues in their large central hydrophilic loop (Friml et al., 2004, Michniewicz et al., 2007). The finding that PID interacts in a calcium-dependent manner with the calmodulin-like protein TCH3 and the small calcium-binding protein PBP1, provided the first molecular evidence for the role of calcium as regulator of PAT (Benjamins et al., 2003). In this chapter, we further investigated the role of PBP1 in plant development in relation to its interaction with PID.

PBP1(H) regulates root growth by enhancing PID activity

PBP1 belongs to a small family of single EF-hand calcium-binding proteins (Reddy et al., 2004), and was found to enhance the PID kinase activity in *in vitro* phosphorylation assays (Benjamins et al., 2003; Chapter 2, this thesis). To analyze the *in planta* role of PBP1 in the PID pathway, we isolated loss- and gain-of function mutants in the *PBP1* gene and its close homologue *PBP1H*. Morphometric analysis of these mutant lines indicated that PBP1 and PBP1H are partially redundant to repress root growth, and although we could not find clear evidence for a change in sensitivity of the mutant lines to auxin, PAT inhibitors or *PID* overexpression, it is likely that PBP1 and PBP1H mediate their effect on root growth through their role as positive regulators of PID activity. PID overexpression may lead to increased auxin transport to the root elongation zone (Benjamins et al., 2001, Friml et al., 2004, Lee and Cho, 2006), which in turn inhibits root growth and thus explains the longer root in *pbp1(h)* loss-of-function lines and the shorter root in *PBP1* overexpression lines. This positive regulatory function of PBP1(H) in PID pathway in roots is similarly observed during embryogenesis by the enhanced penetrance and/or severity of seedling phenotypes in *pid-14 pbp1-1*, *pid-14 hpPBP1H*, *pid-14 pbp1-1 hpPBP1H-16* mutant lines as compared to *pid-14*.

In chapter 2, we showed auxin-induced and calcium-dependent sequestration of PID in epidermis cells of the root elongation zone. Here we present data that this occurs independent of PBP1, and that, in fact *PBP1* overexpression even enhances the membrane-

association of PID. On the one hand, these results corroborate our model that TCH3 is involved in PID sequestration, and on the other hand, it shows that PBP1 not only positively regulates PID action by enhancing its kinase activity, but also by retaining the kinase at the plasma membrane, in proximity of its phosphorylation targets, the PIN proteins.

PBP1(H) assists PID in establishing organ boundaries during embryogenesis

Upon germination, seedlings have a bilateral symmetry marked by the presence of two cotyledons separated by the shoot-root axis. This symmetric structure can be traced back to the early embryogenesis, when the initiation of cotyledon primordia in the globular embryo marks the transition to the heart stage. Proper auxin distribution, based on the PAT activity, is primordial for the embryo patterning at crucial transition steps (Friml et al., 2003, Weijers et al., 2005, Weijers and Jürgens, 2005). The auxin efflux carriers PIN1, PIN3, PIN4 and PIN7 are involved in controlling the auxin gradients during embryogenesis (Friml et al., 2003). At heart stage, the establishment of the cotyledons boundaries is based on the presence of an auxin maximum at the cotyledon tips. Treatment of embryos with exogenous auxin or PAT inhibitors gives rise to seedlings with abnormally positioned or fused cotyledons (Friml et al., 2003, Furutani et al., 2004). And mutations in *PIN1* and *PID* generate seedlings with an abnormal number of cotyledons. The *pin1 pid* double mutant seedlings have no cotyledons and fused leaves with an aberrant phyllotaxis. Both proteins, by controlling auxin distribution, are responsible for the establishment of a bilateral symmetry and the cotyledon outgrowth during embryogenesis (Furutani et al., 2004). We have observed that in the *pid-14* mutant background the absence of the PID positive regulators PBP1 and PBP1H perturbed embryogenesis even more, giving rise to seedlings with no to four cotyledons, whereas only tricotyledon seedlings were observed in *pid-14*. Such phenotypes were previously described for strong alleles of *pid* or in the combination of *pid* with the *enhancer of pid* mutation (Bennett et al., 1995, Treml et al., 2005). Together these results confirm the proposed role of PID in the regulation of organ boundaries establishment (Furutani et al., 2004) and the function of PBP1 and PBP1H as positive regulator of PID kinase activity during embryogenesis and seedling development.

In *pid-14 hpPBP1H-16* and *pid-14 pbp1-1 hpPBP1H-16*, seedlings with strong patterning defects such as absence of hypocotyl or both hypocotyl and root were observed at low frequencies. Similar phenotypes have been reported for mutants impaired in auxin transport and signaling during embryogenesis like *pin1 pin3 pin4 pin7* quadruple mutant, *gnom*, *monopteros* and *bodenlos* (Friml et al., 2003). In these mutants, miss-specification of the embryonic hypophysis leads to an absence of the root pole. This reveals the importance of auxin transport and signaling for proper embryo patterning and the establishment of the shoot-root axis. It is therefore likely that PID is not only involved in cotyledon positioning,

but also in the establishment/maintenance of the shoot-root axis by regulating the highly dynamic and regulated auxin transport during embryo development.

Phyllotaxis regulation by PID activity

The regular arrangement of leaves and flowers around the stem, so-called phyllotaxis, is also a highly auxin-dependent regulated mechanism (Reinhardt et al., 2003). Besides the cotyledon defects during embryo development, *pin1* and *pid* loss-of-function mutants are both defective in aerial organ formation during their adult phase, which is characterized by oddly positioned and shaped leaves and pin-like inflorescences carrying a few aberrant flowers. Interestingly, *pin1* and *pid* loss-of-function mutants react differently to auxin application at the tip of their pin-like inflorescences. In *pin1* mutants, auxin treatment generates the formation of a ring-shape primordium, indicating that PIN1 plays a crucial role in organ separation in the inflorescence meristem as was observed in seedlings. In *pid* mutants, an auxin dose-dependent number of normal sized flowers were induced, suggesting that the mechanism of auxin transport is still present and functional in *pid*, and that the inflorescence meristem retains part of its patterning capacity (Reinhardt et al., 2003). In *pid-14 pbp1-1*, partial rescue of the *pid-14* pin-like structure by *pbp1-1* was observed with the formation of *pid*-like flowers, mimicking auxin application at the inflorescence meristem (Reinhardt et al., 2003). Such phenotypes as well as the formation of functional shoot apical meristems in *pid-14 pbp1-1* are also observed in weak *pid* alleles (Bennett et al., 1995).

Although an enhancement of the *pid* phenotype by *pbp1* or by *pbp1h* was anticipated, the partial rescue of the *pid* inflorescence phenotypes in the *pid-14 pbp1-1* double mutant suggests that PIN1, basal localized in epidermal cells in *pid* inflorescence meristem (Friml et al., 2004), may be restored at its normal, apical, subcellular localization in *pid-14 pbp1-1*, resulting in a normal auxin distribution in the inflorescence meristem and an induction of the flower formation. These results and previous observations suggest that PID may not be involved in the formation of primordia boundaries in the inflorescence meristem, as it does during embryogenesis, since a phyllotactic pattern can be observed upon auxin application (Reinhardt et al., 2003) or in absence of its positive regulators (this work). One has to keep in mind, however, that PID is a member of the AGCVIII family of protein kinases, and that in Arabidopsis it groups together in the AGC3 clade that comprises three PID-related kinases (PRKs) (Galván-Ampudia and Offringa, 2007). We are currently investigating the possibility that these other kinases act redundantly with PID in inflorescence development, and if this is the case, whether the expression of one of these kinases is up-regulated in the *pid-14 pbp1-1* double mutant and not in *pid-14*. Interestingly, the rescue of *pid-14* phenotype observed in *pid-14 pbp1-1* plants is not presented anymore

in the *pid-14 wag1 wag2 pbp1-1* quadruple mutant, suggesting that this is indeed the case (Galván-Ampudia et al., manuscript in preparation).

Materials and methods

Plasmids and molecular cloning

Molecular cloning was performed following standard procedures (Sambrook et al., 1989). Bacteria were grown on LC medium containing 100 µg/ml carbenicillin (Cb) for *E. coli* strains DH5α or Rosetta (Novagen), 50 µg/ml kanamycin (Km) or 250 µg/ml spectinomycin for respectively binary vectors pCAMBIA1300 and pART27 in *E. coli* DH5α or *Agrobacterium tumefaciens* strain LBA1115. For the latter strain, 20 µg/ml rifampicin was included in the LC medium.

The construct pSDM6015 (pBS-SK-PBP1) was previously described (Benjamins et al., 2003). For the *35Spro:PBP1* construct, the *PBP1* cDNA was excised as a *Sal*I-*Spe*I fragment from pSDM6015 and cloned into pCambia1300int-35Snos, given rise to pSDM6085. To obtain the *PBP1H* RNAi construct, a *PBP1H* fragment was PCR amplified from pET-PBP1H (pSDM6042) using the primers 5'TC-*Eco*RI-ATGGCGTCACCAAAGTCACC3' and 5'CAAATCTCTCCAGTG-*Kpn*I-ATGC3', and ligated as anti-sense *Eco*RI-*Kpn*I fragment into the pHANNIBAL vector (Wesley et al., 2001). The sense fragment was excised as a *Cla*I-*Bam*HI fragment from pET-PBP1H and cloned into the corresponding restriction sites in pHANNIBAL. The resulting *PBP1H* RNAi expression cassette (pSDM6043) was transferred to the pART27 binary vector as a *Not*I fragment (pSDM6302).

Arabidopsis lines, plant growth and transformation

The *35Spro:PID-21* (Benjamins et al., 2001) and the *PIDpro:PID:VENUS* (Michniewicz et al., 2007) lines were described previously. The *pid-14* (SALK_049736), *pbp1-1* (Ds transposon line GT6553) and *pbp1h-1* and *-2* alleles (SALK_013868 and SALK_048098) were obtained from NASC for the SALK lines (Alonso et al., 2003) and from the Cold Spring Harbor Laboratory for the transposon insertion line (Sundaresan et al., 1995). For the detection of the insertions, we used gene-specific primers 5'TCTCTTCCGCCAGGTAAAAA3' and 5'CGCAAGACTCGTTGGAAAAG3' for *PID*, 5'TACCCTTACGTGAGCTTCCAA3' and 5'TCACCTCCGTCACAACACAC3' for *PBP1*, 5'CATGCAATTAGAGAACGGGCA3' and 5'AGGAACATCCATGGAAGCCA3' for *PBP1H* and the insertion-specific primers LBaI and Ds3-2 for respectively the SALK lines and the transposon line. The flanking region of each insertion was sequenced to

confirm the insertion position and RT-PCR analysis was performed to determine if the insertion resulted in a complete loss-of-function allele.

Arabidopsis seeds were surfaced-sterilized by incubation for 15 min in 50 % commercial bleach solution and rinsed four times with sterile water. Seeds were vernalized for 2 to 4 days at 4°C and germinated (21°C, 16 h-photoperiod and 3000 lux) on solid MA medium (Masson and Paszkowski, 1992) supplemented with antibiotics when required. Two- to three-week old plants were transferred to soil and grown at 21°C and 70 % relative humidity with a 16 h photoperiod of 10000 lux.

Arabidopsis thaliana ecotype Columbia (Col) was transformed by the floral dip method as described (Clough and Bent, 1998). Primary transformants were selected on medium supplemented with 20 µg/ml hygromycin (Hm) for pSDM6085 or 70 µg/ml Km for pSDM6302 and 100 µg/ml timentin to inhibit the Agrobacterium growth. For further analysis, single locus insertion lines were selected by germination on 10 µg/ml Hm or 25 µg/ml Km and checked for transgene expression by Northern blot or RT-PCR analysis.

Northern blot and RT-PCR analysis

Total RNA was purified using the RNeasy Plant (Qiagen) and Invisorb Spin Plant RNA (Invitek) Mini kits. Subsequent RNA blot analysis was performed as described (Memelink et al., 1994) using 10 µg of total RNA per sample. The following modifications were made: pre-hybridizations and hybridizations were conducted at 65°C using 10 % Dextran sulfate, 1 % SDS, 1 M NaCl, 50 µg/ml of single strand Herring sperm DNA as hybridization mix. The hybridized blots were washed for 20 min at 65°C in 2x SSPE 0.5 % SDS, and for 20 min at 42°C in respectively 0.2x SSPE 0.5 % SDS, 0.1x SSPE 0.5 % SDS and 0.1x SSPE. Blots were exposed to X-ray film FUJI Super RX. Probes were PCR amplified and column purified (Qiagen): 5'CCTCAACAAGACCAAACCAAG3', 5'TCACCTCCGTCACAACACAC3' for *PBP1* from pSDM6007; 5'ATGGCGTCACCAAAGTCACC3', 5'TGTTCAACACATCTGATCAAAGA3' for *PBP1H*, 5'AGGCACGTGACAACGTCTC3', 5'CGCAAGACTCGTTGGAAAAG3' for *PID*, 5'CGGGAAGGATCGTGATGGA3', 5CCAACCTTCTCGATGGCCT3' for *AtROC5*, 5'CGGAATTCATGAGAGAGATCCTTCATATC3', 5'CCCTCGAGTTAAGTCTCGTACTCCTCTTC3' for *αTubulin* from Col genomic DNA. Probes were radioactively labeled using α-^{32}P-ATP (Amersham) and the Prime-a-gene kit (Promega).

RT-PCRs were performed as described (Weijers et al., 2001) using 10 µg of total RNA from one-week old seedlings for the RT reaction. The PCR reactions were performed with one tenth of the RT volume with the same gene specific primers used for the probe amplification in the Northern blot analysis. A RT reaction from Col seedlings RNA in which the reverse-transcriptase was omitted served as a negative control.

Biological assays

For the root meristem collapse assay, about 100 seedlings per line were grown in triplicate on vertical plates containing solid MA medium. The development of the seedling root was monitored and scored each day during eight days for the collapse of the primary root meristem. For the phenotypic analysis of the crosses with *pid-14*, about 300 seeds (100 seeds for *pid-14 pbp1-1* and controls) were plated in triplicate, germinated and grown for one week on solid MA medium. The number of dicotyledon seedlings and of seedlings with cotyledon defects was counted and the penetrance of the phenotypes was calculated based on a 1:3 segregation ratio for homozygous *pid/pid* seedlings. For root length measurements, at least 50 seedlings for each genotype were grown in triplicate on vertical plate for eight days and roots were photographed. Root lengths were measured using ImageJ (http://rsb.info.nih.gov/ij/). To observe the auxin-induced changes in the subcellular localization of PID in Arabidopsis roots, vertically grown three day-old *PIDpro:PID:VENUS* and *PIDpro:PID:VENUS 35Spro:PBP1-29* seedlings were treated with 5 µM IAA (in MA medium) following 30 min pre-treatment with a calmodulin inhibitor (0.5 mM Tetracain, Sigma) or a calcium channel blocker (1.25 mM Lanthanum, Sigma).

Confocal microscopy

Arabidopsis *PIDpro:PID:VENUS* roots were observed using a 40x oil objective with a ZEISS Axioplan microscope equipped with a confocal laser scanning unit (MRC1024ES, BioRad, Hercules, CA). The YFP fluorescence was monitored with a 522-532 nm band pass emission filter (488 nm excitation). All images were recorded using a 3CCD Sony DKC5000 digital camera. The images were processed by ImageJ and assembled in Adobe Photoshop 7.0.

Accession Numbers

The *Arabidopsis* Genome Initiative locus identifiers for the genes mentioned in this chapter are as follows: *PBP1/KRP2* (At5g54490), *PBP1H/KRP1* (At4g27280), *KIC* (At2g46600), *PID* (At2g34650), *TCH3* (At2g41100), *KCBP* (At5g65930), *KIPK* (At3g52890), *ROC* (At4g38740), *αTubulin* (At5g44340).

Acknowledgments

The authors thank Carlos Galván-Ampudia for valuable discussions and critical reading, Marcus Heisler and Pieter Ouwerkerk for kindly providing the *PIDpro:PID:VENUS* line

and pCambia1300int-35Snos, respectively, and Gerda Lamers and Ward de Winter for their help with the microscopy and the tissue culture, respectively

References

Alonso,J.M., Stepanova,A.N., Leisse,T.J., Kim,C.J., Chen,H., Shinn,P., Stevenson,D.K., Zimmerman,J., Barajas,P., Cheuk,R., Gadrinab,C., Heller,C., Jeske,A., Koesema,E., Meyers,C.C., Parker,H., Prednis,L., Ansari,Y., Choy,N., Deen,H., Geralt,M., Hazari,N., Hom,E., Karnes,M., Mulholland,C., Ndubaku,R., Schmidt,I., Guzman,P., Aguilar-Henonin,L., Schmid,M., Weigel,D., Carter,D.E., Marchand,T., Risseeuw,E., Brogden,D., Zeko,A., Crosby,W.L., Berry,C.C., and Ecker,J.R. (2003). Genome-Wide Insertional Mutagenesis of Arabidopsis thaliana. Science **301**:653-657.

Benjamins,R., Galván-Ampudia,C.S., Hooykaas,P.J., and Offringa,R. (2003). PINOID-mediated signaling involves calcium-binding proteins. Plant Physiol **132**:1623-1630.

Benjamins,R., Quint,A., Weijers,D., Hooykaas,P., and Offringa,R. (2001). The PINOID protein kinase regulates organ development in Arabidopsis by enhancing polar auxin transport. Development **128**:4057-4067.

Benková,E., Michniewicz,M., Sauer,M., Teichmann,T., Seifertová,D., Jürgens,G., and Friml,J. (2003). Local, efflux-dependent auxin gradients as a common module for plant organ formation. Cell **115**:591-602.

Bennett,S.R.M., Alvarez,J., Bossinger,G., and Smyth,D.R. (1995). Morphogenesis in Pinoid Mutants of Arabidopsis-Thaliana. Plant Journal **8**:505-520.

Christensen,S.K., Dagenais,N., Chory,J., and Weigel,D. (2000). Regulation of auxin response by the protein kinase PINOID. Cell **100**:469-478.

Clough,S.J. and Bent,A.F. (1998). Floral dip: a simplified method forAgrobacterium-mediated transformation ofArabidopsis thaliana. The Plant Journal **16**:735-743.

Day,I.S., Miller,C., Golovkin,M., and Reddy,A.S. (2000). Interaction of a kinesin-like calmodulin-binding protein with a protein kinase. J.Biol.Chem. **275**:13737-13745.

Dela Fuente,R.K. and Leopold,A.C. (1973). A Role for Calcium in Auxin Transport. Plant Physiol **51**:845-847.

Felle,H. (1988). Auxin causes oscillations of cytosolic free calcium and pH in Zea mays coleoptiles. Planta **V174**:495-499.

Friml,J., Yang,X., Michniewicz,M., Weijers,D., Quint,A., Tietz,O., Benjamins,R., Ouwerkerk,P.B.F., Ljung,K., Sandberg,G., Hooykaas,P.J.J., Palme,K., and Offringa,R. (2004). A PINOID-dependent binary switch in apical-basal PIN polar targeting directs auxin efflux. Science **306**:862-865.

Friml,J., Vieten,A., Sauer,M., Weijers,D., Schwarz,H., Hamann,T., Offringa,R., and Jurgens,G. (2003). Efflux-dependent auxin gradients establish the apical-basal axis of Arabidopsis. Nature **426**:147-153.

Friml,J., Wisniewska,J., Benková,E., Mendgen,K., and Palme,K. (2002). Lateral relocation of auxin efflux regulator PIN3 mediates tropism in Arabidopsis. Nature **415**:806-809.

Furutani,M., Vernoux,T., Traas,J., Kato,T., Tasaka,M., and Aida,M. (2004). PIN-FORMED1 and PINOID regulate boundary formation and cotyledon development in Arabidopsis embryogenesis. Development **131**:5021-5030.

Galván-Ampudia,C.S. and Offringa,R. (2007). Plant evolution: AGC kinases tell the auxin tale. Trends Plant Sci. **12**.

Gehring,C.A., Irving,H.R., and Parish,R.W. (1990). Effects of auxin and abscisic acid on cytosolic calcium and pH in plant cells. Proc.Natl.Acad.Sci.U.S.A **87**:9645-9649.

Lee,S.H. and Cho,H.T. (2006). PINOID Positively Regulates Auxin Efflux in Arabidopsis Root Hair Cells and Tobacco Cells. Plant Cell **18**:1604-1616.

Masson,J. and Paszkowski,J. (1992). The Culture Response of Arabidopsis-Thaliana Protoplasts Is Determined by the Growth-Conditions of Donor Plants. Plant Journal **2**:829-833.

Memelink,J., Swords,K.M.M., Staehelin,L.A., and Hoge,J.H.C. (1994) Southern, Northern and Western blot analysis. In Plant Molecular Biology Manuel, (Dordrecht, NL: Kluwer Academic Publishers).

Michniewicz,M., Zago,M.K., Abas,L., Weijers,D., Schweighofer,A., Meskiene,I., Heisler,M.G., Ohno,C., Huang,F., Weigel,D., Meyerowitz,E.M., Luschnig,C., Offringa,R., and Friml,J. (2007). Phosphatase 2A and PID kinase activities antagonistically mediate PIN phosphorylation and apical/basal targeting in *Arabidopsis*. Cell **130**:1044-1056.

Okada,K., Ueda,J., Komaki,M.K., Bell,C.J., and Shimura,Y. (1991). Requirement of the Auxin Polar Transport System in Early Stages of Arabidopsis Floral Bud Formation. Plant Cell **3**:677-684.

Petrášek,J., Mravec,J., Bouchard,R., Blakeslee,J.J., Abas,M., Seifertová,D., Wisniewska,J., Tadele,Z., Kubes,M., Covanová,M., Dhonukshe,P., Skupa,P., Benková,E., Perry,L., Krecek,P., Lee,O.R., Fink,G.R., Geisler,M., Murphy,A.S., Luschnig,C., Zazimalova,E., and Friml,J. (2006). PIN Proteins Perform a Rate-Limiting Function in Cellular Auxin Efflux. Science **312**:914-918.

Reddy,A.S. and Day,I.S. (2000). The role of the cytoskeleton and a molecular motor in trichome morphogenesis. Trends Plant Sci. **5**:503-505.

Reddy,V.S., Day,I.S., Thomas,T., and Reddy,A.S. (2004). KIC, a novel Ca2+ binding protein with one EF-hand motif, interacts with a microtubule motor protein and regulates trichome morphogenesis. Plant Cell **16**:185-200.

Reinhardt,D., Pesce,E.R., Stieger,P., Mandel,T., Baltensperger,K., Bennett,M., Traas,J., Friml,J., and Kuhlemeier,C. (2003). Regulation of phyllotaxis by polar auxin transport. Nature **426**:255-260.

Sabatini,S., Beis,D., Wolkenfelt,H., Murfett,J., Guilfoyle,T., Malamy,J., Benfey,P., Leyser,O., Bechtold,N., Weisbeek,P., and Scheres,B. (1999). An auxin-dependent distal organizer of pattern and polarity in the Arabidopsis root. Cell **99**:463-472.

Sambrook,J., Fritsch F., and Maniatis,T. (1989) Molecular cloning - A laboratory Manual. C.Nolan, ed Cold Spring Harbor Laboratory press, NY, USA).

Shishova,M. and Lindberg,S. (2004). Auxin induces an increase of Ca2+ concentration in the cytosol of wheat leaf protoplasts. J Plant Physiol **161**:937-945.

Sundaresan,V., Springer,P., Volpe,T., Haward,S., Jones,J.D., Dean,C., Ma,H., and Martienssen,R. (1995). Patterns of gene action in plant development revealed by enhancer trap and gene trap transposable elements. Genes and Development **9**:1797-1810.

Tanaka,H., Dhonukshe,P., Brewer,P.B., and Friml,J. (2006). Spatiotemporal asymmetric auxin distribution: a means to coordinate plant development. Cell Mol.Life Sci. **63**:2738-2754.

Treml,B.S., Winderl,S., Radykewicz,R., Herz,M., Schweizer,G., Hutzler,P., Glawischnig,E., and Ruiz,R.A.T. (2005). The gene ENHANCER OF PINOID controls cotyledon development in the Arabidopsis embryo. Development **132**:4063-4074.

Weijers,D. and Jürgens,G. (2005). Auxin and embryo axis formation: the ends in sight? Curr.Opin.Plant Biol. **8**:32-37.

Weijers,D., Sauer,M., Meurette,O., Friml,J., Ljung,K., Sandberg,G., Hooykaas,P., and Offringa,R. (2005). Maintenance of embryonic auxin distribution for apical-basal patterning by PIN-FORMED-dependent auxin transport in Arabidopsis. Plant Cell **17**:2517-2526.

Weijers,D., Franke-van Dijk,M., Vencken,R.J., Quint,A., Hooykaas,P., and Offringa,R. (2001). An Arabidopsis Minute-like phenotype caused by a semi-dominant mutation in a RIBOSOMAL PROTEIN S5 gene. Development **128**:4289-4299.

Wesley,S.V., Helliwell,C.A., Smith,N.A., Wang,M., Rouse,D.T., Liu,Q., Gooding,P.S., Singh,S.P., Abbott,D., Stoutjesdijk,P.A., Robinson,S.P., Gleave,A.P., Green,A.G., and Waterhouse,P.M. (2001). Construct design for efficient, effective and high-throughput gene silencing in plants. The Plant Journal **27**:581-590.

Wisniewska,J., Xu,J., Seifertová,D., Brewer,P.B., Ruzicka,K., Blilou,I., Rouquié,D., Benková,E., Scheres,B., and Friml,J. (2006). Polar PIN localization directs auxin flow in plants. Science **312**:883.

Chapter 4

BT scaffold proteins: a crucial function in plant development

Hélène Robert, Ab Quint, Daan Brand, Adam Vivian-Smith, Remko Offringa

Abstract

BTB domain scaffold proteins are present in many organisms. In *Arabidopsis thaliana* they form a family of eighty proteins that have been implied in a variety of signaling pathways. We have identified the BTB and TAZ domain protein1 (BT1) as interactor and regulator of the PINOID (PID) kinase. BT1 has a typical domain structure that is only observed in land plants. Here we present a detailed functional analysis of the Arabidopsis *BT* family, which comprises five members, named BT1 to BT5, of which at least four are encoded by auxin responsive genes. BT1 is a short-lived protein, which characteristic as target for degradation by the 26S proteasome is linked to the BTB domain. Expression pattern, genomic structure and sequence alignment analyses indicate that BT1 and BT2 are close relatives that localize both to the nucleus and the cytosol, whereas BT4, BT5 and probably also BT3 are cytosolic. Detailed molecular and phenotypic analysis of plants segregating for loss-of-function mutations in the different *BT* genes shows that there is considerable functional redundancy among the *BT* members, and that BT function is crucial for early steps in both male and female gametophyte development. *BT2* is the dominant gene in this process, in which it is functionally replaced by *BT3* and also partially by *BT1* in *bt2* loss-of-function mutants, through reciprocal transcription regulation. This expression compensation is an important mechanism in the functional redundancy among *BT* genes. Based on our findings and recent data of other research groups we speculate that BT proteins, as regulators of PID activity, are likely part of a feed-back loop that affects auxin distribution.

Introduction

Effector proteins in basic cellular processes, such as protein kinases in signal transduction, transcription factors in gene expression and F-box proteins in protein degradation, act generally as part of a protein complex that is held together by one of more scaffold- or linker proteins. Although the importance of scaffold proteins has for a long time been undervalued, the finding that loss-of-function leads to lethality, for example for CULLIN1 and CULLIN3 (CUL3) in targeted proteolysis (Hellmann et al., 2003, Gingerich et al., 2005), Tic proteins in plastid biogenesis (Inaba et al., 2005) and the extensin RSH in cytokinesis (Hall and Cannon, 2002), has stressed their importance and revived the interest in them.

Scaffold proteins are characterized by their protein-protein interaction domains, which are conserved and form the basis of their classification. One of the largest families of scaffold proteins is formed by proteins that contain a so-called BTB domain. This domain mediates protein-protein interactions, and has first been identified in *Drosophila melanogaster* proteins that are part of Bric-à-brac, Tramtrack and Broad (BTB) protein

complexes of transcriptional regulators. It is also referred to as POZ domain because of its occurrence in many POx virus Zinc finger proteins (Albagli et al., 1995). Currently BTB proteins have been identified in many other eukaryotes including yeasts, *C. elegans*, mammals and plants (Bardwell and Treisman, 1994, Stogios et al., 2005).

The genomes of the model plants *Arabidopsis thaliana* and rice encode, respectively, 80 and 149 BTB proteins classified in ten subfamilies (Gingerich et al., 2005, Gingerich et al., 2007), of which only a few have been studied in detail. Most but not all Arabidopsis BTB proteins combine the BTB domain with at least one other protein-protein interaction domain that assigns a specific cellular function to these proteins. For example, the ankyrin and armadillo domains that are found in BTB proteins are involved in transcriptional regulation (Cao et al., 1997, Ha et al., 2004, Hepworth et al., 2005, Norberg et al., 2005), whereas the MATH and TPR domains in BTB/POZ-MATH, ETHYLENE OVERPRODUCER1 (ETO1) and ETO1-like proteins EOL1 and 2 form E3 ubiquitin protein ligase complexes with CUL3 that label proteins for degradation by the 26S proteasome (Wang et al., 2004, Dieterle et al., 2005, Gingerich et al., 2005, Weber et al., 2005). Furthermore, NON-PHOTOTROPIC HYPOCOTYL3 (NPH3) and Transcriptional Adaptor Zinc finger (TAZ) domains were found in scaffold proteins that organize protein complexes (Motchoulski and Liscum, 1999, Kemel Zago, 2006). These additional domains are not exclusive for BTB proteins, but are also found in other proteins. For example, the TAZ domain of the BTB and TAZ domain (BT) proteins (Du and Poovaiah, 2004) is also present in histone acetyltransferases of the p300/CREB binding protein (CBP) family. The CBP-type histone acetyltransferases 1, 2, 4, 5 and 12 are multidomain proteins with up to two TAZ and two ZZ zinger finger domains and a CBP-type histone acetyltransferase domain (Pandey et al., 2002). The TAZ and ZZ zinc finger domains are known to mediate protein-protein interaction with transcriptional factors (Ponting et al., 1996). Plant BTB proteins take part in a variety of cellular processes, such as phototropic responses for NPH3 (Motchoulski and Liscum, 1999), leaf and flower morphogenesis for BLADE-ON-PETIOLE1 and 2 (Ha et al., 2004, Hepworth et al., 2005, Norberg et al., 2005), and in the abscissic acid and ethylene responses for ARIA and for ETO1, EOL1 and EOL2, respectively (Wang et al., 2004, Kim et al., 2004).

The BTB domain protein BT1 (At5g63160) consists of an N-terminal BTB domain, a TAZ domain and a C-terminal Calmodulin Binding domain (CaMBD), a combination that is plant specific. We identified BT1 as an interacting partner of the protein serine/threonine kinase PINOID (PID), and we therefore initially named the protein PINOID BINDING PROTEIN2 (PBP2) (Benjamins, 2004). Besides BT1/PBP2, four other proteins with the same protein structure have been identified, namely BT2/PBP2H1 (At3g48360), BT3/PBP2H2 (At1g05690), BT4/PBP2H4 (At5g67480) and BT5/PBP2H3 (At4g37610) (Du and Poovaiah, 2004). All five BT proteins are interacting with the potato Calmodulin6 (CaM6) in a calcium-dependent manner through the CaMBD (Du and

Poovaiah, 2004), BT1, 2 and 4 were found to bind to the bromodomain proteins BET10 (Bromodomain and extraterminal domain protein), also called GTE11 (Global Transcriptional Factor group E), and BET9/GTE9 (Florence and Faller, 2001, Pandey et al., 2002, Du and Poovaiah, 2004). Besides PID, BT1 was found to interact with several transcriptional factors and cytoskeleton binding proteins (Kemel Zago, 2006). Furthermore BT2 seems to be part of a feed-back loop that enhances auxin responses, such as root growth inhibition or telomerase activation in vegetative tissues by exogenous auxin (Ren et al., 2007).

Here we present a detailed functional analysis of the BT family in Arabidopsis. We show that the expression of specific *BT* genes is upregulated in loss-of-function mutants of other *BT* family members. The subcellular localization of the BT proteins in Arabidopsis protoplasts is either nuclear, nuclear and cytoplasmic or only cytoplasmic, and correlates well with the presence of nuclear localization and export signals in the different BT proteins sequences. In addition, by generating plants containing multiple loss-of-function mutations in the different *BT* genes, we show that this protein family is essential for plant development. Both male and female gametophyte development relies on BT proteins, because strict segregation distortion and gametophyte development defects occurred in plants containing multiple mutations. *BT2* appeared to be the penultimate regulator of gametophyte and potentially plant development, as the absence of *BT2* could not be achieved in the quintuple loss-of-function mutant, nor in the *bt2 bt3* double mutant. Our results demonstrate that BT proteins play an essential role during megagametogenesis, and possibly throughout plant development.

Results

The BT protein family is land-plant specific

In *Arabidopsis thaliana*, the BT family comprises five members. Orthologues of the BT proteins are found in rice (Gingerich et al., 2007), Medicago, red clover, Solanaceae (SOL genomic network, http://www.sgn.cornell.edu) and Physcomitrella, but not in algae, yeast, fungi or animals, indicating that the domain structure of the BT family is restricted to land plants (Figure 1A).

A comparison of the amino acid sequences of BT1 homologues from *Arabidopsis* distinguishes three groups (Figure 1A) (Du and Poovaiah, 2004). The first group comprises BT1 and BT2, the second one BT3 and the last one BT4 and BT5. The sequence identity between the groups in *Arabidopsis* is between 38% and 49%. Interestingly, BT1 and BT2, as well as BT4 and BT5, are part of segmental genome duplications between chromosomes 3 and 5, and chromosomes 4 and 5, respectively (http://www.tigr.org/tdb/e2k1/ath1/duplication_listing.html), something that is reflected in

the exon/intron gene structure (Figure 1B), and suggests that these genes are likely to be functionally redundant. BT1 and BT2 possess, respectively, three and one nuclear localization signals (NLS: aa57-60, aa193-203 and aa342-345, PSORT prediction) (la Cour et al., 2004) and one and two leucine-rich Nuclear Export Signals (NES, NetNES prediction), whereas the three other BT proteins do not contain clear subcellular targeting signals.

Different studies indicate that BT proteins may act as scaffold proteins in various signaling pathways and may be functionally redundant (Du and Poovaiah, 2004, Kemel Zago, 2006, Ren et al., 2007). In order to further investigate the possible function of these proteins in Arabidopsis, lines with T-DNA- or transposon insertions in the corresponding genes were obtained from available collections and loss-of-function of the disrupted gene was verified. Phenotypic analysis indicated that all insertion mutants, shown to be complete loss-of-function, were indistinguishable from their parental wild type ecotype (Figures 1B-G and data not shown). These results corroborate the conclusion drawn from the BT family analysis that there is strong redundancy among BT family members.

Subcellular localization of BT proteins reflects the predicted nuclear im- and export signals

Up to now the subcellular localization of BT proteins have not been analyzed in detail. We therefore made a C-terminal fusion of BT1 to 5 with YFP, and transfected protoplasts. A C-terminal YFP fusion to BT1 transfected in Arabidopsis protoplasts showed that BT1:YFP is cytoplasmic in 38 % of the protoplasts (n = 21, Figure 2A), whereas it is both cytosolic and nuclear in 62 % of the protoplasts (Figure 2B). The predominant BT1 nuclear localization is in line with previous localization studies using tobacco BY-2 cells (Du and Poovaiah, 2004). When the C-terminal YFP fusions for BT2 was expressed in Arabidopsis protoplasts, 90 % (n = 31) of the cells showed cytoplasmic localization (Figure 2C), and 10 % of the cells showed both nuclear and the cytosolic localization (Figure 2D). The less predominant nuclear localization of BT2 compared to BT1 reflects the ratio of NLSs and NESs, which is 3:1 in the case of BT1, and 2:2 in the case of BT2 (Figure 1B), and confirms the functionality of the NLS and NES in BT1 and BT2 (Figure 1B). BT4:YFP and BT5:YFP were only found in the cytoplasm (n = 40 and 33, respectively, Figures 2E and 2F), corresponding to the fact that no NLS is found in these proteins. Western blot analysis showed the integrity of the protoplast expressed BT:YFP fusion proteins (Figure 2H). Unfortunately, we were not able to clone the *BT3* cDNA to complete this analysis, but based on the absence of predicted NLS (Figure 1) we expect this protein to be cytosolic.

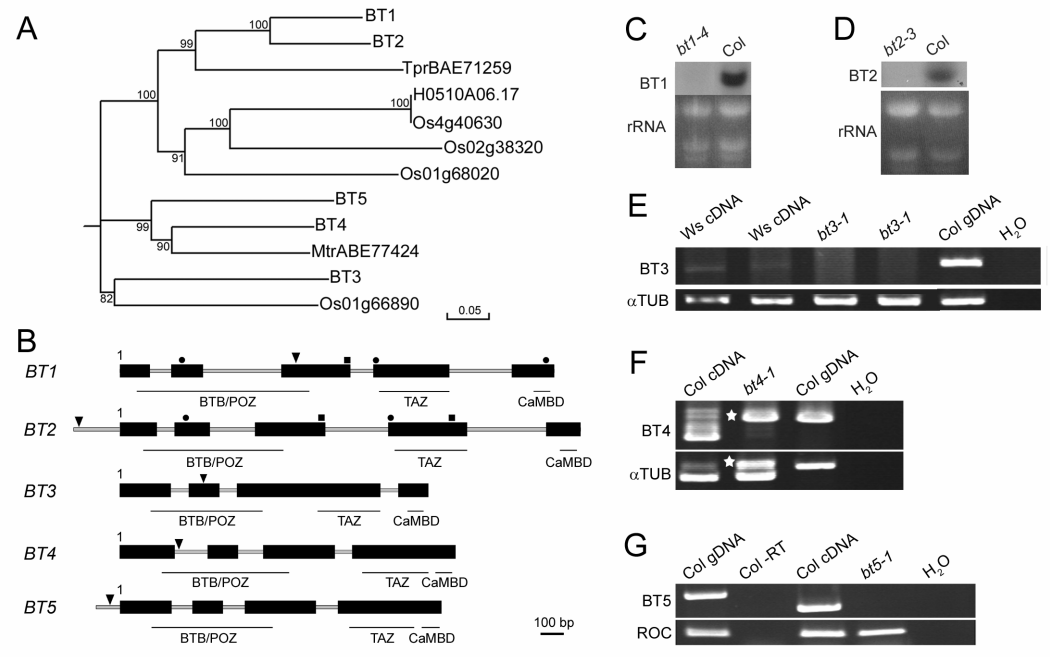


Figure 1. The Arabidopsis BT family comprises 5 members that classify into three groups.

(A) Phylogenic tree showing the relationship between BT1, its four *Arabidopsis* homologous and its orthologues from Rice (Japonica nipponbare and Indica cultivars), *Medicago truncatula* and *Trifolium pratense*. The tree is based on an alignment of the protein sequences using ClustalW and is constructed using the Neighbor-Joining method with a Bootstrap test of 10 000 iterations.

(B) The structure of the five *BT* genes is depicted. The black boxes represent the exons. The parts encoding the N-terminal BTB domain, the TAZ domain and the C-terminal CaMBD are underlined. The positions of predicted Nuclear Localization Signals (NLSs, PSORT prediction) and of the leucine-rich Nuclear Export Signals (NESs, NetNES prediction) are indicated by a circle and a square, respectively. For BT1, three NLSs and one NES are found at positions aa57-60, aa193-203, aa342-345 and aa181-183, respectively. For BT2, two NLSs and two NESs are found at position aa65-81, aa203-212 and aa191-197, aa294-302, respectively The position of the T-DNA or transposon insertion is indicated by a black arrowhead for each gene: *bt1-4* (GT2847), *bt2-3* (SALK_084471), *bt3-1* (Flag_396E01), *bt4-1* (SALK_045370) and *bt5-1* (GABI-Kat 771C08) at position +748 bp, -173 bp, +357 bp, +430 bp and -42 bp relative to the ATG.

(C-G) Northern blots (C, D) and RT-PCR (E-G) analyses on 8-day old seedlings showing the complete loss-of-function of the mutant alleles used in this study for BT1 (C), BT2 (D), BT3 (E), BT4 (F), BT5 (G). Positive controls are the Col and Ws cDNA and genomic DNA (gDNA). Negative controls are a reverse transcription reaction in which the enzyme was omitted (Col -RT) and water (H_2O). rRNA, αTubulin and ROC expression were used as loading controls. Note that for the *bt4-1* sample, some genomic DNA contamination was amplified (stars) but not the cDNA.

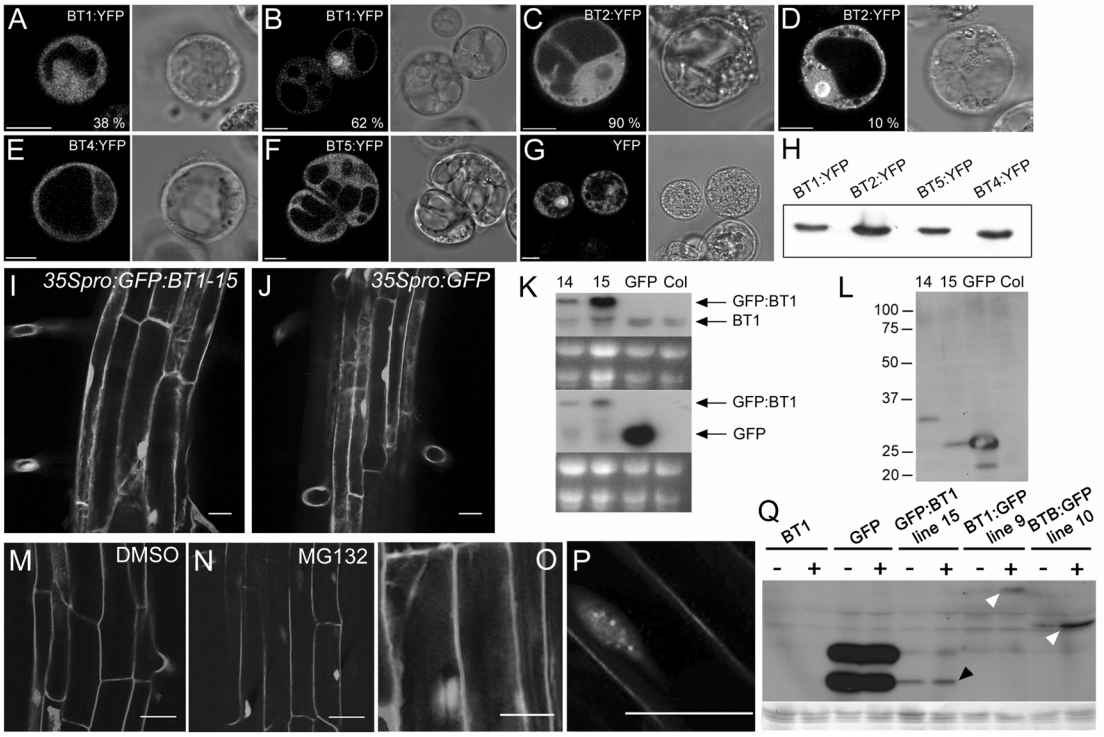


Figure 2. The subcellular localization of Arabidopsis BT proteins.

(A-G) A confocal fluorescent image (left) and the corresponding transmitted light image (right) of Arabidopsis protoplasts expressing C-terminal YFP:HA fusions of BT1 (A, B), BT2 (C, D), BT4 (E) and BT5 (F), or YFP:HA alone (G). For BT1:YFP and BT2:YFP, the percentage of cells showing cytoplasmic (A, C) or both cytoplasmic and nuclear localization (B, D) is indicated. The scale bars represent 10 µm.

(H) Western blot analysis of extracts of cells shown in (A-F) with an anti-HA confirms the expression of full-length BT:YFP fusion proteins.

(I, J) Confocal images of root epidermal cells of the lines *35Spro:GFP:BT1-15* (I) and *35Spro:GFP* (J) show identical cytoplasmic and nuclear localized GFP signal.

(K) Northern blot analysis with the *BT1* (top) or the *GFP* probe (bottom) shows that a full-length *GFP:BT1* mRNA is produced in *35Spro:GFP:BT1* lines 14 and 15.

(L) Western blot probed with anti-GFP antibodies showing that the strong fluorescent signal in lines *35Spro:GFP:BT1-14* and *-15* is caused by respectively a partial GFP:BT1 fusion (30 kDa) or unfused GFP (27 kDa; GFP:BT1 is 69 kDa).

(M-P) BT1:GFP is detected in line *35Spro:BT1:GFP-9* after 4 h of MG132 treatment (N-P), but not in the DMSO treated control (M). MG132 treatment results in a GFP signal in both the cytoplasm (N, O) and the nucleus (N, P).

(Q) Western blot analysis using anti-GFP antibodies confirming the instability of the BT1:GFP and BTB:GFP fusions. Samples were treated 4 h with MG132 (+) or DMSO (-). Plants overexpressing BT1 or GFP were used as negative and positive controls, respectively. Note that the stability of the GFP protein in line *GFP:BT1-15* is not enhanced by MG132 treatment (black arrow head), whereas the full length C-terminal fusions become more abundant after MG132 treatment (white arrow heads).

Scale bars are 10 µm in (A-G) and 20 µm in (I, J, M-P).

BT1 is a short-lived protein in Arabidopsis

Next, we generated stable transformants using both *35Spro:BT1:GFP* and *35Spro:GFP:BT1* constructs. For each construct at least twenty-five independent T2 lines were generated and studied. All lines showed wild-type phenotypes, and none of the *35Spro:BT1:GFP* lines and only few of the *35Spro:GFP:BT1* lines showed a clear cytosolic fluorescent signal in the root (Figure 2I), resembling that of soluble GFP (Figure 2J). Further analysis demonstrated that no full-length fusion protein could be detected in these GFP positive lines, even though a full-length *GFP:BT1* mRNA was produced (Figures 2K and L). The above result together with the lack of fluorescent signal in all the lines carrying the C-terminal fusion (Figure 2M) suggested to us that BT1 and the BT1:GFP fusions were unstable. To test this, seedlings expressing BT1:GFP were treated with the 26S proteasome inhibitor MG132. After 4 hours of treatment, a fluorescent signal was observed both in the nucleus and the cytoplasm of root cells of different lines (Figures 2N-P). Under higher magnification, the nuclear localization was not uniform but consisted of bright dots (Figure 2P) possibly corresponding to MG132-stabilized BT1:GFP present in nuclear bodies of the ubiquitin-proteasome pathway (Tao et al., 2005). Western blot analysis confirmed the presence of the full-length fusion protein in the MG132 treated samples (Figure 2Q). Although the fusion protein in untreated samples could be detected by Western blot, the amount was not sufficient to be observed by confocal microscopy. Different treatments with auxin or auxin transport inhibitors did not influence the stability, nor the subcellular localization of the BT1:GFP fusion protein in the MG132-treated samples (data not shown). Fluorescent microscopy on other tissues than the root (leaves, inflorescences) did not identify tissue-specific stabilization of the BT1:GFP fusion. In conclusion, our *in planta* results indicate that BT1 is a short-lived target for the 26S proteasome pathway, and that this predominantly nuclear protein is also present in the cytoplasm.

Also plants overexpressing a C-terminal fusion of the BTB domain of BT1 with GFP (*35Spro:BTB:GFP*) were indistinguishable of wild type plants. The BTB:GFP fusion protein, like BT1:GFP, was not detectable by confocal microscopy or Western blotting in untreated plants, but could be stabilized by MG132 treatment (Figure 2Q). The subcellular localization of stabilized BTB:GFP is identical to that observed for BT1:GFP (Figures 2M-P), showing predominant nuclear (the NLSs aa57-60 and aa192-203 are included in the fusion) but also cytoplasmic localization (data not shown). These data corroborate our observations that BT1 is an inherently unstable protein, and indicate that its proteasome-mediated degradation is linked to the N-terminal BTB domain-containing part of the protein.

"Expression compensation" among BT family members possibly mediated by auxin

In addition to the subcellular localization of the BT proteins, we investigated the expression of Arabidopsis *BT* family members by Northern blot analysis (Figure 3A). The four *BT* genes analyzed are most abundantly expressed in rosette leaves. *BT1 and BT5* are also strongly expressed in stems, and at low levels in the other tissues tested. *BT2* is highly expressed in seedlings, whereas *BT4* is strongly expresses in flowers and siliques.

Interestingly, *bt1-4* loss-of-function caused a clear increase of expression of *BT2* and *BT5* in seedlings, roots, stems and flowers, whereas *BT4* expression was enhanced in stems. Likewise, *bt2* loss-of-function enhanced the expression of *BT1* and *BT5* in roots, whereas *BT5* expression in stems was significantly reduced (Figure 3A). The observed *bt* loss-of-function induced changes in gene expression of *BT* family members indicates that the genes are under reciprocal transcription regulation, where the expression of one gene has a direct compensatory effect for the loss of another *BT* gene expression. This could be through a direct effect of the BT proteins on the transcription of the other BT family members, or through indirect feed-back control on *BT* expression.

Recently, evidence was presented that BT2 potentiates auxin responses (Ren et al., 2007), and this opens the possibility that the feed back control on *BT* expression is mediated by auxin. We therefore tested whether the *BT* genes are auxin responsive. *BT1*, *BT2* and *BT5* showed a rapid and transient induction of expression, at different strength levels, with a peak at 30 minutes after auxin (IAA) treatment. *BT4* expression was also enhanced at this time point, but the RNA levels increased until 4 hours, and enhanced levels persisted at least until 24 hours after auxin treatment (Figure 3B). These results indicate a clear link between auxin signaling and *BT* gene expression, and suggest that the reciprocal transcription regulation within the *BT* gene family is at least in part mediated by feed back control on auxin signaling.

BT proteins are essential for gametophyte development

Since the single loss-of-function mutants did not show a phenotype, mutant combinations were generated to bypass the possible functional redundancy of the BT proteins and show their relevance for plant development. Unfortunately, the different combinations of double and triple mutants produced were indistinguishable from wild type (data not shown). To definitively establish or distinguish whether BT proteins are essential for plant development, the generation of a quintuple mutant was initiated by crossing a triple, *bt1 bt2 bt4*, and a double mutant, *bt3 bt5*. In the progeny of this cross, only two combinations of homozygous quadruple mutants out of the five possible could ever be obtained: *bt1 bt2 bt4 bt5* and *bt1 bt3 bt4 bt5*. This implied that quadruple mutants where *bt2* and *bt3* alleles were both homozygous could not be obtained. Furthermore in an attempt to identify the quintuple loss-of-function mutant, only *bt1 bt2/+ bt3/+ bt4 bt5* and *bt1 bt2/+ bt3 bt4 bt5*

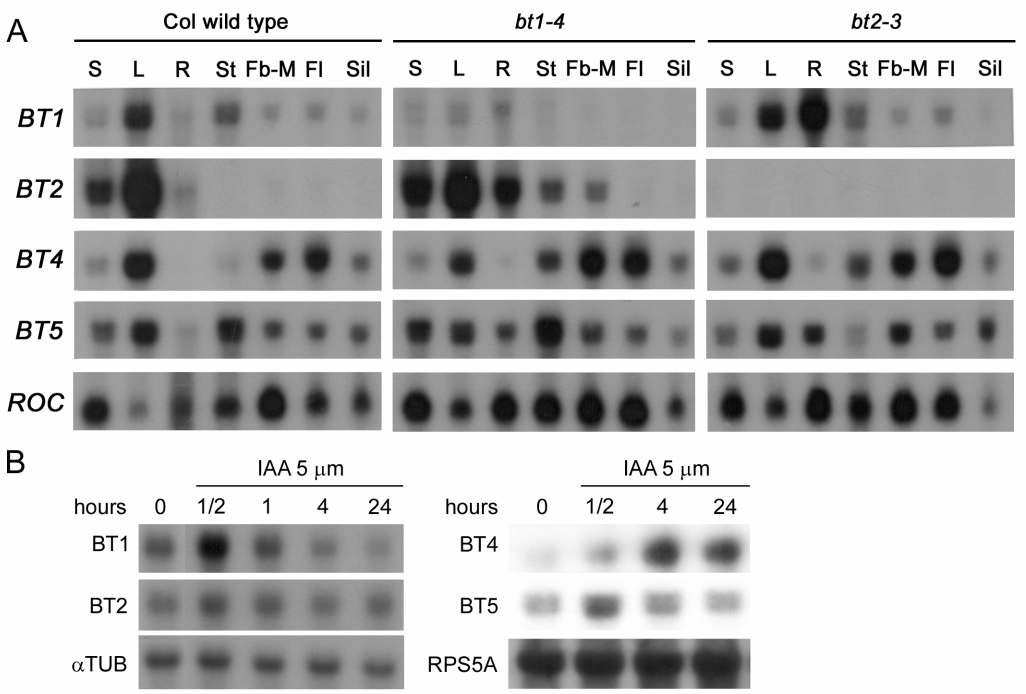


Figure 3. *BT* gene expression shows reciprocal transcriptional regulation

(A) Northern blot analysis of the expression pattern of four of the *BT* genes (*BT1*, *BT2*, *BT4*, *BT5*) in 8-day old seedlings (S), or rosette leaves (L) and roots (R) of 3-week old seedlings or stems (St), flower buds and inflorescence meristems (Fb-M), flowers (Fl) and siliques (Sil) from 6-week old plants of Col wild-type (right), *bt1-4* (middle) and *bt2-3* (left). The *ROC* expression was used as control. The blots probed with *BT1* and *BT2* were exposed overnight, with *ROC* for 48 hours and with *BT4* and *BT5* for 72 hours.

(B) Northern blot analysis of the BT gene expression (*BT1, BT2, BT4, BT5*) after auxin (5 μm IAA) treatment for the indicated time. The *αTubulin* and *RPS5A* expression were used as control. The blot probed with *BT1* was exposed for 48 hours, with *BT2* for 6 hours, with *BT4*, *BT5*, *αTubulin* and *RPS5A* for 16 hours.

were obtained. As *BT2* and *BT3* are located on chromosomes 3 and 1, respectively, physical linkage can not explain the absence of seedlings carrying both insertion alleles. The self-pollinated population of *bt1 bt2/+ bt3/+ bt4 bt5* was screened in order to analyze the observed segregation distortion. In over 200 seedlings that were screened from this genotype (Table 1), neither quintuple homozygous mutants, nor *bt1 bt2 bt3/+ bt4 bt5* seedlings were found. As the expected segregation ratio for these genotypes is 1/16 and 2/16, respectively, their absence from the test population is highly significant. Furthermore, quadruple mutants homozygous wild type for either *BT2* or *BT3* were obtained in a higher proportion than expected (25 % and 15 % against 6.3 %, respectively, Table 1). Allele frequencies for the other possible genotypes were in range with the expected ratios.

Table 1. Segregation ratio of the progeny of the quintuple *bt1 bt2/+ bt3/+ bt4 bt5* mutant.

bt1 bt2/+ bt3/+ bt4 bt5 progeny	observed proportion	expected proportion
bt1 bt2 bt3 bt4 bt5	**0 %**	**6.3 %**
bt1 bt2 bt3/+ bt4 bt5	**0 %**	**13 %**
bt1 bt2 BT3 bt4 bt5	**15 %**	**6.3 %**
bt1 bt2/+ bt3 bt4 bt5	**8 %**	**13 %**
bt1 bt2/+ bt3/+ bt4 bt5	32 %	25 %
bt1 bt2/+ BT3 bt4 bt5	10 %	13 %
bt1 BT2 bt3 bt4 bt5	**25 %**	**6.3 %**
bt1 BT2 bt3/+ bt4 bt5	**6 %**	**13 %**
bt1 BT2 BT3 bt4 bt5	5 %	6.3 %

Based on this analysis we hypothesized that it is impossible to produce gametes containing both *bt2* and *bt3* loss-of-function mutations. To confirm this hypothesis, reciprocal backcrosses between *bt1 bt2/+ bt3/+ bt4 bt5* and Col wild type were analyzed. Genotyping of the F1 progeny of the two reciprocal backcrosses showed a segregation ratio of 1:2:1 for the gamete genotypes *BT2 bt3* : *BT2 BT3* : *bt2 BT3* (n = 96, Chi-square < 9.348 for p = 0.01 in both cases), whereas the *bt2 bt3* genotype was never found. The results suggest that the mutations do not lead to embryo arrest, since plants heterozygous for both mutations are fully viable, and indicate that the single *bt2* and *bt3* mutations hamper gametophyte development, thus leading to segregation distortion, and that megagametogenesis and microsporogenesis, respectively female and male gametophyte development, arrest when both loss-of-function mutations are present. Similar segregation ratios have been observed for other mutations affecting both male and female gametophyte development (Yadegari and Drews, 2004).

To confirm the results of the segregation and backcrosses analyses, embryo and ovule development was studied in *bt1 bt2/+ bt3/+ bt4 bt5* plants. Cleared siliques of *bt1 bt2/+ bt3/+ bt4 bt5* showed empty spaces (Figures 4A and 4C), whereas *bt1 bt3 bt4 bt5* siliques contained full seed set (Figures 4A and 4B). Closer inspection showed that in *bt1 bt2/+ bt3/+ bt4 bt5* siliques, about 70 % of the ovules were not fertilized and desiccated, and that the seed set in these plants was reduced to 30 % (Figure 4C and Table 2). The embryos and endosperm in the seeds that succeeded to develop were normal (data not shown). All these data are consistent with two mutations affecting female gametophyte development (Christensen et al., 1998). As a result of the reduced seed set, the silique length was significantly reduced in *bt1 bt2/+ bt3/+ bt4 bt5* plants (8.7 mm +/- 1.6 mm, n = 7), compared to Col wild type (15 mm +/- 1.3 mm, n = 5, Student's t-test, $p < 0.01$) or *bt1 bt3 bt4 bt5* plants (14.6 mm +/- 1.7 mm, n = 5, Student's t-test, $p < 0.01$) (Table 3).

Table 2. Seed set in the different mutant combinations.

	seeds per silique(%)[1]	s. d.	n
Col	96.5	3.8	2
bt2	95.8	4.1	4
bt1/+ bt2	92	9.2	1
bt1 bt2/+	**50.1**	10.5	5
bt1 bt2	98.3	2.8	2
bt1 bt5	98.8	1.4	1
bt1 bt2 BT3 bt4 bt5	93.6	5.7	11
bt1 BT2 bt3 bt4 bt5	96.6	5.2	7
bt1 bt2/+ bt3/+ bt5	**31.4**	10.1	3
bt1 bt2/+ bt3/+ bt4 bt5	**30**	6	10

[1] mean of the developed seeds versus total seed per silique for four siliques per plant

Table 3. *bt* mutant has a reduced silique length.

	silique length (mm)*	s. d.	n
Col	15	1.3	5
bt1 BT2 bt3 bt4 bt5	14.6	1.7	5
bt1 bt2/+ bt3/+ bt4 bt5	8.7[*] [†]	1.6	7

[*] Significantly different from Col wild type (Student's t-test, $p < 0.01$)

[†] Significantly different from *bt1 BT2 bt3 bt4 bt5* (Student's t-test, $p < 0.01$)

BT function essential during early stages of female gametophyte development

To analyze during which stages of megagametogenesis BT function is essential, we searched mature ovules at terminal development stage (FG7) (Christensen et al., 1997) for aberrant morphology of the female gametophyte. Unfertilized ovules were dissected out of emasculated carpels and observed by confocal microscopy after propidium iodide staining. Wild type gametophytes are highly polarized structure made of seven cells (Figures 4D and 4E). At the micropyle pole (bottom on Figures 4D-J), two synergid cells are surrounding the egg cell. The nuclei of the synergids are facing the micropyle whereas the nucleus of the egg cell is located toward the chalazal pole (top left on Figures 4D-J). In the middle of the gametophyte, a bi-nucleate cell with a huge vacuole is forming the central cell composed of two fused nuclei, called polar nuclei, facing the egg cell. Three remaining cells, the antipodal cells, are located at the chalazal pole and will degenerate during the final stages of megagametogenesis (Figures 4D and 4E) (Christensen et al., 1997, Drews and Yadegari, 2002).

In the quintuple *bt1 bt2/+ bt3/+ bt4 bt5* gynoecium, besides wild type gametophytes, three different mutant phenotypes were observed. First, gametophytes with unfused polar nuclei

were found (9 out of 42 [counts include the wild type phenotype] counted on two siliques, Figures 4F and 4G). Unfused polar nuclei can also be found in immature gametophytes (stage FG5) and in mutants of the category 4 such as *magatama1* and *3*, *gametophytic factor2* (*gfa2*), and *gfa3* (Christensen et al., 1998, Shimizu and Okada, 2000, Drews and Yadegari, 2002) or seed shortly after fertilization (stage F2) (Faure et al., 2002). Therefore either these ovules are delayed in growth, or their polar nuclei failed to fuse. In some other gametophytes, the synergid cells were collapsed (7 out of 42, Figure 4H). Collapse of the synergid cells does not occur if pollination is prevented, but it is usually observed at the time of, or shortly before, the fertilization in wild type seeds due to the pollen tube penetration and discharge of the sperm cells (Faure et al., 2002). Viable synergid cells are required for the pollen guidance and attraction to the gametophyte for a proper fertilization (Higashiyama et al., 2001). The segregation distortion observed in *bt1 bt2/+ bt3/+ bt4 bt5* plants may in part be explained by a reduction of the pollen tube attraction due to the collapsed synergid cells in some of the gametophytes. Finally the last and more striking phenotype was a total absence of gametophyte (19 out of 42 [7 out of 42 were n/a], Figures 4I and 4J) and the presence of some degenerated structures instead of the synergid cells, suggesting that the defect occurred very early during the megagametogenesis. Based on the segregation ratios of this last phenotype, it is likely that the quintuple *bt* loss-of-function mutant belongs to the category 1 of gametophytic mutations, such as *gfa4, gfa5*, *female gametophyte2* and *3* (Christensen et al., 1998, Drews and Yadegari, 2002) , where the mutants are affected at the earliest step of the gametophyte development and do not progress after the one-nuclei stage (FG1) (Christensen et al., 1997). The presence of the BT proteins seems to be essential during early stages of female gametophyte development. The male gametophyte development was not analyzed in detail but according to the results obtained in the backcrosses analysis, it is likely that BT function is also essential during early stages of male gametophyte development.

BT2 ***acts redundantly with*** **BT3** ***and*** **BT1** ***during female gametophyte development***

Because it appeared that the gametophytic phenotype in the quintuple *bt* mutant was caused by the absence of *BT2* and *BT3* expression, as the combination of *bt2* and *bt3* loss-of-function could not be obtained, we analyzed more in detail whether the female gametophyte development was also impaired in the different mutant combinations we had generated. Reduced seed set and shorter siliques were observed in *bt1 bt2/+, bt1 bt2/+ bt3 bt4 bt5 and bt1 bt2/+ bt3/+ bt5* plants (Table 2), indicating that the phenotype is more strongly linked to *bt2* loss-of-function. Interestingly, however, the siliques were full in the quadruple *bt1*

Figure 4. (continued)
small arrow), or is completely absent except for a white fluorescent structure at the micropyle pole (I,J). MC: micropyle pole, CHZ: chalazal pole, PN: polar nuclei, EC: egg cell, Sy: synergid cell, UPN: unfused polar nuclei, CSy: collapsed synergids. Scale bars represent 20 µm.

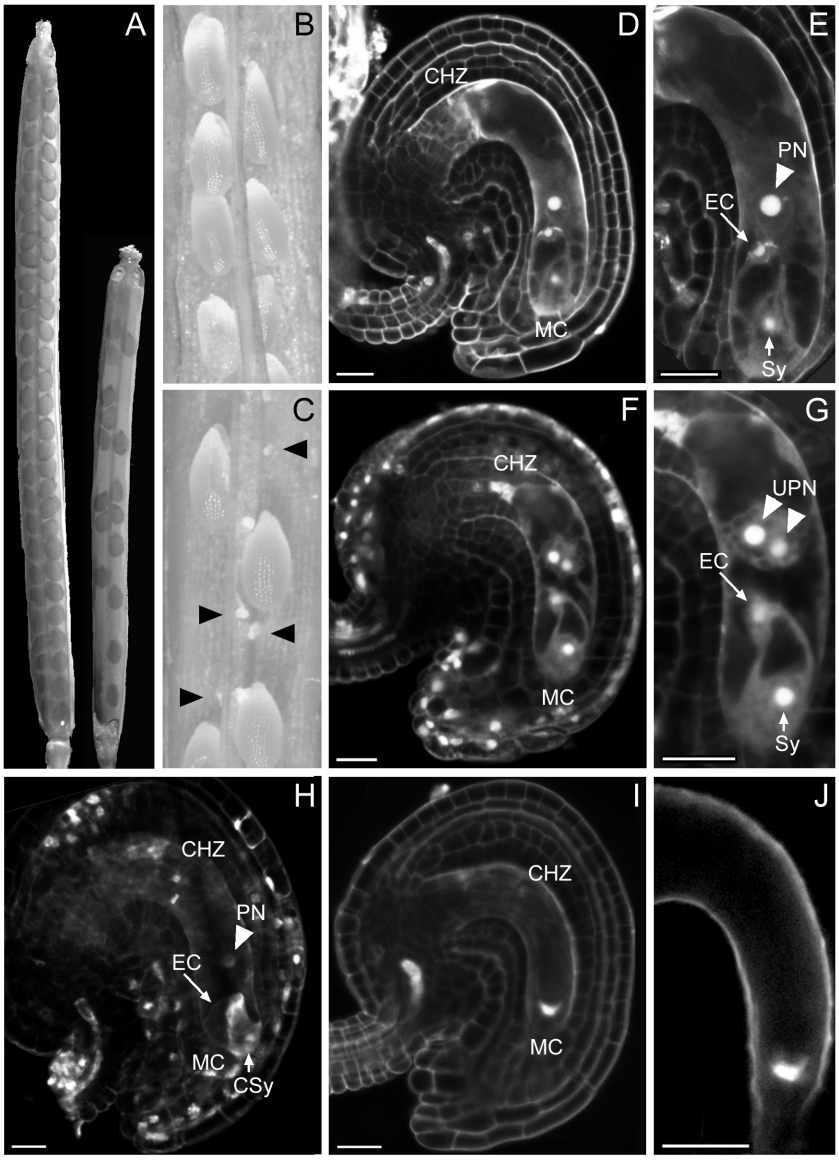


Figure 4. *bt* loss-of-function is gametophytic lethal.

(A) Cleared siliques of a *bt1 bt2*/+ *bt3*/+ *bt4 bt5* plant (right) show many random empty positions, whereas a silique of a *bt1 bt3 bt4 bt5* plant (left) shows full seed set. Note that the *bt1 bt2*/+ *bt3*/+ *bt4 bt5* silique is significantly shorter than the one with full seed set.

(B-C) Details of opened siliques of a *bt1 bt3 bt4 bt5* plant (B) and a *bt1 bt2*/+ *bt3*/+ *bt4 bt5* plant (C). The empty spaces in the quintuple mutant are from unfertilized ovules, as indicated by the dried and white structures (black arrowheads).

(D-J) Confocal sections of unfertilized female gametophytes at mature stage (FG7) stained with propidium iodide. (D, E) Mature wild type female gametophytes are characterized by fused polar nuclei (arrowhead), the egg cell (large arrow) and synergid cells (small arrow). (F-J) *bt1 bt2*/+ *bt3*/+ *bt4 bt5* ovules in which the female gametophyte shows unfused polar nuclei (double arrowheads) in the central cell (F,G), collapsed synergid cells (H,

bt2 bt4 bt5, suggesting in this case that *BT3* is the redundant copy of *BT2*.

To test whether *BT2* and *BT3* are the crucial and redundant *BT* genes during female gametophyte development, the progeny of a cross between *bt2* and *bt3* were analyzed. Remarkably, only crosses with *bt3* as pollen donor and *bt2* as ovule acceptor did lead to germinating seeds. The short silique and reduced seed set phenotypes were observed in 14 plants out of 20 of the F2 progeny of *bt2/+ bt3/+* F1 plants (not shown). This corroborates our hypothesis that the absence of these two genes is sufficient to induce defective female gametophyte development, and also indicates that the three other *bt* genes are not able to fully complement the double mutant. The 14 plants showing the phenotype were double heterozygous for *bt2* and *bt3*. The 6 remaining wild type looking F2 plants were homozygous for one of the *bt* mutations and wild type for the other *BT* gene, confirming that the two mutations can only coexist in one plant when heterozygous.

Interestingly, when we compared seed set in *bt2*, *bt1 bt2* or *bt1 bt2/+* plants, the first two mutants showed full siliques, whereas the seed set was reduced to 50 % in *bt1 bt2/+* plants (Table 2). These results indicate that expression compensation by *BT1* (Figure 3) is needed to functionally replace BT2 in the *bt2/+* background. Apparently, the *bt2/+* heterozygous situation is not sufficient to trigger the full expression compensation by *BT3* that is clearly observed in the *bt1 bt2* double and *bt1 bt2 bt4 bt5* quadruple mutant plants. As suggested by the possibility to get the double homozygous *bt1 bt2* mutant and by the segregation analysis of the quintuple mutant *bt1 bt2/+ bt3/+ bt4 bt5*, the penetrance of the gametophytic phenotype is partial in double, triple and quadruple mutants because of functional redundancy, until the complete gene family is knocked out. Then the phenotype is fully penetrant and gametophytic lethal.

Discussion

BTB domain proteins form a large family of scaffold proteins that are found in a wide range of organisms. Here we studied the function of a specific subfamily, the BT proteins, in Arabidopsis. Based on their structure BT proteins are land plant-specific BTB domain proteins. Previous work indicated that these proteins are multi-functional scaffolds that interact with a variety of other proteins such as a protein kinase, transcriptional factors and cytoskeleton motor proteins (Du and Poovaiah, 2004, Kemel Zago, 2006). BT2 was found to be involved in the induction of the telomerase activity ((Du and Poovaiah, 2004, Kemel Zago, 2006, Ren et al., 2007). In addition, we have shown that PBP2/BT1 interacts with and regulates the activity of PID, a protein kinase that directs the transport of the plant hormone auxin (Chapter 5, this thesis, Friml et al., 2004). Here we present a detailed functional analysis of the Arabidopsis *BT* gene family, and demonstrate that there is considerable functional redundancy among the family members. Detailed analysis of

Arabidopsis plants segregating loss-of-function mutations of the five *BT* genes indicated that the BT proteins are essential for gametophyte development, and probably also for other stages of plant development.

Redundancy of the BT proteins

Since the loss-of-function allele *bt1-4* is wild type looking, functional redundancy among the BT protein family was hypothesized and demonstrated using expression pattern analysis and a genetic analysis with T-DNA/transposon insertion lines. First, each of the *BT* genes is expressed in a large panel of tissues where their respective expression pattern overlaps rather than being tissue-specific. Secondly, these expressions are cross-regulated within the gene family, since in the loss-of-function mutants *bt1-4* and *bt2-3*, the absence of *BT1* and *BT2* expression, respectively, is compensated by the other functional family members, which may explain the absence of phenotype in these mutants. Similar redundancy and cross-regulation of gene expression have previously been observed for the *PIN* auxin efflux carrier gene family (Vieten et al., 2007). For the *PIN* genes, expression compensation is achieved via their auxin responsiveness, since *pin* loss-of-function leads to alterations in auxin distribution. The *BT* genes were also found to be auxin responsive, and given that BT2 was found to alter auxin responses, and that BT1 to regulate the activity of PID (Chapter 5, this thesis), a protein kinase regulating auxin transport, it is likely that the reciprocal transcriptional regulation of the *BT* genes is auxin-controlled. Finally, to get insight in the function of the BT proteins, single insertion lines which disrupt gene expression of each of the five genes were isolated. None of them as well as combinations of double, triple or quadruple mutants with *bt1-4*, *bt3-1*, *bt4-1* and *bt5-1* resulted in mutant phenotypes. Combinations with *bt2-3* showed an alteration in the gametophyte development which was fully penetrant only when the *bt3-1* mutation was present. A total absence of the BT proteins in the plant is lethal since it results in an absence of female gametophyte formation. These data together indicate that the BT protein family is able to compensate for the lost of one of the family members and is functionally redundant.

***Impaired gametophytic development in* bt1 bt2/+ bt3/+ bt4 bt5**

Our attempt to knock-out BT function using Arabidopsis plants segregating for multiple *bt* loss-of-function mutations demonstrated that the BT2 protein is essential for female and male gametophyte development, and that in the mutant background either *BT1* or *BT3* can compensate for *bt2* loss-of-function. *bt2* loss-of-function could co-exist with the *bt3-1* allele in plant only in the heterozygous state, but their co-occurrence in the haploid megaspore resulted in an aberrant gametophyte development (Drews and Yadegari, 2002). Ovules are developed from a diploid megaspore that undergoes meiosis giving rise to four haploid megaspores from which three die. The remaining one (stage FG1) follows three round of mitosis and becomes an eight-nucleate cell (stage FG5), which, after nuclear

migration and fusion, and cellularization, turns into a seven-cell structure (stage FG7) (Christensen et al., 1997). Segregation of *BT2* and *BT3* in *bt1 bt2/+ bt3/+ bt4 bt5* gave rise to four different kinds of female gametophytes: (1) wild type looking, presumably derived from *bt1 BT2 BT3 bt4 bt5* megaspores; (2) with unfused polar nuclei and (3) with collapsed synergid cells, presumably derived from *bt1 BT2 bt3 bt4 bt5* or *bt1 bt2 BT3 bt4 bt5* megaspores*;* and (4) with an empty embryo sac, most likely derived from *bt1 bt2 bt3 bt4 bt5* megaspores. According to the segregation analysis, it seems likely that the three first phenotypes are able to develop normally to give fertile ovules, whereas the last one collapsed. Additional backcrosses analysis indicated that it is likely that the pollen microspore with *bt1 bt2 bt3 bt4 bt5* haplotype is not able to develop either. Together these data suggest that the BT proteins are essential during female and male gametophyte development, probably as early as the first meiosis.

BT proteins and the telomerase activity in gametes

Recently, the *BT2* gene has been shown to be directly and specifically induced by TELOMERASE ACTIVATOR1 (TAC1) transcriptional factor, indicating that BT2 is required for the activation of the telomerase activity in Arabidopsis mature leaves (Ren et al., 2007). Telomerases are enzymes that synthesize and maintain telomeric DNA at the end of the chromosomes, mainly during the transition between the vegetative to reproductive phase, meaning in the gametophytes (Riha and Shippen, 2003). Telomerase activity is usually absent in leaves but can be induced by exogenous auxin as well as by TAC1 overexpression (Ren et al., 2004). And BT2 is sufficient and necessary to stimulate TAC1-dependent telomerase activity in leaves by inducing the expression of *Arabidopsis thaliana TELOMERASE REVERSE TRANSCRIPTASE* (*ATTERT*) (Ren et al., 2007). One hypothesis could be that the gametophyte phenotype observed in the quintuple *bt* mutant is caused by the absence of telomerase activity. However, Arabidopsis *attert* mutants can survive up to the tenth generation without telomerase activity, during which they accumulate phenotypes from leaf morphology aberration at the sixth generation to vegetative termination at the tenth generation (Riha et al., 2001). In contrast, *bt1 bt2/+ bt3/+ bt4 bt5* plants are initially wild type looking, but their defected gametophyte development eventually causes a reduction in seed set and silique length. Quintuple homozygous plants could not be produced. Hence the gametophyte lethality observed in the quintuple homozygous *bt* mutant was probably not the direct result of the absence of activation of *ATTERT* expression by BT2, but rather the consequence of a more general function of these proteins as scaffolds in a variety of signaling pathways.

BT proteins are multifunctional scaffold proteins

Functional analyses of some BTB proteins in yeast and *C. elegans* indicated that these proteins are involved in targeting proteins for degradation as part of CULLIN3 (CUL3)

containing E3 Ubiquitin ligases (Geyer et al., 2003, Furukawa et al., 2003, Pintard et al., 2004, Moon et al., 2004). In such E3 ligases, the BTB protein acts as a scaffold protein that interacts with CUL3 through the BTB domain, and selects the target proteins for ubiquitination through its affinity for the second protein-protein interaction domain (Krek, 2003, Moon et al., 2004). In Arabidopsis, members of several BTB proteins subfamilies, such as NPH3 and the BTB-MATH protein family, were found to interact with CUL3, but for the BT clade the reports are contradictory (Wang et al., 2004, Dieterle et al., 2005, Figueroa et al., 2005, Gingerich et al., 2005, Weber et al., 2005). Moreover, in a yeast two-hybrid screen with BT1, we have not identified CUL3 as BT1 interactors (Kemel Zago, 2006). Interestingly, the experiments presented here indicate that the BT1 protein itself is a target for degradation by the 26S proteasome pathway, as the proteasome inhibitor MG132 is able to stabilize the protein. The BT1 instability and degradation by the 26S proteasome could be part of a feed back regulation of BT1 function. Considering the variety of interacting proteins identified for the BT proteins, the presence of two protein-protein interaction domains in the structure and the drastic effect of the loss of the BT function in Arabidopsis, it is likely that BT proteins are multifunctional scaffolds that act in, or maybe even interconnect, multiple cellular pathways. The finding that BT proteins interacts with PID through their BTB domain (Chapter 5), that BT2 has been found to potentiate auxin responses (Ren et al., 2007), and that the reciprocal transcriptional control between *BT* genes is possibly mediated by auxin (this chapter), make it tempting to hypothesize that their key role is to modulate auxin distribution by regulating the activity of the PID protein kinase. Further research on this hypothesis is presented in Chapter 5 of this thesis.

Material and methods

Arabidopsis lines, plant growth, transformation and protoplast transfections

The loss-of-function *bt2-3* (SALK_084471) and *bt4-1* alleles (SALK_045370) were obtained from NASC (Alonso et al., 2003). The loss-of-function *bt1-4* allele (Ds transposon line GT2847) was obtained from the Cold Spring Harbor Laboratory (Sundaresan et al., 1995). The loss-of-function *bt3-1* allele (Flag 396E01) was obtained from INRA (Versailles, France) (Samson et al., 2002). The loss-of-function *bt5-1* allele *(*GABI-Kat 771C08) was provided by MPI for Plant Breeding Research (Cologne, Germany) (Rosso et al., 2003). For detection of the insertion, we used gene-specific primers 5'TCTCTTCCGCCAGGTAAAAA3' and 5'CGCAAGACTCGTTGGAAAAG3' for *pid-14*, 5'TTCTCCGAGGTTCGTCTTTC3' and 5'GGACACGGCAAGATTCAGAT3' for *bt1-4,* 5'TCATGATCTCCACGGACCAAA3' and 5'GGACGGACATTGCGACAAGA3' for *bt2-3,* 5'TGAGGTTGCATCAGATTAGGG3' and 5'TCATCACTTTCCATCCCTCTG3' for *bt3-1*; 5'CACAACACATCTCATTTCTCCGC3'

and 5'TACATTAAGCTCGTAAGCGACAGA3' for *bt5-1*, 5'GGCTAAAGAATCGACAATAT3' and 5'TACGGTGAGATATGAGGCTA3' for *bt4-1* and the insertion-specific primers LBaI, Ds3-2, LB4 and GABI-LB for respectively the SALK, the Ds transposon, the FLAG and the GABI-Kat lines (Sundaresan et al., 1995, Samson et al., 2002, Rosso et al., 2003, Alonso et al., 2003). The flanking region of each insertion was sequenced to confirm the insertion position and Northern blot or RT-PCR analysis was performed to determine if the insertion resulted in a complete loss-of-function allele.

Arabidopsis seeds were surfaced-sterilized by incubation for 15 min in 50 % commercial bleach solution and rinsed four times with sterile water. Seeds were vernalized for 2 to 4 days before germination at 21°C with a 16-hour photoperiod and 3000 lux on solid MA medium (Masson and Paszkowski, 1992) supplemented with antibiotics when required. Two- to three-week old plants were transferred to soil and grown at 21°C with a 16-hour photoperiod of 10000 lux and at 70 % relative humidity.

Protoplasts were obtained from *Arabidopsis thaliana* Col cell suspension cultures that were propagated as described (Schirawski et al., 2000). Protoplast isolation and PEG-mediated transfections were performed as initially described (Axelos et al., 1992) and adapted by Schirawski and coworkers (Schirawski et al., 2000). Transfections were performed with 10 µg of plasmid DNA, after which the cells were incubated for at least 16 h prior observation using confocal laser scanning microscopy.

Molecular cloning and constructs

Molecular cloning was performed following standard procedures (Sambrook et al., 1989). Bacteria were grown on LC medium containing 100 µg/ml carbenicillin (Cb) or 50 µg/ml Km for *E. coli* strains DH5α or Rosetta (Novagen) containing typical high copy cloning plasmids or the binary vector pCambia1300, respectively, or 20 µg/ml rifampicin and 50 µg/ml Km for Agrobacterium strains containing binary vectors. The *BT1* cDNA was amplified, using the Expand High Fidelity kit (Roche) from a cDNA batch made from Arabidopsis seedlings, using primers 5'CC-*Sal*I-GCTATAAACCGCCACTCA3' and 5'CCGGAACAAGTTAATGTGA-*Pst*I-AA3'. The amplified cDNA was cloned in the *Sal*I and *Pst*I sites in pBluescript-SK+ giving rise to pSDM6014. The *BT2* cDNA was amplified from pUNI10183 (Yamada et al., 2003) with the primers 5'G-*Eco*RI-ATGGAAGCTGTTCTTGTCGC3' and 5'CG-*Bam*HI-TTAAACCCCTTGTGCTTGTT3' and cloned (*Eco*RI-*Bam*HI) into pUC28, giving rise to pSDM6069. The *BT4* cDNA was cloned (*Stu*I-*Nco*I) from pUNI13579 (Yamada et al., 2003) into pUC28 giving rise to pSDM6092. For the sub-cellular localization analysis in protoplast cells, *35Spro:BT1:YFP*, *35Spro:BT2:YFP*, *35Spro:BT4:YFP and 35Spro:BT5:YFP* were constructed using the Gateway Technology (Invitrogen). Genes of interest were PCR amplified from pSDM6014, pSDM6069, pSDM6092 and BX827434 (Castelli et al., 2004), respectively with primers

containing *att*B recombination sites (underlined):
5'GGGGACAAGTTTGTACAAAAAAGCAGGCTTAATGGCTATAACCGCCACT3'
and 5'GGGGACCACTTTGTACAAGAAAGCTGGGTACATTAACTTGTTCCGGAT3'
for BT1;
5'GGGGACAAGTTTGTACAAAAAAGCAGGCTTAATGGAAGCTGTTCTTGTC3'
and 5'GGGGACCACTTTGTACAAGAAAGCTGGGTAAACCCCTTGTGCTTGTTC3'
for BT2;
5'GGGGACAAGTTTGTACAAAAAAGCAGGCTTAATGGTGACAGGTTGTGTT3'
and 5'GGGGACCACTTTGTACAAGAAAGCTGGGTAACAGTTTGTCACCGGTAA3'
for BT4 and
5'GGGGACAAGTTTGTACAAAAAAGCAGGCTTAATGGAGAACATGGACGAT3'
and 5'GGGGACCACTTTGTACAAGAAAGCTGGGTATAAAGTAACATCAATTGC3'
for BT5. BP reactions were performed in pDONOR207 according to manufacturer's instructions (Invitrogen). Recombinant plasmids were isolated and sequenced. LR reactions were performed in pART7 plasmids containing a Gateway cloning cassette in frame with a YFP:HA tag coding region (C. Galván-Ampudia, unpublished data). For the *35Spro:BT1* construct (pSDM6086), the *BT1* cDNA was cloned as a *SalI-SpeI* fragment from pSDM6014 into the pCambia1300int-35Snos binary vector. To create *35Spro:GFP:BT1* (pSDM6025), the *BT1* coding sequence was cloned as a *Xho*I-*Sma*I fragment from pSDM6014 in pTH2 (Chiu et al., 1996). For *35Spro:BT1:GFP* (pSDM6063), the complete cDNA of *BT1*, including the start codon and excluding the stop codon, was amplified from pSDM6014 using the M13 forward primer and BT1-R-minusTGA-*Sal*I (5'TAGC-*Sal*I-CATTAACTTGTTCCG3'). The amplified fragment was cloned as *Sal*I fragment in pTH2 (pSDM6062). For *35Spro:BTB:GFP* (pSDM6066), the BTB domain containing part of BT1 was cloned as a *Nco*I fragment from pGEX-BT1 into pTH2 (pSDM6098). The N- and C-terminal *GFP* fusions were cloned as *Eco*RI-*Hin*dIII fragments into the binary vector pCambia1300.

Northern blot analysis

Auxin treatments were done on 8-day old Col wild type seedlings with 5 µm IAA for the indicated time. Total RNA was purified using the RNeasy Plant Mini kit (Qiagen). Subsequent RNA blot analysis was performed as described (Memelink et al., 1994) using 10 µg of total RNA per sample. The following modifications were made: pre-hybridizations and hybridizations were conducted at 65^{o}C with 10 % Dextran sulfate, 1 % SDS, 1 M NaCl, 50 µg/ml of single stranded Herring sperm DNA as hybridization mix. The hybridized blots were washed for 20 min at 65^{o}C in 2x SSPE 0.5 % SDS, and for 20 min at 42^{o}C in respectively 0.2x SSPE 0.5 % SDS, 0.1x SSPE 0.5 % SDS and 0.1x SSPE. Blots were exposed to X-ray film FUJI Super RX. Probes were PCR amplified and column purified (Qiagen) using primers 5'CATCCCAAACATTACAAAGGGC3',

5'TTCTCCGAGGTTCGTCTTTC3' for *BT1* from pSDM6006, *5'CTCACCATGGGTTTCCACAAGATCATA3', 5'GGCAACATCCTGGGGCACAA3' for GFP from pSDM6025,* 5'TGTTCCTCACCACGCTCTTC3', 5'TGCTCAAAACATTCCTCACC3' for *BT5, ,* 5'GACGCCGAATCGGTAAACT3', 5'TTTGTAATCGCGAAACAACGGA3' for *BT2*, 5'GGCTAAAGAATCGACAATAT3', 5'TACGGTGAGATATGAGGCTA3' for *BT4,* 5'CTCTCATTCGCGCGACGCAAACG3', 5'GGGTTCAAGTCAGACAAGAGGTGG3' for *RPS5A* and 5'CGGGAAGGATCGTGATGGA3', 5'CCAACCTTCTCGATGGCCT3' for *AtROC* from Col wild type genomic DNA. Probes were radioactively labeled with α-^{32}P-ATP (Amerscham) using the Prime-a-gene kit (Promega).

RT-PCRs were performed as described (Weijers et al., 2001) using 10 µg of total RNA from 8-day old seedlings for the RT reaction. The PCR reactions were performed with one tenth of the RT volume with the same gene specific primers used for the probe amplification in the Northern blot analysis and with 5'ATGTCTAGTAGTACCAAGAACATTCCAAAAC3', 5'TATCAAACCAGAAGAACGTGACGAG3' for *BT3* and 5'CGGAATTCATGAGAGAGATCCTTCATATC3', 5'CCCTCGAGTTAAGTCTCGTACTCCTCTTC3' for *αTubulin*. A RT reaction from Col seedlings RNA in which the reverse-transcriptase was omitted served as a negative control.

Western blot analysis

To check YFP-tagged proteins integrity, total protein was extracted from transfected protoplasts. Half volume of the transfected cells were pelleted at full-speed at 4^{o}C, resuspended in 30 µl of 1x Laemmeli sample buffer and boiled for 5 min. Proteins (half volume) was separated on a SDS-PAGE gel (10 %) with PageRuler Prestained Protein Ladder (Fermentas) as a size marker. To analyze the GFP-tagged BT1 in Arabidopsis, total protein was extracted from 7-day old seedlings as previously described (Kurata et al., 2005). The protein concentration was determined by Bradford assay and per sample 40 µg of protein was separated on a SDS-PAGE gel (12 %) with PageRuler Prestained Protein Ladder (Fermentas) as a size marker. A parallel gel was run and stained with Coomassie to correct for loading differences. Gels for Western blot analyses were transferred to nitrocellulose membranes (Immobilon-P, Millipore) which were incubated with rat HRP-conjugated anti-HA (3F10) antibody (1/2000, Roche) or rabbit anti-GFP primary antibody (1/5000, Molecular Probes) and an anti-rabbit horse radish peroxidase (HRP)-conjugated secondary antibody (1/5000, Promega). Detection followed the protocol of the Phototope-HRP Western Blot Detection Kit (New England Biolabs).

Microscopy and phenotypic analysis

The 26S-proteasome inhibitor MG132 (Sigma) was used at 50 µM during 4 h. Propidium iodide (0.1 µg/ml in distilled water) was used to stain the cell walls of living cells and the nuclei of the female gametophyte. The female gametophyte phenotypes and GFP fusion lines were observed using 40x dry and oil objectives on a ZEISS Axioplan microscope equipped with a confocal laser scanning unit (MRC1024ES, BIO-RAD, Hercules, CA). The GFP fluorescence was monitored with a 522-532 nm band pass emission filter (488 nm excitation). Propidium iodide was visualized using the 585 nm long pass emission filter (568 nm excitation). All images were recorded using a 3CCD Sony DKC5000 digital camera. For the subcellular localization of the BT proteins in protoplast cells, a Leica DM IRBE confocal laser scanning microscope was used with a 63x water objective. The fluorescence was visualized with an Argon laser for excitation at 514 nm and with a 522-532 nm (YFP) emission filter. Images were processed by ImageJ (http://rsb.info.nih.gov/ij/) and assembled in Adobe Photoshop 7.0.

Silique seed set was determined in cleared siliques after treatment with a derivative of Hoyer's solution (Boisnard-Lorig et al., 2001) using a Leica MZ12 stereomicroscope equipped with a 3CCD Sony DKC-5000 digital camera. Quantification of seed set was performed by slitting opened siliques for at least 4 siliques of 5 plants per genotype and counting the number of seeds and ovules. Silique length was measured for 10 mature siliques per plant.

Accession Numbers

The *Arabidopsis* Genome Initiative locus identifiers for the genes mentioned in this article are as follows: *BT1/PBP2* (At5g63160), *BT2/PBP2H1* (At3g48360), *BT3/PBP2H2* (At1g05690), *BT4/PBP2H4* (At5g67480), *BT5/PBP2H3* (At4g37610), *ROC* (At4g38740), *αTubulin* (At5g44340), *RPS5A* (At3g11940), *NPH3* (At5g64330), *RPT2* (At2g30520), *CUL3a* and *b* (At1g26830 and At1g69670), *BET10/GTE11* (At3g01770), *BET9/GTE* (At5g14270) and *TAC1* (At3g09290). The TIGR *Rice* Genome initiation locus identifiers for the japonica nipponbare cultivar *BT* family genes used the Figure 1B are as follows: *Os01g66890*, *Os01g68020*, *Os02g38320* and *Os04g40630*. The GeneBank locus names of the *BT* homologues are H0510A06.17 for the rice indica cultivar *BT* gene, AC146856.8 (protein ABE77424) for the *Medicago truncatula BT* gene and AB236807 (protein BAE71259) for the *Trifolium pratense BT* gene.

Acknowledgments

The authors would like to thank Gerda Lamers for her helpful comments concerning microscopy, Ward de Winter for his technical assistance, Pieter Ouwerkerk for providing

the pCambia1300int-35Snos and pCAMBIA1300 plasmids and the *35Spro:GFP Arabidopsis* line and the Arabidopsis Biological Resource center to provide us with BT2 and BT4 cDNAs. A. V-S. was supported by a STW grant (LB6822).

References

Albagli,O., Dhordain,P., Deweindt,C., Lecocq,G., and Leprince,D. (1995). The BTB/POZ domain: a new protein-protein interaction motif common to DNA- and actin-binding proteins. Cell Growth Differ **6**:1193-1198.

Alonso,J.M., Stepanova,A.N., Leisse,T.J., Kim,C.J., Chen,H., Shinn,P., Stevenson,D.K., Zimmerman,J., Barajas,P., Cheuk,R., Gadrinab,C., Heller,C., Jeske,A., Koesema,E., Meyers,C.C., Parker,H., Prednis,L., Ansari,Y., Choy,N., Deen,H., Geralt,M., Hazari,N., Hom,E., Karnes,M., Mulholland,C., Ndubaku,R., Schmidt,I., Guzman,P., Aguilar-Henonin,L., Schmid,M., Weigel,D., Carter,D.E., Marchand,T., Risseeuw,E., Brogden,D., Zeko,A., Crosby,W.L., Berry,C.C., and Ecker,J.R. (2003). Genome-Wide Insertional Mutagenesis of Arabidopsis thaliana. Science **301**:653-657.

Axelos,M., Curie,C., Mazzolini,L., Bardet,C., and Lescure,B. (1992). A Protocol for Transient Gene-Expression in Arabidopsis-Thaliana Protoplasts Isolated from Cell-Suspension Cultures. Plant Physiology and Biochemistry **30**:123-128.

Bardwell,V.J. and Treisman,R. (1994). The POZ domain: a conserved protein-protein interaction motif. Genes Dev. **8**:1664-1677.

Benjamins, R. (2004). Functional analysis of the PINOID protein kinase in *Arabidopsis thaliana*. Institute of Biology, Leiden University, The Netherlands.

Boisnard-Lorig,C., Colon-Carmona,A., Bauch,M., Hodge,S., Doerner,P., Bancharel,E., Dumas,C., Haseloff,J., and Berger,F. (2001). Dynamic analyses of the expression of the HISTONE::YFP fusion protein in arabidopsis show that syncytial endosperm is divided in mitotic domains. Plant Cell **13**:495-509.

Cao,H., Glazebrook,J., Clarke,J.D., Volko,S., and Dong,X. (1997). The Arabidopsis NPR1 Gene That Controls Systemic Acquired Resistance Encodes a Novel Protein Containing Ankyrin Repeats. Cell **88**:57-63.

Castelli,V., Aury,J.M., Jaillon,O., Wincker,P., Clepet,C., Menard,M., Cruaud,C., Quétier,F., Scarpelli,C., Schächter,V., Temple,G., Caboche,M., Weissenbach,J., and Salanoubat,M. (2004). Whole Genome Sequence Comparisons and "Full-Length" cDNA Sequences: A Combined Approach to Evaluate and Improve Arabidopsis Genome Annotation. Genome Res. **14**:406-413.

Chiu,W.l., Niwa,Y., Zeng,W., Hirano,T., Kobayashi,H., and Sheen,J. (1996). Engineered GFP as a vital reporter in plants. Current Biology **6**:325-330.

Christensen,C.A., King,E.J., Jordan,J.R., and Drews,G.N. (1997). Megagametogenesis in *Arabidopsis*wild type and the *Gf* mutant. Sex Plant Reprod **10**:49-64.

Christensen,C.A., Subramanian,S., and Drews,G.N. (1998). Identification of Gametophytic Mutations Affecting Female Gametophyte Development inArabidopsis. Developmental Biology **202**:136-151.

Dieterle,M., Thomann,A., Renou,J.P., Parmentier,Y., Cognat,V., Lemonnier,G., Muller,R., Shen,W.H., Kretsch,T., and Genschik,P. (2005). Molecular and functional characterization of Arabidopsis Cullin 3A. Plant J. **41**:386-399.

Drews,G.N. and Yadegari,R. (2002). Development and function of the angiosperm female gametophyte. Annu.Rev.Genet. **36**:99-124.

Du,L.Q. and Poovaiah,B.W. (2004). A novel family of Ca2+/calmodulin-binding proteins involved in transcriptional regulation: interaction with fsh/Ring3 class transcription activators. Plant Molecular Biology **54**:549-569.

Faure,J.E., Rotman,N., Fortuné,P., and Dumas,C. (2002). Fertilization in Arabidopsis thaliana wild type: developmental stages and time course. Plant J. **30**:481-488.

Figueroa,P., Gusmaroli,G., Serino,G., Habashi,J., Ma,L.G., Shen,Y.P., Feng,S.H., Bostick,M., Callis,J., Hellmann,H., and Deng,X.W. (2005). Arabidopsis has two redundant Cullin3 proteins that are essential for embryo development and that interact with RBX1 and BTB proteins to form multisubunit E3 ubiquitin ligase complexes in vivo. Plant Cell **17**:1180-1195.

Florence,B. and Faller,D.V. (2001). You BET-CHA: A novel family of transcriptional regulators. Front.Biosci. **6**:D1008-D1018.

Friml,J., Yang,X., Michniewicz,M., Weijers,D., Quint,A., Tietz,O., Benjamins,R., Ouwerkerk,P.B.F., Ljung,K., Sandberg,G., Hooykaas,P.J.J., Palme,K., and Offringa,R. (2004). A PINOID-dependent binary switch in apical-basal PIN polar targeting directs auxin efflux. Science **306**:862-865.

Furukawa,M., He,Y.J., Borchers,C., and Xiong,Y. (2003). Targeting of protein ubiquitination by BTB-Cullin 3-Roc1 ubiquitin ligases. Nat.Cell Biol. **5**:1001-1007.

Geyer,R., Wee,S., Anderson,S., Yates,J., and Wolf,D.A. (2003). BTB/POZ domain proteins are putative substrate adaptors for cullin 3 ubiquitin ligases. Mol.Cell **12**:783-790.

Gingerich,D.J., Gagne,J.M., Salter,D.W., Hellmann,H., Estelle,M., Ma,L.G., and Vierstra,R.D. (2005). Cullins 3a and 3b assemble with members of the broad complex/tramtrack/bric-a-brac (BTB) protein family to form essential ubiquitin-protein ligases (E3s) in Arabidopsis. J.Biol.Chem. **280**:18810-18821.

Gingerich,D.J., Hanada,K., Shiu,S.H., and Vierstra,R.D. (2007). Large-Scale, Lineage-Specific Expansion of a Bric-a-Brac/Tramtrack/Broad Complex Ubiquitin-Ligase Gene Family in Rice. Plant Cell:2329-2348.

Ha,C.M., Jun,J.H., Nam,H.G., and Fletcher,J.C. (2004). BLADE-ON-PETIOLE1 Encodes a BTB/POZ Domain Protein Required for Leaf Morphogenesis in Arabidopsis thaliana. Plant Cell Physiol. **45**:1361-1370.

Hall,Q. and Cannon,M.C. (2002). The Cell Wall Hydroxyproline-Rich Glycoprotein RSH Is Essential for Normal Embryo Development in Arabidopsis. Plant Cell **14**:1161-1172.

Hellmann,H., Hobbie,L., Chapman,A., Dharmasiri,S., Dharmasiri,N., del Pozo,C., Reinhardt,D., and Estelle,M. (2003). Arabidopsis AXR6 encodes CUL1 implicating SCF E3 ligases in auxin regulation of embryogenesis. EMBO J. **22**:3314-3325.

Hepworth,S.R., Zhang,Y., McKim,S., Li,X., and Haughn,G.W. (2005). BLADE-ON-PETIOLE-Dependent Signaling Controls Leaf and Floral Patterning in Arabidopsis. Plant Cell **17**:1434-1448.

Higashiyama,T., Yabe,S., Sasaki,N., Nishimura,Y., Miyagishima,S.y., Kuroiwa,H., and Kuroiwa,T. (2001). Pollen Tube Attraction by the Synergid Cell. Science **293**:1480-1483.

Inaba,T., Alvarez-Huerta,M., Li,M., Bauer,J., Ewers,C., Kessler,F., and Schnell,D.J. (2005). Arabidopsis Tic110 Is Essential for the Assembly and Function of the Protein Import Machinery of Plastids. Plant Cell **17**:1482-1496.

Kemel Zago, M. (2006). Components and targets of the PINOID signaling complex in *Arabidopsis thaliana*. Institute of Biology, Leiden University, The Netherlands.

Kim,S., Choi,H.i., Ryu,H.J., Park,J.H., Kim,M.D., and Kim,S.Y. (2004). ARIA, an Arabidopsis Arm Repeat Protein Interacting with a Transcriptional Regulator of Abscisic Acid-Responsive Gene Expression, Is a Novel Abscisic Acid Signaling Component. Plant Physiol. **136**:3639-3648.

Krek,W. (2003). BTB proteins as henchmen of Cul3-based ubiquitin ligases. Nat.Cell Biol. **5**:950-951.

Kurata,T., Ishida,T., Kawabata-Awai,C., Noguchi,M., Hattori,S., Sano,R., Nagasaka,R., Tominaga,R., Koshino-Kimura,Y., Kato,T., Sato,S., Tabata,S., Okada,K., and Wada,T. (2005).

Cell-to-cell movement of the CAPRICE protein in Arabidopsis root epidermal cell differentiation. Development **132**:5387-5398.

la Cour,T., Kiemer,L., Molgaard,A., Gupta,R., Skriver,K., and Brunak,S. (2004). Analysis and prediction of leucine-rich nuclear export signals. Protein Engineering, Design and Selection **17**:527-536.

Masson,J. and Paszkowski,J. (1992). The Culture Response of Arabidopsis-Thaliana Protoplasts Is Determined by the Growth-Conditions of Donor Plants. Plant J. **2**:829-833.

Memelink,J., Swords,K.M.M., Staehelin,L.A., and Hoge,J.H.C. (1994) Southern, Northern and Western blot analysis. In Plant Molecular Biology Manuel, (Dordrecht, NL: Kluwer Academic Publishers).

Moon,J., Parry,G., and Estelle,M. (2004). The Ubiquitin-Proteasome Pathway and Plant Development. Plant Cell **16**:3181-3195.

Motchoulski,A. and Liscum,E. (1999). Arabidopsis NPH3: A NPH1 photoreceptor-interacting protein essential for phototropism. Science **286**:961-964.

Norberg,M., Holmlund,M., and Nilsson,O. (2005). The BLADE ON PETIOLE genes act redundantly to control the growth and development of lateral organs. Development **132**:2203-2213.

Pandey,R., Muller,A., Napoli,C.A., Selinger,D.A., Pikaard,C.S., Richards,E.J., Bender,J., Mount,D.W., and Jorgensen,R.A. (2002). Analysis of histone acetyltransferase and histone deacetylase families of Arabidopsis thaliana suggests functional diversification of chromatin modification among multicellular eukaryotes. Nucl.Acids Res. **30**:5036-5055.

Pintard,L., Willems,A., and Peter,M. (2004). Cullin-based ubiquitin ligases: Cul3-BTB complexes join the family. EMBO J. **23**:1681-1687.

Ponting,C.P., Blake,D.J., Davies,K.E., Kendrick-Jones,J., and Winder,S.J. (1996). ZZ and TAZ: new putative zinc fingers in dystrophin and other proteins. Trends in Biochemical Sciences **21**:11-13.

Ren,S., Johnston,J.S., Shippen,D.E., and McKnight,T.D. (2004). TELOMERASE ACTIVATOR1 induces telomerase activity and potentiates responses to auxin in Arabidopsis. Plant Cell **16**:2910-2922.

Ren,S., Mandadi,K.K., Boedeker,A.L., Rathore,K.S., and McKnight,T.D. (2007). Regulation of Telomerase in Arabidopsis by BT2, an Apparent Target of TELOMERASE ACTIVATOR1. Plant Cell **19**:23-31.

Riha,K., McKnight,T.D., Griffing,L.R., and Shippen,D.E. (2001). Living with genome instability: plant responses to telomere dysfunction. Science **291**:1797-1800.

Riha,K. and Shippen,D.E. (2003). Telomere structure, function and maintenance in Arabidopsis. Chromosome.Res. **11**:263-275.

Rosso,M.G., Li,Y., Strizhov,N., Reiss,B., Dekker,K., and Weisshaar,B. (2003). An *Arabidopsis thaliana* T-DNA mutagenized population (GABI-Kat) for flanking sequence tag-based reverse genetics. Plant Molecular Biology **53**:247-259.

Sambrook,J., Fritsch F., and Maniatis,T. (1989) Molecular cloning - A laboratory Manual. New York: Cold Spring Harbor Laboratory press, ed.

Samson,F., Brunaud,V., Balzergue,S., Dubreucq,B., Lepiniec,L., Pelletier,G., Caboche,M., and Lecharny,A. (2002). FLAGdb/FST: a database of mapped flanking insertion sites (FSTs) of Arabidopsis thaliana T-DNA transformants. Nucl.Acids Res. **30**:94-97.

Schirawski,J., Planchais,S., and Haenni,A.L. (2000). An improved protocol for the preparation of protoplasts from an established Arabidopsis thaliana cell suspension culture and infection with RNA of turnip yellow mosaic tymovirus: a simple and reliable method. Journal of Virological Methods **86**:85-94.

Shimizu,K.K. and Okada,K. (2000). Attractive and repulsive interactions between female and male gametophytes in Arabidopsis pollen tube guidance. Development **127**:4511-4518.

Stogios,P., Downs,G., Jauhal,J., Nandra,S., and Prive,G. (2005). Sequence and structural analysis of BTB domain proteins. Genome Biology **6**:R82.

Sundaresan,V., Springer,P., Volpe,T., Haward,S., Jones,J.D., Dean,C., Ma,H., and Martienssen,R. (1995). Patterns of gene action in plant development revealed by enhancer trap and gene trap transposable elements. Genes Dev. **9**:1797-1810.

Tao,L.Z., Cheung,A.Y., Nibau,C., and Wu,H.M. (2005). RAC GTPases in Tobacco and Arabidopsis Mediate auxin-induced formation of proteolytically active nuclear protein bodies that contain AUX/IAA proteins. Plant Cell **17**:2369-2383.

Vieten,A., Sauer,M., Brewer,P.B., and Friml,J. (2007). Molecular and cellular aspects of auxin-transport-mediated development. Trends in Plant Science **12**:160-168.

Wang,K.L.C., Yoshida,H., Lurin,C., and Ecker,J.R. (2004). Regulation of ethylene gas biosynthesis by the Arabidopsis ETO1 protein. Nature **428**:945-950.

Weber,H., Bernhardt,A., Dieterle,M., Han,P., Hano,P., Mutlu,A., Estelle,M., Genschik,P., and Hellmann,H. (2005). Arabidopsis AtCUL3a and AtCUL3b form complexes with members of the BTB/POZ-MATH protein family. Plant Physiol. **137**:83-93.

Weijers,D., Franke-van Dijk,M., Vencken,R.J., Quint,A., Hooykaas,P., and Offringa,R. (2001). An Arabidopsis Minute-like phenotype caused by a semi-dominant mutation in a RIBOSOMAL PROTEIN S5 gene. Development **128**:4289-4299.

Yadegari,R. and Drews,G.N. (2004). Female Gametophyte Development. Plant Cell **16**:S133-S141.

Yamada,K., Lim,J., Dale,J.M., Chen,H., Shinn,P., Palm,C.J., Southwick,A.M., Wu,H.C., Kim,C., Nguyen,M., Pham,P., Cheuk,R., Karlin-Newmann,G., Liu,S.X., Lam,B., Sakano,H., Wu,T., Yu,G., Miranda,M., Quach,H.L., Tripp,M., Chang,C.H., Lee,J.M., Toriumi,M., Chan,M.M.H., Tang,C.C., Onodera,C., Deng,J.M., Akiyama,K., Ansari,Y., Arakawa,T., Banh,J., Banno,F., Bowser,L., Brooks,S., Carninci,P., Chao,Q., Choy,N., Enju,A., Goldsmith,A.D., Gurjal,M., Hansen,N.F., Hayashizaki,Y., Johnson-Hopson,C., Hsuan,V.W., Iida,K., Karnes,M., Khan,S., Koesema,E., Ishida,J., Jiang,P.X., Jones,T., Kawai,J., Kamiya,A., Meyers,C., Nakajima,M., Narusaka,M., Seki,M., Sakurai,T., Satou,M., Tamse,R., Vaysberg,M., Wallender,E.K., Wong,C., Yamamura,Y., Yuan,S., Shinozaki,K., Davis,R.W., Theologis,A., and Ecker,J.R. (2003). Empirical Analysis of Transcriptional Activity in the Arabidopsis Genome. Science **302**:842-846.

Chapter 5

A BTB domain protein interacts with the protein kinase PINOID to fine tune its activity

Hélène Robert, Marcelo K. Zago, René Benjamins[1], Yang Xiong[2], Carlos Galván-Ampudia, Ab Quint, Niels Wattel, Douwe Doevendans, Fang Huang, Remko Offringa

[1] Current address: Molecular Genetics Group, Department of Biology, Utrecht University, Padualaan 8, 3584 CH Utrecht, The Netherlands.

[2] Current address: College of Life Sciences, Peking University, Beijing 100871, China

Abstract

Polar transport of auxin directs plant development by producing dynamic gradients through the concerted action of asymmetrically localized PIN-FORMED (PIN) auxin efflux carriers. The PINOID (PID) serine/threonine protein kinase determines the direction of auxin transport by regulating the polar subcellular targeting of PIN proteins. A yeast two-hybrid screen using PID as bait identified *Arabidopsis thaliana* BTB and TAZ domain protein1 (BT1) as PID BINDING PROTEIN2 (PBP2). In Arabidopsis, *BT1/PBP2* belongs to a small gene family comprising five members, encoding proteins with the same land plant-specific domain structure: an N-terminal BTB domain, a TAZ domain and a C-terminal Calmodulin binding domain. At least four of the five BT proteins interact with PID through their BTB domain, and *in vitro* phosphorylation assays indicate that BT1 is not a target for phosphorylation by PID, but that BT1 binding reduces its kinase activity. BT1 localizes in the nucleus and the cytoplasm, and upon co-expression with PID, BT1 is found at the plasma membrane whereas PID becomes partially nuclear. Overexpression of BT1 leads to a reduction of *PID* gain-of-function seedling phenotypes and enhanced *pid* loss-of-function embryo phenotypes. Furthermore, *bt* loss-of-function rescues seedling phenotypes and enhances adult plant phenotypes of *35Spro:PID* plants. Together these data indicate that on the one hand BT1 functions as a repressor of PID kinase activity, and that on the other hand recruitment of PID by the BT-orchestrated protein complex is a crucial aspect of PID signaling. We present evidence that the BT1 scaffold protein is possibly involved in feed back control between PID-directed auxin transport and KNOX-BEL controlled internode patterning in the inflorescence.

Introduction

The phytohormone auxin plays a crucial function in plant developmental processes such as embryogenesis, phyllotaxis and root meristem maintenance (Sabatini et al., 1999, Reinhardt et al., 2003, Benková et al., 2003). Characteristic for auxin action is its polar transport, which generates gradients and maxima that are instrumental in directing cell division, -elongation and -differentiation (Tanaka et al., 2006). Auxin transport can be chemically inhibited resulting in inflorescence meristems that lose the capacity to produce leaves and flowers and therefore form pin-like structures (Okada et al., 1991). The Arabidopsis *pin-formed1* (Okada et al., 1991) and the *pinoid* (Bennett et al., 1995) loss-of-function mutants phenocopy plants that have been treated with polar auxin transport inhibitors. The *PIN-FORMED1* (*PIN1*) gene is part of a family of eight genes in Arabidopsis that encodes major transporter membrane proteins characterized by two groups of five conserved transmembrane domains (Paponov et al., 2005). These PIN proteins were shown to be the

rate limiting factor in auxin efflux (Petrášek et al., 2006) and to determine the direction of polar auxin transport through their asymmetric subcellular localization (Wisniewska et al., 2006). The *PINOID* (*PID*) gene encodes a plant specific protein serine/threonine kinase (Christensen et al., 2000) that has been implied as a regulator of polar auxin transport (Benjamins et al., 2001), and was shown to induce the subcellular targeting of PIN proteins to the apical (shoot apex facing) plasma membrane (Friml et al., 2004). Recent evidence that PID was able to phosphorylate the PIN proteins allowed to identify the mechanism of PID-dependent PIN targeting (Michniewicz et al., 2007). In order to clarify this pathway, we used PID as bait in a yeast two-hybrid screen to identify PID BINDING PROTEINs (PBPs). Two of these PBPs, TOUCH3 (TCH3) and PBP1, are calcium-binding proteins that regulate PID kinase activity in *in vitro* phosphorylation assays (Benjamins et al., 2003), suggesting the involvement of calcium in regulating and directing auxin-mediated plant development.

Here we analyze the functional interaction of PID with PBP2, a BTB (Broad-Complex, Tramtrack, Bric-à-Brac) domain protein that was previously identified as a potato calmodulin interactor, and was named BT1 after BTB and TAZ domain protein1 (Du and Poovaiah, 2004). BTB domain proteins are known to act as scaffold- or linker-proteins that organize protein complexes (Albagli et al., 1995). The Arabidopsis genome encodes eighty BTB domain proteins that can be grouped in ten subfamilies (Gingerich et al., 2005). Most of the BTB proteins contain a second protein domain that specifies their function (Motchoulski and Liscum, 1999, Sakai et al., 2000, Wang et al., 2004, Weber et al., 2005, Dieterle et al., 2005). Besides the N-terminal BTB domain, BT1 contains two additional protein-protein interaction domains: a TAZ domain (Transcriptional Adaptor Zinc finger) (Ponting et al., 1996) and a C-terminal calmodulin binding domain (Du and Poovaiah, 2004). Our data demonstrate that PID interacts with the BTB domain containing part of BT1, and that BT1 is not a phosphorylation target of PID but a repressor of its kinase activity. Overexpression of BT1 reduces PID overexpression phenotypes and enhances *pid* loss-of-function phenotypes. Using GFP-tagged proteins, we show that BT1 co-localizes with PID at the plasma membrane, and also causes PID to localize to the nucleus. This nuclear localization of PID is only observed in the presence of BT1, and suggests a new function for PID signaling in the nucleus. Interestingly, phenotypes obtained by meristem-specific ectopic expression of the BTB domain of BT1 suggest a link between the KNOX-BEL transcription factors and PID-regulated polar auxin transport during internode patterning in the inflorescence. Apart from BT1, also other members of the BT protein family were found to interact with PID, and a multiple *bt* knock-out rescued *PID* gain-of-function seedling phenotypes, suggesting that despite their function as multifunctional scaffolds, their role as regulator of PID is conserved for all BT proteins.

Results

PINOID interacts with BT proteins through their BTB domain

Two Arabidopsis yeast two-hybrid cDNA libraries were screened for proteins that interact with the PID protein serine/threonine kinase (Benjamins, 2004). One of the identified PID partners was BT1/PBP2. BT1 contains an N-terminal BTB domain, which is well-known to mediate both homo- and hetero-dimerization of proteins (Bardwell and Treisman, 1994, Figueroa et al., 2005, Weber et al., 2005), and two other protein-protein interaction domains: a TAZ domain that also mediates protein-protein interactions (Ponting et al., 1996) and a C-terminal domain that was found to interact with a potato calmodulin CaM6 (Du and Poovaiah, 2004) (Figure 1A). To test which domain binds to PID, GST-tagged full length BT1, or the GST-tagged BTB or TAZ domains alone (Figure 1A) were incubated *in vitro* with crude extracts from *E. coli* cell expressing His-tagged PID. Western blot analysis using anti-His antibodies showed that PID efficiently binds the BTB domain, whereas the TAZ domain only pulls down background levels of the kinase (Figure 1B).

BT1 is part of a small protein family comprising five members in Arabidopsis that not only share the BT1 domain structure, but also interact with the same proteins. The five Arabidopsis BT proteins have been shown to bind the potato CaM6, and BT1, BT2 and BT4 were found to interact with bromodomain transcription factors (Du and Poovaiah, 2004). To test the possibility that PID also binds other BT family members, *in vitro* pull-down assays were performed using His-tagged BT1, -BT2, -BT4 and -BT5. All four proteins were efficiently pulled down from a crude *E. coli* extract by the GST-tagged PID, but not by the GST tag alone (Figure 1C). Although we were not able to test His-BT3, our results suggest that PID is a conserved interaction partner for all five Arabidopsis BT proteins. Genetic and expression analyses of the *BT* family already indicated that there is functional redundancy between the *BT* genes (Chapter 4, this thesis), and our results suggest that the BT proteins also act redundantly in the PID pathway.

BT1 is a likely regulator of PID kinase activity

PID is an auto-activated protein serine/threonine kinase that can auto- and trans-phosphorylate in *in vitro* reactions (Figure 1D, lane 1) (Christensen et al., 2000, Benjamins et al., 2003), thus we tested whether BT1 is a PID phospho-target *in vitro*. No phosphorylation of BT1 was observed, but, interestingly, the presence of BT1 in the reaction mixture resulted in a significant reduction of the PID kinase activity, as indicated by the reduced levels of PID auto-phosphorylation and of the phosphorylation of the general protein kinase substrate Myelin Basic Protein (MBP) (Figure 1D). These results suggest that BT1 has a negative effect on both auto- and trans-phosphorylation activity of PID and imply that BT1 is not a target of PID phosphorylation, but that instead it functions as a negative regulator of PID activity.

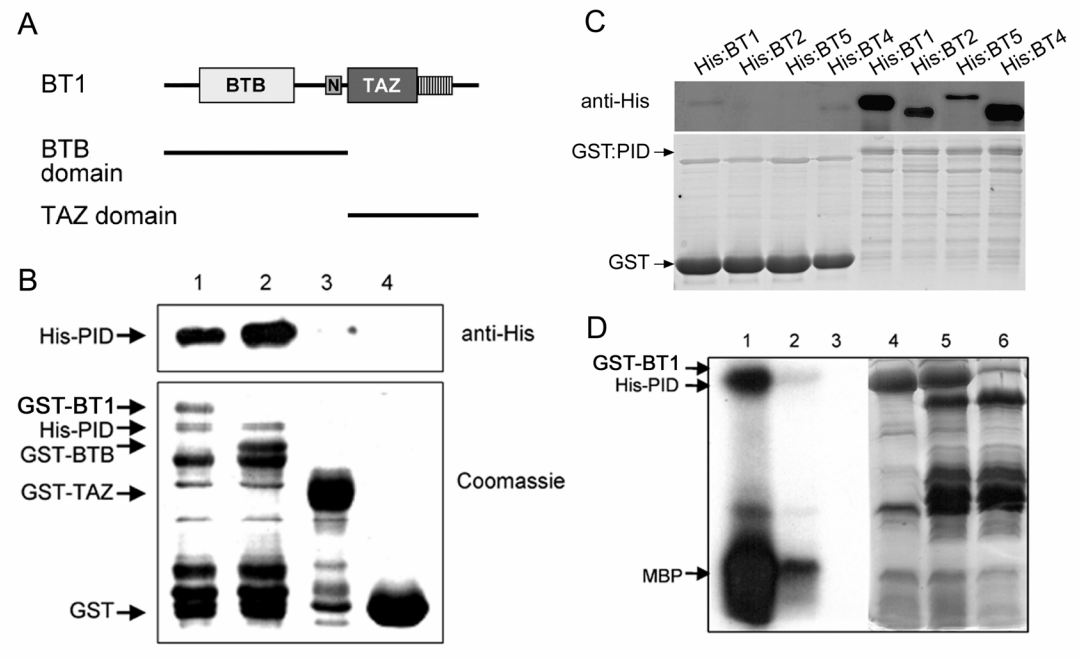


Figure 1. Binding of PINOID to the BTB domain of BT1 represses its kinase activity *in vitro*.
(A) Schematic representation of BT1 (365 aa) and the two deletion versions comprising either the BTB or the TAZ domains. The N-box and the striped box indicate the positions of respectively a nuclear localization signal (aa 193-203) and a putative calmodulin binding site (Du and Poovaiah, 2004).
(B) Western-blot analysis (top panel) with anti-His antibodies detects His-tagged PID after pull-down with GST:BT1 (lane 1) or the GST-tagged BTB domain (lane 2), but not with the GST-tagged TAZ domain (lane 3) or GST alone (lane 4), from the soluble fraction of *E. coli* protein extracts. The bottom panel shows the Coomassie stained gel of the pull-down reactions, with the positions of the different proteins indicated.
(C) Western blot with the anti-His antibody (top panel) showing specific pull-down of His-tagged BT1, -BT2, -BT5 and -BT4 by GST-tagged PID (right), and only background levels when GST is used in the pull-down assay (left). The bottom panel represents a Coomassie stained gel of the same experiment showing the presence of the GST and the GST-tagged PID.
(D) Autoradiograph (lanes 1, 2 and 3) and Coomassie stained gel (lanes 4, 5 and 6) of a phosphorylation assay containing PID and MBP (lanes 1 and 4), PID, BT1 and MBP (lanes 2 and 5), or BT1 and MBP (lanes 3 and 6).

BT1 *expression overlaps with that of* PINOID

For PID and BT1 to interact *in planta,* it is crucial that their spatio-temporal expression patterns overlap. To investigate this, Northern blot analysis was performed and the results were compared with the available Genevestigator micro-array data (Zimmermann et al., 2004) and the previously published *PID* expression pattern (Christensen et al., 2000, Benjamins et al., 2001). *PID* expression is most abundant in roots, young developing flowers and siliques, and it is expressed at relatively low levels in seedling and plant shoots (Figure 2A). In these tissues, PID is expressed in the young vascular tissues and around

organ primordia (both in root and shoot) (Benjamins et al, 2001). *BT1* mRNA is particularly abundant in seedling shoots, but can also be detected in seedling roots, and in stems and flower buds (Figure 2B). Furthermore, the expression of both *PID* and *BT1* is auxin inducible (Figure 2C). These data indicate that *PID* and *BT1* expression patterns partially overlap, which corroborates a possible *in vivo* interaction between the two proteins.

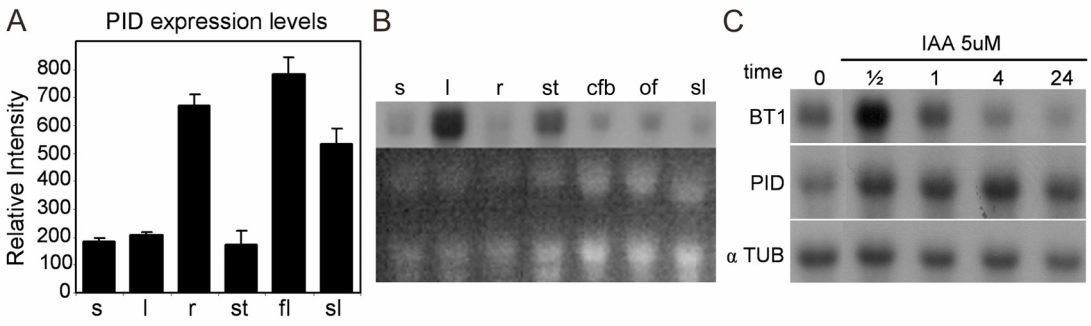


Figure 2. The auxin responsive *BT1* gene is co-expressed with *PID.*

(A) The Genevestigator micro-array data show that *PID* expression is high in roots (r), flowers (fl) and siliques (sl), and lower in seedlings (s), leaves (l) and stems (st).

(B) Northern blot analysis showing the expression of *BT1* mRNA in wild-type Arabidopsis Columbia tissues. Leaf (l) and root (r) tissues are from 2-week old seedlings (s). Stems (st), flower buds (cfb), opened flowers (of) and siliques (sl) are from 6-week old plants.

(C) Northern blot showing that *BT1* (upper panel) and *PID* (middle panel) expression is induced in 8-day old seedlings as soon as 30 min after auxin treatment. The expression of *αTubulin* (lower panel) is used as loading control.

PID and BT1 co-localize at the plasma membrane and in the nucleus

Previous experiments indicated that PID is a plasma membrane-associated protein (Lee and Cho, 2006), whereas BT1 is predominantly nuclear localized in *35Spro:BT1:GFP* transfected protoplasts or in *35Spro:BT1:GFP* plant lines (Chapter 4, this thesis). This raised the question where PID and BT1 meet in the cell to form a complex. Closer inspection of *35Spro:PID:GFP* transfected protoplasts revealed however, that only 38 % of the protoplasts showed purely plasma membrane localization of PID:GFP (Figure 3A, n = 122), and that in 62 % PID:GFP is both at plasma membrane and in the cytosol (Figure 3B). This corresponds to more recent observations using a *PIDpro:PID:VENUS* Arabidopsis line (Michniewicz et al., 2007), and indicates that PID and BT1 can meet in the cytosol.

Co-transfection of Arabidopsis protoplasts with *35Spro:PID:CFP* and *35Spro:BT1:YFP* indeed showed the expected overlap in localization in the cytosol.

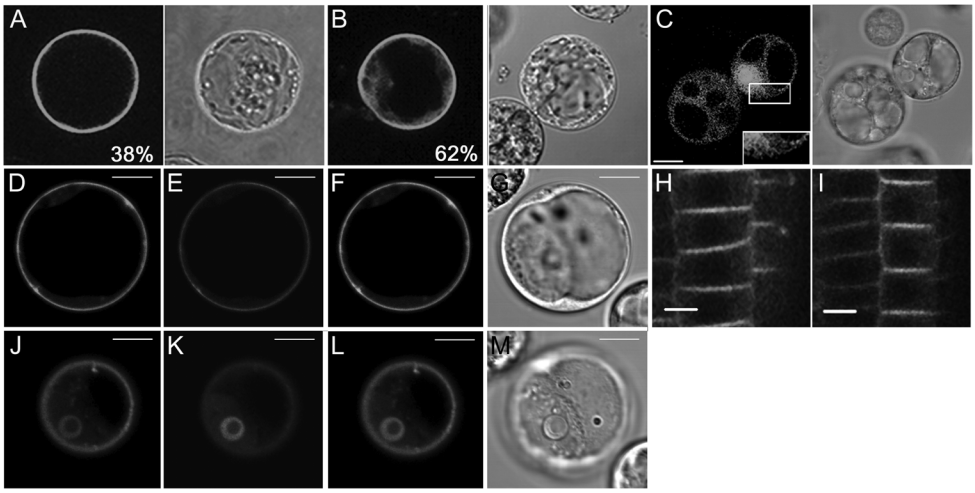


Figure 3. BT1 and PID co-localize at the plasma membrane and in the nucleus in Arabidopsis protoplasts.
(A-C) Confocal images (left) and the corresponding transmission light images (right) of representative Arabidopsis protoplasts transfected with *35Spro:GFP:PID* (A, B) or *35Spro:BT1:YFP* (C). In 38 % of the cells GFP:PID localizes at the plasma membrane (A), whereas 62 % of the cells show both cytosolic and plasma membrane localization (B). BT1:YFP localizes in the nucleus and the cytosol (C), but no clear signal is observed at the plasma membrane (detail).
(D-G) and (J-K) Different confocal sections of an Arabidopsis protoplast co-transfected with *35Spro:PID:CFP* and *35Spro:BT1:YFP*. PID:CFP shows plasma membrane (D), cytosolic (D, J) and nuclear (J) localization, whereas BT1:YFP, beside its normal cytosolic and nuclear localization (K), now localizes at the plasma membrane (E). Merged (F, L) and transmitted light (G, M) images are shown.
(H-I) A confocal microscopy section through the root meristem shows the subcellular localization of PID in epidermal cells in *PIDpro:PID:VENUS* (H) and in *PIDpro:PID:VENUS 35Spro:BT1-1* (I).
Scale bars are 10 μm.

Interestingly, however, in the co-transfected cells a clear signal was observed for BT1:YFP at the plasma membrane (Figure 3E), whereas PID:CFP could now be detected in thenucleus (Figure 3J). Control transfections with single constructs showed plasma membrane and cytosolic localization for PID:CFP, and nuclear and cytosolic localization for BT1:YFP (data not shown). Not only do these results provide important *in vivo* evidence for the interaction between PID and BT1, but they also indicate that a portion of BT1 is recruited to the plasma membrane through its interaction with PID, whereas PID is imported to the nucleus upon BT1 interaction (Figures 3D-F and 3J-L). The nuclear localization of the BT1-PID complex suggests that one of the functions of BT1 in the PID signaling pathway is to regulate the subcellular localization of PID, and also uncovers a new role for PID signaling in the nucleus. We used *35Spro:BT1:GFP* and *PIDpro:PID:VENUS* plants to find *in planta* evidence for the BT1-mediated nuclear import of PID. However, BT1:GFP localization and instability was not affected in a *PID*-overexpression background (data not shown), neither did *BT1* overexpression significantly

alter the baso-apical plasma membrane localization of PID:VENUS in root epidermal cells of seedlings (Figures 3H and 3I). The difference between the observations in protoplasts and in plants may be explained by the fact that BT1 in plants, due to its instability (see Chapter 4, this thesis), is not sufficiently abundant to visualize the recruitment of PID or BT1 to respectively the nucleus and the plasma membrane.

Overexpression of* BT1 *enhances* pid-14 *phenotypes and inhibits* 35Spro:PID *root collapse

To obtain more *in vivo* conformation on the possible role of BT1 as negative regulator of PID activity, we generated *35Spro:BT1* overexpression lines and selected two lines showing significantly increased *BT1* transcript levels for further analysis (Figure 4A). As neither of them showed mutant phenotypes, we examined the effect of *BT1* overexpression on the intermediately strong *pid-14* allele. About 40 % of the *pid-14* mutant embryos developed three instead of two cotyledons (Bennett et al., 1995), and in the *BT1* overexpression background the penetrance of the tricotyledon phenotype was significantly increased up to 58 % (Figures 4B and 4F). In addition, seedlings with more severe cotyledon phenotypes were observed, such as no-cotyledons (1 %, Figure 4C), monocotyledons (2 %, Figure 4D) and even tetracotyledons (1 % only for *35Spro:BT1-2 pid-14*, Figure 4E), phenotypes that were never found among progeny of the *pid-14* mutant line (Figure 4F). These severe phenotypes are observed in some strong *pid* alleles (Bennett et al., 1995), indicating that *BT1* overexpression enhances the mutant phenotypes of the *pid-14* allele during embryo development, which fits with a role of BT1 as negative regulator of PID. At adult plant stage, however, no phenotypes additional to the typical *pid* inflorescence were observed.

To further support the previous results, we also crossed the selected overexpression lines *35Spro:BT1-1* and *-2* with the *35Spro:PID-21* overexpression line. *PID* overexpression leads to the absence of auxin accumulation at the root meristem due to a polarity switch in the subcellular localization of PIN auxin efflux carriers (Friml et al., 2004). This results in agravitropic root growth and in the differentiation of root meristem initials, leading to the collapse of the main root meristem (Benjamins et al., 2001). *35Spro:PID-21*-induced root meristem collapse is observed in 17 % of the seedlings at 3.5 days after germination (dag) and in 91 % of the seedlings at 5.5 dag (Figure 4G and Benjamins et al, 2001). Overexpression of *BT1* resulted in a significant reduction of the *35Spro:PID-21* induced root collapse between 3.5 (3 % and 7 % for *PID-21 BT1-1* and *-2* respectively) and 5.5 dag (71 % and 80 % for *PID-21 BT1-1* and *-2*, respectively) (Figure 4G). The level of *PID* overexpression in *35Spro:PID-21 35Spro:BT1-2* did not significantly differ from that in the parental *35Spro:PID-21* line (Figure 4A), but in *35Spro:PID-21 35Spro:BT1-1* we can not completely exclude that reduced root collapse is

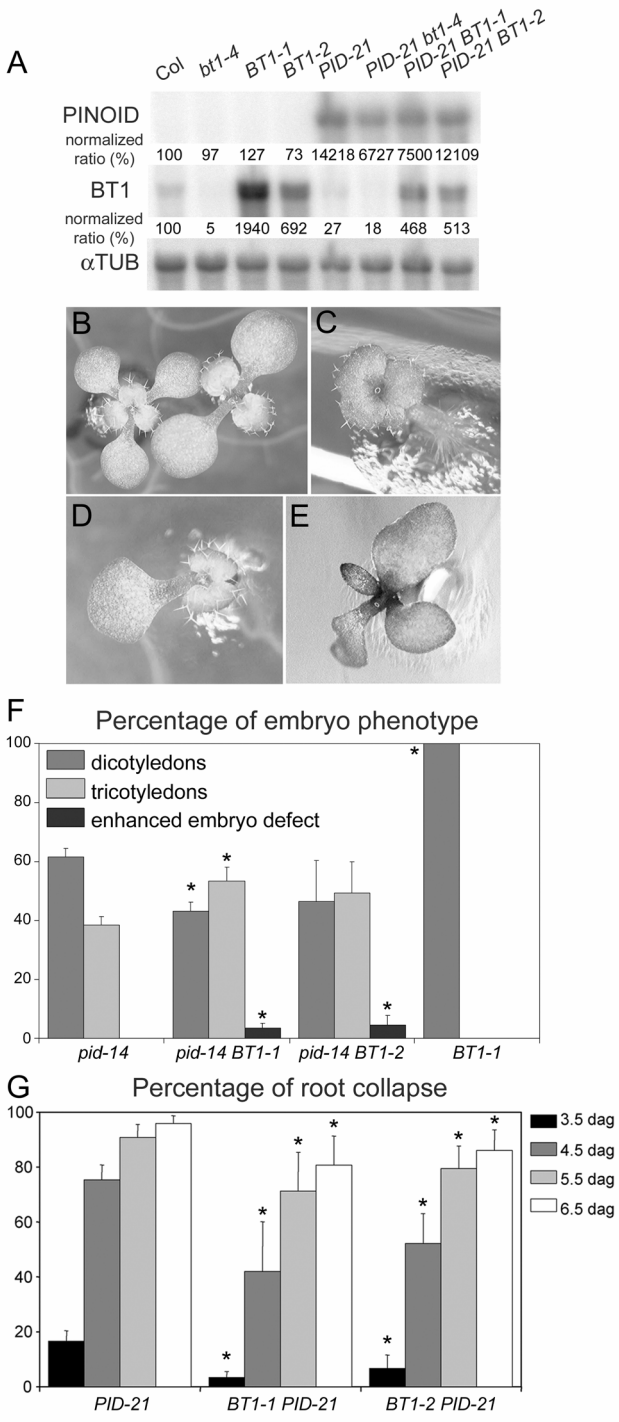


Figure 4. Overexpression of *BT1* enhances *pid-14* embryo phenotypes and inhibits *35Spro:PID-21* root meristem collapse.

(A) Northern blot analysis showing *PINOID* (top), *BT1* (middle) and *αTubulin* (bottom) expression in seedlings of the Col wild-type, *bt1-4*, the *35Spro:BT1* overexpression lines -1 and -2, *35Spro:PID-21* and in seedlings of the crosses *35Spro:PID-21 bt1-4*, *35Spro:PID-21 35Spro:BT1-1* and *35Spro:PID-21 35Spro:BT1-2*. The expression levels were quantified using ImageQuant, corrected for loading differences using *αTubulin* as a reference and normalized to the expression level in wild type.

(B) Segregation of cotyledon phenotypes observed in the *pid-14* mutant line, with the tricotyledon phenotype (left) indicative for seedlings homozygous for the *pid-14* allele.

(C-E) The enhanced cotyledon phenotypes observed in the *pid-14 35Spro:BT1* line range from no cotyledon (C), monocotyledon (D) and tetracotyledon (E) seedlings.

(F) Graph showing the proportion of tri- and di-cotyledons seedlings and seedlings with enhanced embryo phenotype (no-, mono- or tetracotyledons) in *pid-14* (n = 290, 424, 298), *pid-14 35Spro:BT1-1* (n = 372, 658, 367), *pid-14 35Spro:BT1-2* (n = 302, 688, 408) and *35Spro:BT1-1* (n = 191, 193). Stars (*) indicated that the values are significantly higher compared to *pid-14* (Student's t-test, $p < 0.05$).

(G) Graph showing the percentage of root collapse at 3.5, 4.5, 5.5 and 6.5 days after germination (dag) in *35Spro:PID-21* (n = 199, 186, 275), *35Spro:PID-21 35SproBT1-1* (n = 233, 321, 344), *35Spro:PID-21 35Spro:BT1-2* (n = 214, 315, 348). For each time point the values of the *35Spro:PID-21 35Spro:BT1* lines were significantly lower than those of *35Spro:PID-21* (Stars (*), Student's t-test, $p < 0.01$).

due to reduced *PID* expression levels. Together these results corroborate our previous conclusion that BT1 is a negative regulator of PID activity. Similar to the single overexpression lines, no striking phenotype could be observed in *35Spro:PID-21 35Spro:BT1* lines at adult plant stage.

BT1 ***overexpression does not change PIN1 and PIN2 localization in the root***

Previously, we have shown that PID is required for the correct asymmetric subcellular localization of PIN proteins and that above-threshold levels of PID expression causes the apicalization of the PIN proteins (Friml et al., 2004, Michniewicz et al., 2007). To investigate whether the observed negative effect of BT1 on PID activity results in changes in PIN polar targeting, we immunolocalized PIN1 and PIN2 in wild type, *35Spro:PID-21*, *35Spro:BT1-1* and *35Spro:PID-21 35Spro:BT1-1* seedlings. As expected, in wild type roots, PIN1 localized at the basal (root tip facing) membrane in endodermis and stele cells (Figure 5A), whereas PIN2 localized basally in the epidermis and apically (shoot apex facing) in the cortex (Figure 5B). In *35Spro:PID-21* seedlings roots, PIN1 and PIN2 localized to the apical plasma membrane in the cells where they are expressed. No significant changes in PIN1 or PIN2 localization were observed in root tips of *35Spro:BT1-1* or *35Spro:PID-21 35Spro:BT1-1* seedlings as compared to wild type or *35Spro:PID-21*, respectively (Figure 5). These observations indicate that *BT1* overexpression does not reverse the effect of PID overexpression on the subcellular PIN1 and PIN2 localization in root tips, and suggest that BT1 is involved in fine-tuning rather than completely inhibiting PID kinase activity.

PID-BT interaction is necessary for proper PID signaling

The inability of *BT* overexpression to induce changes in PIN localization indicates that BT is not merely a negative regulator of PID kinase activity. BT proteins may rather be involved in fine-tuning PID action, either by down-regulating its activity, or by offering another subset of phospho-substrates through the recruitment of PID to a specific domain of the cell (such as the nucleus). To further test this possibility and since our analysis of the Arabidopsis BT family in Chapter 4 of this thesis indicated that there is considerable functional redundancy among the *BT* genes, and we show here that at least four of the five Arabidopsis BT proteins interact with PID, we introduced the *PID* overexpression locus of line *35Spro:PID-21* in *bt* quintuple loss-of-function mutant background. *35Spro:PID-21 bt1 bt2/+ bt3/+ bt4 bt5* plants are bushy and have even shorter siliques than *bt1 bt2/+ bt3/+ bt4 bt5*, whereas siliques length of *35Spro:PID-21* plants does not significantly differ from wild type siliques (Table 1). Since quintuple homozygous seedlings in *35Spro:PID-21* background could not be obtained, we conclude that *PID* overexpression does not rescue the gametophytic lethality of the *bt* quintuple mutant (Chapter 4, this thesis). The seedling phenotype observed in *35Spro:PID-21*, collapse of the main root meristem and root

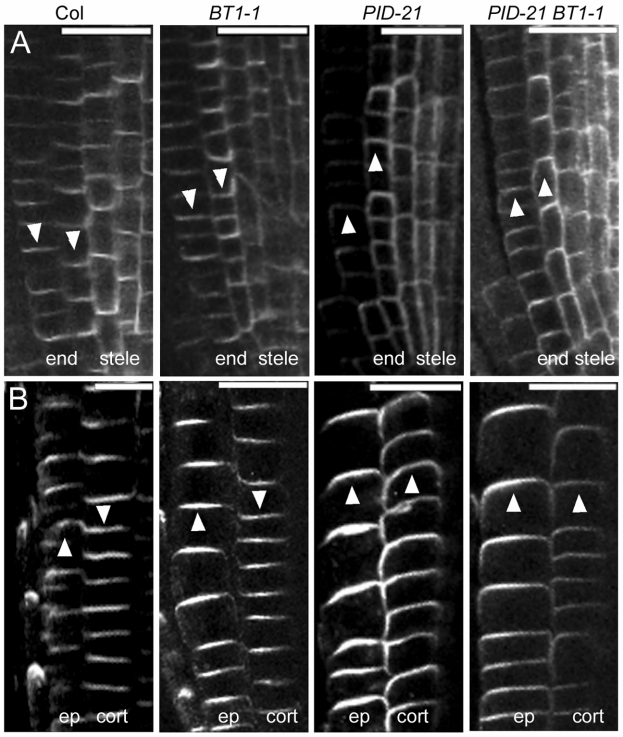


Figure 5. PIN1 and PIN2 polar targeting is not significantly changed by *BT1* overexpression.
Immunolocalization of PIN1 (A) and PIN2 (B) in Arabidopsis Columbia wild type, *35Spro:BT1-1*, *35Spro:PID-21* and *35Spro:PID-21 35Spro:BT1-1*.
(A) PIN1 is expressed in the endodermis (end) and stele of the root tip, where it is localized at the basal (root tip facing) plasma membrane in wild type and *35Spro:BT1-1* root tips, whereas apical (shoot apex facing) PIN1 localization can be observed in these cell layers in both *35Spro:PID-21* and *35Spro:PID-21 35Spro:BT1-1* root tips.
(B) PIN2 is expressed in the cortex (cort) and in the epidermis (ep) where it shows respectively basal and apical localization in wild type and *35Spro:BT1-1* roots. In *35Spro:PID-21* and *35Spro:PID-21 35Spro:BT1-1* root tips, PIN2 localizes apically in both cell layers.
Scale Bars are 50 μM.

Table 1. *bt* loss-of-function leads to reduced silique length.

	silique length (mm)*	s. d.	n
Col	15	1.3	5
bt1 bt2/+ bt3/+ bt4 bt5	8.7[*]	1.6	7
35Spro:PID-21	14.4	1	5
35Spro:PID-21 bt1 bt2/+ bt3/+ bt4 bt5	5.3[*†#]	0.6	6

[*] Significantly different from Col wild type (Student's t-test, $p < 0.01$)
[†] Significantly different from *35Spro:PID-21* (Student's t-test, $p < 0.01$)
[#] Significantly different from *bt1 bt2/+ bt3/+ bt4 bt5* (Student's t-test, $p < 0.01$)

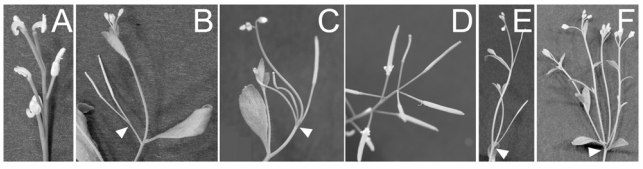
agravitropism, is absent in *35Spro:PID-21 bt1 bt2/+ bt3/+ bt4 bt5* seedlings. These observations indicate that the two characteristics of *PID* overexpression in seedlings were rescued by the (nearly) absence of the BT function in *bt1 bt2/+ bt3/+ bt4 bt5*. Although we can not exclude that *PID* overexpression levels are reduced in the quintuple *bt* mutant background, the fact that the presence of the *35Spro:PID-21* construct does have a strong effect on the development of the quintuple mutant at the adult plant stage indicates that the overexpression construct is still actively transcribed. Based on these results we conclude

that BT proteins are not merely negative regulators of PID activity, but that the PID-BT complex is an essential signaling component.

Meristem-specific BTB domain expression leads to flower and axillary branching defects

For *PID*, the *35S* promoter is not sufficiently strong during embryogenesis or inflorescence development to induce clear phenotypic defects at these stages. Only when *PID* expression was placed under control of the cell division-specific *RPS5A* promoter (Weijers et al., 2001, Weijers et al., 2003), strong defects related to auxin transport were observed in these tissues (Friml et al., 2004). Since *35S* promoter-controlled overexpression of *BT1* or its BTB domain alone did not provide mutant phenotypes, we decided to test their overexpression using the *RPS5A* promoter. *RPS5Apro>>BT1* plants showed no clear developmental defects, and also *RPS5Apro>>BTB* seedlings were normal upon germination. In 7- to 8-week old *RPS5Apro>>BTB* plants, however, significant defects in floral development and axillary branching could be observed. Flower initiation at the primary inflorescence meristem terminated prematurely, and the flowers that were formed were aberrant and did not set seed (Figure 6A). Correlating with this, 7-week old *RPS5Apro>>BTB* plants showed reduced apical dominance and developed significantly more secondary inflorescences (3.5 to 4.75 [for 3 independent transformants, n = 8] compared to 2.1 for Col wild-type [n = 8]). In comparison, *RPS5Apro>>PID* plants showed an enhanced apical dominance and only started to develop secondary stems around 7 to 8 weeks after germination (n = 7). In addition, changes in axillary branching were observed (Figures 6B-G). Siliques that are fused at the petiole (Figure 6B) or clustered siliques at the same axil of a bract (Figure 6C) were observed. In some *RPS5Apro>>BTB* lines, secondary inflorescence meristems terminated precociously resulting in clustered siliques at the tip of the stem (Figures 6D and 6G). Single siliques were also observed at an axil of a cauline leaf (Figure 6G), and in several cases, both siliques and axillary stems (paraclades) developed from an axil (Figures 6E-F). These observations indicate that the internodes, stem portions between two siliques or leaves, were missing or reduced, and that this defect appears to be random along the stem axis since normal-sized internodes were often visible.

Overexpression of *BT1* alone, either driven by the *35S* or *RPS5A* promoters, did not result in similar phenotypes, suggesting that this is a dominant negative effect of meristem-specific expression of the BTB domain. Interestingly, in *RPS5Apro>>PID* plants and in plants overexpressing both *PID* and *BT1*, some of these internode and axillary branching defects were also observed (Figure 6G). This suggests that these phenotypes are not strictly related to the down-regulation of PID activity, but rather that internode size determination is dependent on the local balance between *PID* and *BT1* expression levels, and that the interaction between PID and BT1 plays an important role in internode patterning.



G

Phenotypes							n
PID-21 BT1-1	0.4/pl			0.5/pl	0.4/pl	0.6/pl	8
PID-21 BT1-2	1.5/pl			0.5/pl		1.3/pl	8
RPS5A>>BTB-1	2.9/pl	0.6/pl	0.6/pl	0.6/pl	0.3/pl	1.1/pl	8
RPS5A>>BTB-4	1.3/pl	0.4/pl	0.5/pl	0.5/pl			8
RPS5A>>BTB-5	1.3/pl		0.1/pl	0.1/pl		0.3/pl	8
RPS5A>>PID	0.6/pl						7
Col							9
PID-21							9
BT1-1					0.1/pl		8
BT1-2							8

Figure 6. *RPS5Apro>>BTB* expression results in axillary branch and inflorescence meristem defects.
(A-F) Phenotypes observed in *RPS5A>>BTB* plants. (A) Most of the plants develop primary inflorescence stems with few aberrant flowers that do not produce seeds. (B-F) Secondary inflorescences do develop fertile flowers and siliques that are occasionally fused at the petiole ((B), arrowhead), or clustered ((C), here three, arrowhead). Clustering of siliques is also observed at the inflorescence apex (D), probably due to early termination of the inflorescence meristem. Sometimes, single siliques can be found together with a paraclade at the axil of a cauline leaf ((E), arrowhead), or two paraclades are found at the same axil (F). Note that the next axil of a cauline leave also develops a paraclade, and that the internode length is strongly reduced.
(G) Table summarizing the frequencies of the different phenotypes (expressed as occurrence per plant) observed in the *RPS5Apro>>BTB* lines. Interestingly, some phenotypes are also observed in *35Spro:PID 35Spro:BT1* and *RPS5Apro>>PID* plants.

Discussion

An important characteristic of the plant hormone auxin is its polar transport which generates gradients and maxima that are instructive for cell division and growth during plant development. The chemiosmotic hypothesis proposed in the 1970's for the cell-to-cell transport of this hormone predicted that transporter proteins that drive the cellular efflux of auxin are themselves polarly localized (Rubery and Sheldrake, 1974, Raven, 1975). Later, the PIN proteins have been identified as auxin efflux carriers that determine the direction of transport through their asymmetric subcellular localization (Gälweiler et al., 1998, Wisniewska et al., 2006, Petrášek et al., 2006). In addition the protein kinase PID was found to control the direction of the auxin flux by regulating the subcellular localization of the PIN proteins (Friml et al., 2004). PID acts antagonistic to phosphatases through direct phosphorylation of PINs (Michniewicz et al., 2007). How this regulates the subcellular

targeting of PIN proteins, and which components are involved in the PID signaling pathway is largely unknown.

A yeast two-hybrid screen identified several PID interacting proteins, of which the two calcium binding proteins TCH3 and PBP1 have been described previously (Benjamins et al., 2003). Here we report the functional analysis of the plant specific BTB protein PINOID BINDING PROTEIN2 (PBP2), previously named BTB and TAZ domain protein1 (BT1). The interaction between PID and BT1/PBP2 was first identified in a yeast two-hybrid screen, and confirmed and confined to the BTB domain of BT1 by *in vitro* pull-down experiments. Northern blot analysis showed that the expression patterns of the two proteins overlap. Moreover, co-expression of CFP-tagged PID and YFP-tagged BT1 in Arabidopsis protoplasts resulted in recruitment of PID to the nucleus and BT1 to the plasma membrane, subcellular compartments where the single expressed proteins did not localize. This provided *in vivo* evidence for the interaction between PID and BT1.

BT1 as a negative regulator of PID kinase activity

For PBP1 and TCH3 it was demonstrated previously that they are not phospho-targets of PID, but that they bind PID to regulate its kinase activity in response to cytosolic calcium levels (Benjamins et al., 2003). Here we show that also BT1 is not phosphorylated by PID. Instead, BT1 reduced the activity of the kinase in *in vitro* phosphorylation assays, suggesting a role for BT1 as negative regulator of the PID pathway. This role was corroborated by the fact that *BT1* overexpression enhanced the *pid-14* loss-of-function embryo phenotypes and reduced the *PID* overexpression phenotypes. However, even though *BT1* overexpression reduced *PID* overexpression phenotypes, no striking and direct effect was observed on the PID-dependent basal to apical switch of PIN protein localization in *35Spro:PID-21 35Spro:BT1-1* roots. This result suggests that BT1 is not purely a negative regulator of PID activity, but that it rather modulates and fine tunes PID activity in different developmental processes.

This is corroborated by the observation that *BT1* overexpression does not affect *pid-14* inflorescences, whereas an enhancement of the pin-like phenotype is anticipated analogous to the enhanced cotyledon phenotypes of *pid-14 35Spro:BT1-1* embryos. The *35S* promoter is known to be active in floral meristems and in flowers (Bossinger and Smyth, 1996, Meister et al., 2005), and overexpression of other genes, e.g. MADS-box genes, using this promoter has lead to clear flower/inflorescence phenotypes (Robles and Pelaz, 2005). The absence of the effect of *BT1* overexpression on the *pid* inflorescence phenotype may be due to either (i) the non-availability of the BT1 scaffold protein for binding to other interactors in these tissues, (ii) a tissue specificity in the interaction between BT1 and PID and/or (iii) the increased instability of the BT1 protein in these tissues.

In Chapter 4 of this thesis we show that BT1 is an instable protein that is a target for degradation by the 26S proteasome, and that the instability is linked to the BTB domain. It would be interesting to test whether PID is part of this degradation process, and whether BT1 is involved in PID turn-over. The instability could explain why BT1 overexpression, both under control of the 35S or the meristem-specific *RPS5A* promoter (Weijers et al., 2001, Weijers et al., 2003) does not lead to clear phenotypic defects. However, meristem-specific overexpression of the BTB domain alone does provide clear dominant negative inflorescence phenotypes, which is expected if the BTB domain titrates out BT1 interactors such as PID to prevent their incorporation into their appropriate complexes.

Recently, a second BTB protein, the NPH3-like MACCHI BOU4/ENHANCER OF PINOID/NAKED PINS IN YUC MUTANTS1 (MAB4/ENP/NPY1), has been connected to the PID signaling pathway (Cheng et al., 2007, Furutani et al., 2007). The *mab4* loss-of-function mutation enhances *pid* phenotypes and affects PIN1 localization and expression in inflorescence meristem and embryo. MAB4 localizes in intracellular compartments, suggesting that MAB4, similar to BT1 is not a direct phospho-target of PID, but either a regulatory component of PID signaling or involved in a second parallel pathway that affects PIN polar targeting.

BT proteins as scaffold proteins in PINOID pathway

As predicted from its domain structure, BT1 is likely to serve as a scaffold protein that recruits PID to the appropriate signaling complex. PID interacts with the BTB domain of BT1, which in turn interacts with several other proteins, such as cytoskeleton related proteins or MYB domain proteins, through its TAZ domain (Kemel Zago, 2006). Analysis of the *35Spro:PID-21 bt1 bt2/+ bt3/ bt4 bt5* mutant indicates that the (nearly) absence of the BT function rescued the agravitropic growth and root meristem collapse observed in the *35Spro:PID-21* seedlings. This indicates that BT proteins are not merely negative regulators, but that they are important components of the PID signaling pathway. The inhibitory effect of BT1 on PID activity observed in *in vitro* phosphorylation assays and by overexpressing *BT1* in *pid-14* and *35Spro:PID-21* background may be the effect of BT1 blocking the PID catalytic domain during binding. In order to validate this conclusion, it would be interesting to investigate whether the apicalized PIN localization in is restored in the *bt* quintuple mutant. Moreover, besides rescue of the *PID* overexpression seedlings phenotypes, the *bt* quintuple mutant enhances phenotypes at the adult plant stage. Flowering *35Spro:PID-21* plants do not show clear phenotypes, whereas *35Spro:PID-21* quintuple *bt* mutant plants are bushy and develop short siliques, even shorter than observed in the quintuple *bt* mutant. This indicates that the effect of *PID* overexpression in the wild type background is masked by the BT proteins.

PID and BT1, a possible feed back loop between auxin and KNOX proteins

Interestingly, expressing the PID binding BTB domain under the *RPS5A* promoter leads to precocious arrest of the inflorescence meristem, production of infertile flowers, reduced internode elongation and apical dominance- and axillary branching defects. The fact that such phenotypes were not observed by overexpressing *BT1*, suggests that overexpression of the BTB domain has a dominant negative effect due to absence of the TAZ domain. However, some, but not all, of the axillary branching defects were also observed in the *RPS5Apro>>PID* and *35Spro:PID 35Spro:BT1* lines, indicating that these inflorescence phenotypes are not only caused by a reduction of PID activity. Based on the current data we hypothesize that rather an imbalance in the availability of PID and BT1 to interact, either by overexpressing one, both or a partial component, leads to subtle defects in the polar auxin transport. Correct localization of the PIN proteins at the SAM is crucial for a correct positioning of the auxin maxima that in turn controls the initiation and out growth of lateral organs, such as leaves and flowers (Reinhardt et al., 2003). Perturbing the correct activity of PID in these tissues affects the downstream PID-dependent processes and the siliques phyllotaxis.

Remarkably, clustered siliques are specific for the *RPS5Apro>>BTB* lines. Similar phenotypes are observed in loss-of-function mutants of the *BEL1-like homeobox* (*BEL*) gene *PENNYWISE* (*PNY*) (Smith and Hake, 2003). PENNYWISE and its orthologous protein POUND-FOOLISH (PNF) interact with the Knotted1-like homeobox (KNOX) proteins BREVIPEDICELLUS (BP) and SHOOTMERISTEMLESS (STM) (Kanrar et al., 2006). These BEL-KNOX heterodimers are responsible for internode patterning. Interestingly, BP and a microtubule-associated protein MPB2C (Kragler et al., 2003) were found to interact with BT1 in the yeast two-hybrid system (Kemel Zago, 2006)). Recently, MPB2C was found to interact with STM to prevent its cell-to-cell transport (Winter et al., 2007). At the same time, auxin and the PIN transporter protein-mediated polar distribution of this hormone control inflorescence architecture, by regulating apical dominance, internode elongation and phyllotaxis (Reinhardt et al., 2003, Leyser, 2003, Woodward et al., 2005). A recent paper identified the LOB domain protein JAGGED LATERAL ORGANS (JLO) as activator of BP expression and repressor of PIN expression (Borghi et al., 2007). Loss-of-function *bp* partially rescues *pid* and *pin1* flower phenotype, and correct auxin transport regulation is necessary to promote leaf development by repressing *BP* expression (Hay et al., 2006). Moreover, the maize *rough sheat2* mutant that overexpresses three *KNOX* genes shows decreased polar auxin transport (Tsiantis et al., 1999). Clearly there is a complex network of interactions between auxin transport and signaling and the action of KNOX and BEL proteins. The BT1 scaffold protein could be part of a feed back loop through its interaction with PID, MPB2C and BP.

Material and Methods

Yeast two-hybrid screen, molecular cloning and constructs

The yeast two-hybrid screen has been described previously (Benjamins et al., 2003). Molecular cloning was performed following standard procedures (Sambrook et al., 1989). The complete coding region of *PID*, excluding the start codon, was amplified using primers PID-*Sal*I-F1 (5'GG-*Sal*I-TTACGAGAATCAGACGGTGAG3') and PID-*Xba*I-R1 (5'CC-*Xba*I-CCGTAGAAAACGTTCAAAAGT3') and cloned into pBluescriptSK+ to create pSDM6005. The cDNA of *PID* was then N-terminally fused (*Xmn*I-*Sal*I) to the His-tag (10x His) present in pET16H (Klenow blunted *BamH*I-*Xho*I), a derivative of pET16B (J. Memelink, unpublished results). The construct pSDM6004 (pGEX-PID) has been described elsewhere (Benjamins et al., 2003). The *35Spro:PID:GFP* construct was generated by amplifying the *PID* cDNA using the primers 5'TTAATATGACTCACTATAGG3' and 5'GCTCACCATAAAGTAATCGAACGC3' and the *eGFP* coding region using the primers 5'GATTACTTTATGGTGAGCAAGGGC3' and 5'TCAATCTGAGTACTTGTACAG3'. Both PCR products were used in a fusion PCR with outer primers, and the amplified *PID:GFP* fragment was cloned into pUC28 digested with *Nco*I and *Hin*cII, and excised again with *Eco*RI and *Stu*I (blunted) for ligation into *Eco*RI-*Sma*I digested pART7. The *35Spro:PID:CFP* construct was made using the Gateway Technology (Invitrogen). *PID* cDNA was PCR amplified from pSDM6004 (pGEX:PID) (Benjamins et al., 2003) with primers containing *att*B recombination sites (underlined):
5'GGGGACAAGTTTGTACAAAAAAGCAGGCTTCAGCATGTTACGAGAATCAGAC GGT3' and
5'GGGGACCACTTTGTACAAGAAAGCTGGGTCAAAGTAATCGAACGCCGCTGG3' BP reaction was performed in pDONOR207 according to manufacturer's instructions (Invitrogen). Recombinant plasmid was isolated and sequenced. LR reaction was performed in pART7 plasmids containing the CFP fluorescent markers in frame with the gateway recombinant cassette (C. Galvan-Ampudia, unpublished data).

The plasmids pSDM6014 (pBS-BT1), pSDM6069 (pUC28-BT2), pSDM6086 (pC1300-BT1), pSDM6092 (pUC28-BT4), pSDM6099 (pART7-BT1:YFP) and pDM6309 (pDONOR207-BT3) were previously described (Chapter 4, this thesis). The cDNA of *BT1* (*Xho*I-*Sma*I digested from pSDM6014), excluding the start codon, was cloned into pGEX-KG (Guan and Dixon, 1991) to obtain pGEX-BT1 encoding an N-terminal GST-BT1 fusion. The plasmid pGEX-BTB, encoding the GST-tagged BT1 BTB/POZ domain, was generated by digesting pGEX-BT1 with *Nde*I and filling in with Klenow. The plasmid pGEX-TAZ, encoding the GST-tagged BT1 TAZ domain, was constructed by deleting the *Nco*I fragment from pGEX-BT1. For the N-terminal His-BT1 fusion used within the *in vitro* pull-down and the *in vitro* phosphorylation assay experiments, the *BT1* coding region

which excluded the start codon was cloned as a *Xho*I-*Sma*I fragment into pET16H (pSDM6006).The *BT2* cDNA was cloned (*Eco*RI-*Bam*HI from pSDM6069) in frame with a His-tag in pET16H (pSDM6078). The *BT4* cDNA was cloned (*Eco*RI-*Bam*HI from pSDM6092) in frame with the His-tag in pET16H (pSDM6093). The translational fusion between *BT5* cDNA (from pSDM6309) and the His-tag was generated into the pET16H derived destination vector (pSDM6310) (C. Galvan-Ampudia, unpublished data) using the Gateway technology (Invitrogen). To construct pEF-BT1, *BT1* cDNA was cloned as an *Eco*RI-*Kpn*I fragment from pSUMFUNdelta*Nco*I-BT1s (Y. Xiong, unpublished data) into pIC-UAS-E-tNOS, derived from pSDM7022 (Weijers et al., 2003). To construct pEF-BTB, the *Nco*I fragment containing the BTB part of BT1 from pGEX-BT1 was cloned into pUC28. The BTB domain (*Bam*HI-*Eco*RI) was then fused to the UAS promoter into pIC-UAS-E-tNOS. The expression cassettes *UAS-E-BT1-tNOS* and *UAS-E-BTB-tNOS* were then transferred as a *Hin*dIII fragment from pIC-UAS-E-BT1-tNOS or pIC-UAS-E-BTB-tNOS respectively into pSDM7006 (Weijers et al., 2003).

***Arabidopsis* lines, plant growth, transformation and protoplast transfections**

The *35Spro:PID*-21 line (Benjamins et al., 2001), the *PIDpro:PID:VENUS* line (Michniewicz et al., 2007), the quintuple mutant *bt1 bt2/+ bt3/+ bt4 bt5* (Chapter 4, this thesis) and *pid-14* allele (SALK_049736) (Chapter 2, this thesis) were described previously.

Arabidopsis seeds were surfaced-sterilized by incubation for 15 min in 50 % commercial bleach solution and rinsed four times with sterile water. Seeds were vernalized for 2 to 4 days before germination (21^{o}C, 16-hour photoperiod and 3000 lux) on solid MA medium (Masson and Paszkowski, 1992) supplemented with antibiotics when required. Two- to three-week old plants were transferred to soil and grown at 21^{o}C with a 16-hour photoperiod of 10000 lux and at 70 % relative humidity.

Arabidopsis thaliana ecotype Columbia (Col) was transformed by floral dipping method as described (Clough and Bent, 1998) using *Agrobacterium tumefaciens* strain LBA1115. The binary construct *35Spro:BT1* was transformed into *Arabidopsis* Col plants. The constructs *EF-BT1* and *EF-BTB* were transformed into the *ACT-RPS5A*-5 line (Weijers et al., 2003). Primary transformants were selected on medium supplemented with 20 µg/ml hygromycin for the *35S* constructs or 30 µg/ml phosphinotricin and 25 µg/ml kanamycin for the *EF* constructs and 100 µg/ml timentin to inhibit *Agrobacterium* growth. For further analysis, single locus insertion lines were selected by segregation on hygromycin at 10 µg/ml or phosphinotricin at 15 µg/ml and analyzed for expression by Northern blot analysis (*35Spro:BT1*).

Protoplasts were obtained from Arabidopsis Col cell suspension cultures that were propagated as described (Schirawski et al., 2000). Protoplast isolation and PEG-mediated transfections were performed as initially described (Axelos et al., 1992) and adapted by

Schirawski and coworkers (Schirawski et al., 2000). Transfections were performed with 20 µg (*35Spro:GFP*, *35Spro:PID:GFP*) or 5 µg (*35Spro:PID:CFP*, *35Spro:BT1:YFP*) of plasmid DNA, after which the cells were incubated for at least 16 h prior observation using confocal laser scanning microscopy.

***In vitro* pull down experiments**

E. coli strain Rosetta (Novagen) was transformed with pGEX, pSDM6004, pSDM6006, pSDM6078, pSDM6093 and pSDM6310. And His-tagged PID and GST-tagged BT1, BTB/POZ and TAZ or GST alone were expressed and purified from *E. coli* strain BL21-DE03. *E. coli* cells containing one of the constructs were grown at 37^{o}C to OD_{600} 0.8 in 50 ml LC supplemented with antibiotics. The cultures were then induced for 4 h with 1 mM IPTG at 30^{o}C, after which cells were harvested by centrifugation (10 min, 4000 rpm) and stored at -20^{o}C. Precipitated cells were resuspended in 2 ml Extraction Buffer (EB: 1x PBS, 2 mM EDTA, 2 mM DTT) supplemented with 0.1 mM PMSF (Phenylmethanesulfonyl Fluoride), 0.1 mM Leupeptin and 0.1 mM Aprotinin for the GST-tagged proteins or in 2 ml Binding Buffer (50 mM Tris-HCl pH 6.8, 100 mM NaCl, 10 mM $CaCl_2$) supplemented with 0.1 mM PMSF, 0.1 mM Leupeptin and 0.1 mM Aprotinin for His-tagged proteins and sonicated for 2 min on ice. From this point on, all steps were performed at 4^{o}C. Eppendorf tubes containing the sonicated cells were centrifuged at 14000 rpm for 20 min. The supernatant containing His-tagged proteins was left on ice, while 100 µl Glutathione Sepharose 4B resin (Amersham-Pharmacia) (pre-equilibrated with three washes of 10 resin volumes of 1x PBS followed by three washes of 10 resin volumes of 1x EB at 500 g for 5 min) was added to the GST-fusion proteins containing supernatants. Resin-containing mixtures were incubated for 1 h with gentle agitation, subsequently centrifuged at 500 g for 3 min and the precipitated resin was washed three times with 20 resin volumes of EB. Next, His-tagged proteins containing supernatant (approximately 2 ml) was added to GST-fusions-containing resins, and the mixtures were incubated for 1 h with gentle agitation. After incubation, supernatants containing GST resins were centrifuged at 500 g for 3 min, the new supernatants were discarded and the resins subsequently washed three times with 20 resin volumes of EB. Protein loading buffer was added to the resin samples, followed by denaturation for 5 min at 95^{o}C. Proteins were subsequently separated on a 10 % (BT proteins pull-down assay) or 12 % (Domains pull-down assay) polyacrylamide gel prior to transfer to an Immobilon-P PVDF (Millipore) membrane. Western blots were hybridized using a horse radish peroxidase (HRP)-conjugated anti-penta Histidine antibody (Qiagen) and detection followed the protocol described for the Phototope-HRP Western Blot Detection Kit (New England Biolabs). A parallel gel was run and stained with Coomassie as loading control.

***In vitro* phosphorylation assays**

His-tagged proteins were purified from 5 aliquots of 50 ml cultures of *E. coli*. BL21 cells which were grown, induced, pelleted and frozen as described above for the *in vitro* pull down experiments. Commercial Myelin Basic Protein (MBP, Sigma) was used a positive control. Each aliquot of frozen cell pellet was resuspended in 2 ml Lysis Buffer (LB: 25 mM Tris-HCl pH 8.0, 500 mM NaCl, 20 mM Imidazol, 0.1 % Tween-20) supplemented with 0.1 mM PMSF, 0.1 mM Leupeptin and 0.1 mM Aprotinin and sonicated for 2 min on ice. Further steps were performed at 4°C. Sonicated cells were centrifuged at 14000 rpm for 20 min, supernatants from all aliquots of the same construct were transferred to a 15 ml tube containing 100 µl of pre-equilibrated Ni-NTA resin (Qiagen) (pre-equilibration performed with three washes of 10 resin volumes of LB at 500 g for 5 min). Supernatant and resin were mixed, incubated with gentle agitation for 1 h, after which the resin was collected by centrifugation at 500 g for 3 min. The resin was washed three times with 20 resin volumes of LB, once with 20 resin volumes of Wash Buffer 1 (25 mM Tris-HCl pH 8.0, 500 mM NaCl, 40 mM Imidazol, 0.05 % Tween-20) and once with 20 resin volumes of Wash Buffer 2 (25 mM Tris-HCl pH 8.0, 600 mM NaCl, 80 mM Imidazol). After the last washing step, the resin was incubated in 20 volumes of Elution Buffer (25 mM Tris-HCl pH 8.0, 500 mM NaCl, 500 mM Imidazol) for 15 min with gentle agitation. The resin was centrifuged for 3 min at 500 g, and the supernatant containing the desired protein was diluted a 1000-fold in Tris Buffer (25 mM Tris-HCl pH 7.5, 1 mM DTT) and concentrated to a workable volume (usually 50 µl) using Vivaspin microconcentrators (10 kDa cut off, maximum capacity 600 µl, Vivascience). Glycerol was added as preservative to 10 % final concentration and samples were stored at -80°C.

Approximately 1 µg of purified His-tag protein (PID and substrate) was added to a 20 µl kinase reaction mix, containing 1x kinase buffer (25 mM Tris-HCl pH 7.5, 1 mM DTT, 5 mM $MgCl_2$) and 1 x ATP solution (100 µM $MgCl_2$, 100 µM ATP-Na_2, 1 µCi ^{32}P-γ-ATP). Reactions were incubated at 30°C for 30 min and stopped by addition of 5 µl of 5x protein loading buffer (310 mM Tris-HCl pH 6.8, 10 % SDS, 50 % Glycerol, 750 mM β-Mercaptoethanol, 0.125 % Bromophenol Blue) and 5 min boiling. Reactions were subsequently separated over 12.5 % acrylamide gels, which were washed three times for 30 min with Kinase Gel Wash Buffer (5 % Trichoroacetic Acid, 1 % $Na_2H_2P_2O_7$), Coomassie stained and dried. Autoradiography was performed for 24 to 48 h at -80°C using Fuji Super RX X-ray films and intensifier screens.

RNA extraction and Northern Blots

Total RNA was purified using the RNeasy Plant Mini kit (Qiagen). Subsequent RNA blot analysis was performed as described (Memelink et al., 1994) using 10 µg of total RNA per sample. The following modifications were made: pre-hybridizations and hybridizations were conducted at 65°C using a different hybridization mix (10 % Dextran sulfate, 1 %

SDS, 1 M NaCl, 50 µg/ml of single strand Herring sperm DNA). The hybridized blots were washed for 20 min at 65°C in 2x SSPE 0.5 % SDS, and for 20 min at 42°C in respectively 0.2x SSPE 0.5 % SDS, 0.1x SSPE 0.5 % SDS and 0.1x SSPE. Blots were exposed to X-ray film FUJI Super RX. Probes were PCR amplified and column purified (Qiagen): 5'CATCCCAAACATTACAAAGGGC3', 5'TTCTCCGAGGTTCGTCTTTC3' for *BT1* from pSDM6006; 5'AGGCACGTGACAACGTCTC3', 5'CGCAAGACTCGTTGGAAAAG3' for *PID* from Col genomic DNA; 5'CGGAATTCATGAGAGAGATCCTTCATATC3', 5'CCCTCGAGTTAAGTCTCGTACTCCTCTTC3' for *αTubulin* from Col genomic DNA; 5'CGGGAAGGATCGTGATGGA3', 5'CCAACCTTCTCGATGGCCT3' for *AtROC* from Col genomic DNA. Probes were radioactively labeled using α-^{32}P-ATP (Amerscham) and a Prime-a-gene kit (Promega).

Immunolocalization

Whole-mount immunolocalizations were performed on 3-day old seedlings fixed in 4 % paraformaldehyde in MTSB buffer as described previously (Friml et al., 2003) using medium size baskets format in an InSituPro robot (INTAVIS, Cologne, Germany). Rabbit anti-PIN1 and anti-PIN2 primary antibodies (1/400) and Alexa 488-conjugated anti-rabbit secondary antibodies (1/200, Molecular Probes) were used for detection. Samples were observed using confocal laser scanning microscopy.

Biological assays

For the root meristem collapse assay, about 200 seedlings per line were grown in triplicate on vertical plates on MA medium, while the development of the seedling root was monitored and scored each day during eight days for the collapse of the primary root meristem. For the phenotypic analysis of *35Spro:BT1 pid-14/+* lines, about 300 seeds (200 for *35Spro:BT1-1*) were plated in triplicate on MA medium and germinated for one week. The number of dicotyledon seedlings and of seedlings with specific cotyledon defects was counted and the penetrance of the specific phenotypes was calculated based on a 1:3 segregation ratio for *pid/pid* seedlings. To test for auxin responsive gene expression, one-week old Arabidopsis Col seedlings were transferred to liquid MA medium under shaking conditions. After 3 days of culture, seedlings were treated with 5 µM IAA for the indicated time.

Confocal Laser Scanning Microscopy

YFP fusion lines and immunolocalizations were observed using 40x dry and oil objectives on a ZEISS Axioplan microscope equipped with a confocal laser scanning unit (MRC1024ES, BIO-RAD, Hercules, CA). The YFP and Alexa 488 fluorescences were monitored with a 522-532 nm band pass emission filter (488 nm excitation). All images

were recorded using a 3CCD Sony DKC5000 digital camera. For the protoplast experiments, a Leica DM IRBE confocal laser scanning microscope was used with a 63x water objective. The fluorescence was visualized with an Argon laser for excitation at 488 nm (GFP), 514 nm (YFP) and 457 nm (CFP) with 522-532 nm (GFP), 527-560 nm (YFP) and 467-499 nm (CFP) emission filters. The images were processed by ImageJ (http://rsb.info.nih.gov/ij/) and assembled in Adobe Photoshop 7.0.

Accession Numbers

The Arabidopsis Genome Initiative locus identifiers for the genes mentioned in this article are as follows: *BT1/PBP2* (At5g63160), *BT2/PBP2H1* (At3g48360), *BT3/PBP2H2* (At1g05690), *BT4/PBP2H4* (At5g67480), *BT5/PBP2H3* (At4g37610), *PID* (At2g34650), *PIN1* (At1g73590), *PIN2* (At5g57090), *TCH3* (At2g41100), *PBP1* (At5g54490), *ROC* (At4g38740), *αTubulin* (At5g44340), *PNY* (At5g02030), *PNF* (At2g27990), *BP* (At4g08150), *STM* (At1g62230), *JLO* (At4g00220), *NPH3* (At5g64330), *RPT2* (At2g30520), *CUL3a* and *b* (At1g26830 and At1g69670), *MAB4/ENP* (At4g31820), *BET10/GTE11* (At3g01770), *BET9/GTE* (At5g14270) and *TAC1* (At3g09290).

Acknowledgements

We would like to thank Ward Winter for their technical assistance, Gerda Lamers for her helpful advises concerning microscopy, Jiří Friml and Christian Luschnig for providing respectively PIN1 and PIN2 antibodies, M. Heilser for the *PIDpro:PID:VENUS* seeds and Pieter Ouwerkerk for kindly providing the pCambia1300int-35Snos and pCAMBIA1300 plasmids. This work was financially supported by the Brazilian Funding Agency for Post-Graduation Education-CAPES (M.K.Z.), and by Earth and Life Sciences (ALW) with financial support from the Dutch Organization of Scientific Research (NWO, C. G-A.).

References

Albagli,O., Dhordain,P., Deweindt,C., Lecocq,G., and Leprince,D. (1995). The BTB/POZ domain: a new protein-protein interaction motif common to DNA- and actin-binding proteins. Cell Growth Differ **6**:1193-1198.

Axelos,M., Curie,C., Mazzolini,L., Bardet,C., and Lescure,B. (1992). A Protocol for Transient Gene-Expression in Arabidopsis-Thaliana Protoplasts Isolated from Cell-Suspension Cultures. Plant Physiology and Biochemistry **30**:123-128.

Bardwell,V.J. and Treisman,R. (1994). The Poz Domain - A Conserved Protein-Protein Interaction Motif. Genes & Development **8**:1664-1677.

Benjamins, R. (2004). Functional analysis of the PINOID protein kinase in *Arabidopsis thaliana*. Institute of Biology, Leiden University, The Netherlands.

Benjamins,R., Galván-Ampudia,C.S., Hooykaas,P.J., and Offringa,R. (2003). PINOID-mediated signaling involves calcium-binding proteins. Plant Physiol **132**:1623-1630.

Benjamins,R., Quint,A., Weijers,D., Hooykaas,P., and Offringa,R. (2001). The PINOID protein kinase regulates organ development in Arabidopsis by enhancing polar auxin transport. Development **128**:4057-4067.

Benková,E., Michniewicz,M., Sauer,M., Teichmann,T., Seifertová,D., Jürgens,G., and Friml,J. (2003). Local, efflux-dependent auxin gradients as a common module for plant organ formation. Cell **115**:591-602.

Bennett,S.R.M., Alvarez,J., Bossinger,G., and Smyth,D.R. (1995). Morphogenesis in Pinoid Mutants of Arabidopsis-Thaliana. Plant J. **8**:505-520.

Borghi,L., Bureau,M., and Simon,R. (2007). Arabidopsis JAGGED LATERAL ORGANS Is Expressed in Boundaries and Coordinates KNOX and PIN Activity. Plant Cell:1795-1808.

Bossinger,G. and Smyth,D.R. (1996). Initiation patterns of flower and floral organ development in Arabidopsis thaliana. Development **122**:1093-1102.

Cheng,Y., Qin,G., Dai,X., and Zhao,Y. (2007). NPY1, a BTB-NPH3-like protein, plays a critical role in auxin-regulated organogenesis in Arabidopsis. Proc.Natl.Acad.Sci.U.S.A.

Christensen,S.K., Dagenais,N., Chory,J., and Weigel,D. (2000). Regulation of auxin response by the protein kinase PINOID. Cell **100**:469-478.

Clough,S.J. and Bent,A.F. (1998). Floral dip: a simplified method forAgrobacterium-mediated transformation ofArabidopsis thaliana. Plant J. **16**:735-743.

Dieterle,M., Thomann,A., Renou,J.P., Parmentier,Y., Cognat,V., Lemonnier,G., Muller,R., Shen,W.H., Kretsch,T., and Genschik,P. (2005). Molecular and functional characterization of Arabidopsis Cullin 3A. Plant J. **41**:386-399.

Du,L.Q. and Poovaiah,B.W. (2004). A novel family of Ca2+/calmodulin-binding proteins involved in transcriptional regulation: interaction with fsh/Ring3 class transcription activators. Plant Molecular Biology **54**:549-569.

Figueroa,P., Gusmaroli,G., Serino,G., Habashi,J., Ma,L.G., Shen,Y.P., Feng,S.H., Bostick,M., Callis,J., Hellmann,H., and Deng,X.W. (2005). Arabidopsis has two redundant Cullin3 proteins that are essential for embryo development and that interact with RBX1 and BTB proteins to form multisubunit E3 ubiquitin ligase complexes in vivo. Plant J. **17**:1180-1195.

Friml,J., Benková,E., Mayer,U., Palme,K., and Muster,G. (2003). Automated whole mount localisation techniques for plant seedlings. Plant J. **34**:115-124.

Friml,J., Yang,X., Michniewicz,M., Weijers,D., Quint,A., Tietz,O., Benjamins,R., Ouwerkerk,P.B.F., Ljung,K., Sandberg,G., Hooykaas,P.J.J., Palme,K., and Offringa,R. (2004). A PINOID-dependent binary switch in apical-basal PIN polar targeting directs auxin efflux. Science **306**:862-865.

Furutani,M., Kajiwara,T., Kato,T., Treml,B.S., Stockum,C., Torres-Ruiz,R.A., and Tasaka,M. (2007). The gene MACCHI-BOU 4/ENHANCER OF PINOID encodes a NPH3-like protein and reveals similarities between organogenesis and phototropism at the molecular level. Development.

Gälweiler,L., Guan,C., Müller,A., Wisman,E., Mendgen,K., Yephremov,A., and Palme,K. (1998). Regulation of polar auxin transport by AtPIN1 in Arabidopsis vascular tissue. Science **282**:2226-2230.

Gingerich,D.J., Gagne,J.M., Salter,D.W., Hellmann,H., Estelle,M., Ma,L.G., and Vierstra,R.D. (2005). Cullins 3a and 3b assemble with members of the broad complex/tramtrack/bric-a-brac (BTB) protein family to form essential ubiquitin-protein ligases (E3s) in Arabidopsis. J.Biol.Chem. **280**:18810-18821.

Guan,K.L. and Dixon,J.E. (1991). Eukaryotic Proteins Expressed in Escherichia-Coli - An Improved Thrombin Cleavage and Purification Procedure of Fusion Proteins with Glutathione-S-Transferase. Analytical Biochemistry **192**:262-267.

Hay,A., Barkoulas,M., and Tsiantis,M. (2006). ASYMMETRIC LEAVES1 and auxin activities converge to repress BREVIPEDICELLUS expression and promote leaf development in Arabidopsis. Development **133**:3955-3961.

Kanrar,S., Onguka,O., and Smith,H. (2006). Arabidopsis inflorescence architecture requires the activities of KNOX-BELL homeodomain heterodimers. Planta **224**:1163-1173.

Kemel Zago, M. (2006). Components and targets of the PINOID signaling complex in *Arabidopsis thaliana*. Institute of Biology, Leiden University, The Netherlands.

Kragler,F., Curin,M., Trutnyeva,K., Gansch,A., and Waigmann,E. (2003). MPB2C, a microtubule-associated plant protein binds to and interferes with cell-to-cell transport of tobacco mosaic virus movement protein. Plant Physiol **132**:1870-1883.

Lee,S.H. and Cho,H.T. (2006). PINOID positively regulates auxin efflux in Arabidopsis root hair cells and tobacco cells. Plant Cell **18**:1604-1616.

Leyser,O. (2003). Regulation of shoot branching by auxin. Trends Plant Sci. **8**:541-545.

Masson,J. and Paszkowski,J. (1992). The Culture Response of Arabidopsis-Thaliana Protoplasts Is Determined by the Growth-Conditions of Donor Plants. Plant J. **2**:829-833.

Meister,R.J., Oldenhof,H., Bowman,J.L., and Gasser,C.S. (2005). Multiple Protein Regions Contribute to Differential Activities of YABBY Proteins inReproductive Development. Plant Physiol. **137**:651-662.

Memelink,J., Swords,K.M.M., Staehelin,L.A., and Hoge,J.H.C. (1994) Southern, Northern and Western blot analysis. In Plant Molecular Biology Manuel, (Dordrecht, NL: Kluwer Academic Publishers).

Michniewicz,M., Zago,M.K., Abas,L., Weijers,D., Schweighofer,A., Meskiene,I., Heisler,M.G., Ohno,C., Huang,F., Weigel,D., Meyerowitz,E.M., Luschnig,C., Offringa,R., and Friml,J. (2007). Antagonistic regulation of PIN phosphorylation by PP2A and PINOID directs auxin flux. Cell **130**:1044-1056.

Motchoulski,A. and Liscum,E. (1999). Arabidopsis NPH3: A NPH1 photoreceptor-interacting protein essential for phototropism. Science **286**:961-964.

Okada,K., Ueda,J., Komaki,M.K., Bell,C.J., and Shimura,Y. (1991). Requirement of the Auxin Polar Transport System in Early Stages of Arabidopsis Floral Bud Formation. Plant Cell **3**:677-684.

Paponov,I.A., Teale,W.D., Trebar,M., Blilou,I., and Palme,K. (2005). The PIN auxin efflux facilitators: evolutionary and functional perspectives. Trends Plant Sci. **10**:170-177.

Petrášek,J., Mravec,J., Bouchard,R., Blakeslee,J.J., Abas,M., Seifertová,D., Wisniewska,J., Tadele,Z., Kubes,M., Covanová,M., Dhonukshe,P., Skupa,P., Benková,E., Perry,L., Krecek,P., Lee,O.R., Fink,G.R., Geisler,M., Murphy,A.S., Luschnig,C., Zazimalová,E., and Friml,J. (2006). PIN Proteins Perform a Rate-Limiting Function in Cellular Auxin Efflux. Science **312**:914-918.

Ponting,C.P., Blake,D.J., Davies,K.E., Kendrick-Jones,J., and Winder,S.J. (1996). ZZ and TAZ: new putative zinc fingers in dystrophin and other proteins. Trends in Biochemical Sciences **21**:11-13.

Raven,J.A. (1975). Transport of indolaceticacid in plant cells in relation to pH and electrical potential gradients, and its significance for polar IAA transport. New Phytologist **74**:163-172.

Reinhardt,D., Pesce,E.R., Stieger,P., Mandel,T., Baltensperger,K., Bennett,M., Traas,J., Friml,J., and Kuhlemeier,C. (2003). Regulation of phyllotaxis by polar auxin transport. Nature **426**:255-260.

Robles,P. and Pelaz,S. (2005). Flower and fruit development in Arabidopsis thaliana. Int.J.Dev.Biol. **49**:633-643.

Rubery,P.H. and Sheldrake,A.R. (1974). Carrier-mediated auxin transport. Planta **118**:101-121.

Sabatini,S., Beis,D., Wolkenfelt,H., Murfett,J., Guilfoyle,T., Malamy,J., Benfey,P., Leyser,O., Bechtold,N., Weisbeek,P., and Scheres,B. (1999). An auxin-dependent distal organizer of pattern and polarity in the Arabidopsis root. Cell **99**:463-472.

Sakai,T., Wada,T., Ishiguro,S., and Okada,K. (2000). RPT2. A signal transducer of the phototropic response in Arabidopsis. Plant Cell **12**:225-236.

Sambrook,J., Fritsch F., and Maniatis,T. (1989) Molecular cloning - A laboratory Manual. New York: Cold Spring Harbor Laboratory press, ed.

Schirawski,J., Planchais,S., and Haenni,A.L. (2000). An improved protocol for the preparation of protoplasts from an established Arabidopsis thaliana cell suspension culture and infection with RNA of turnip yellow mosaic tymovirus: a simple and reliable method. Journal of Virological Methods **86**:85-94.

Smith,H.M.S. and Hake,S. (2003). The Interaction of Two Homeobox Genes, BREVIPEDICELLUS and PENNYWISE, Regulates Internode Patterning in the Arabidopsis Inflorescence. Plant Cell **15**:1717-1727.

Tanaka,H., Dhonukshe,P., Brewer,P.B., and Friml,J. (2006). Spatiotemporal asymmetric auxin distribution: a means to coordinate plant development. Cell Mol.Life Sci. **63**:2738-2754.

Tsiantis,M., Brown,M.I.N., Skibinski,G., and Langdale,J.A. (1999). Disruption of Auxin Transport Is Associated with Aberrant Leaf Development in Maize. Plant Physiol. **121**:1163-1168.

Wang,K.L.C., Yoshida,H., Lurin,C., and Ecker,J.R. (2004). Regulation of ethylene gas biosynthesis by the Arabidopsis ETO1 protein. Nature **428**:945-950.

Weber,H., Bernhardt,A., Dieterle,M., Han,P., Hano,P., Mutlu,A., Estelle,M., Genschik,P., and Hellmann,H. (2005). Arabidopsis AtCUL3a and AtCUL3b form complexes with members of the BTB/POZ-MATH protein family. Plant Physiol. **137**:83-93.

Weijers,D., Franke-van Dijk,M., Vencken,R.J., Quint,A., Hooykaas,P., and Offringa,R. (2001). An Arabidopsis Minute-like phenotype caused by a semi-dominant mutation in a RIBOSOMAL PROTEIN S5 gene. Development **128**:4289-4299.

Weijers,D., van Hamburg,J.P., van Rijn,E., Hooykaas,P.J.J., and Offringa,R. (2003). Diphtheria Toxin-Mediated Cell Ablation Reveals Interregional Communication during Arabidopsis Seed Development. Plant Physiol. **133**:1882-1892.

Winter,N., Kollwig,G., Zhang,S., and Kragler,F. (2007). MPB2C, a microtubule-associated protein, regulates non-cell-autonomy of the homeodomain protein KNOTTED1. Plant Cell **19**:3001-3018.

Wisniewska,J., Xu,J., Seifertová,D., Brewer,P.B., Ruzicka,K., Blilou,I., Rouquié,D., Benková,E., Scheres,B., and Friml,J. (2006). Polar PIN localization directs auxin flow in plants. Science **312**:883.

Woodward,C., Bemis,S.M., Hill,E.J., Sawa,S., Koshiba,T., and Torii,K.U. (2005). Interaction of auxin and ERECTA in elaborating Arabidopsis inflorescence architecture revealed by the activation tagging of a new member of the YUCCA family putative flavin monooxygenases. Plant Physiol **139**:192-203.

Zimmermann,P., Hirsch-Hoffmann,M., Hennig,L., and Gruissem,W. (2004). GENEVESTIGATOR. Arabidopsis microarray database and analysis toolbox. Plant Physiol. **136**:2621-2632.

Summary

Plant architecture is determined by tightly regulated developmental processes that largely depend on the action of the plant hormone auxin (Tanaka et al., 2006). Auxin has been first discovered as the signaling molecule that directs tropic responses of plants to unidirectional abiotic stimuli such as gravity and light (Darwin, 1880). A major determinant in auxin action, besides its signaling pathway, is its polar cell-to-cell transport (PAT) throughout the plant, which generates dynamic concentration gradients and maxima that are instrumental for organ positioning, meristem maintenance, embryo development and tropic growth responses (Benková et al., 2003, Friml et al., 2002, Friml et al., 2003, Reinhardt et al., 2003, Sabatini et al., 1999). The drivers of PAT are the PIN auxin efflux carriers that control the direction of PAT through their asymmetric subcellular localization (Wisniewska et al., 2006). The polar distribution of PIN proteins is highly dynamic, mediated by actin cytoskeleton-guided vesicle trafficking, and regulated by PIN protein degradation and auxin signaling (Abas et al., 2006, Geldner et al., 2001, Sauer et al., 2006) .

The AGCVIII PINOID (PID) protein serine/threonine kinase is the first, and yet only, identified determinant in the polar subcellular targeting of PIN proteins. Above threshold levels of PID activity induce a polarity switch in PIN localization from the basal (root facing) to the apical (shoot facing) side of the cell (Friml et al., 2004). Recently, it was shown that PID is a membrane-associated kinase (Lee and Cho, 2006) and that PID and PINs partially co-localize at the plasma membrane (Michniewicz et al., 2007). Furthermore, evidence was provided for the PID-dependent phosphorylation of PIN proteins in their large hydrophilic loop, and for the antagonistic action of PID and PP2A phosphatases on the phosphorylation status of PIN proteins (Michniewicz et al., 2007). Although these findings do clarify how PID functions as a regulator of PAT (Benjamins et al. 2001), several important questions about the regulation of the localization and the activity of PID remain unanswered. For example, 1) what are the upstream regulators of the PID kinase, 2) what determines the subcellular PID localization, 3) does PIN phosphorylation occur at the plasma membrane or in the endosomal compartments, and 4) is PID-dependent PIN phosphorylation sufficient to induce a switch in PIN polarity?

Previously, a yeast two-hybrid screen identified two calcium binding proteins PINOID BINDING PROTEIN1 (PBP1) and TOUCH3 (TCH3) and the BTB domain protein PBP2 as PID-interacting proteins. PBP1 is a small protein with a single calcium binding pocket (EF-hand). The corresponding encoding gene is part of a small gene family in Arabidopsis that includes *PBP1H* (for *PBP1 homologue*) and *KIC* (Reddy et al., 2004). TCH3 is an atypical 6 EF-hand calmodulin-like protein that is encoded by a single copy touch-inducible gene in Arabidopsis (Braam and Davis, 1990, Sistrunk et al., 1994). TCH3 and PBP1 bind to PID in a calcium-dependent manner. PBP2 was previously named BTB and TAZ domain protein1 (BT1) (Du and Poovaiah, 2004). BT1 is part of a family of five proteins characterized by the presence an N-terminal BTB domain, a TAZ domain and a C-terminal calmodulin-binding domain, a combination that is land plant specific. BTB

proteins are known to act as scaffold- or linker-proteins that organize protein complexes in various pathways (Albagli et al., 1995), and the specificity of their function may be dependent on the presence of extra domains. Interestingly, none of the PBPs are of targets PID, and instead they negatively (TCH3 and PB2) and positively (PBP1) regulate the activity of this kinase in *in vitro* phosphorylation reactions (Benjamins et al., 2003, Benjamins, 2004). The objective of the study described in this thesis was to identify the *in vivo* significance of the interaction between the PBPs and the PID kinase.

Chapters 2 and 3 describe the further functional analysis of the calcium-binding proteins. *In vitro* and *on chip* phosphorylation assays confirmed the regulatory role of TCH3 and PBP1 on PID activity, and for TCH3 it could be shown that it interacts with the catalytic domain of PID, whereas PBP1 seems to interact with the N- and C-terminal parts of this kinase. Furthermore, loss- and gain-of-function mutants in *TCH3* and *PBP1* were used to investigate and confirm that both proteins are regulators of the PID kinase activity. *pid* loss-of-function mutant embryos appeared to be sensitized to changes in *TCH3* expression, in that both loss- and gain-of-function of *TCH3* enhanced cotyledon defects. Moreover, overexpression of the *TCH3* coding region reduced the *PID* overexpression phenotype, which is in line with the model that TCH3 negatively modulates PID kinase activity (**Chapter 2**). On the other hand, *pbp1* and *pbp1h* loss-of-function mutations synergistically enhanced *pid* embryo phenotypes, which fits with their stimulatory effect on the *in vitro* PID phosphorylation activity. In addition, PBP1 and PBP1H were found to act as repressors of root growth, possibly though the enhancement of PID function. In contrast, *pbp1-1* loss-of-function partially rescued the *pid-14* inflorescence phenotype. Preliminary observations suggest that this rescue is not observed when two PID-related kinases (*WAG1* and *WAG2*) or *PBP1H* are also knocked out, suggesting that *pbp1* loss-of-function induces feed-back regulation on the activity of the redundantly acting PID-related kinases (**Chapter 3**).

Co-expression of a PID:CFP fusion with TCH3 or PBP1 fused to YFP in Arabidopsis protoplasts and the subsequent detection of Förster Resonance Energy Transfer (FRET) confirmed that PID and the two proteins interact *in vivo*. Interestingly, in both co-transfections the membrane-associated PID:CFP was sequestered from the plasma membrane to the cytosol. This sequestration was auxin-dependent, as it was not observed in auxin-starved protoplasts. Recently, Zegzouti and co-workers provided evidence that association of PID with the plasma membrane is mediated by the amino acid insertion in the PID catalytic domain that is characteristic for the AGCVIII kinases. They suggested that membrane-association was mediated by binding of this insertion domain to phosphatidic acids and phosphorylated inositides (Zegzouti et al., 2006). The sequestration of PID could thus be caused by TCH3 and PBP1 blocking the lipid binding site(s) in PID.

The auxin-dependency of PID sequestration could be related to the well-documented auxin-induced increase in cytoplasmic calcium (Dela Fuente and Leopold,

1973, Felle, 1988, Gehring et al., 1990, Shishova and Lindberg, 2004), which should enhance the binding of PID to the interacting calcium-binding proteins. Indeed, in root epidermis cells, where the expression of *PID* and *TCH3* is known to overlap, auxin treatment provoked a rapid transient release of PID to the cytoplasm, a response that appeared to be dependent on the action of calcium channels and calmodulin proteins such as TCH3 (**Chapter 2** and Figure 1). Preliminary results indicate that *PBP1* overexpression renders PID more resistant to this auxin-induced release from the plasma membrane (**Chapter 3** and Figure 1). It is thus likely that (auxin-induced) elevated levels of cytosolic calcium facilitate the interaction of TCH3 to the PID catalytic domain, preventing a kinase-

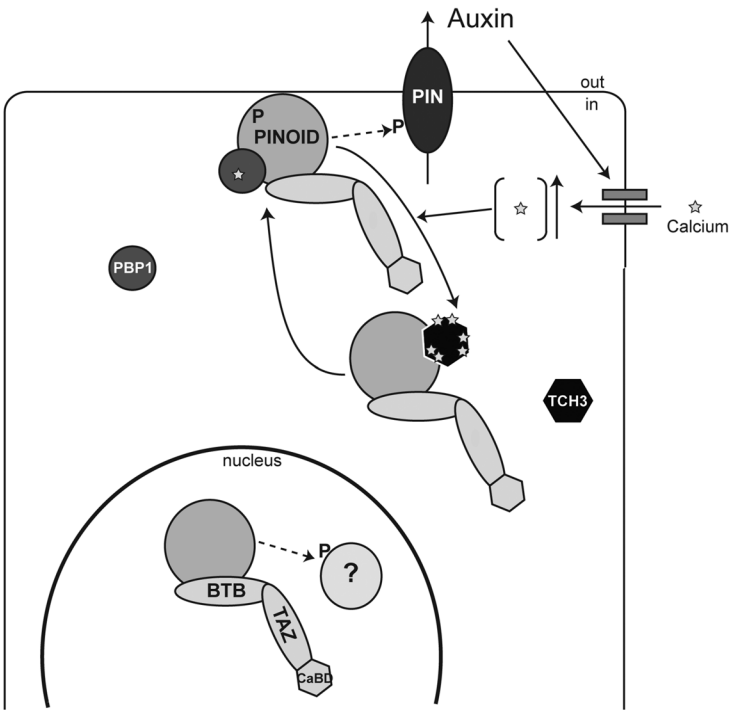


Figure 1. PID activity and subcellular localization is mediated by BT1, calcium and the calcium-binding proteins TCH3 and PBP1.

PID is a plasma membrane-associated protein kinase in proximity of its phospho-targets, the PIN auxin efflux carriers. Through its BTB domain, BT1 might regulate PID localization, notably in the nucleus, where yet unknown PID phosphorylation targets are localized. Low calcium levels stabilize membrane association and potentiate PID activity by interaction with PBP1. Increases in calcium concentrations, via calcium channels in the plasma membrane, for example in response to elevated auxin levels, stimulate the interaction with the calmodulin-like TCH3, and this inhibits PID activity and triggers the dissociation of PID from the plasma membrane. P: phosphate group from a phosphorylation event, stripped line: phosphorylation reaction, plain line: signaling event, stars: calcium.

lipid interaction and resulting in sequestration of the kinase away from its phospho-targets to the cytoplasm (Figure 1). Changes in subcellular localization are a commonly used cellular mechanism to regulate protein activity by sequestering proteins away from their targets. To our knowledge, however, the calcium- and calmodulin-dependent release of the PID kinase represents a novel mechanism of how the activity of kinases that steer the polar subcellular targeting of transporter proteins is regulated.

Chapter 4 describes the functional analysis of the Arabidopsis *BT* gene family to which *PBP2/BT1* belongs. A comparison of gene structure and amino acid sequence analysis of the encoded proteins indicated that the five genes group into three clades, that the genes have a clade-specific expression pattern, and that the corresponding proteins have a clade-specific subcellular localization. Furthermore, BT1 is shown to be a short-lived protein targeted for degradation by the 26S proteasome. Genetic analysis of the *BT* family indicated that the genes are functionally redundant and that *BT2* and *BT3* are essential for both male and female gametophyte development.

Chapter 5 describes a study on the link between BT proteins and PID. BT1 was found to interact with PID through its BTB domain, and to repress PID kinase activity *in vitro*. Moreover, *BT1* and *PID* expression patterns in Arabidopsis plants overlap, and PID:CFP and BT1:YFP fusion proteins co-localize in the cytoplasm of Arabidopsis protoplasts, indicating that *in vivo* interaction is possible. In fact, the proteins were found to alter each other subcellular localization. In protoplasts expressing both fusion proteins, BT1:YFP is also found at the plasma membrane, whereas PID:CFP becomes localized to the nucleus. Not only does this provide *in vivo* evidence for the interaction between BT1 and PID, but it also uncovers that PID possibly functions in the nucleus (Figure 1). *In vitro* pull-down assays indicate that at least four of the five BT proteins interact with PID, which corroborates the observed functional redundancy among the *BT* genes (**Chapter 4**).

The negative regulatory function of BT1 was confirmed *in vivo* by the fact that *BT1* overexpression enhanced *pid* loss-of-function mutant phenotypes and reduced *PID* overexpression phenotypes. Interestingly, *PID* overexpression, which normally does not lead to strong inflorescence phenotypes, significantly enhanced the *bt* loss-of-function inflorescence and silique phenotype. This indicates that the effect of *PID* overexpression on the inflorescence is normally suppressed by BT proteins, and only becomes visible in plants carrying multiple *bt* mutations. In contrast, the multiple *bt* mutations rescued the *PID* overexpression seedling phenotypes, indicating that BT scaffold proteins do not only repress PID activity, but are also essential components of PID signaling (**Chapter 5)**.

In conclusion, the functional analyses of the PBPs described in this thesis uncover a new mechanism of protein kinase activity regulation via calcium signaling, and present novel roles for the BT proteins, not only in PID signaling, but also more in general in plant development. Interesting questions about the biological relevance of the fine tuning of PID activity by these upstream regulators remain unanswered. For example, how does the

subcellular sequestration of PID by calcium signaling affect the PIN function and localization? And what is the exact function of the BT proteins in the PID signaling pathway, and which other proteins are parts of the BT-PID complex? The first steps and components in PID signaling have now been established, but clearly much more details need to be uncovered before the molecular mechanisms behind the dynamic kinase-dependent steering of polar auxin transport in response to endogenous developmental programs and external (abiotic) signals will be completely understood.

References

Abas,L., Benjamins,R., Malenica,N., Paciorek,T., Wisniewska,J., Moulinier-Anzola,J.C., Sieberer,T., Friml,J., and Luschnig,C. (2006). Intracellular trafficking and proteolysis of the Arabidopsis auxin-efflux facilitator PIN2 are involved in root gravitropism. Nat.Cell Biol. **8**:249-256.

Albagli,O., Dhordain,P., Deweindt,C., Lecocq,G., and Leprince,D. (1995). The BTB/POZ domain: a new protein-protein interaction motif common to DNA- and actin-binding proteins. Cell Growth Differ **6**:1193-1198.

Benjamins, R. (2004). Functional analysis of the PINOID protein kinase in *Arabidopsis thaliana*. Institute of Biology, Leiden University, The Netherlands.

Benjamins,R., Ampudia,C.S., Hooykaas,P.J., and Offringa,R. (2003). PINOID-mediated signaling involves calcium-binding proteins. Plant Physiol **132**:1623-1630.

Benková,E., Michniewicz,M., Sauer,M., Teichmann,T., Seifertova,D., Jurgens,G., and Friml,J. (2003). Local, efflux-dependent auxin gradients as a common module for plant organ formation. Cell **115**:591-602.

Braam,J. and Davis,R.W. (1990). Rain-, wind-, and touch-induced expression of calmodulin and calmodulin-related genes in Arabidopsis. Cell **60**:357-364.

Cheng,Y., Qin,G., Dai,X., and Zhao,Y. (2007). NPY1, a BTB-NPH3-like protein, plays a critical role in auxin-regulated organogenesis in Arabidopsis. Proc.Natl.Acad.Sci.U.S.A.

Darwin,C. (1880) *The Power of Movement in Plants*. London: John Murray.

Dela Fuente,R.K. and Leopold,A.C. (1973). A Role for Calcium in Auxin Transport. Plant Physiol **51**:845-847.

Du,L.Q. and Poovaiah,B.W. (2004). A novel family of Ca2+/calmodulin-binding proteins involved in transcriptional regulation: interaction with fsh/Ring3 class transcription activators. Plant Molecular Biology **54**:549-569.

Felle,H. (1988). Auxin causes oscillations of cytosolic free calcium and pH in Zea mays coleoptiles. Planta **V174**:495-499.

Friml,J., Wisniewska,J., Benkova,E., Mendgen,K., and Palme,K. (2002). Lateral relocation of auxin efflux regulator PIN3 mediates tropism in Arabidopsis. Nature **415**:806-809.

Friml,J., Yang,X., Michniewicz,M., Weijers,D., Quint,A., Tietz,O., Benjamins,R., Ouwerkerk,P.B.F., Ljung,K., Sandberg,G., Hooykaas,P.J.J., Palme,K., and Offringa,R. (2004). A PINOID-dependent binary switch in apical-basal PIN polar targeting directs auxin efflux. Science **306**:862-865.

Friml,J., Vieten,A., Sauer,M., Weijers,D., Schwarz,H., Hamann,T., Offringa,R., and Jurgens,G. (2003). Efflux-dependent auxin gradients establish the apical-basal axis of Arabidopsis. Nature **426**:147-153.

Furutani,M., Kajiwara,T., Kato,T., Treml,B.S., Stockum,C., Torres-Ruiz,R.A., and Tasaka,M. (2007). The gene MACCHI-BOU 4/ENHANCER OF PINOID encodes a NPH3-like protein and reveals similarities between organogenesis and phototropism at the molecular level. Development.

Gehring,C.A., Irving,H.R., and Parish,R.W. (1990). Effects of auxin and abscisic acid on cytosolic calcium and pH in plant cells. Proc.Natl.Acad.Sci.U.S.A **87**:9645-9649.

Geldner,N., Friml,J., Stierhof,Y.D., Jurgens,G., and Palme,K. (2001). Auxin transport inhibitors block PIN1 cycling and vesicle trafficking. Nature **413**:425-428.

Kemel Zago, M. (2006). Components and targets of the PINOID signaling complex in *Arabidopsis thaliana*. Institute of Biology, Leiden University, The Netherlands.

Lee,S.H. and Cho,H.T. (2006). PINOID positively regulates auxin efflux in Arabidopsis root hair cells and tobacco cells. Plant Cell **18**:1604-1616.

Michniewicz,M., Zago,M.K., Abas,L., Weijers,D., Schweighofer,A., Meskiene,I., Heisler,M.G., Ohno,C., Huang,F., Weigel,D., Meyerowitz,E.M., Luschnig,C., Offringa,R., and Friml,J. (2007). Phosphatase 2A and PID kinase activities antagonistically mediate PIN phosphorylation and apical/basal targeting in *Arabidopsis*. Cell **130**:1044-1056.

Reddy,V.S., Day,I.S., Thomas,T., and Reddy,A.S. (2004). KIC, a novel Ca2+ binding protein with one EF-hand motif, interacts with a microtubule motor protein and regulates trichome morphogenesis. Plant Cell **16**:185-200.

Reinhardt,D., Pesce,E.R., Stieger,P., Mandel,T., Baltensperger,K., Bennett,M., Traas,J., Friml,J., and Kuhlemeier,C. (2003). Regulation of phyllotaxis by polar auxin transport. Nature **426**:255-260.

Ren,S., Mandadi,K.K., Boedeker,A.L., Rathore,K.S., and McKnight,T.D. (2007). Regulation of Telomerase in Arabidopsis by BT2, an Apparent Target of TELOMERASE ACTIVATOR1. Plant Cell **19**:23-31.

Sabatini,S., Beis,D., Wolkenfelt,H., Murfett,J., Guilfoyle,T., Malamy,J., Benfey,P., Leyser,O., Bechtold,N., Weisbeek,P., and Scheres,B. (1999). An auxin-dependent distal organizer of pattern and polarity in the Arabidopsis root. Cell **99**:463-472.

Sauer,M., Balla,J., Luschnig,C., Wisniewska,J., Reinohl,V., Friml,J., and Benkova,E. (2006). Canalization of auxin flow by Aux/IAA-ARF-dependent feedback regulation of PIN polarity. Genes Dev. **20**:2902-2911.

Shishova,M. and Lindberg,S. (2004). Auxin induces an increase of Ca2+ concentration in the cytosol of wheat leaf protoplasts. J Plant Physiol **161**:937-945.

Sistrunk,M.L., Antosiewicz,D.M., Purugganan,M.M., and Braam,J. (1994). Arabidopsis TCH3 encodes a novel Ca2+ binding protein and shows environmentally induced and tissue-specific regulation. Plant Cell **6**:1553-1565.

Tanaka,H., Dhonukshe,P., Brewer,P.B., and Friml,J. (2006). Spatiotemporal asymmetric auxin distribution: a means to coordinate plant development. Cell Mol.Life Sci. **63**:2738-2754.

Wisniewska,J., Xu,J., Seifertova,D., Brewer,P.B., Ruzicka,K., Blilou,I., Rouquie,D., Scheres,B., and Friml,J. (2006). Polar PIN localization directs auxin flow in plants. Science **312**:883.

Zegzouti,H., Li,W., Lorenz,T.C., Xie,M., Payne,C.T., Smith,K., Glenny,S., Payne,G.S., and Christensen,S.K. (2006). Structural and functional insights into the regulation of Arabidopsis AGC VIIIa kinases. J.Biol.Chem. **281**:35520-35530.

Samenvatting

De architectuur van planten wordt bepaald door strak gereguleerde ontwikkelingsprocessen, die in belangrijke mate worden gestuurd door het plantenhormoon auxine. Auxine is initieel ontdekt als het signaalmolecuul dat de tropische groeiresponsen van planten ten opzichte van directionele abiotische stimuli zoals licht en zwaartekracht stuurt. Een belangrijke factor in de activiteit van auxine is, naast de signaaltransductie, het polaire transport van dit hormoon door de plant. Polair auxinetransport (PAT) genereert dynamische gradiënten en maxima van auxine die de posities van organen bepalen, tropische groeiresponsen sturen, en de functionaliteit van meristemen waarborgen. De aanjagers van PAT zijn de PIN auxinetransporters, die de richting van PAT bepalen door hun asymmetrische subcellulaire lokalisatie in de cel. De polaire distributie van PIN eiwitten is zeer dynamisch, en wordt gemedieerd door cyclisch transport van membraanblaasjes via het actinecytoskelet, en gereguleerd door auxinesignaaltransductie en gerichte afbraak van PIN eiwitten.

Het Arabidopsis proteïne serine/threonine kinase PINOID (PID) is geïdentificeerd als de eerste determinant in de polaire subcellulaire targeting van PIN eiwitten. Wanneer de expressie en daarmee de activiteit van PID boven een drempelwaarde uitkomt, dan induceert dit een verandering in de polaire lokalisatie van PIN eiwitten van de basale (naar de wortelpunt wijzende) naar de apicale (naar het scheutmeristeem wijzende) kant van cellen. Recentelijk is aangetoond dat PID een membraangeassocieerd kinase is, en dat PID en PIN eiwitten gedeeltelijk colokaliseren op het plasmamembraan van cellen. Tevens is er bewijs gevonden voor de PID-afhankelijke fosforylering van PIN eiwitten, en dat PP2A phosphatases en PID antagonisch werken op de lokalisatie en fosforylatiestatus van PIN eiwitten. Deze vindingen laten de essentie zien van hoe PID werkt als regulator van PAT, maar ze laten ook een aantal belangrijke vragen nog onbeantwoord. Wat reguleert de activiteit van PID, en wat bepaalt de subcellulaire lokalisatie van dit kinase? Fosforyleert PID PIN eiwitten wanneer deze op het plasmamembraan aanwezig zijn, of heeft dit plaats in endosomale compartimenten, en is PID-afhankelijke PIN fosforylering voldoende om veranderingen in PIN polariteit te induceren?

In voorgaand onderzoek zijn er door middel van een twee-hybride screen in gist een drietal PID BINDENDE EIWITTEN (PBPs) geïdentificeerd, te weten de calciumbindende eiwitten PINOID BINDING PROTEIN1 (PBP1) en TOUCH3 (TCH3), en het BTB domein eiwit PBP2. PBP1 is een klein eiwit met een enkele calciumbindingsplaats (EF-hand). Het corresponderende gen maakt deel uit van een kleine genfamilie in Arabidopsis, met *KIC* en het directe homoloog *PBP1H* als familieleden. TCH3 is een atypisch calmoduline-achtig eiwit met 6 EF-hands, dat wordt gecodeerd door een uniek gen in Arabidopsis waarvan de expressie geïnduceerd wordt door aanraking. PBP1 en TCH3 binden PID op een calciumafhankelijke wijze. PBP2 is identiek aan het eerder geïdentificeerde BTB en TAZ domein eiwit 1 (BT1). BT1 maakt deel uit van een familie van vijf eiwitten in Arabidopsis die gekarakteriseerd worden door een plantspecifieke combinatie van eiwit-eiwit interactiedomeinen, te weten een N-terminaal BTB domein, een

TAZ domein en een C-terminaal calmodulinebindend domein. Van BTB eiwitten is bekend dat ze als linkereiwitten bij een grote verscheidenheid van processen betrokken zijn, en dat hun specificiteit wordt bepaald door de aanwezigheid van de extra eiwit-eiwit interactiedomeinen.

Interessant genoeg worden geen van de PBPs in *in vitro* reacties door PID gefosforyleerd, maar lijken ze eerder als positieve (PBP1) en negatieve (TCH3 en PBP2) regulatoren van de PID activiteit op te treden. Het doel van het in dit proefschrift beschreven onderzoek was de interactie tussen PBPs en PID *in vivo* aan te tonen, en de functionele significantie daarvan verder te analyseren.

Hoofdstukken 2 en 3 beschrijven de verdere functionele analyse van de calciumbindende eiwitten. Additionele *in vitro* en *on chip* fosforylatieassays bevestigden dat PBP1 en TCH3 de PID activiteit respectievelijk positief en negatief beïnvloeden. Voor TCH3 kon worden aangetoond dat het specifiek bindt aan het katalytische domein van PID, terwijl PBP1 met name een interactie lijkt aan te gaan met de N- en C-terminale uiteinden van het kinase. Verder zijn er verlies- en winst-van-functie mutanten van *TCH3* en *PBP1* gebruikt om *in vivo* bewijs te krijgen voor de rol van deze eiwitten als regulators van PID. *pid* mutante embryos bleken gevoeliger voor veranderingen in *TCH3* expressie. Zowel *tch3* verlies-van-functie als *TCH3* overexpressie leidde tot versterking van de *pid* zaadlobfenotypes. Tevens leidde overexpressie van *TCH3* tot een reductie van het *PID* overexpressie fenotype, een resultaat dat de rol van TCH3 als negatieve regulator van PID activiteit bevestigt (**Hoofdstuk 2**). In overeenstemming met het stimulerende effect van PBP1 en PBP1H op de *in vitro* activiteit van PID, leidden zowel *pbp1* als *pbp1h* verlies-van-functie mutaties tot een versterking van het *pid* embryo fenotype. Daarentegen bleek de *pbp1-1* verlies-van-functie gedeeltelijk het *pid-14* bloeiwijzefenotype te herstellen. Voorlopige resultaten suggereren dat dit herstel niet optreedt wanneer de genen coderend voor PBP1H of voor de PID-gerelateerde kinases WAG1 en WAG2 ook uitgeschakeld zijn, wat impliceert dat *pbp1* verlies-van-functie leidt tot terugkoppeling, resulterend in verhoogde transcriptie van deze genen (**Hoofdstuk 3**).

Co-expressie in Arabidopsis protoplasten van een PID:CFP (cyaan fluorescent eiwit) fusie met een fusie tussen TCH3 of PBP1 en YFP (geel fluorescent eiwit) en de daaropvolgende detectie van "Förster Resonance Energy Transfer" (FRET) bevestigde dat PID ook *in vivo* een interactie aangaat met de twee calcium-bindende eiwitten. Interessant genoeg verplaatst PID zich in aanwezigheid van TCH3 of PBP1 van het plasmamembraan naar het cytoplasma. Deze verplaatsing bleek afhankelijk van auxine, en werd niet geobserveerd in auxinegehongerde protoplasten. Recentelijk is er bewijs gevonden dat PID met het plasmamembraan associeert door binding van de karakteristieke aminozuurinsertie in het katalytische domein van PID met fosfatidylzuur en gefosforyleerde inositides. De verplaatsing van PID naar het cytoplasma van protoplasten wordt mogelijk veroorzaakt

door afscherming van de fosfolipide-bindingsplaatsen in PID door de binding van PBP1 en TCH3.

De auxineafhankelijkheid van de PID verplaatsing zou verklaard kunnen worden door de auxinegeïnduceerde verhoging van de cytoplasmatische calciumconcentratie, welke vervolgens leidt tot een sterkere interactie tussen PID en de calciumbindende eiwitten PBP1 en TCH3. Inderdaad werd in wortelepidermiscellen, waar de expressie van *PID* en *TCH3* overlappen, na auxinebehandeling een snelle transiënte dissociatie van PID van het plasmamembraan geobserveerd. Deze respons bleek afhankelijk van de activiteit van calciumkanalen en calmodulines (**Hoofdstuk 2**). Daarentegen bleek *PBP1* overexpressie PID juist meer resistent te maken tegen de auxinegeïnduceerde dissociatie van het plasmamembraan in wortelepidermiscellen. Ook bleek overexpressie van *PBP1* en *PBP1H* te leiden tot verminderde wortelgroei, mogelijk door versterking van de PID functie (**Hoofdstuk 3**). Hieruit is het model gedestilleerd dat auxinegeïnduceerde verhoging van calciumconcentraties leidt tot een sterkere interactie tussen TCH3 en het katalytische domein van PID, waarbij de fosfolipidebindingsplaats afgeschermd wordt, resulterend in dissociatie van het plasmamembraan, weg van de PIN fosforylatietargets. Veranderingen in de subcellulaire lokalisatie van eiwitten is een algemeen gebruikt mechanisme om de activiteit van het betreffende eiwit te reguleren. Voor zover ons bekend, is dit echter het eerste voorbeeld van een calcium- en calmoduline-afhankelijke membraandissociatie van een kinase dat de subcellulaire targeting van transporteiwitten stuurt.

Hoofdstuk 4 beschrijft de functionele analyse van de Arabidopsis *BT* genfamilie waartoe *PBP2*/*BT1* behoort. Een vergelijking van genstructuur en aminozuurvolgorde van de gecodeerde eiwitten laat zien dat de vijf genen groeperen in 3 claden. Per clade laten de genen een specifiek expressiepatroon zien, en de corresponderende BT eiwitten vertonen een specifieke subcellulaire lokalisatie. BT1 is een onstabiel eiwit dat afgebroken wordt door het 26S proteasoom. Genetische analyse van de *BT* familie laat zien dat de genen onderling functioneel redundant zijn, en dat *BT2* en *BT3* essentieel zijn voor zowel mannelijke als vrouwelijke gametogenese.

Met het in **hoofdstuk 5** beschreven onderzoek is de rol van de BT eiwitten in PID signaaltransductie nader onderzocht. BT1 interacteert met PID via het BTB domein, en onderdrukt de *in vitro* activiteit van dit kinase. Daarnaast vertonen *BT1* en *PID* overlappende expressiepatronen in Arabidopsis planten, en co-localiseren PID:CFP en BT1:YFP fusie-eiwitten in het cytoplasma van Arabidopsis protoplasten, wat aangeeft dat de *in vivo* interactie tussen de eiwitten mogelijk is. Interessant genoeg blijken de eiwitten elkaars subcellulaire lokalisatie te beïnvloeden. In protoplasten die beide eiwitten tot expressie brengen, wordt BT1:YFP gevonden op het plasma-membraan, terwijl PID:CFP kernlokalisatie laat zien. Dit bevestigt de interactie tussen de twee eiwitten, en geeft aan dat PID zeer waarschijnlijk een functie heeft in de kern van de plantencel. Tenminste vier van

de vijf BT eiwitten blijken in *in vitro* pull down assays met PID te binden, wat de in **hoofstuk 4** beschreven functionele redundantie tussen de *BT* genen onderstreept.

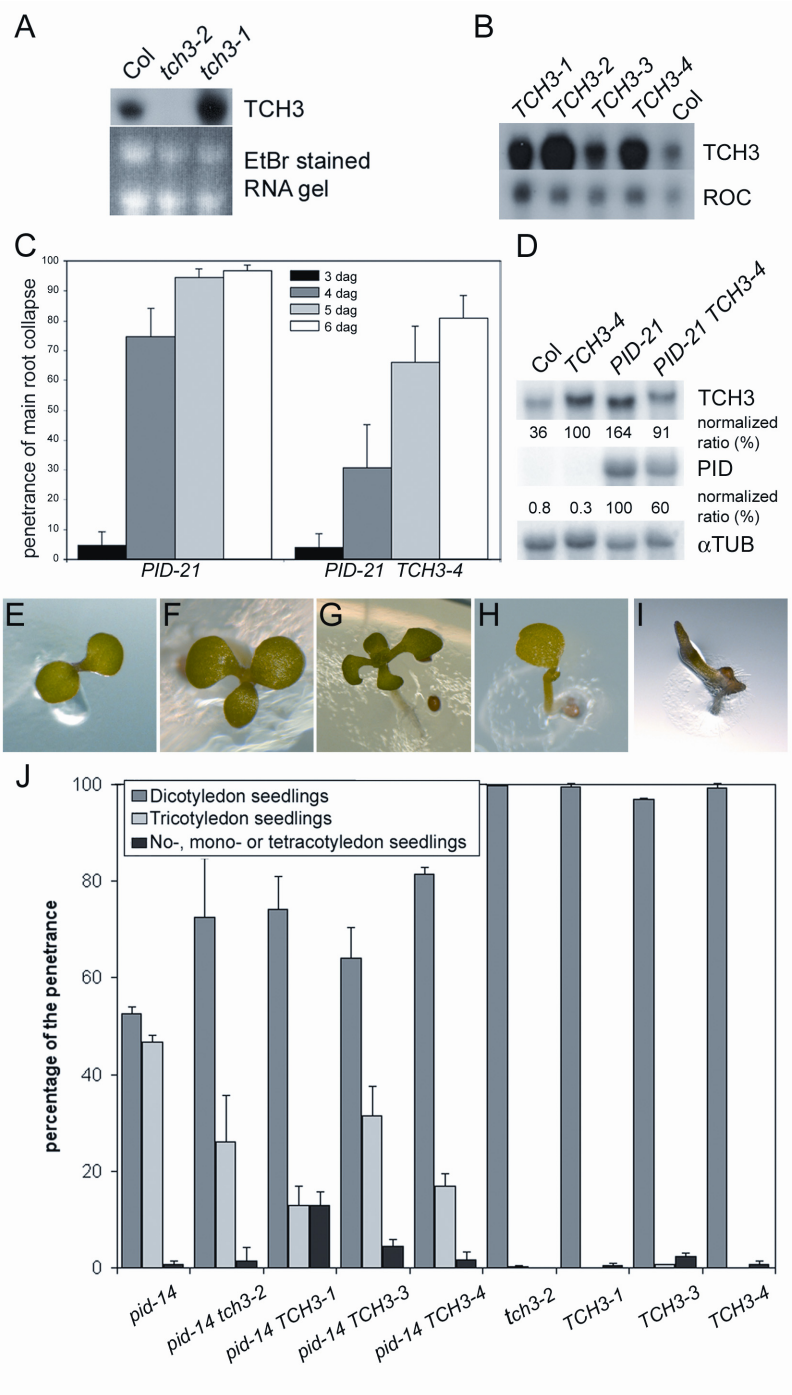
De rol van BT1 als negatieve regulator van PID werd bevestigd door het feit dat *BT1* overexpressie leidde tot een versterking van het *pid* verlies-van-functie fenotype, terwijl het *PID* overexpressie fenotype werd afgezwakt. *PID* overexpressie planten vertonen normaal geen fenotype in de bloeiwijze, maar in planten die meerdere *bt* mutaties dragen bleek *PID* overexpressie het *bt* verlies-van-functie fenotype in de bloeiwijze duidelijk te versterken. Hieruit concluderen wij dat het effect van *PID* overexpressie normaal onderdrukt wordt door BT eiwitten, en dat het alleen zichtbaar wordt in planten met meerdere *bt* mutaties. Verrassend genoeg leidden meerdere *bt* mutaties tot een volledig herstel van de zaailing fenotypes van PID overexpressie. Dit suggereert dat BT scaffold eiwitten niet alleen de PID activiteit onderdrukken, maar dat ze in ieder geval gedurende zaailingontwikkeling essentiële componenten in PID signaaltransductie zijn.

De in dit proefschrift beschreven functionele analyse van de PBPs heeft enerzijds een nieuw regulatiemechanisme van eiwit kinases door calciumsignaaltransductie blootgelegd, en anderzijds zijn er nieuwe functies van BT eiwitten gevonden, niet alleen in PID signaaltransductie, maar ook meer algemeen gedurende plantenontwikkeling. Een interestante vraag blijft echter wat de biologische relevantie is van de fijnregulatie van PID activiteit door deze bindende eiwitten. Hoe heeft de verplaatsing van PID door calcium van het plasmamembraan naar het cytosplasma effect op de functie en lokalisatie van PIN eiwitten? En wat is de precieze functie van BT eiwitten in de PID signaaltransductieroute, en welke andere eiwitten zijn onderdeel van het BT-PID complex? De eerste stappen en componenten in PID signalering zijn nu in kaart gebracht, maar het mag duidelijk zijn dat er nog veel valt te ontdekken, voordat we de moleculaire mechanismen achter de dynamische kinase-gemedieerde sturing van auxine transport in respons op interne ontwikkelingsprogramma's en externe (abiotische) signalen volledig zullen doorgronden.

Curriculum Vitae

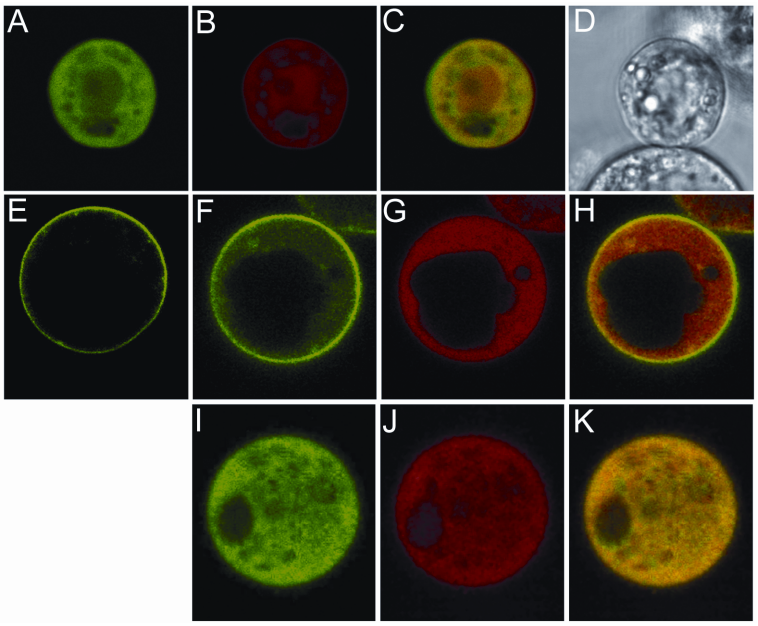
Hélène Robert-Boisivon was born on January, 10th 1977 in Mont-Saint-Aignan (76), France. She attended to the Lycée Sembat at Sotteville-lès-Rouen (76), France. In September 1995, she started Medicine studies at the University of Rouen (76), France, for two years, and in September 1997 she was accepted to the second year of Diplôme d'Etudes Universitaires Générales (General Academic Studies Diploma) in Animal and Plant Biology and Geology at the same university. In 1999 and 2000, she obtained her Licence and Maitrise in Cell Biology and Physiology with an option in Plant Physiology and Biotechnology. Then from February 2000 to December 2001, Hélène was a research trainee under the supervision of Dr. Frédéric Berger in the laboratory of Reproduction and Development of Plants at the Ecole Normale of Lyon (69), France. The traineeship concerned the analysis of establishment of endosperm polarity during seed development in *Arabidopsis thaliana*. In September 2001, Hélène received her master degree in Differentiation, Genetics and Immunology from the Ecole Normale of Lyon (69), France. From January to May 2002, she worked as an assistant ingenieur in the group of Dr. Jim Haseloff at the Cellular Development Laboratory at the Plant Sciences Department, University of Cambridge, UK, where she worked on the generation and screening of enhancer trap Arabidopsis lines. In June 2002 she joint the research group of Dr. Remko Offringa at the Molecular Developmental Genetics Department in the Institute of Biology of Leiden University, The Netherlands, to study the role of PINOID BINDING PROTEINs as regulators of transport of the plant hormone auxin in *Arabidopsis thaliana* (this thesis). From September 2007 on, she works as a post-doc in the Auxin group at the Plant System Biology Department of the Flemish Institute of Biotechnology in Ghent, Belgium. Under the supervision of Prof Jiří Friml, she continues her studies on auxin transport in Arabidopsis, but now with a focus on early embryo development and the still unknown function of the BIG protein in this process.

Color supplements



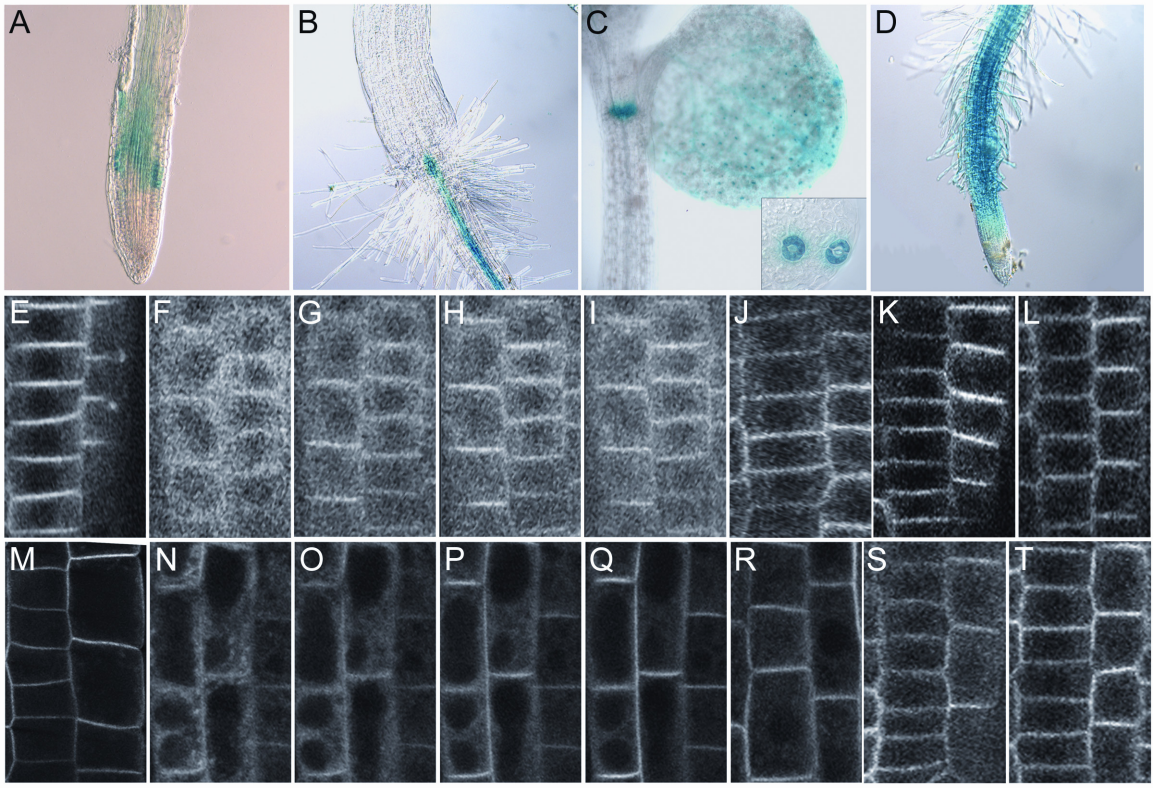
Chapter 2, Figure 3, page 38.

TOUCH3 is a negative regulator of PINOID *in vivo*.



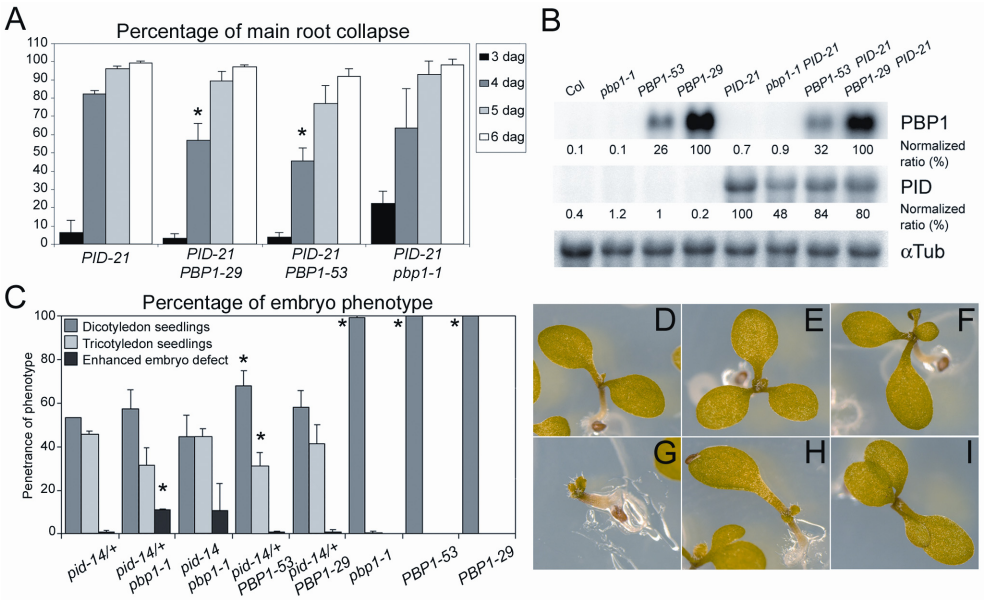
Chapter 2, Figure 4, page 40.

TOUCH3 and PINOID co-localization is auxin-dependent.



Chapter 2, Figure 6, page 42.

TOUCH3 and auxin cause PINOID to dissociate from the plasma membrane.



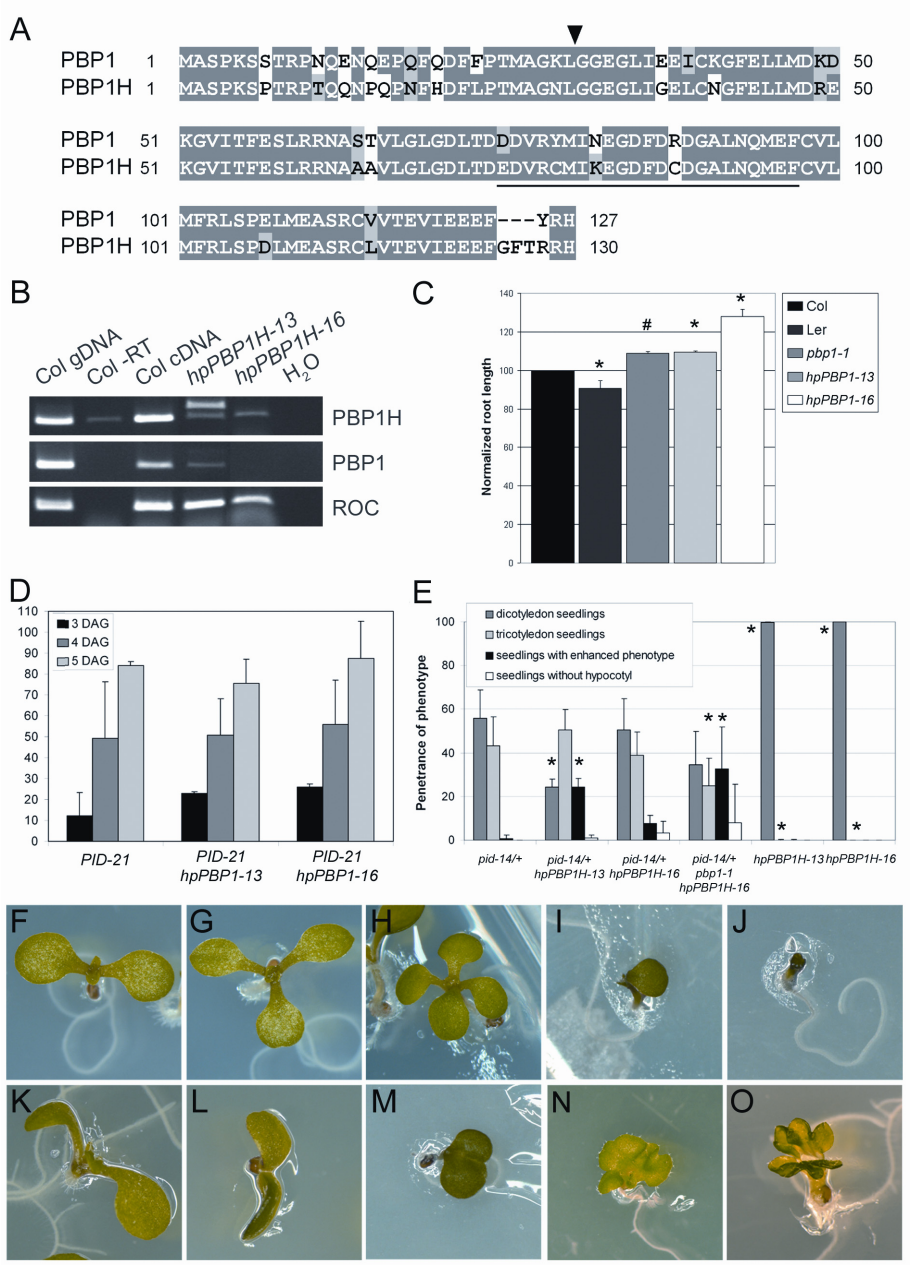
Chapter 3, Figure 2, page 60.

pbp1-1 loss-of-function enhances *pid-14* embryo phenotypes.



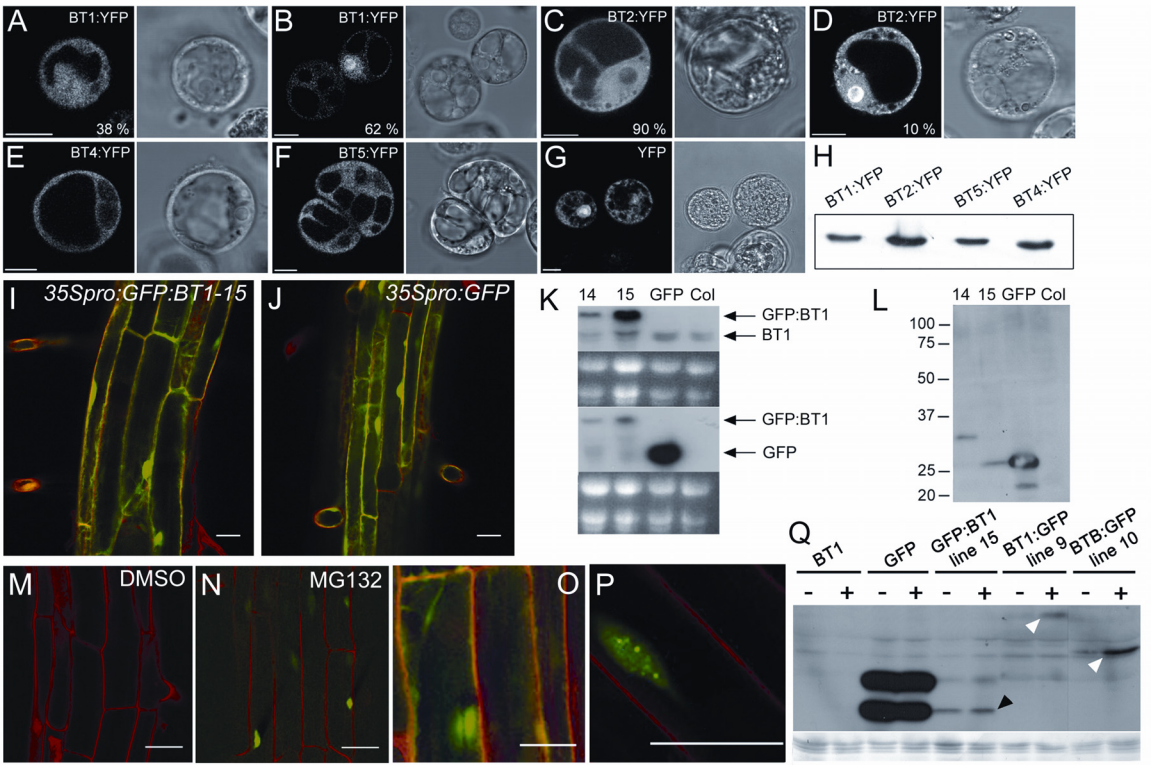
Chapter 3, Figure 3, page 63.

pbp1-1 loss-of-function partially rescues *pid-14* inflorescences.



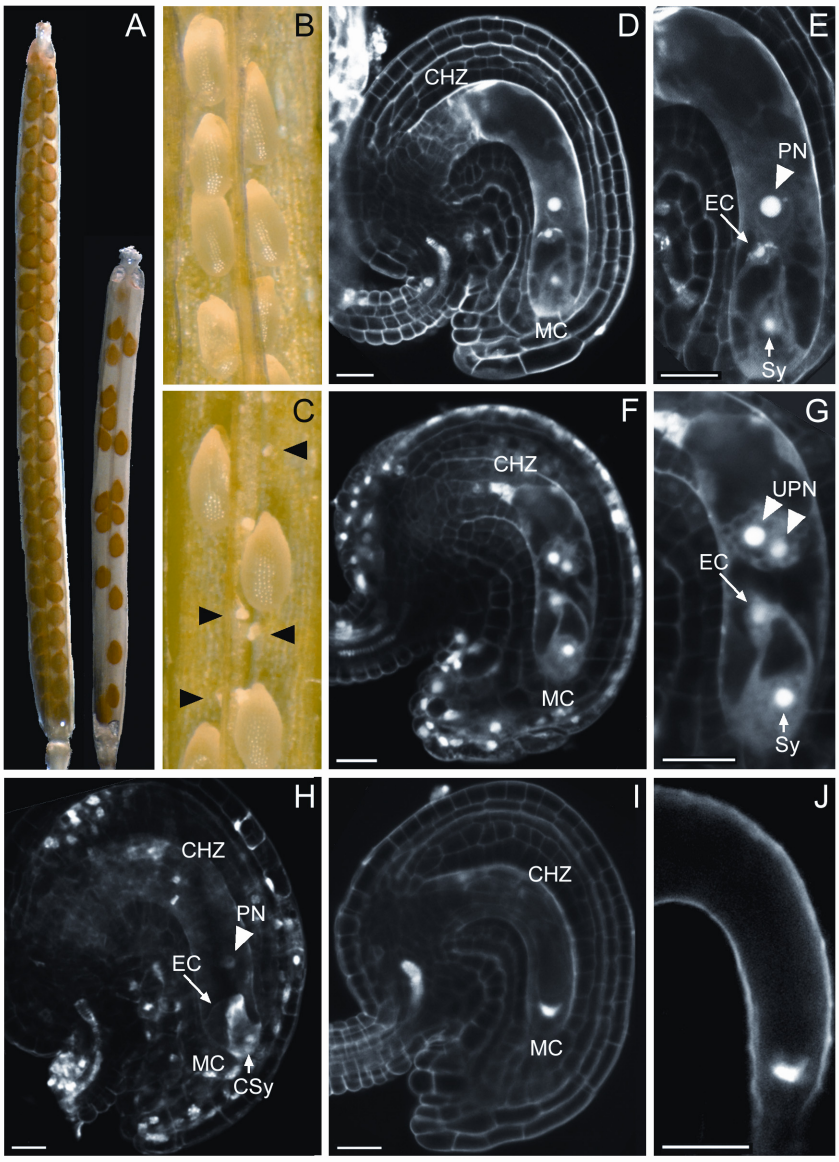
Chapter 3, Figure 5, page 65.

PBP1 and PBP1H act redundantly on root growth, embryo patterning and leaf phyllotaxis.



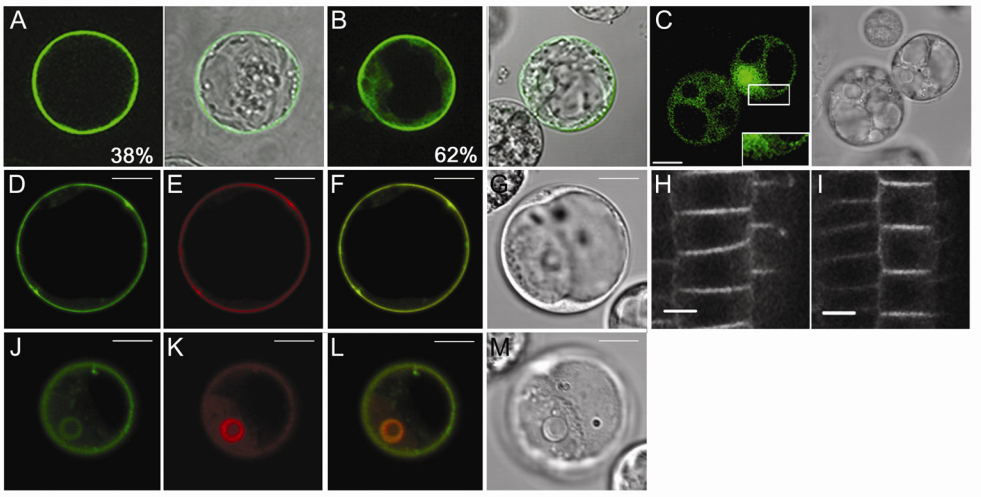
Chapter 4, Figure 2, page 81.

The expression pattern of the BT proteins suggests a genetic redundancy among the family members.



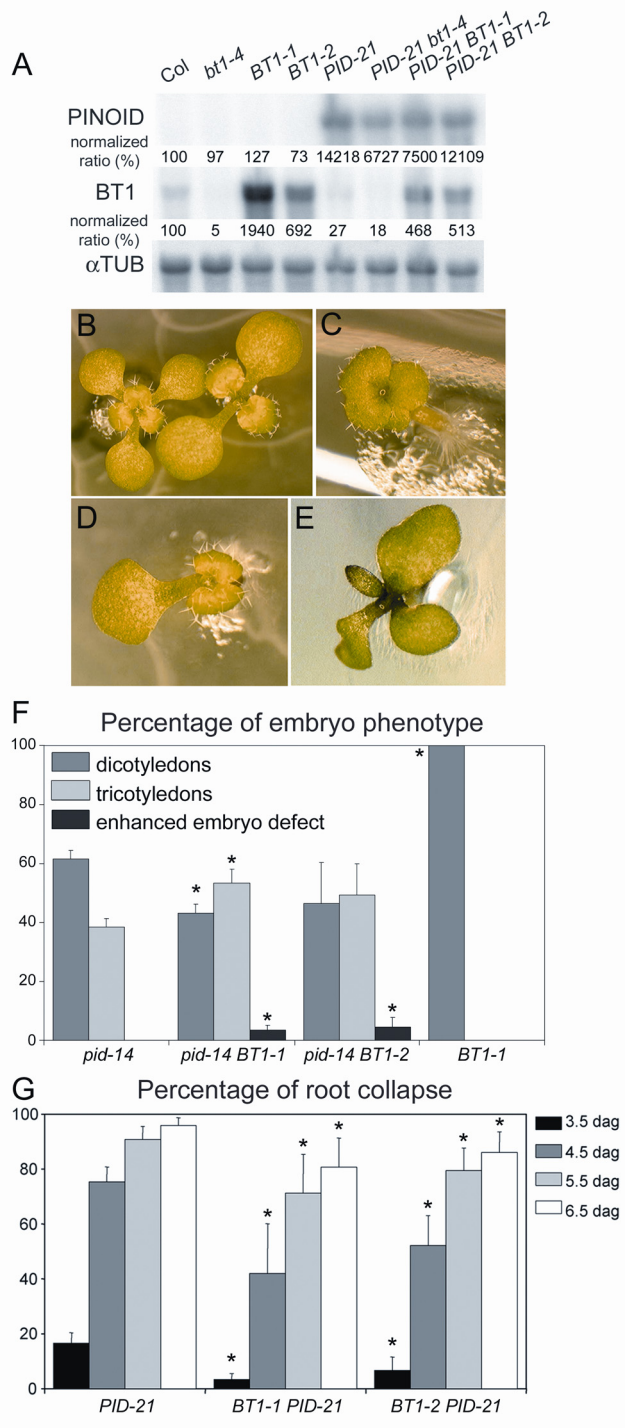
Chapter 4, Figure 4, page 86.

The quintuple *bt* loss-of-function is gametophytic lethal.



Chapter 5, Figure 3, page 105.

BT1 and PINOID co-localize at the plasma membrane in Arabidopsis protoplasts.



Chapter 5, Figure 4, page 107.

Overexpression of *BT1* enhances *pid-14* embryo phenotypes and inhibits *35Spro:PID-21* root meristem collapse.



G

Phenotypes							n
PID-21 BT1-1	0.4/pl			0.5/pl	0.4/pl	0.6/pl	8
PID-21 BT1-2	1.5/pl			0.5/pl		1.3/pl	8
RPS5A>>BTB-1	2.9/pl	0.6/pl	0.6/pl	0.6/pl	0.3/pl	1.1/pl	8
RPS5A>>BTB-4	1.3/pl	0.4/pl	0.5/pl	0.5/pl			8
RPS5A>>BTB-5	1.3/pl		0.1/pl	0.1/pl		0.3/pl	8
RPS5A>>PID	0.6/pl						7
Col							9
PID-21							9
BT1-1					0.1/pl		8
BT1-2							8

Chapter 5, Figure 6, page 110.

RPS5Apro>>BTB expression results in axilliary branch and inflorescence meristem defects.